Time-lapse studies of neural precursor cell divisions *in vitro*

Nina Amelia Lucy Callard

The Wolfson Institute for Biomedical Research, University College London

A thesis submitted to the University of London in part fulfilment of the degree of Doctor of Philosophy

February 2008

ProQuest LLC
789 East Eisenhower Parkway
P.O. Box 1346
Ann Arbor, MI 48106-1346

Abstract

The entire adult central nervous system (CNS) derives from an initially small population of apparently homogeneous neuroepithelial precursor cells (NEPs) which produce specific differentiating cell types in a highly organised fashion with respect to both the time and place at which they are generated. A unifying phenomenon throughout the CNS is that neurons are always generated before glia. To better understand what mechanisms might be involved, the dynamics of precursor lineages need to be described. Here, single NEPs from the murine dorsal embryonic neocortex were cultured at clonal density and filmed using time-lapse microscopy to monitor their divisions over time. The progeny they gave rise to were identified by immunocytochemical methods and expression of the oligodendrocyte lineage-affiliated transcription factor, *olig2* was directly observed by using a transgenic mouse that expressed enhanced green fluorescent protein (EGFP) in *olig2*-expressing cells. (The transgenic mouse line was created by phage artificial chromosome (PAC) transgenesis). This data enabled lineage trees for individual clones to be retrospectively drawn to include the timing of *olig2* expression alongside the final identification of the daughter cells produced. In this way, the effects of different growth factors with respect to the induction of glial in preference to neuronal phenotypes were assessed.

Using this system it was possible to determine what cell types could be derived from a single precursor and with what pattern within a lineage *olig2* might be expressed under different culture conditions. Both FGF-2 and a Sonic Hedgehog agonist were seen to produce mixed clones in which *olig2* was transcribed at early branch points within a lineage and later down-regulated in a selection of daughter cells. This means that *olig2* expression does not denote commitment to the oligodendrocyte lineage and, furthermore, that induction is a sporadic event which seems to be dictated at the level of the individual progenitor cells rather than by an intrinsic cell-timer dictated within the original NEP.

Acknowledgements

My list of thanks really should extend longer than this thesis itself; the longer it has taken to come into fruition, the more people I seem to have recruited to help make it happen. It goes without saying that the parental-creatures who have nurtured me thus far in life, upped the anti during thesis-writing time. Special thanks must go to Dad for his unerring support, encouragement and advice throughout – he even offered to read it for me! And to Mum who, even from the other side of the world, checked up on a daughter who was out there somewhere, writing something big. Of course I have to thank my sisters too – Ali, Em and Helen where would I be without you?! Thanks for being wonderfully wonderful always! Then there is my James who has seen the good, the bad and the ugly and has provided me with laughter, kindness, midnight pizza in the park and lots of love throughout. Thank you! I don't think I would have done it without you. I have also had friends in abundance to keep me going and to promise to still *be* my friend even if I don't see them for a year! Kamala – always a pleasure and a pick-me up, you and Cornwall have been a saving grace, the Snorbens crew who persistently ask if I'm nearly done yet!, Burd for emergency coffee and incentive devices!, Leanne and Kaylene for fun n' laughter in and out of the lab, Raquel for late-night chats over the cryostat, Sergeant Setzu for showing me it *can* be done, and Melanie for giving me that creative buzz when dotting the i's and crossing the t's became too much and who got me to resonate in the field again!

Thanks to Bill Richardson and all the lab members who made the whole experience something to remember. Special thanks to Nigel Pringle without whose painstaking construction and maintenance of the time-lapse set-up and constant advice on the world of tissue culture, I would have been lost. Thanks of course to Mat G for his patient educating of me in the world of molecular biology, street talk and how to whistle that half a semi-note out of tune to drive everyone else nuts! Also mountains of thanks to Ulla for all her help and support, and to Palma for helping make my mice possible. Thanks to the Wellcome Trust for getting and keeping me here and to David Attwell for pointing me in the right direction! And thanks to Martin Raff who valiantly read the first drafts and helped edit without completely covering it in red pen!

Declaration

I, Nina Amelia Lucy Callard, confirm that the work presented in this thesis is my own. Where information has been derived from other sources, I confirm that this has been indicated in this thesis.

Signed

Table of Contents

Abbreviations

AEP - Anterior Entopeduncular Area

BMP – Bone Morphogenetic Protein

Bp – Base pairs (of DNA)

CGE – Caudal Ganglionic eminence

Cm^R – Chloramphenicol resistance

CNS – Central Nervous System

DMEM – Dulbecco's Modified Eagle's Medium

DMSO – Dimethylsulphoxide

DNA – Deoxyribonucleic Acid

DNase – Deoxyribonuclease

dNTP – Deoxyribonucleotide triphosphate

DSHB – Developmental Studies Hybridoma Bank

E# - Embryonic day # (number of days after conception)

EBSS – Earle's Balanced Salt Solution

EDTA – Ethylenediaminetetracetic Acid

EGF – Epidermal Growth Factor

EGFP – Enhanced Green Fluorescent Protein

FCS – Foetal Calf Serum

FGF-2 – Fibroblast Growth Factor 2

FGFR – Fibroblast Growth Factor Receptor

FITC – Fluorescein isothiocyanate

GFAP – Glial Fibrillary Acidic Protein

GRP – Glial Restricted Precursor

HD – Homeodomain

Hrs – Hours

IAA – Indole acetic acid

IHH – Indian Hedgehog

Kb – Kilobase pairs (of DNA)

LB – Luria Bertani Broth

LGE – Lateral ganglionic eminence

LMP – Low melting point (agarose)

MBP – Myelin basic protein

MGE – Medial ganglionic eminence

MN – Motor neuron

MNP – Motor neuron precursor

mRNA – Messenger Ribonucleic Acid

NEP – Neuroepithelial precursor cell

NRP – Neuron Restricted Precursor

O-2A – Oligodendrocyte and Type-2-Astrocyte precursor

OD_{600} – Optical Density at 600 nm wavelength

Olig2 – Oligodendrocyte lineage transcription factor 2

OLP – Oligodendrocyte precursor

ORF – Open reading frame

P# - Postnatal day # (number of days after birth)

PAC – P1 bacteriophage-derived Artificial Chromosome

PBS – Phosphate Buffered Saline

PCR – Polymerase Chain Reaction

PDGFRα – Platelet-Derived Growth Factor Receptor α

PFA – Paraformaldehyde

PFGE – Pulse Field Gel Electrophoresis

PLP – Proteolipid Protein

RNase – Ribonuclease

Rpm – Revolutions per minute

SDS – Sodium Dodecyl Sulphate

SHH – Sonic Hedgehog

SVZ – Subventricular Zone

TE – Tris EDTA Solution

TGF-β – Transforming Growth Factor β

VZ – Ventricular Zone

List of Tables and Figures

Chapter 1 – Introduction

Chapter 2 – Methods and Materials

Chapter 3 – *Olig2* Transgenesis

Chapter 4 – Time-lapse Microscopy of Neuroepithelial Precursor cells *in vitro*

Chapter 1

Introduction

1.1 Development of the Central Nervous System

The specification of neural tissue begins at a relatively late stage of embryogenesis, after gastrulation, when the zygote has already multiplied and differentiated into the three 'germ layers' of the embryo - the endoderm, mesoderm and ectoderm, which represent the inner, middle and outer layers respectively (Figure 1.1).

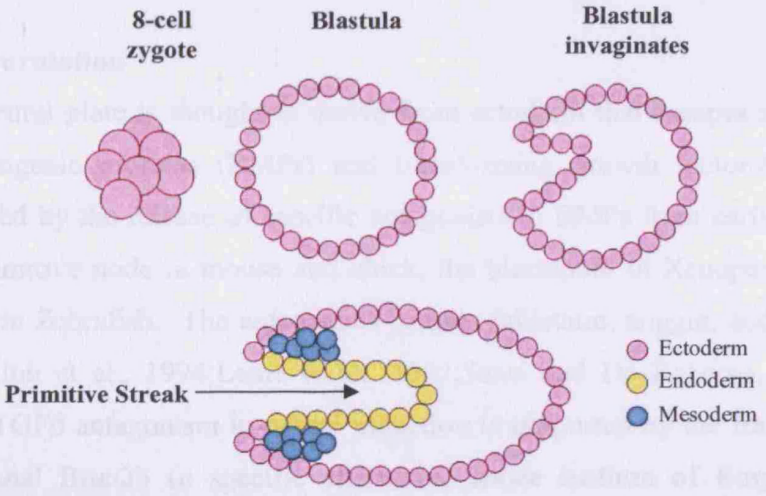

Figure 1.1 Schematic representation of gastrulation. From the fertilized zygote, the early blastula is formed – a hollow ball made up of a layer of cells surrounding a central cavity. Gastrulation is the process by which cells of the blastula invaginate to form a long furrow called the primitive streak. During the course of invagination, cell-cell contact and intercellular communication induce cell differentiation, resulting in the formation of three germ cell layers; the outer layer becomes ectoderm, the lining of the primitive streak (the inner layer) becomes endoderm and the cells in between the ectoderm and endoderm become mesoderm. From these three layers, all of the tissues of the body are generated; ectoderm produces skin, nervous system, cornea and lens; endoderm produces digestive tract, lung epithelium, liver and many endocrine glands; mesoderm produces notochord, skeleton, muscles and circulatory system.

Neural tissue is specified from a region of the ectoderm layer and from this layer of cells the early central nervous system (CNS) develops in four principal stages:

1) Neurulation (specification of the neural plate within the ectoderm and formation of the neural tube)
2) Regionalisation (early patterning of the neural tube)
3) Neurogenesis (formation of differentiated neurons and glia)
4) Axon path-finding and synaptogenesis (generation of neural networks)

My thesis work focussed on elements of neurogenesis, with particular emphasis on the generation of neurons and glia from neuroepithelial precursor cells (NEPs) that express the basic helix-loop-helix (bHLH) transcription factor *olig2* (*oligodendrocyte lineage transcription factor 2*).

1.2 Neurulation

The neural plate is thought to derive from ectoderm that escapes signalling from bone morphogenic proteins (BMPs) and transforming growth factor-β (TGFβ). This is achieved by the release of specific antagonists to BMPs from early organising centres; the primitive node in mouse and chick, the blastopore in Xenopus and the embryonic shield in Zebrafish. The antagonists include follistatin, noggin, and chordin (Hemmati-Brivanlou et al., 1994;Lamb et al., 1993;Sasai and De Robertis, 1997). A role for BMP/TGFβ antagonism in neural induction is supported by the finding that absence of functional Bmp2b (a specific alternative splice isoform of Bmp2), in *bmpb2/swirl* Zebrafish mutants, results in the expansion of the neural plate at the expense of non-neural ectoderm (Nguyen et al., 1998). Antagonistic interactions between fibroblast growth factor (FGF), retinoic acid (RA) and Wnt (mammalian homologues of the *wingless/int* family) signalling are also thought to be involved in neural specification, particularly with respect to defining anterior/posterior fate (Altmann and Brivanlou, 2001;Molotkova et al., 2005;Sasai and De Robertis, 1997). Once the neural plate has been established, it begins to fold, forming the neural groove (Figure1.2). As the flanking ectoderm moves towards the midline, the neural groove, pivoted at the medial

hinge point cells which are anchored to the underlying notochord, subsequently closes at the dorsal aspect, thus creating the neural tube (Figure 1.2).

Figure 1.2 Neurulation. After the neural plate has been specified, it begins to invaginate. This is facilitated by the medial hinge point cells of the neural plate attaching and anchoring to the underlying notochord and changing shape, while the flanking non-neural ectoderm migrates inwards towards the midline. This causes the flanking neural plate to rise into the neural folds and the neural groove is established. The groove finally closes at the dorsal aspect, thus creating the neural tube. Non-neural ectoderm entirely covers the dorsal neural tube and becomes epidermis. The remnants of the neural folds break away and become neural crest cells (adapted from Scott F. Gilbert, Developmental Biology 7th edition).

Figure 1.3 Vesicle formation in the developing brain. After neural tube closure, the anterior neural tube balloons into 3 vesicles; the prosencephalon (forebrain), mesencephalon (midbrain) and rhombencephalon (hindbrain). These then subdivide further to generate 5 vesicles; the forebrain subdivides to form the telencephalon and diencephalon, the hindbrain subdivides to form the metencephalon and the myelencephalon and the midbrain remains as it is (the mesencephalon). The main structures of the brain derive from these 5 vesicles as labeled (adapted from images from the Department of Zoology, University of Guelph, Guelph, Ontario, Canada N1G 2W1).

1.3 Regionalisation of the neural tube

Following neural tube closure, the anterior neural tube expands and forms a series of vesicles which prefigure the forebrain (prosencephalon), midbrain (mesencephalon) and hindbrain (rhombencephalon). The forebrain further subdivides to form the telencephalon and diencephalon and the hindbrain subdivides into the metencephalon and myelencephalon. The midbrain undergoes no further subdivision (Figure 1.3). Thereafter, a dramatic period of cell division commences so the tube changes from being one cell thick to being multi-layered. This is a tightly controlled process that generates a sufficient pool of neuroepithelial precursor cells (NEPs) from which neural cells are

specified. Cell specification is, in turn, a tightly temporally and spatially regulated process involving many transcription factor interactions.

By the time of neural tube closure, adjacent mesodermal tissue along the anterior/posterior (A/P) and dorsal/ventral (D/V) axes secrete signalling molecules that engage early signalling processes for cell specification throughout the tube. The axial mesoderm forms the notochord which underlies the length of the CNS at its ventral-most aspect (excluding the anterior forebrain and prechordal plate) and secretes the morphogen sonic hedgehog (SHH), which is largely responsible for ventral cell type specification (Echelard et al., 1993). Simultaneously, BMPs are released from overlying non-neural dorsal ectoderm which assist in the dorsalisation of the spinal cord in the absence of secretion of antagonists at this stage (Chesnutt et al., 2004;Gross et al., 1996;Vallstedt et al., 2005). Thus, the neural tube is polarised along the D/V axis. With respect to A/P specification, surrounding paraxial mesoderm condenses into blocks to form laterally flanking somites which generate muscle and vertebrae. Somitic mesoderm is also thought to synthesise and secrete retinoic acid (Niederreither et al., 1997) which, in combination with FGF signalling, is important in the posteriorisation of the neural tube (Molotkova et al., 2005;Moreno and Kintner, 2004). Thus, early differentiation of spinal cord cell types is initiated by signals from surrounding mesodermal tissue. Regionalisation of the brain is more complex due to the invaginations and dynamic cell movements that occur. Nevertheless, the factors that have been identified as being involved in dorsal and ventral cell type specification in the brain are largely the same as those in the spinal cord; SHH is principally important in ventral specification and Wnts, in combination with FGF-8 signalling, in dorsal specification (Gunhaga et al., 2003).

Mechanisms of cell specification are more easily studied in the spinal cord since it is a relatively simple structure. SHH signalling is critical for D/V patterning of the CNS (Echelard et al., 1993;Hammerschmidt et al., 1997;Roelink et al., 1995) and this role is particularly well described in the spinal cord where it is initially released from the notochord and diffuses dorsally, thus establishing a ventral-to-dorsal morphogenetic

gradient of SHH signalling. Different genes are induced or repressed in cells according to the concentration of SHH that they are exposed to, which is largely determined by their distance from the ventral midline where SHH is secreted (Figure 1.4). Genes whose expression are affected by SHH signalling are classified as being Class I or Class II according to whether they are repressed or activated by SHH, respectively (Figure 1.4; Jacob and Briscoe., 2003). Class I genes include transcription factors such as *pax6*, *pax7*, *irx3* and *dbx1* which are expressed in dorsal domains and repressed ventrally. Class II genes include *nkx6.1*, *nkx2.2* and *olig2* and they are activated in ventral cells where SHH is present at its highest concentrations. SHH signalling thus initiates broad domains of transcription factor expression which are spatio-temporally integrated. Interactions between transcription factors at the boundaries of these broad domains subsequently establish a series of smaller, refined domains of transcription factor expression along the D/V axis of the spinal cord, largely via co-repression between the proteins that share a boundary (Figure 1.5). Similarly, BMPs released from dorsal epidermal ectoderm and roof plate cells form a concentration gradient opposite and antagonistic to that of SHH. Thus, BMP signalling both contributes to the dorsalisation of the spinal cord as well as refining SHH signalling in more intermediate and ventral domains (Chesnutt et al., 2004;Gross et al., 1996;Mekki-Dauriac et al., 2002;Vallstedt et al., 2005). In total, six dorsal domains (dP1-dP6) and five ventral domains (p0, p1, p2, pMN and p3 domains) are established according to their unique compliment of transcription factor expression and the different neuronal and glial subtypes that they consequently generate (Figures 1.4 and 1.5). The motor neuron progenitor (pMN) domain, for example, is found in the ventral half of the spinal cord, between p2 and p3 (Figures 1.4 and 1.5), and is defined by the exclusive expression of *olig2* and the exclusion of *irx3* and *nkx2.2*. The pMN domain generates motor neurons (MNs) and oligodendrocyte progenitor cells (OLPs) (Figure 1.5).

Figure 1.4 Domains of transcription factor expression in the spinal cord. Sonic Hedgehog (SHH) released from the underlying notochord at the ventral-most aspect of the spinal cord represses Class I genes (which are therefore expressed more dorsally) and activates Class II genes (which are therefore expressed more ventrally). Different homeodomain (HD) and basic helix-loop-helix (bHLH) proteins are therefore expressed at different positions relative to their distance from the notochord and SHH-secreting floorplate (FP). Domains of combinatorial transcription factor expression are thus established; p0-p3 and the motor neuron precursor (pMN) domain are the 5 ventral domains and dP1-dP6 are the 6 dorsal domains. Dorsal domain specification is also assisted by the release of BMPs from ectoderm overlying the dorsal-most aspect of the spinal cord. Co-repression between transcription factors facilitates the refining of these domains so distinct boundaries of homeodomain and basic helix-loop-helix protein expression are established (adapted from Kessaris et al., 2001). FP = floor plate, RP = roof plate.

Figure 1.5 Formation of discrete spinal cord domains defined by SHH-regulated transcription factor expression. The morphogenetic gradient of SHH released from the ventral notochord and floorplate cells establishes a series of broad domains of gene expression (A) according to the concentration of SHH the receptive cells are exposed to. Class I genes are repressed by SHH and Class II genes are activated. These broad domains of gene expression are refined by cross-regulatory interactions between them at expression boundaries (B). Nkx2.2 and Pax6 are two homeodomain (HD) proteins that are mutually exclusive, as are Nkx6.1 and Dbx2. Such co-repressive interactions generate distinct boundaries between refined domains of unique combinations of Class I and Class II gene expression (C). These domains subsequently give rise to unique neuronal cell types and glia. The basic helix-loop-helix (bHLH) transcription factor Olig2 is co-repressive with the HD protein Irx3 and these form the dorsal boundary of the motor neuron progenitor (pMN) domain from which motor neurons and oligodendrocyte progenitors are derived (Adapted from Jacob and Briscoe., 2003).

1.4 The Neuron/Glia Switch

Throughout the CNS, neurons are generated before glia, but it is not yet known how this timing is regulated. One school of thought is that NEPs within the ventricular zone (VZ) segregate early in development to become either neuron-restricted or glial-restricted precursors (NRPs or GRPs) which produce differentiating neurons or glia respectively at different times (Noble et al., 2004). Alternatively, neurons and glia (or NRPs and GRPs) may derive from a common precursor that generates neurons or NRPs first and then switches to produce glia or GRPs (Figure 1.6). These have been termed the 'segregating' and 'switching' models, respectively (Richardson et al., 2000). In favour of the segregating model, both NRPs and GRPs have been identified throughout the neuroepithelium at different developmental ages. Putative GRPs (including oligodendrocyte type-2 astrocyte precursors identified by Raff et al (Raff et al., 1983))

have been isolated from the full extent of the neuroectoderm by several groups. Most GRPs express the marker A2B5 and generate only glia and never neurons *in vitro* (even over weeks of expansion) and after transplantation *in vivo* (Gregori et al., 2002;Rao et al., 1998;Rao and Mayer-Proschel, 1997). PSA-NCAM-positive (poly-sialated neural cell adhesion molecule) NRPs have also been isolated which can give rise to multiple neuronal phenotypes, but no glia (Mayer-Proschel et al., 1997). The discovery of such lineage-restricted precursors in vertebrates has been predated by experimental analysis in Drosophila. An example of this is the early asymmetric division of precursors in the thoracic segment which generates separate neuron- and glial-restricted progenitors (kiyama-Oda et al., 1999). The discovery of NRPs and GRPs does not exclude the switching model as a possibility since one precursor cell could give rise to both NRPs and GRPs. However, the question remains regarding at what point are NRPs and GRPs lineally segregated.

In support of the 'switching' model, Temple and co-workers showed that not only can both neurons and glia derive from a single, multipotent cortical neuroepithelial precursor cell (NEP) *in vitro* (Davis and Temple, 1994), but that they do so sequentially – neurons first, followed by glia (Qian et al., 2000). This was demonstrated with the use of long term time-lapse microscopy and will be discussed in more detail later. Experiments by Park and Appel (Park and Appel, 2003) indicate that OLPs and Motor Neuron Precursors (MNPs) derive from a common *olig2+* precursor since alteration in the numbers of one class of precursor has a reciprocal effect on the other (e.g increasing numbers of MNPs sees a decrease in the number of OLPs). Notch signalling in the pMN domain supports the maintenance of proliferative NEPs in the ventricular zone (VZ), promoting the production of OLPs by preventing *olig2+* NEPs from differentiating into MNs. Deficiencies in Notch signalling result in the production of excess MNs at the expense of OLPs and vice versa in the presence of excess Notch signalling (Park and Appel, 2003). This indicates that a common progenitor pool in the pMN might support the generation of both MNs and OLPs and when generation of one cell type is encouraged, the other is consequently reduced. Alternatively, the numbers of MNPs and OLPs could depend upon feedback between the two precursor populations which is

disrupted when one or other precursor type is disrupted. Changes in the expression of the pro-neural bHLH factor *ngn2* also alters the relative proportions of MNPs and OLPs that are generated; precocious expression of *ngn2* promotes neuronal differentiation at the expense of dividing cells which may be OLPs in the pMN domain (Mizuguchi et al., 2001) while *ngn1/ngn2* double mutants generate no MNs, but OLP production is increased (Sugimori et al., 2007). MN specification is coincident with up-regulation of *ngn2* in concert with down-regulation of *olig2* (Lee et al., 2005). It is possible that MNs and OLPs derive from a common *olig2+* progenitor and that specific combinations of *olig2* with other cell-specific transcription factors in daughter cells might determine whether they become MNs or OLPs and changes in the expression of these transcription factors may therefore alter the proportions of MNs and OLPs produced.

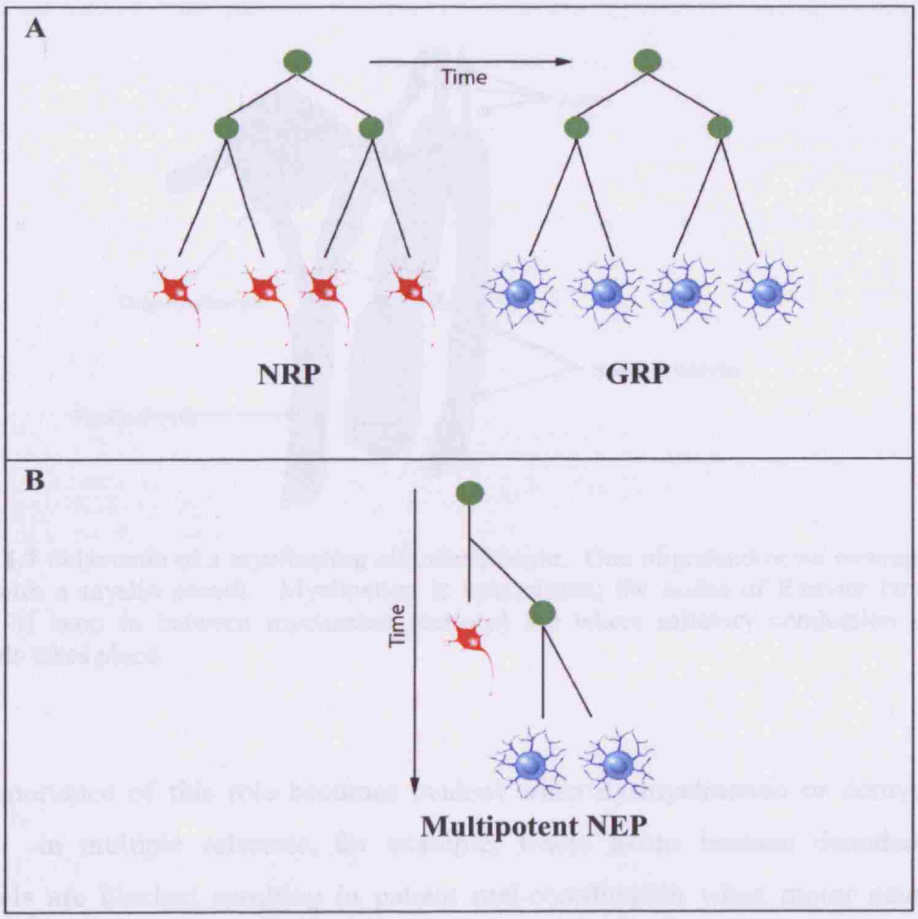

Figure 1.6 (above) Segregating (A) versus switching (B) models of neuronal and glial generation in the developing CNS. The two principal schools of thought regarding the temporal succession of neuronogenesis followed by gliogenesis are; the segregating model whereby neuroepithelial precursor cells (NEPs) segregate early in development to be committed to making only neurons (neuron-restricted precursors (NRPs)) or only glia (glial-restricted precursors (GRPs)) and that GRPs are activated at a later time than NRPs; and the switching model whereby neurons and glia derive from a common precursor that first produces neurons and then switches to make glia at a later time point.

1.5 The oligodendrocyte lineage

Oligodendrocytes are the myelinating cells of the CNS. They spirally enwrap the axons of CNS neurons with a fatty myelin membrane, thus enabling fast, saltatory conduction of action potentials. One oligodendrocyte usually myelinates several axons simultaneously (Figure 1.7).

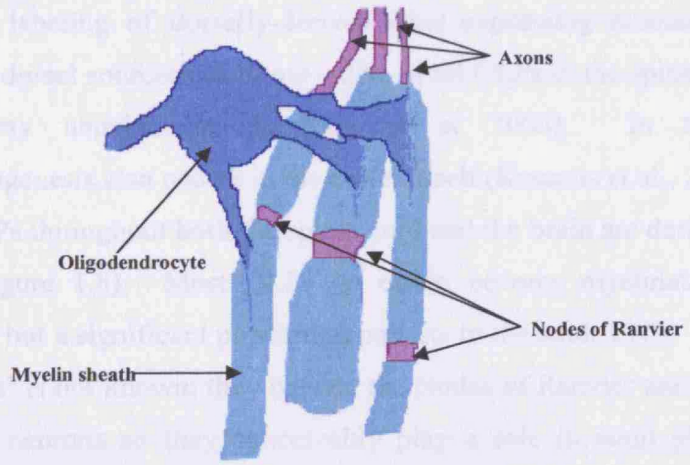

Figure 1.7 Schematic of a myelinating oligodendrocyte. One oligodendrocyte enwraps several axons with a myelin sheath. Myelination is intermittent; the nodes of Ranvier (small nude lengths of axon in between myelinated portions) are where saltatory conduction of action potentials takes place.

The importance of this role becomes evident when dysmyelination or demyelination occurs. In multiple sclerosis, for example, where axons become denuded, action potentials are blocked resulting in patient mal-coordination when motor neurons are affected, loss of sight when visual system neurons are affected and dementia when

cortical neurons are affected. A great deal of research has gone into the characterization of the oligodendrocyte lineage and the investigation of mechanisms involved in their development and differentiation in the hope that understanding their normal development will give us clues to how to stimulate regeneration of oligodendrocytes and myelin during demyelinating diseases.

In both the spinal cord and the brain, the first OLPs are found in ventral domains; in the pMN domain of the spinal cord (Pringle and Richardson, 1993) and the medial Ganglionic eminence (MGE) and the anterior entopeduncular area (AEP) of the ventral forebrain (Pringle and Richardson, 1993;Tekki-Kessaris et al., 2001;Zhou et al., 2000). OLPs from these domains migrate to populate the dorsal regions as well, but along with the ventral origins of OLPs in the CNS, there has more recently been identified some indigenous dorsal sources of OLPs which emerge at around E16.5 in the mouse. Transgenic labeling of dorsally-derived *dbx1*-expressing precursors has shown that OLPs from dorsal sources constitute ~20% of all OLPs in the spinal cord (Fogarty et al., 2005)(Fogarty unpublished, Kessaris et al 2006). In the perinatal brain, oligodendrogenesis also occurs in the cortex itself (Kessaris et al., 2006). Consequently, by E19 OLPs throughout both the spinal cord and the brain are derived from a variety of sources (Figure 1.8). Most OLPs go on to become myelinating oligodendrocytes postnatally, but a significant population persists in the adult CNS. The function of these 'adult OLPs' is not known; they contact the Nodes of Ranvier and also receive synaptic input from neurons so they conceivably play a role in adult physiology as well as providing a potential new source of oligodendrocytes.

Figure 1.8 Schematic representation of 'waves' of oligodendrogenesis in the spinal cord (A) and brain (B). In the spinal cord, the first (and principal) source of OLPs is from *olig2*+ precursors in the pMN domain. These first appear around E12 and migrate to disperse throughout the cord. From around E16 onwards, a second source of OLPs is generated from *dbx*+ precursors in dorsal domains of the cord. These, along with other dorsal sources of OLPs finally constitute about 10-15% of all OLPs in the spinal cord. In the brain, the first wave of oligodendrogenesis originates from the anterior entopeduncular area (AEP) and medial ganglionic eminence (MGE) from E11.5, followed by a second wave from the lateral and caudal ganglionic eminences (LGE and CGE) at around E15, finally a third wave is generated within the cortex itself postnatally. Each wave of oligodendrogenesis can be sourced to precursor cells expressing different transcription factors, unique to their domains of origin, as shown (Adapted from Fogarty et al., 2005 and Kessaris et al., 2006).

1.6 OLPs to Oligodendrocytes

Early OLPs are proliferative and highly migratory cells. They can be identified by the expression of *platelet-derived growth factor receptor α (pdgfrα)* (Hall et al., 1996), *SRY-box-containing gene 10 (sox10)* (Stolt et al., 2002) and *olig2* (Lu et al., 2000;Zhou et al., 2000). Once they reach their destination they undergo a limited proliferation and start to differentiate into pro-myelinating oligodendrocytes (Pro-OLs) characterised by expression of O4 and downregulation of PDGFRα. Pro-OLs have a highly processed morphology and although they are still proliferative (less so than OLPs), they are no longer migratory and form small, localised groups of cells (Bansal and Pfeiffer, 1997). The final stages of differentiation involve withdrawal from the cell cycle and extension of processes to enwrap axons and generate myelin sheaths. These terminally differentiated myelinating oligodendrocytes express structural components of myelin such as myelin basic protein (MBP), proteolipid protein (PLP), myelin oligodendrocyte protein (MOG), galactocerebroside (GC) etc (Bansal and Pfeiffer, 1997).

There are evident morphological changes from OLPs to mature oligodendrocytes along with their different proliferative and migratory activities and immunogenic profiles. The transition from one phase to the next could conceivably be mediated by FGF-2 since expression of different FGF receptor (FGFR) isoforms also changes at different stages of the oligodendrocyte lineage (Bansal et al., 1996). The different stages of the oligodendrocyte lineage can be defined by the expression profile of FGFRs and by their responses to FGF-2 (Figure 1.9). FGFR1 is expressed in early progenitors with increasing levels of expression as the cells progress to mature oligodendrocytes. FGF-2 signalling through FGFR1 promotes proliferation and migration which are typical features of early OLPs. FGFR3 has low levels of expression up until a peak at the Pro-OL stage; signalling through FGFR3 promotes proliferation and is thought to be involved in the arrest of differentiation in late progenitors in response to FGF-2. FGFR2 is expressed only in mature oligodendrocytes and is thought to be involved in signaling terminal differentiation (Fortin et al., 2005). How the timely expression of these different receptors is controlled and regulated is unknown, but FGF-2 signalling has been shown to regulate the expression of some FGFR isoforms so may itself be involved

in regulating the responses of cells of the oligodendrocyte lineage. How OLPs are first specified is not yet fully known, but, along with SHH signalling, FGF-2 could also be involved.

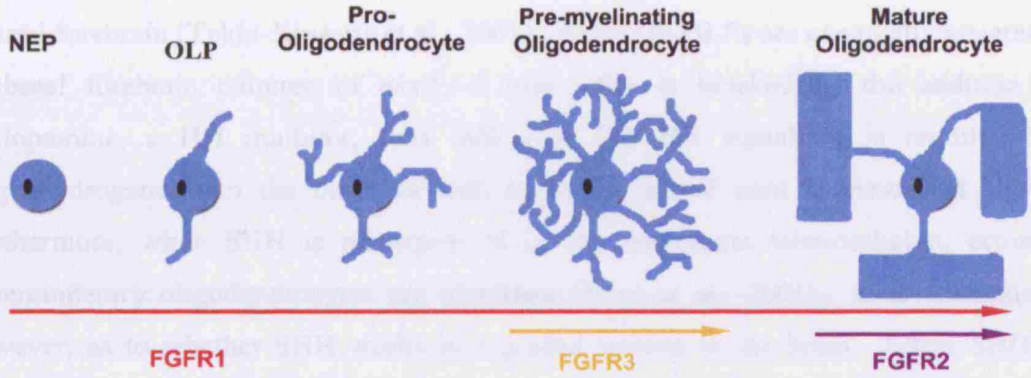

Figure 1.9 Stages of the oligodendrocyte lineage and corresponding profiles of FGFR isoform expression. Oligodendrocyte precursors (OLPs) are derived from neuroepithelial cells (NEPs) and express FGFR1, which increases in levels as the lineage progresses with peaking levels at the pre-myelinating and mature oligodendrocyte stage. FGFR3 has a brief period of expression at the pre-myelinating stage and is thought to assist transition to the mature, differentiated oligodendrocyte via FGF-2 signal transduction. FGFR2 is only expressed in mature, myelinating oligodendrocytes.

1.7 Control of oligodendrogenesis

The principle factor involved in pMN domain oligodendrogenesis is SHH (as outlined above) via signaling at a particular range of concentrations (Orentas et al., 1999;Pringle et al., 1996;Roelink et al., 1995). Ectopic expression of SHH in the dorsal part of the spinal cord results in ectopic generation of MNs and OLPs (Pringle et al., 1996), while, in *shh-/-* mutants, oligodendrocytes and motor neurons are absent (Lu et al., 2000). SHH signaling is required over an extended period for OLPs to be generated (Orentas et al., 1999), transient exposure not being sufficient. There may be some functional redundancy between SHH and other members of the hedgehog (HH) family however, since *shh-/-* mutants have a less severe phenotype than *smo-/-* mutants in which all HH signalling (i.e. from Sonic, Desert and Indian Hedgehogs) is prevented (Wijgerde et al., 2002).

Oligodendrogenesis and the involvement of SHH in the brain are less well defined than in the spinal cord, but similar principles apply. Zones of SHH expression coincide with oligodendrogenic domains and OLP production in the forebrain is delayed or abolished in *nkx2.1-/-* mutant mice in which there is no (or very reduced) SHH expression in the ventral forebrain (Tekki-Kessaris et al., 2001). Although OLPs are eventually generated in basal forebrain cultures of *nkx2.1-/-* mice, this is blocked by the addition of cyclopamine, a HH inhibitor, thus indicating that HH signalling is required for oligodendrogenesis in the brain as well as in the spinal cord as described above. Furthermore, when SHH is misexpressed in the embryonic telencephalon, ectopic, supernumerary oligodendrocytes are identified (Nery et al., 2001). It is contentious however, as to whether SHH works in a graded fashion in the brain. When SHH is applied to telencephalic explants at an early stage (E9 or earlier in rat), ventral medial ganglionic eminence (MGE)-like features are identified (Kohtz et al., 1998). However, when SHH is added to slightly older explants (E10-E11.5 in rat), a lateral ganglionic eminence (LGE)-like phenotype is generated, which is a more dorsal feature of the telencephalon, regardless of the level of SHH that is applied (Kohtz et al., 1998). Thus, responsiveness to SHH signalling is demonstrated to change over time.

1.8 SHH-independent OLP specification

Dorsal NEPs presumably do not receive the same level of SHH signalling as those in the ventral CNS (if they are exposed to SHH at all), suggesting that a SHH-independent mechanism of OLP specification might exist. This has been supported by the finding that NEPs from *shh-/-* null mice can still generate OLPs *in vitro* (Chandran et al., 2003) although this could be attributed to signalling by other HH proteins as described above. Chandran et al demonstrated that FGF-2 induces oligodendrocytes from MEPs derived from the dorsal spinal cord, in the absence of SHH signalling. They therefore proposed that FGF-2 could be a candidate molecule for SHH-independent oligodendrogenesis (Chandran et al., 2003). Dorsal cortical NEPs from E13.5 mouse embryos have also been induced to generate OLPs *in vitro* in the presence of FGF-2 (Kessaris et al., 2004;Qian et al., 1997). Both Chandran et al (Chandran et al., 2003) and Kessaris et al

(Kessaris et al., 2004) showed that FGF-2 still was able to induce OLPs in the presence of cyclopamine, which blocks all HH signaling, indicating that it acted independently of SHH. Kessaris et al also showed that SHH-mediated induction of OLPs *in vitro* was abolished in the presence of the FGFR inhibitor PD173074, indicating that FGF-2 signalling is necessary for SHH-induced oligodendrogenesis, possibly by activating the MAP kinase pathway (Kessaris et al., 2004). More recent experiments have demonstrated that FGF-2 is capable of inducing OLPs in the brain *in vivo* (Naruse et al., 2006).

1.9 Olig2 and the oligodendrocyte lineage

Olig2 expression defines OLP and MN precursors in the pMN domain and is a marker and transcription factor throughout the oligodendrocyte lineage. It was identified along with *olig1* and *olig3* by three independent research groups; Zhou et al 2000 (Zhou et al., 2000), Lu et al 2000 (Lu et al., 2000) and Takebayashi et al (Takebayashi et al., 2000). Zhou et al identified the *olig* genes while screening for previously uncharacterised bHLH factors that may function as mediators of glial cell fate in the central nervous system (CNS). bHLH transcription factors were already well known to be key regulators of many cell types in various tissues across a variety of organisms (Garrell and Campuzano, 1991), but in the CNS were implicated in neuronal rather than glial specification (Lee et al., 1995;Ma et al., 1994). However, given that there were many bHLH transcription factors at the time that still remained uncharacterised it was postulated that some of these may be involved in glial fate determination.

Concurrent with the discovery of *olig1 and olig2* by Zhou et al, Lu et al cloned rat *olig1* and *olig2* after identifying them as genes up-regulated in E14.5 rat neuroepithelial cell cultures upon induction of OLPs by FGF (Lee et al., 1995;Lu et al., 2000). They further showed, by *in situ* hybridisation analysis, that the pattern of *olig2* expression has a profile matching that of oligodendrogenic zones in the early embryo. *Olig2* was also found to be expressed at E13.5 in the retina and in the olfactory epithelium by E11.5 where no OLPs develop, suggesting that it may also be involved in developing sensory organs. In the spinal cord, *olig2* is not only common to motor neuron progenitors and

OLPs, but is also *required* for their generation since *olig2-/-* knock-outs have no OLPs or MNs in the spinal cord (Lu et al., 2000). Co-expression of *olig2* with other transcription factors is thought to promote the generation of different cell types. For example, co-expression of *ngn2* with *olig2* is thought to promote MN differentiation in the pMN domain (Mizuguchi et al., 2001), although *olig2* is then rapidly down-regulated in post-mitotic MNs (Lee et al., 2005). *Ngn1* and *ngn2* are down-regulated in the pMN domain after the period of motor neuron production. In the chick spinal cord there is then a dorsal expansion of *nkx2.2* expression from the p3 domain into the pMN domain in (Fu et al., 2002) and the consequent overlap of *olig2* and *nkx2.2* expression has been proposed to assist the onset of oligodendrogenesis (Zhou et al., 2001). This story is complicated, however, because in the mouse spinal cord, expression domains of *olig2* and *nkx2.2* remain separate (restricted to pMN and p3 domains respectively) at the onset of oligodendrogenesis. Dorsal expansion of *nkx2.2* expression into the pMN domain occurs about two days after OLPs begin to migrate from the pMN domain (Fu et al., 2002), indicating that *nkx2.2* is not necessary for the onset of oligodendrogenesis in the mouse. The idea that *nkx2.2* expression alone is not sufficient to induce OLPs (Zhou et al., 2001) is supported by the finding that mutations in the *nkx2.2* gene cause a reduction in MBP and PLP expression, but not in earlier OLP markers (Qi et al., 2001). However, *olig2* may co-operate with *nkx2.2* for the specification and differentiation of oligodendrocytes *in vivo* since ectopic co-expression of these two transcription factors can result in ectopic oligodendrocyte differentiation in the embryonic chicken spinal cord (Zhou et al., 2001). Furthermore, all differentiating oligodendrocytes in the white matter co-express *olig2* and *nkx2.2* in both mouse and chick (Fu et al., 2002). In the brain things are even more complex. Despite a huge reduction in OLPs in the embryonic brains of *olig2-/-* mutants, there is still generation of OLPs in small regions of the forebrain and normal numbers of OLPs are seen in the midbrain (Zhou and Anderson, 2002). All *olig2-/-* OLPs express *olig1* however, suggesting a level of redundancy between these transcription factors in the brain. Co-expression of *nkx2.2* and *olig2* seems to be important in the specification of OLPs in the brain since Vallstedt et al (Vallstedt et al., 2005) showed that *olig1/2+* cells in the anterior hindbrain appear to be derived from *nkx2.2+* progenitors. *Nkx2.2* is expressed early in a ventral domain

of the anterior hindbrain and its dorsal boundary is maintained by Nkx6-mediated repression. In *nkx6-/-* mutants, the region of *nkx2.2* expression expands dorsally and ectopic oligodendrocyte differentiation occurs in register with this (Richardson et al., 2006;Vallstedt et al., 2005).

In both the brain and spinal cord, *olig2* clearly has an important, instructive role in OLP specification. Induction of *olig2* expression *in vivo* is largely dependent on SHH signaling, although SHH-independent mechanisms are now also being suggested; FGF-2 being a prime candidate. In culture, the addition of a sonic agonist to preparations of primary neocortical NEPs results in the up-regulation of the *olig2* within 24 hours of treatment (Kessaris et al., 2004). In the absence of SHH, FGF-2 induces *olig2,* and OLPs are derived thereafter (Chandran et al., 2003;Kessaris et al., 2004). The mechanisms of signaling of these two molecules will be described further.

1.10 SHH signalling

Sonic Hedgehog is a 45 kDa protein that undergoes auto-catalytic cleavage to yield a 20 kDa N-terminal domain and a 25 kDa C-terminal domain. The N-terminal domain is thought to carry all of the signalling properties of SHH and it is modified by the addition of a cholesterol and a palmitate moiety which converts it to a soluble form that can be released extracellularly. It is this soluble form of the N-terminal SHH fragment that is freely diffusible and is able to form the concentration gradient in the spinal cord. Diffusion gradients are one means of regulating the potency of SHH signalling; alternatively, SHH can act at different potencies if recipient cells alter the density of its receptor, Patched 1 (Ptc1) at their surface. In line with this idea, there has been found to be a ventral to dorsal gradient of *ptc1* mRNA in cells of the spinal cord (Pearse et al., 2001). This may have been established via the initial gradient of diffusing SHH since it has been demonstrated that SHH signalling can increase *ptc1* expression (Marigo and Tabin, 1996). The intracellular context of a cell also determines how it interprets the concentration of SHH signalling it receives. The main transcriptional regulators of SHH target genes are a group of zinc finger transcription factors; *cubis interruptis* in

Drosophila (Methot and Basler, 1999), and the *gli* family in vertebrates (Jacob and Briscoe, 2003).

Ci was first identified in Drosophila and has both a transcriptional activator (CiA) and a repressor (CiR) isoform, the repressor isoform being generated by cleavage of CiA (za-Blanc et al., 1997). Ptc1 activity regulates the activity of the seven-pass transmembrane protein Smoothened (Smo). In turn, Smo regulates proteolytic cleavage of the bi-functional Ci or Gli proteins. In the mouse, there are three Gli isoforms; Gli1-3, which are characterised by five tandem C2-H2 zinc finger motifs (for a review see (Gunhaga et al., 2003;Jacob and Briscoe, 2003). Although they have cleavage sites and are therefore potentially bi-functional like Ci, only the repressor isoform of Gli3 (Gli3R) has been identified *in vivo*. The regulation of Gli3R generation is mediated via control of Smo activity as for Ci modification in Drosophila. In the absence of Ptc1-mediated suppression, Smo inhibits the cleavage of the full-length activator isoforms of Ci or Gli3 into their repressor isoforms. Since SHH signalling inhibits Ptc1-mediated suppression of Smo it therefore indirectly maintains the activator isoforms of Ci or Gli3 by preventing their cleavage. However, in the absence of SHH signalling, Ptc1 inhibits Smo activity and thus the repressor isoforms of Ci and Gli3 are generated and move to the nucleus (Figure 1.10). Gli1 and 2 have only been identified in their activator forms and are expressed in ventral domains of the CNS (Bai et al., 2002;Hui et al., 1994). Gli1 does not have a pivotal role in SHH signal transduction, however, since *gli1 -/-* mutants are phenotypically normal (Park et al., 2000). Gli2, on the other hand, is principally involved in transducing the ventralising activity of SHH and *gli2-/-* mutants have severe phenotypes (Park et al., 2000). Conversely, Gli3 has a prominent role as a transcriptional repressor and is expressed in more intermediate and dorsal domains of the spinal cord. Gli3 repressor (Gli3R) activity is important in the specification of intermediate cell types in intermediate domains and the inhibition of ventral cell types in dorsal domains (Litingtung and Chiang, 2000). The relative distribution of Gli proteins across the D/V axis of the CNS could feasibly contribute to the differential D/V effects of SHH. The targets of SHH signalling include homeodomain transcription factors, characterised by a specific 60 amino acid helix turn helix motif. As a consequence,

SHH signalling has the capacity to trigger a cascade of transcriptional regulation which results in combinations of genes being expressed in specific regions as described above.

Figure 1.10 Sonic Hedgehog (SHH)-regulated processing of Drosophila Cubis Interruptus (Ci) and vertebrate Gli proteins. Smoothened (Smo) normally inhibits the processing of the full-length activator isoforms of Ci and Gli (CiA and GliA) into the repressor isoforms (CiR and GliR). In the absence of SHH activity, Patched 1 (Ptc1) represses Smo-mediated inhibition of CiR and GliR formation and thus the repressor isoforms are generated. However, upon SHH-binding to Ptc1, Smo keeps Ci and Gli as the activator isoform (Adapted from Motoyama, 2006).

1.11 FGFs in CNS development

Members of the fibroblast growth factor (FGF) family are involved at many stages in CNS development (Goldfarb, 1996). They are first involved in the specification of neural tissue with FGF-8, FGF-2, FGF-4 and FGF-3 being present in the anterior neural streak (ANS), a prominent signalling centre before and during gastrulation (Riese et al., 1995;Storey et al., 1998;Streit et al., 2000). In combination with other factors, different FGFs are involved in proliferation and differentiation of various cell types within the developing CNS. Of particular interest here are the roles and mechanisms of FGF-2 signalling.

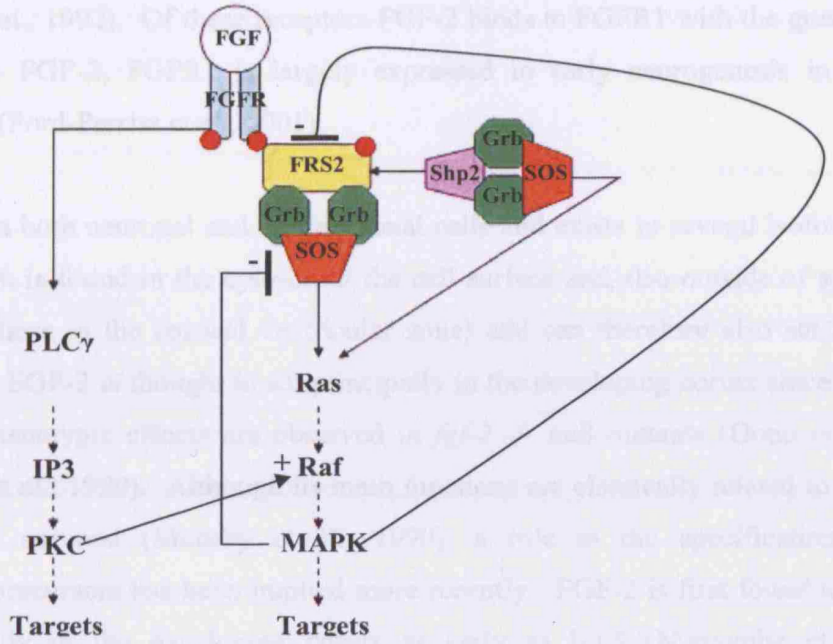

Figure 1.11 FGF signaling pathways. FGFRs dimerise upon ligand-binding and consequently cross-phosphorylate at intracellular tyrosine residues (red circles indicate phosphate groups). The phosphorylated receptors recruit and phosphorylate docking proteins such as fibroblast growth factor receptor substrate 2 (FRS2), which subsequently recruit other proteins to generate a large complex. Via SOS activation, the MAPK pathway can be activated through Ras and Raf activation, ultimately culminating in transcriptional activation of target genes in the nucleus. Phospholipase C (PLC) can be directly activated by phosphorylated FGFRs which activate target genes via protein kinase C (PKC) activation and activation of the MAPK pathway through Raf. MAPK activation, in turn, inhibits FRS2 and SOS activity and thus creates negative feedback loops. These are just some of the pathways accessed by FGFR activation.

FGFRs are tyrosine kinase receptors (TKRs) which are activated upon ligand-induced dimerisation, which promotes auto-phosphorylation of intracellular tyrosine residues as a result. This instigates the recruitment of docking proteins such as FRS2 (fibroblast growth factor receptor substrate 2) which, in turn, are also phosphorylated and recruit intracellular signalling components. Few FGF-induced signalling cascades are activated directly by the phosphorylated FGF receptor and thus most FGF-induced signalling is transduced by docking complexes (Figure 1.11). A series of negative feedback loops, mainly via MAP-Kinase activation, are also in play, meaning FGFR-mediated signalling is a complex series of interactions (Schlessinger, 2004). In the CNS, four FGFR

isoforms are known to be expressed (FGFR-1-4), each of which has multiple splice variants (Miki et al., 1992). Of these receptors FGF-2 binds to FGFR1 with the greatest affinity and, like FGF-2, FGFR1 is largely expressed in early neurogenesis in the developing brain (Ford-Perriss et al., 2001).

FGF-2 is found in both neuronal and non-neuronal cells and exists in several isoforms. The 18kD isoform is found in the cytosol, at the cell surface and also outside of some cells (including those in the cortical ventricular zone) and can therefore also act as a diffusible signal. FGF-2 is thought to act principally in the developing cortex since this is where most phenotypic effects are observed in *fgf-2 -/-* null mutants (Dono et al., 1998;Vaccarino et al., 1999). Although its main functions are classically related to cell proliferation and survival (Murphy et al., 1990), a role in the specification of oligodendrocyte precursors has been implied more recently. FGF-2 is first found to be expressed ventrally in the developing cortex as early as E9.5 (Nurcombe et al., 1993;Raballo et al., 2000) with an increase in expression identified from E14-18; around the time of gliogenesis (Giordano et al., 1992;Powell et al., 1991;Weise et al., 1993). Moreover, early studies showed that low concentrations of FGF-2 induce E10 stem cells to produce mainly neurons but that increased levels of FGF-2 generate more and more glia (Reimers et al., 2001), raising the possibility that FGF-2 could be involved in oligodendrogenesis *in vivo*.

1.12 Time-lapse microscopy as a tool for lineage-tracing studies

Time-lapse microscopy has been employed over the last decade to observe the activities of single progenitor cells *in vitro*. Observing cell division and behaviour in real time enables lineage trees to be traced retrospectively since the cell types generated can be identified by immunocytochemical analysis and their lineal relationships can be determined by tracing the divisions that occurred. Cell behaviour is regulated by both cell-intrinsic and environmental factors. The contributions of such factors to the generation of cell lineages can be assessed using time-lapse microscopy. Individual cell behaviour can be recorded and compared when cultured in different conditions, via the addition of different signalling molecules. It is possible to observe directly, for example,

whether the cell types derived from a single progenitor are altered in different culture environments. In this way, cell-intrinsic tendencies can be separated, to a certain extent, from the effects of extrinsic signalling events.

Using time-lapse microscopy Qian et al (Qian et al., 2000) addressed the timing of the emergence of neurons and glia from embryonic cortical NEPs in the presence of 10 ng/ml FGF-2 as a mitogen. Recording NEPs from E10.5 mice, an age at which neurogenesis is still on-going, they showed that, as *in vivo*, neurons were generated first, followed by glia over 10 days *in vitro*. They observed repeated patterns of cell division whereby neurons were generated largely via asymmetric divisions while glia were generated by symmetric divisions. They also showed that lower concentrations of FGF-2 generated more neurons in multipotent clones while higher concentrations of FGF-2 reduced the number of neurons and increased the number of differentiated glia over time (Qian et al., 1997). Thus, they showed that while the NEPs maintained the pattern of generation of neurons being followed by glia in different concentrations of FGF-2, the relative proportions of neurons:glia in mixed clones could be altered. They also showed that the number of neurons generated in mixed clones decreased when NEPs from older embryonic cortices were used further indicating that there is a change in cortical NEPs over time with respect to the proportion of neurons and glia that were generated in mixed clones derived from them *in vitro* in the presence of FGF-2 (Qian et al., 2000). My thesis work revisits these time-lapse studies.

The first aim was to investigate further into the observation by Kessaris et al (Kessaris et al., 2004) that an increase in concentration of FGF-2 in cultures of E13.5 NEPs causes an increase in the number of OLPs that are generated over 3 days. This increase in numbers of OLPs could occur via a number of mechanisms; increased proportion of NEPs in the starting culture that give rise to OLPs, increased proliferation of OLPs that are generated, preferential survival of OLPs within a mixed population, or a combination of any of these mechanisms. Using time-lapse to monitor cell divisions in real time and using immunolabelling to identify daughter cells that were generated in a lineage,

lineage trees could be drawn retrospectively and cell division times and cell survival could be monitored to answer this question.

A second aim was to monitor the dynamics of *olig2* expression in lineages derived from embryonic cortical NEPs. In particular, the aim was to determine whether there were any differences in *olig2* expression patterns in response to different concentrations of FGF-2 in order to drill down further into how higher concentrations of FGF-2 might induce more OLPs to be generated. This was enabled through use of a transgenic mouse line[n.1] that was generated to express the reporter molecule enhanced green fluorescent protein (EGFP) under the same transcriptional regulatory control as endogenous *olig2*. Use of this transgenic line for these time-lapse experiments meant that *olig2*-expressing cells could be visualised directly *in vitro* by the visualisation of EGFP fluorescence. Thus, the patterns of *olig2* expression within emerging clones could be characterised. Since *olig2* is the earliest known marker of the oligodendrocyte lineage, the dynamics of *olig2* expression within a lineage, captured by time-lapse, could indicate the points at which OLPs might be specified. Since not all *olig2*+ cells give rise to OLPs, however, immunolabelling at the end of experiments was also necessary in order to identify the cell types that were generated from both *olig2*+ and *olig2*- precursor cells.

A third aim was to investigate the responses to FGF-2 of NEPs derived from younger embryonic cortices than E13.5. Qian et al (Qian et al., 2000) observed that younger NEPs produce clones with more neurons and fewer OLPs even over 7 days and in 10 ng/ml FGF-2. However, they did not investigate the response to higher concentrations of FGF-2 than 10 ng/ml. Thus, the question addressed by my thesis experiments was whether younger (E10.5, E11.5, E12.5) cortical NEPs were intrinsically less responsive to the induction of OLPs by increasing concentrations of FGF-2 than E13.5 NEPs. It is possible that some NEPs in the younger populations are more refractory to FGF-2 signalling than others and therefore that an increase in FGF-2 concentration could ultimately induce OLP generation comparable to that in E13.5 cultures. Alternatively, younger NEPs may be intrinsically unresponsive to FGF-2-induced OLP generation at any concentration of FGF-2. This was examined using time-lapse microscopy.

It is important to note that my thesis experiments investigate the dynamics of cell division and differentiation in an *in vitro* setting and over a limited time frame and therefore cannot be strictly extrapolated to report on the behaviour of these cells *in vivo*. These time-lapse experiments give data on the potential of the cultured cortical NEPs to respond to different concentrations of FGF-2 in these specified culture conditions. Whether the cell fate potentials observed *in vitro* are recapitulated in the live animal would need to be answered with *in vivo* models.

Note. 1: The Olig2:EGFP transgenic mouse line was originally constructed in order to perform *in vitro* analysis of PMN domain cells from E9.5 spinal cords to observe the generation of OLPs and Motor Neurons (MNs) using time-lapse. This was with the aim of determining whether both cell types were always generated from a single *olig2+* precursor or whether there are also segregated populations of *olig2+* precursors that are dedicated to generating either MNs or OLPs, and at what stage in embryonic development might such specification of OLP-dedicated and MN-dedicated precursors occur. However, the culture system proved to be unsustainable. Such early spinal cord cells were unable to be kept alive as clonal cultures or dense cultures and explants were unable to be observed in focus in the time-lapse set-up.

Chapter 2

Materials and Methods

Unless otherwise stated, all chemicals and reagents where purchased from VWR Chemicals limited and were of AnalaR grade wherever possible.

Restriction enzymes and molecular biology reagents were purchased from New England Biolabs.

Radio-nucleotides were purchased from Amersham International.

Specialized bacterial media components were obtained from Difco laboratories Ltd, Detroit, Michigan, USA.

Most of the molecular techniques described here are taken from Sambrook *et al* (1989)

Unless otherwise stated all culture media, foetal bovine serum (FBS), sheep serum and supplements were purchased from Invitrogen Life Technologies Ltd.

General chemicals and reagents were obtained from Sigma Aldrich Co Ltd apart from Laminin which was purchased from GIBCO BRL Life Technologies and Trypsin from Roche Molecular Biochemicals.

Falcon sterile plastic-ware was from Beckton Dickenson

13mm diameter glass cover-slips were a Chance Propper Ltd product

Human recombinant FGF2 was purchased from ImmunoKontact

The small molecule agonist of Hedgehog signaling (Cur-0188168 or SHH-Ag1.2) (Frank-Kamenetsky et al., 2002) was provided by Curis Inc. Unless otherwise stated, the working concentrations of reagents were as follows: FGF2, 10 ng/ml (~0.6 nM); SHHAg1.2, 100nM.

2.1 Bacteriology

For general cloning and sub-cloning of recombinant plasmids *Escherichia coli* (*E.coli*) XL1-Blue was used. For Phage artificial chromosome (PAC) cloning and sub-cloning *E.Coli* strain EL250 was used. This is a modified DH10B strain (Gibco) containing defective lambda prophage (Yu et al., 2000) and arabinose *flpe* gene (Lee et al., 2001a).

2.1.1 Growth Media and agar plates

Bacteria were grown in Luria Bertani broth (LB broth; containing 10g Tryptone, 5g NaCl, 5g bacto-yeast extract (SIGMA) per litre), or on LB agar plates (LB broth + 30g/L bacto-agar). Solutions were sterilized by autoclaving at 15lb/square inch for 20 minutes and were stored at 4°C. When appropriate Ampicillin (AMP, final concentration 100μg/ml for plasmid transformed bacteria and 20μg/ml for Phage artificial chromosome (PAC) transformed bacteria.), Kanamycin (15μg/ml for plasmid transformed and 12.5μg/ml for PAC) or Chloramphenicol (30μg/ml for plasmid and 15μg/ml for PAC transformed) was added to LB broth or LB agar. Antibiotics were added to LB broth or LB agar after the temperature had cooled below 55°C. Agar was poured into 10cm Petri dishes (Falcon) and allowed to set at room temperature. Plates were stored at 4°C and were air dried for 1 hour before use. All XL1-Blue cultures were grown at 37°C and *E.Coli* EL250 cultures were grown at 32°C. Liquid cultures were continuously agitated in a rotating environment shaker at 250rpm

2.1.2 Long term storage of transformed bacteria

Glycerol stocks of bacteria were made by adding glycerol to a final concentration of 15% (v/v) to exponentially growing cultures and storing at -80°C. These were subsequently thawed and used to inoculate LB broth (plus antibiotic where appropriate) or streaked onto LB agar plates (plus antibiotic where appropriate) to derive single bacterial colonies.

2.1.3 Preparation of Competent bacterial cells

Transformation of bacteria was done by electroporation of the specified DNA into electrocompetent bacteria; *E.Coli* strain XL-1 Blue or EL250. Electrocompetent cells were prepared using the following method (Dower et al., 1988);

To prepare electrocompetent XL-1 blue *E.Coli* for electroporation, 10ml of Super Optimal broth with Catabolite repression (SOC) medium (20% bacto-tryptone (w/v), 5% bacto-yeast extract (w/v), 0.5% NaCl (w/v) 2.5mM KCL 20mM glucose, adjusted to pH 7.0 with 5N NaOH) was inoculated with 5μl of relevant bacterial suspension from glycerol stocks and grown at 37°C in a shaking incubator overnight at 250rpm. 4ml of this overnight culture was used to inoculate 400ml of SOC medium and grown at 37°C. Samples were removed and the optical density at 600nm (OD_{600}) measured periodically until it reached at least 0.5 indicating that the bacteria were reaching the peak of their exponential growth cycle (3-4 hours in culture). 16 x 50ml centrifuge tubes were pre-cooled on ice and the culture decanted into these and allowed to cool for 15 minutes. Bacteria were pelleted by centrifugation at 1500 x G for 15 minutes at 4°C in a pre-chilled rotator. All the following steps were done in a cold room at 4°C. The supernatant was discarded and the pellets gently re-suspended in 25ml of pre-chilled ultra-clean (autoclaved) Milli-Q® water. The contents of the 16 tubes were then pooled into 8 tubes which were centrifuged again at 1500 x G for 15 minutes at 4°C. The supernatant was discarded again and the pellets were washed a second time by adding 25ml of cold ultra-clean water to each tube and again gently re-suspending the pellets. The contents of these 8 tubes were then pooled into 4 tubes which were again centrifuged at 1500 x G for 15 minutes at 4°C. The supernatants were discarded and 10ml of cold Milli-Q® water containing 10% glycerol (w/v) was added to each tube and all suspensions were pooled. 42μl aliquots of bacterial suspension were placed into 1.5ml pre-cooled cryo-tubes which were then snap-frozen in liquid nitrogen before transferring to -80°C for storage. The same protocol was used to prepare EL250 bacteria except that the cultures were grown at 32°C and not 37°C.

2.1.4 Electroporation of competent bacterial cells

Electrocompetent bacteria were transformed with either 2μl of a ligation reaction, or with a ligation reaction product that had been ethanol precipitated and re-suspended in 5μl of water. The bacteria were thawed on ice and 40μl mixed with the DNA to be electroporated. This was added to a pre-cooled (on ice) 0.2cm electroporation cuvette (Bio-rad). Electroporation was carried out at 2.5kV (25μFD) capacitance and 200Ω resistance in a Bio-Rad Micropulsar.

Transformed bacteria had 500μl of warm SOC medium added (without antibiotics) and were incubated at 37°C before plating onto LB agar plates containing the appropriate antibiotic. Whenever it was possible blue-white selection was used to screen for recombinant plasmids. This was done when transforming XL1-blue bacteria with a plasmid that provides α-complementation (pBluescript© II) to the host bacteria's expression of the β component of the *lacZ* operon. Modified plasmids have the α-component interrupted since the multi-cloning site interrupts the sequence. For blue-white colony screens X-gal and IPTG were added to the LB plates (20μl of 50mg/ml X-gal in DMF (w/v) and 100μl of 0.1M IPTG per plate) to act as substrates for any complete *LacZ* gene product. Transformed bacteria were thus white if ligation into the transforming plasmid had been successful but blue where ligation had been unsuccessful.

Slight modifications to this protocol were made for electroporation of EL250 *E.coli* with PAC DNA. The addition of PAC DNA to the electrocompetent bacteria and all subsequent steps was carried out using wide-bore pipette tips to avoid shearing of the DNA. Electroporation was at 1.8kV and subsequent recovery time in warm SOC medium extended to 2 hours, all incubations with EL250 bacteria were at 32°C not 37°C, as this lower temperature prevents activation of endogenous *flpe* activity.

2.2 Nucleic Acids

2.2.1 Phenol and Chloroform extractions

Plasmid DNA samples to be extracted were made with TRIS-EDTA (TE) buffer (5mM Tris, pH 75, 0.5mM EDTA pH 8.0). An equal volume of TRIS pH 7.9-saturated phenol-chloroform was added and the mixture was briefly vortexed and then centrifuged at 10,000 x G for 10 minutes at 20°C. The upper aqueous phase was removed and re-extracted with an equal volume of chloroform (containing 4% (v/v) Iso Amyl Alcohol, IAA), centrifuged as before and the upper aqueous phase collected. For phenol-chloroform extraction of PAC DNA some amendments to the protocol were necessary. All mixing was done by inversion with no vortexing and the phenol-chloroform extraction step was repeated twice before re-extraction with chloroform:IAA. The DNA was then ethanol precipitated as described in 2.2.2.

2.2.2 Ethanol Precipitation of DNA

Sodium Acetate (pH 5.3) was added to all plasmid or genomic DNA extractions to a final concentration of 0.3M before precipitating the DNA by adding 2 x the volume of 95% (v/v) Ethanol (ETOH, stored at -20°C). Samples were incubated on ice for at least 15 minutes before centrifuging at 10,000 x G for 10 minutes. The supernatant was discarded and the DNA pellet washed in 70% ETOH and centrifuged again before removing the supernatant. The DNA pellets were air dried before re-suspending in an appropriate buffer. For ethanol precipitation of PAC DNA no sodium acetate was added.

2.2.3 Small scale plasmid preparation

To isolate 1-2μg quantities of DNA, XL1-blue *E-coli* bacteria were first transformed with the specified plasmid (see above for details of transformation). The transformed bacteria preparation was then streaked onto LB agar plates containing the appropriate selection antibiotic and incubated overnight at 37°C. 2ml of LB broth containing antibiotic was inoculated with a single colony of bacteria isolated from the agar plates. The inoculated LB broth was incubated with shaking at 250 rpm overnight (16 hours) at 37°C. The overnight culture was transferred to an eppendorf tube and spun at

10,000 x G for 1 minute. The supernatant was discarded and the pellet resuspended by vortexing in 100μl of Solution I (50mM glucose, 25mM Tris-HCl, pH 8.0 and 10mM EDTA pH 8.0). 200μl of Solution II (1% w/v SDS and 0.2N Sodium Hydroxide, made fresh each time) was added to each tube and the solutions were mixed by inversion. 150μl of Solution III (3M sodium acetate, 11.5% w/v glacial acetic acid) was added and the lysate mixed by inversion before centrifuging at 1600 x G for 10 minutes. The supernatant was transferred to fresh eppendorff tubes and twice the volume of cold (-20°C) 99.7% (v/v) ethanol was added to each tube and mixed by inversion to precipitate the DNA. The DNA suspension was then centrifuged for 10 minutes at 1600 x G at 4°C. The supernatant was discarded and the pellet was washed in 200μl of 70% ethanol (room temperature) and re-spun for 1 minute at 1600 x G. The supernatant was removed completely and the pellet was air dried and then dissolved in 40μl TE buffer.

2.2.4 Large scale plasmid preparation

To prepare $\geq$1mg of plasmid DNA, 50ml of terrific broth (TB, 12g/L bacto-tryptone, 24g/L bacto-yeast extract, 4ml/L glycerol, 0.017M KH_2PO_4, 0.072M K_2HPO_4) with appropriate antibiotic was inoculated with 200μl of an overnight culture or with a single colony taken from an agar plate. This was incubated overnight, shaking, at 37°C.

The overnight culture was spun at 2000 x G at 4°C for 10 minutes. The supernatant was discarded and the pellet re-suspended in 4ml of Solution I by vortexing and then incubated on ice for 5 minutes. 8ml of fresh Solution II was added and mixed by inversion and incubated for a further 5 minutes at room temperature. 6ml of Solution III was then added and they were again mixed by inversion followed by a 5 minute incubation on ice. The solutions were next centrifuged at 2000 x G at 4°C for 15 minutes and the supernatants were filtered through sterile muslin. 17ml of isopropanol were added per 50ml of filtrate and mixed by inversion before a further cycle of centrifugation at 2000 x G at 4°C for 15 minutes. The DNA was pelleted by discarding the supernatant and air drying the pellet before being resuspending in 2ml TE buffer and 2.5ml of 4.4M LiCl. This was incubated on ice for 1 hour and then

centrifuged at 2000 x G at 4°C for 15 minutes. The supernatants were transferred to fresh falcon tubes and 9ml of 99.7% (v/v) ethanol was added to each and incubated at room temperature for 10-15 minutes to precipitate the DNA. They were then centrifuged at 2000 x G at 4°C for 15 minutes, the supernatants removed and the DNA pellets washed with 70% ethanol. The 70% ethanol was removed completely and the pellets were air dried before resuspending in 400μl of TE. This DNA suspension was transferred to fresh eppendorf tubes with 5μl of 4mg/ml DNase-free RNase A and incubated at 37°C for 15 minutes. 10μl of 20% Sodium Dodecyl Sulphate (SDS) was then added and incubated at 70°C for up to 10 minutes before phenol-chloroform extraction and final DNA precipitation as previously described. The supernatants were discarded and the pellets air dried before being resuspended in 200μl of TE buffer.

2.2.5 Large scale PAC preparation

Extra care must be taken in preparing PAC DNA since its large size makes it susceptible to shearing. Thus, all mixing was done by inversion with no vortexing and wide bore pipettes were used for all pipetting or transfer of the DNA that was done.

400 ml of LB media with antibiotic was inoculated with 500μl from a starter culture (EL250 bacteria transformed with PAC DNA grown at 32°C overnight). This was incubated at 32°C shaking at 250rpm overnight. After incubation the culture was split equally into 8 falcon tubes and centrifuged at 2000 x G at 4°C for 10 minutes. The supernatant was discarded and each pellet resuspended in 8ml of PAC Solution I (PI) (50mM Tris-HCl, pH 8.0, 10mM EDTA, pH 8.0, 100μg/ml RNase A) by pipetting with a 10 ml pipette. 8ml of fresh PAC Solution 2 (PII) (0.2N sodium hydroxide, 1% SDS) were then added to each tube and this was mixed by inversion. The tubes were incubated at room temperature for 5 minutes before adding 8ml of solution PAC Solution 3 (PIII) (3.0M sodium acetate, 11.5% w/v glacial acetic acid) which was mixed by inversion until all the PII turned white. The suspensions were then incubated on ice for 1 hour before centrifuging at 2000 x G at 4°C for 15 minutes. The supernatant was transferred to fresh falcon tubes by passing through a double layer of sterile muslin and the filtrate was centrifuged at 2000 x G at 4°C for 15 minutes. The supernatant was again

transferred to fresh falcon tubes and an equal volume of ice-cold isopropanol was added to each and mixed by inversion before incubating at room temperature for 5 minutes to precipitate the DNA before centrifuging again as before. The supernatants were removed completely and the pellets were air dried before resuspending in 0.25ml of TE buffer. The resuspended DNA was pooled and then split into 4 eppendorf tubes. The DNA suspensions were centrifuged at 16000 x G for 5 minutes to remove any debris and the clear supernatants were transferred to 4 fresh eppendorf tubes ready for phenol/chloroform DNA extraction followed by ethanol precipitation as previously described. The supernatants were discarded and the pellets air dried at room temperature until the edges began to look translucent at which point they were resuspended in 100μl of Ultrapure Milli-Q® water without trituration (the DNA should dissolve completely at room temperature within 10 minutes with occasional gentle agitation). Once resuspended, the DNA suspensions were pooled for further use.

2.2.6 Extraction of genomic DNA from mouse biopsy

Mouse genomic DNA was extracted either from small tail biopsies (~3mm lengths taken from postnatal mice) or from embryonic tissue. Samples were incubated in 500μl of extraction buffer (100mM Tris-HCl, pH 8.5, 5 mM EDTA pH 8.0, 200mM NaCl, 0.2% SDS) with 0.48mg/ml of Proteinase K at 55°C overnight. 200μl of 6M ammonium acetate was added to each sample and mixed by vortexing before incubating on ice for at least 10 minutes. After centrifuging at 16000 x G at 4°C for 10 minutes the supernatant was transferred to a fresh eppendorf, 500μl of room temperature isopropanol was added and mixed by briefly vortexing before centrifuging again at 16000 x G at room temperature for 3 minutes. The supernatants were removed and 500μl of room temperature 70% ethanol was added and vortexed briefly before centrifuging for a further 3 minutes at 16000 x G. The supernatants were then completely removed and the pellets left to air dry before resuspending in 100μl of TE.

2.3 Analysis of DNA

2.3.1 Restriction enzyme digests

All restriction enzymes were obtained from New England Biolabs (NEB) and reactions were carried out using the appropriate buffer supplied with each enzyme. When more than one restriction enzyme was used simultaneously, a buffer was selected that enabled optimal activity for both enzymes even if 100% efficiency was not possible for any one of them. The buffer selection was based on efficiency ratings found in the NEB catalogue. For analytical protocols, 50ng of plasmid DNA was digested in a 10-20μl total reaction volume at 37°C for 1 hour. For cloning purposes approximately 1μg of DNA was used to enable recovery of sufficient DNA to be used in subsequent steps of the cloning paradigm.

2.3.2 Agarose gel electrophoresis

Agarose gel electrophoresis was carried out as described in Sambrook et al (1989). Nucleic acid samples were electrophoresed through set gels made up from AnalaR grade agarose melted in Tris Actetate buffer (TAE) (0.04M Tris, 0.001M EDTA, 0.35% glacial acetic acid) using a microwave. A Horizon 11.14 horizontal gel tank (Gibco BRL) was used and was powered by a BioRad Power Pac 300. The voltage applied for electrophoresis varied according to the size of the DNA samples (genomic DNA samples were run at 100V, smaller plasmid DNA was run at 150V). Ethidium bromide was added to the gels to a final concentration of 0.5μg/ml to enable visualisation of the DNA fragments under a UV transilluminator. For gels running plasmid DNA samples, ethidium bromide was added before the gels were set. For gels running genomic DNA the ethidium bromide was added by soaking the gels in a dilute solution for 15 minutes after electrophoresis was complete. This prevents intercalation into the DNA distorting the running track of the samples. For the separation of DNA fragments of sizes 0.1-10 Kb, 1% (w/v) agarose gels were used and 0.8% (w/v) gels were used for separation of larger genomic DNA samples. As a standard size marker, 5μl of a 0.1-10 Kb marker ladder (HyperLadder I Bioline) was run alongside the samples to enable the identification of sample fragments of specified sizes. DNA samples to be run

contained 10% (v/v) loading buffer (10 X stock, 50% (v/v) glycerol, 1mM EDTA, pH 8.0, 0.25% (v/v) bromophenol blue).

2.3.3 Pulse field gel electrophoresis

Pulse field gel electrophoresis (PFGE) was conducted in a BioRad contour-clamped homogeneous electric field elecrophoresis cell powered by a CHEF DR II control module and CHEF DR II drive module (BioRad). This was used for the separation of DNA fragments greater than 10Kb in size. 1% (w/v) agarose gels were made up in 0.5 x Tris-Borate EDTA (TBE) buffer (45mM Tris Borate, 1mM EDTA, pH 8.0) without ethidium bromide. As a standard size marker a 2mm plug of Pulse Marker^{TM} (Sigma, 0.1-200Kb) was placed in one of the wells. The samples of PAC DNA were loaded with 10% loading buffer (as described in 2.3.2) and were run overnight at 4°C in 2 litres of 4°C, 0.5 x TBE being continuously circulated over the gel by a peristaltic pump. The programme of PFGE used was such that the gel was exposed to 6V/cm potential difference with an initial switch time of 2.1 seconds and a final switch time of 10 seconds and this was run over 12 hours. After the gels were run, they were stained with ethidium bromide for visualisation with a UV transilluminator.

2.3.4 Quantitation of double stranded DNA

5μl of a 1/10 dilution (in water) of the sample DNA was run on a 1% agarose gel with ethidium bromide (as described above) alongside 5μl of a standard size marker, Hyperladder I (Bioline). When visualised, the levels of fluorescence of bands of different sizes indicated the concentration of the DNA fragment when compared to the fluorescence of the Hyperladder bands of the same size. This gives sample DNA concentrations to within 10ng DNA/μl which is sufficient for our purposes.

2.3.5 Ligation of fragments

Ligations were performed in 10μl reaction volumes at 16°C overnight. The fragments to be ligated were appropriately digested with restriction enzymes to generate complimentary overhanging ends. The digested fragments were quantified as described and volumes for use were calculated on the basis that 50ng of vector should be used and

the insert fragment should be present in a molar ration of 3:1 (insert : vector). The quantities of insert fragment to be used were thus calculated using the following equation: X = ((50/V) x I) x 3 where X is the quantity of insert fragment required in ng, V is the length of the vector in base pairs and I is the length of the insert fragment in base pairs. The reaction mix included volumes of vector and insert fragment DNA preparations, according to the above calculation, along with 1μl 10 x T4 DNA ligase buffer, 1μl T4 DNA ligase (NEB), 0.5μl 10nM ATP and made up to 10μl with Ultrapure Mill-Q® water.

2.3.6 Blunt Ended ligation reactions

Blunting of overhanging ends on DNA fragments after restriction enzyme digest was done by mixing the DNA with 2μl of 10 x buffer #1 (NEB), 1μl mixed dNTPs (NEB) and 1 unit of the Klenow fragment of DNA Polymerase I from *E. coli* (NEB) per microgram of DNA in 20μl of water. This reaction mixture was incubated at room temperature for 15 minutes before inactivating the Klenow by incubation at 70°C for 20 minutes. These fragments may then be ligated as described above.

2.3.7 Polymerase Chain Reaction

Polymerase Chain Reaction (PCR) was used to; identify orientations of inserts in plasmid and PAC vectors, amplify fragments of DNA from plasmids for cloning, amplify DNA fragments from constructed DNA cassettes to provide samples for DNA sequencing in order to check sequence fidelity and to genotype animals using extracts of genomic DNA as a template. Each PCR reaction contained; 2.5μl of 10x $MgCl_2$-free PCR buffer (promega), 2.0μl of 25mM Magnesium Chloride (Promega), 0.25μl of mixed dNTPs (20mM each of dATP, dGTP, dCTP, dTTP, Amersham Biosciences), 0.1μl forward primer (100μM from MWG), 0.1μl reverse primer (100μM from MWG), 0.25μl Taq Polymerase (5μg/μl, Promega).

The total reaction volume was made up to 23μl with ultra pure Baxter water and then 2μl template DNA preparation was added such that the total reaction volume was 25μl. The reaction tubes were immediately sealed and placed in an MWG-Biotech -Primus 96 PCR

machine and the required PCR programme was run. The basic programme for the PCR was as follows;

Initial denaturing at 94°C for 4 minutes
Denature again at 94°C for 30 seconds
Anneal at 53°C for 45 seconds
Extension of the DNA at 72°C for 1.5 minutes

This denature-anneal-extend cycle was repeated 37 times and then the reactions were held at 72°C for 10 minutes before dropping to 4°C for completion of reaction and storage.

For hi-fidelity amplification PCR reactions a different reaction mix and PCR programme was used. Each reaction contained 5μl of 10x buffer including 25mM $MgCl_2$, 0.5μl 20mM dntps, 0.15μl of each primer and 0.75μl of HiFi Taq Polmerase (Roche) with 1μl template DNA and made up to a total volume of 50μl with Baxter water. The PCR programme was also modified to have a reannealing temperature of 65°C for 4 cycles followed by a step-down from 64-61°C over 4 more cycles with a final reannealing temperature of 60°C for 35 cycles before final extension at 72°C for 10 minutes as before.

Amplification fragment	Forward primer (5'–3')	Reverse primer (5'-3')	Product size
Olig2 NLS:EGFP	GCC ACA ACG TCT ATA TCA TGG CC	TCC TGG GAG TCT CCT ACC CCG CC	600bp
3' homology region	ATA AGC GGC CGC GCC GGC CAG CGG GGG TGC GTC CT	GCC CTT AAT TAA CCC TGG GCC AGG GAT GAA CCT GC	500bp
5' homology region	TTG GCG CGC CGT CCT CAT TTA TTC CAG GCC GG	AGT CCA TGG TCC CAG GGA TGA TCT AAG CTC TCG	500bp
NLS:EGFP	CCA TGG CAC CCA AGA AGA AGA GGA AGG TGG TGA GCA AGG GCG AGG AGC T	ACT AGT TTA CTT GTA CAG CTC GTC CAT GCC	800bp

Table 2.1 Primer sequences for amplification of vector and plasmid fragments.

2.3.8 Preparation of radiolabelled probes

cDNA probes were labelled with ^{32}P by random priming (Feinberg and Vogelstein, 1984). 25ng of the purified probe DNA was diluted to a final volume of 45μl of Ultrapure Milli-Q® water and denatured at 95°C for 5 minutes before rapidly cooling on ice for 2 minutes. It was briefly spun and then added to a reaction tube from the RediprimeTM II kit (Amersham Pharmacia Biotech) containing DNA Polymerase enzyme, random primers, dATP, dTTP and dGTP. 5μl of radioactive [^{32}P] dCTP was added and the reaction mix was incubated in a shielded container at 37°C for 1 hour to allow incorporation of radiolabelled dCTP. The radiolabelled probe was separated from unincorporated dNTPs by spin column chromatography (Micro Bio-Spin® P-30 Tris chromatography columns, BioRad laboratories). The purified radiolabelled probe was then denatured by heating again for 5 minutes at 95°C and then cooling on ice for 2 minutes.

2.3.9 Southern blotting

DNA fragment samples to be analysed were first separated in agarose gels in 1 x TAE as described above in the absence of ethidium bromide to prevent distortion of the running track of the DNA. The samples and a standard marker lane were run at a voltage appropriate to the size of the DNA in the samples. After electrophoresis, the gel was stained with ethidium bromide and visualised. The gel was photographed alongside a ruler such that the positions of different sized DNA fragments could be nominated a measurable position on the gel. The gel was then depurinated by soaking in 0.25M HCl for 30 minutes at room temperature with constant agitation and then washed in distilled water twice before treatment with denaturing solution (0.4M sodium hydroxide, 1.5M sodium Chloride) for 30 minutes at room temperature with agitation. After a further two rinses with distilled water, the gel was treated with neutralising solution (1.0M Tris, 1.5M sodium Chloride, 0.5 M EDTA, pH 8.0, adjusted to pH 7.5 with hydrochloric acid) for 30 minutes, room temperature with agitation before being washed again as above. The gel was then rinsed in 10 x Sodium Chloride Citrate (SCC) (1.5M NaCl, 0.15M sodium citrate) in preparation for capillary transfer onto a Hybond XL nucleic acid transfer membrane (Amersham Biosciences). The gel was placed in direct contact with a nylon membrane optimised for nucleic acid transfer (Hybond^{TM}-XL, Amersham Pharmacia Biotech UK Limited). The gel with the membrane layered on top of it was placed onto a layer of blotting paper soaked in 10 x SCC. A series of absorbent tissues was placed on top and gentle pressure applied overnight. Following transfer the DNA was cross-linked onto the membrane via UV irradiation (254nm, 0.15J/cm2) in a Stragene UV stratalinker. The cross-linked DNA could then be incubated with a specified radiolabelled probe for detection of required sequences. The membrane was pre-wetted with 2 x SCC (0.3M NaCl, 0.03M sodium citrate) in a hybridisation bottle with the side with the transferred DNA facing the inside of the bottle. It was then prehybridised with Salmon Sperm DNA (10mg/ml stock Helena Biosciences). The salmon sperm DNA was denatured by heating for 5minutes at 95°C and then quickly chilled on ice for a minimum of 2 minutes. It was then added to 10ml MIB (0.225M NaCl, 15mM NaH_2PO_4, 1.5mM EDTA, 10% PEG 8000, 7% SDS) to a final concentration of 100μg/ml. The 2 x SCC was removed and the 10ml of MIB with

salmon sperm DNA was added. The membrane was prehybridised at 65°C for one hour with constant rotation of the cylinder to ensure constant wetting in buffer. The denatured probe (prepared as described above) was then added and the bottle was re-sealed and rotated overnight at 65°C. After overnight hybridisation with the labelled probe the membrane was washed with Wash I solution (2 x SCC, 0.1% SDS) at 65°C for 15 minutes with constant agitation. It was then washed in Wash II solution (0.1 x SCC, 0.1% SDS) at 65°C with agitation for 5 minutes or until radioactivity levels dropped to a reasonable and consistent level. The membrane was then transferred to 3mm filter paper and blot-dried briefly before wrapping in Saran Wrap and attaching to a fluorescent labelled pre-exposed HYperfilm MP (Amersham) which acts as a marker to orient the membrane in a sealed light cassette. The membrane was then sealed in a cassette with an intensifying screen and an unexposed HYperfilm. This was incubated at -80°C for a variable amount of time depending on the expected levels of radioactivity. Plasmid DNA contains high proportions of the DNA sequences to be identified and so retains a large amount of probe and thus requires only short exposure times of a few hours before the film is developed. However, when screening genomic DNA, the fragments of interest are in low abundance and thus hybridise very little probe making the signal is week and such blots may have to be left for up to two weeks before exposure is sufficient to develop the film.

2.3.10 DNA sequencing

DNA was sequenced "in house" using the WIBR Scientific Support Services. DNA was prepared and isolated from a small scale preparation as described above. It was washed once with 99.7% (v/v) ethanol, then twice with 70% ethanol and diluted in Ultrapure Milli-Q® water to a final concentration of at least 100fmols and 6μl was required per reaction. Before sequencing the DNA solution it was treated with RNase A (1 in 100 dilution) for 15 minutes at 37°C. The prepared DNA was sequenced using Beckman Coulter DTCS quick start kits (Cat No 608120) along with the appropriate primer. All sequencing was carried out on a Beckman Coulter CEQ 8000 Genetic Analysis System. Primer sequences specific to promoter regions of the plasmids used were as follows (from 5' to 3');

M13 Reverse, GGA AAC AGC TAT GAC CAT G

M13-20, GTA AAA CGA CGG CCA GT

T3,AAT TAA CCC TCA CTA AAG GG; T7, GTA ATA CGA CTC ACT ATA GGG C

Sp6, ATT TAG GTG ACA CTA TAG

2.4 Preparation of DNA constructs

2.4.1 Isolation of DNA for cloning

After separation of DNA by agarose gel electrophoresis the required band was excised from the gel with a clean scalpel. The DNA was extracted from the agarose by placing the excised gel band into a length of dialysis tubing filled with 1x TAE and sealing each end with clips. This was placed at the negative terminal end of a gel electrophoresis tank filled with 1x TAE and subjected to electrophoresis at 120V for 30 minutes. The DNA shifts from the gel into the surrounding 1x TAE within the dialysis tubing and the gel fragment was removed and the 1x TAE containing the DNA was harvested. The DNA was then extracted by one phenol/chloroform extraction followed by one chloroform extraction as previously described. The DNA was then ethanol precipitated as described. The supernatants were removed and the pellets were air dried before being resuspended in either TE or MilliQ® water. The DNA was then quantified in order to calculate the volumes that should be used in future protocols.

2.4.2 TOPO© cloning of PCR-amplified DNA fragments

PCR fragments could be reliably and efficiently inserted into a plasmid vector using the TOPO© cloning kit (Invitrogen Cat no. K4600-01). The kit includes vector DNA with specified modified insert ends (pCR©II-TOPO©) and a topoisomerase enzyme that specifically binds to these ends such that they unravel to accept and covalently bind to any PCR amplified product that is added. All PCR products have an overhanging deoxyadenosine (A) at the 3'end by nature of the activity of Taq Polymerase. The linearised TOPO© vector has single overhanging deoxythymidine (T) residues and is thus complementary to all PCR products. The Topoisomerase I that is included in the kit is covalently bound to the vector making these overhanging ends 'active' for

annealing to and joining with any added PCR product. There are also specific promoter and restriction enzyme site sequences either side of the insert site such that the insert may be rapidly and reliably cloned by amplification and excision thereafter according to the TOPO© instruction manual.

2.5 PAC recombination

2.5.1 Induction of homologous recombination in EL250 *E.coli*

Homologous recombination was carried out based on the protocol described by Lee et.al (Lee et al 2001) EL250 bacteria were first transformed with PAC vector DNA and the transformed bacteria were grown, shaking at 250 rpm, overnight in 5ml LB broth with 12.5μg Kanamycin at 32°C. The overnight culture was then used to inoculate 50ml of fresh LB without kanamycin and grown shaking at 32°C until the OD_{600} reached 0.4-0.8. Homologous recombination between the PAC vector and the linear insert was then induced in a sample of the culture by transferring 10ml of the culture to a 42°C water bath for 15 minutes to activate the arabinose *flpe* enzyme. The remainder of the culture was kept shaking at 32°C as a control. The 42°C-incubated culture was then rapidly cooled by gently agitating on ice for 5 minutes. 10ml of the 32°C uninduced culture was also rapidly cooled as a negative control. Both culture samples were then centrifuged at 2000 x G for 8 minutes at 4°C. The supernatants were discarded and the pellets resuspended in 1ml of ice cold autoclaved, Milli-Q® water. Each suspension was transferred to a 1.5ml eppendorff tube and spun at 16000 x G for 20 seconds. The supernatants were again removed and the pellets washed a second time by resuspending in ice cold ultra pure water before centrifuging as above once more. This washing process was repeated three times and after the final centrifugation, the pellets were finally resuspended in 100μl of sterile water. This yielded 2 cell populations, both containing the PAC vector DNA and one with the bacterial recombination enzymes having been activated. Both preparations were then electroporated with 100-300ng of the linearised targeting construct prepared as above and the transformed bacteria were immediately transferred to 500μl warm LB broth and they were incubated then at 32°C for 90 minutes during which time the homologous recombination should take place in

the bacteria that had been induced. Each preparation was then plated onto a selection of LB agar plates containing either; 15μg/ml chloramphenicol to select for recombined PAC DNA, or kanamycin (12.5μg/ml) as a positive control. These were incubated at 32°C overnight or over 2 nights if necessary (the DNA load can slow down bacterial growth in these preparations). Colonies growing on the chloramphenicol plates indicated successful recombination events in these cells and these are the colonies picked and selected for expansion by inoculating overnight cultures to make large scale PAC DNA preparations ready for Southern blot analysis to be performed to check analytically for the expected recombination event.

2.5.2 Removing the chloramphenicol cassette

It was necessary to remove the Chloramphenicol cassette from the successfully transformed bacteria before *in ovo* injection. This is done by employing the *flpe* enzyme activity in the EL250 bacteria since the Chloramphenicol cassette is flanked by *frt* sites. 15ml of fresh LB broth was inoculated with 300μl overnight culture of the recombinant bacteria. The bacteria were grown, shaking at 37°C until the OD_{600} reached 0.5-0.8 at which point sterile arabinose was added to a final concentration of 2% (v/v). The cultures were then incubated for 1 hour at 32°C and 1ml was then taken to inoculate 10ml of fresh LB broth which was then incubated for a further 2 hours at 32°C. This preparation was then plated on LB agar plates containing both Ampicillin and Chloramphenicol. The ampicillin selects for recombinant bacteria and the Chloramphenicol excludes bacteria that have had the gene successfully excised and is an indicator of the efficiency of excision. The removal of Chloramphenicol can be confirmed by Southern blot analysis of large scale preparations of selected clones. Small scale DNA preparations were made from selected colonies as described. Recombination events were detected by pulse field gel electrophoresis of a restriction enzyme digest of the prepared DNA and analysis by southern blot. Comparisons of recombined DNA before and after Chloramphenicol removal should show a difference of about 1.3kb in size since this is the size of the Chloramphenicol cassette.

2.6 Making the transgenic mice

2.6.1 Linearization of recombined PAC

Transgenesis was achieved by *in ovo* injection of the linearised recombined PAC DNA that includes the transgene. The recombined PAC DNA had first to be amplified by making a large scale DNA preparation as described. The PAC DNA was harvested and 85μl was digested overnight by PvuI restriction enzyme digest. The fragments were separated overnight by Pulse Field Gel Electrophoresis as described with the majority of the digest being run in the central lane with small sample lanes run either side as markers to estimate any drift in the separation across the gel. After the gel was run, the marker lanes were cut out and imaged with ethidium bromide such that the position of the PAC fragments could be identified without contaminating the main sample which is to be used for *in ovo* injection. The band containing the remnant Vector and that of the linearised transgene with up and downstream genomic sequences were identified. Both fragments were excised from the central lane of the gel using the marker lanes as guidance for their positions within the gel.

The two excised bands were then arranged in a mini gel tray as shown in Figure 2.1 A and covered with low melting point (LMP) agarose to be run at 50V for 9hrs at 4°C such that the linearised PAC DNA moves completely from the PFGE band into the LMP agarose (Figure 2.1 B). After the gel has run, the portion with the vector band was cut out and stained with EB to visualise how far the DNA had moved into the LMP gel (Figure 2.1 C). This was used to estimate how much of the LMP gel to excise in order to isolate the insert PAC DNA. This portion (approx 6mm) was cut out with a clean scalpel (Figure 2.1 C) and equilibrated with TENPA buffer (1M Tris-HCl pH7.5 , 0.5M EDTA pH 8.0, 5M NaCl) with 30μM spermine and 70μM spermidine by continuous inversion for 1.5 hrs after which the equilibrated block of gel was transferred to an eppendorf. It was melted by incubation at 68°C for 3 minutes in a water bath. It was then briefly spun in a microfuge followed by further 5 minutes incubation at 68°C in the water bath before being transferred to 42°C for a further 5 minutes. Keeping the bottom of the tube in the water bath to maintain the gel in a molten state, β-agarase was added at

2 units per 100μl of molten agarose. This was mixed into the agarose by gentle pipetting up to 20 times with a wide bore pipette. The agarose was left to digest at 42°C for 3 hours before returning to room temperature upon which the digest should remain as liquid if digestion with the β-agarase has been complete.

Figure 2.1 Vector and insert DNA bands excised from the pulse field gel and arranged in the 4% LMP mini gel (A). Shaded blocks indicate the location of the DNA. The vector and insert DNA move from the pulse field gel bands into the LMP 4% gel during electrophoresis (B). Note the DNA condenses into a smaller band in the 4% gel immediately adjacent to the excised PFGE blocks. Insert DNA is excised (pale block) and the block of vector DNA is visualised to determine where the insert block is located relative to the PFGE bands (C). From M. Grist

The PAC DNA in solution was then pipetted directly in equal volumes (~50μl) using wide bore pipette tips onto three dialysis membranes (Millipore, pore size 0.5μm) which were laid floating upon microinjection buffer (1M Tris-HCL pH7.5, 0.5M EDTA pH 8.0, 5M NaCL filter sterilised) in a 35mm petri dish containing 30μM spermine and 70μM spermidine. The DNA solution was left to thus dialyse for 1hour at room temperature in a flow hood. After dialysis the DNA solution was retrieved with wide bore pipettes and stored at 4°C until required for *in ovo* injection.

Preceding *in ovo* injection, the prepared, dialysed PAC DNA must be quantified in order to estimate the dilution at which it should be injected. This was determined by running 1μl and 10μl overnight by PFGE alongside a standardised PAC DNA preparation. It was then microfuged and diluted accordingly with microinjection buffer before *in ovo* microinjection.

2.6.2 In ovo injection and transplantation

Female (B6 x CBA) F1 mice of 3-4 weeks of age were induced to superovluate by timed injection of follicle stimulating hormone (Folligon, Intervet) at 5pm on nominated day 1 followed by injection with human gonadotrophin (hCG, Chorulon, Intervet) 45 hours later. At 5pm the evening of the injection of hCG when the induction of superovulation is complete, the females were mated with (B6 x CBA) F1 males and the fertilised eggs were harvested the following morning for microinjection of the linear PAC DNA construct. On average, by mating 4-6 superovulated females 100-200 fertilised ova may be obtained.

These ova are incubated in MI6 medium before and after microinjection and may be stored as such over night at 37°C awaiting transfer into the receptive oviducts of pseudopregnant females which were prepared 24 hours in advance by mating females selected for their natural oestrus with vasectomised males. Microinjection was performed by U. Dennehey and P. Ianarelli (Richardson Lab, WIBR). This involved the injection of the linear PAC DNA construct suspension in microinjection buffer (prepared as described above) into the pronuclei of the fertilised ova using a pulled micropipette and visualised under Leica microscope. Following injection of the PAC DNA the ova were left in MI6 medium at 37°C until they reached the 1 or 2-cell stage. Surviving 1 or 2-cell stage embryos were then transferred into the oviducts of the pseudopregnant females (6-24 weeks old) under hypnorm/hypnovel anaesthetic. The litters born from these recipient females were then analysed for the presence of the PAC transgene indicating its successful integration into the genome following the microinjection. Successful (B6 x CBA) F1 transgenic males were mated with CD1 females for timed mating.

2.7 Analysis of mice and screening for transgenes

2.7.1 PCR genotyping

The PCR programme designed to amplify fragments of the transgene was applied to genomic DNA extractions obtained from tissue biopsies from putative transgenic litters. The primers designed to amplify genomic DNA fragments indicative of the inclusion of the NLS:EGFP transgene are in Table 2.1.

2.7.2 Southern blot genotyping

Genomic DNA extractions from tissue biopsies obtained as described were used for this purpose. 10μl of the genomic DNA preparations were used in a restriction enzyme digest to yield fragment sizes of 3kb. The digestion mix was run on a 0.8% agarose gel and blotted as described above. The positive litter mates were identified using a probe that was a radiolabelled 5' homology region fragment cut with NcoI/Asc and purified from the plasmid vector.

2.8 Immunohistochemistry

2.8.1 Tissue fixation and preparation

Embryonic tissue was fixed by immersion in 4% (w/v) Paraformaldehyde (PFA) overnight at 4°C. Postnatal animals were first perfused under terminal anaesthetic with cold 4% PFA and then spinal cord and brain were dissected out and post fixed by immersion in 4% PFA overnight at 4°C. For some antibodies fixation times had to be adjusted since some antigens are fixation sensitive (Table 2.2)

After fixation, all samples were then immersed in 20% sucrose overnight at 4°C for the purpose of cryopreservation before embedding in OCT and being quickly set by freezing on dry ice and stored at -80°C.

2.8.2 Detection of antigens on tissue sections

Frozen tissue was prepared as described above and cut at 15μm by cryostat sectioning (collected onto SuperFrost plus slides) and left to air dry for 1 hour. The sections were then covered in blocking solution (10% foetal calf or sheep serum in 0.1% Triton-X 100, 1x PBS) for 1 hour at room temperature. The block was removed before covering the slides in primary antibody, diluted in blocking solution (for antibody dilutions see table). The slides were incubated in the primary antibody overnight at 4°C. They were then washed (3 x 5 minutes) in 0.1% Triton-X 100 in x1 PBS before adding the appropriate secondary antibody (diluted in blocking solution) and left to incubate on the slides for 2 hours at room temperature. The slides were then washed again as above (3 x 5 minutes) before counterstaining with Hoechst (10mg/ml stock at a 1:1000 dilution in 0.1% Triton-X 100 in 1xPBS) for 5 minutes at room temperature followed by a further wash before mounting with Citiflour mounting medium and sealing the slide.

2.8.3 Detection of antigens on fixed cells on coverslips petri dishes

For cell preparations on coverslips or petri dishes, the growth medium was aspirated off and 4% PFA was added for 2-20minutes at room temperature before washing briefly by immersion into 1x PBS 8-10 times. The protocol for antibody incubation thereafter is the same as for the frozen tissue sections. All primary antibodies were diluted in 0.1% (v/v) Triton-X 100, 10% (v/v) sheep serum in 1X PBS at dilutions summarised in table 2. For the detection of the cell-surface antigens NG2 and O4 permeabilisation of cell membranes must be prevented and thus Triton-X 100 was excluded from both the washing solution and the antibody diluents. Fluorescent secondary antibodies were applied for 30 minutes at room temperature followed by washing by immersion. Nuclei were stained thereafter with Hoescht (sigma 1/1000) for 5 minutes at room temperature and following a further wash the coverslips were mounted in Citiflour (City University, UK) and stored at 4°C in the dark. For the detection of two antigens for which the primary antibodies were both raised in rabbit, a sequential protocol was employed whereby the first rabbit primary was 'masked' by the subsequent incubation of the sections/coverslips with goat anti- rabbit Fab fragments (1/200) for 1 hour at room temperature. The antigen may then be visualised by applying a mouse anti-goat

Cy3-conjugated secondary before adding the second rabbit primary antibody. In these instances the antibodies were diluted in 0.1% Triton-X 100, 10% *foetal calf serum* in 1x PBS since the mouse anti-goat Cy3 secondary would recognise too many components of the sheep serum to give a clear visualisation.

Antibody	Working Dilution	Supplier
Rabbit anti-Olig2 IgG	1:4000	DF308, a gift from David Rowitch
Rabbit anti-NG2 IgG	1:400	Chemicon
Monoclonal mouse anti-O4 IgM-conditioned supernatant	1:4	Original cells from Raff lab (Sommer and Schachner 1981)
Mouse anti- MNR2 IgG-conditioned supernatant	1:4	Developmental Studies Hybridoma Bank (DSHB)
Mouse anti-Panislet IgG	1:10	DSHB
Mouse anti-NeuN IgG	1:500	Chemicon
Mouse anti-Nestin supernatant	1:5	DSHB
Guinea Pig anti-GLAST polyclonal	1:5000	Chemicon
Mouse anti-GFAP IgG	1:400	Sigma
Rabbit anti-GFP	1:6000	AbCam
Rat anti-GFP IgG2a	1:4000	Fine Chemical
Mouse anti RC2 monoclonal IgM supernatant	1:4	DSHB

Table 2.2 Antibodies used for immunohistochemical analyses.

2.9 Tissue Culture

2.9.1 Tissue culture media

Primary cell cultures were grown in modified rat Bottenstein and Sato's medium (Bottenstein and Sato, 1979) as follows:

Dulbecco's modified Eagle's medium (DMEM) with Glutamax-1 and sodium bicarbonate supplemented with transferrin (0.1mg/ml), progesterone (60ng/ml), sodium selenite (40ng/ml), thyroxine (40ng/ml) triiodo-L-thyronine (30ng/ml), putrescine (16μg/ml), insulin (5μg/ml), 1mM N-acetyl-L-cysteine, 100μg/ml penicillin/streptomycin and 0.5% foetal bovine serum. Media was further supplemented with growth factors where appropriate for different experiments.

2.9.2 Animals

Wild-type mice were of the CD1 background (bred in-house at UCL). Transgenic mice were generated from a C57Bl/6J x CBA/Ca F1 (B6 X CBA) background. For breeding purposes, male mice were caged with females at 5pm and a vaginal plug was checked for the following morning. Fertilisation was considered to have occurred at midnight and thus embryonic day zero (E0) was deemed to be the morning that a plug was discovered. Noon on the day of discovery of the vaginal plug was designated embryonic day 0.5 (E0.5). Mid-gestation embryos were staged according to the morphological criteria of Theiler (Theiler, 1972). Pregnant females were culled by terminal anaesthesia in CO_2 followed by cervical dislocation. The embryos were removed under sterile conditions, their stage confirmed by morphology (Theiller 1972) and were culled by decapitation.

2.9.3 Conditioned medium

Whole cortices were removed from E13.5 mice embryos and the meningeal membranes were mechanically dissected away in Earle's balanced salt solution (EBSS). After coarse mechanical dissection with forceps, the tissue was enzymatically dissociated by

incubation with trypsin at a final concentration of 0.00625% (w/v) at 37°C for 40 minutes. DNAse was then added to a final concentration of 52.5μg/ml and the digest was agitated without trituration to break up the tissue. The suspension was centrifuged at 1300 x G for 2 minutes, the supernatant discarded and the pelleted cells resuspended by gentle trituration in 250μl pre-warmed Sato's. The single-cell suspension was seeded onto Poly-D-Lysine (PDL) coated tissue culture flasks in defined Sato's medium with 0.5% FBS (v/v) and penicillin/streptomycin (P/S, 200 units/ml Penicillin & Sodium, 200μg/ml Streptomycin in 0.85% saline). Primary cultures were grown at high density (70% confluency) over 2-3 days in vitro (DIV). The conditioned medium was then harvested and filtered through a 0.22 μm filter before being aliquoted and stored at -80°C.

2.9.4 Preparation of single cell suspension of cortical VZ cells

Mouse E13.5 cortices were dissected according to the protocol outlined by Qian et al, 1997. Briefly, E13.5 mouse brains were dissected from the surrounding tissue in EBSS and the cortices were removed and transferred immediately to DNAse (52.5μg/ml) with Dispase (0.5mg/ml Roche Diagnostics) in EBSS and incubated for 15 minutes at room temperature. The meningeal membranes were mechanically removed and the denuded cortices transferred to fresh room temperature EBSS for further dissection. The Medial and Lateral Ganglionic Eminences (MGE and LGE respectively) were mechanically removed and the remaining neocortex was enzymatically dissociated in 0.0625% (w/v) trypsin in EBSS for 40 minutes at 37°C. After incubation, the suspension was gently agitated to mechanically dissociate the cells in the presence of DNAseI (52.5μg/ml) without trituration and immediately transferred 12ml pre-warmed, room temperature DMEM for centrifugation at 1300 x G for 2 minutes. The supernatant was removed and the pellet gently triturated with a P1000 pipette 4-6 times in 250μl 37°C, 0.5%-FBS Sato's medium. Sediment and undissociated lumps were left to settle for 2 minutes and the cell density of the top fraction of single cell suspension was then calculated using a haemocytometer. Appropriate dilutions of the cell suspension were made according to the experimental paradigm and the cells were accordingly seeded onto PDL-coated (mol. Weight > 300,000) petri dishes or glass coverslips.

2.10 Time-lapse microscopy

2.10.1 The Time-lapse Imaging system

The time-lapse imaging system is composed of an inverted research microscope (Leica H107 DMIRB or an Olympus IMT-2) equipped with fluorescence and phase or brightfield optics. The microscope is contained within a Perspex heat jacket with a heater and thermostat keeping the microscope body, lenses and culture dishes at 37°C. A custom made adaptor, fitted onto a motorised stage (Prior), fits 3 x 35mm plastic culture dishes in airtight grooves directly above the lens. The stage, housed within a second Perspex box, is moved to locate fields of interest within the culture dishes. The second Perspex housing incorporates a CO_2 sensor/controller (International Controlled Atmosphere Ltd) which regulates a flow of humidified air fan-mixed with CO_2 to maintain the environment at 98% relative humidity and 10% CO_2 / 90% air (v/v).

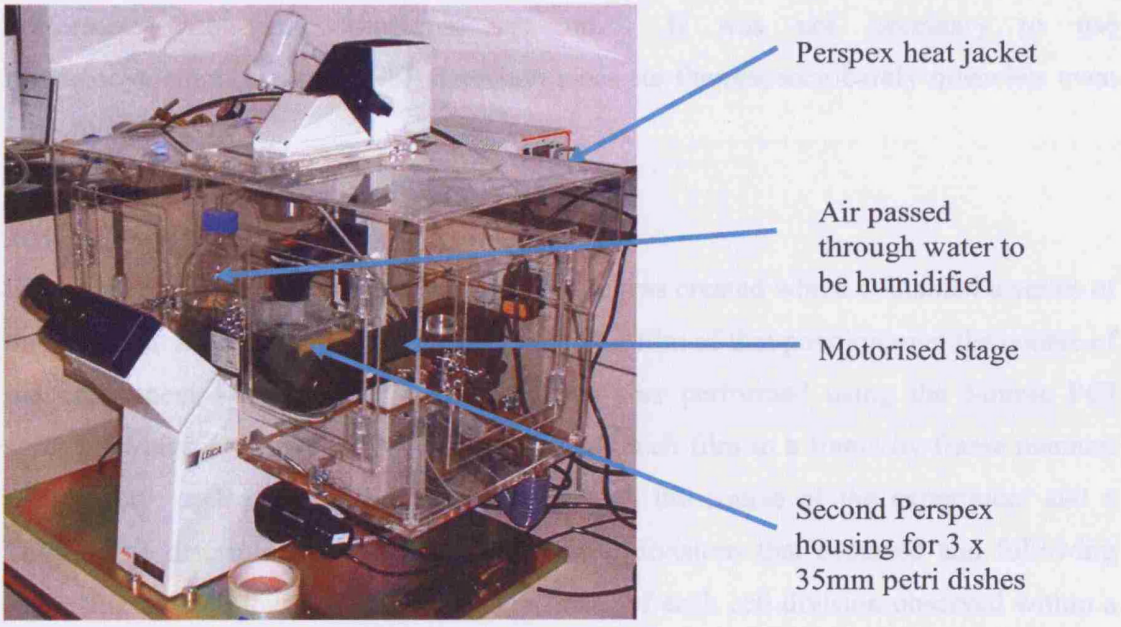

Figure 2.2 Time-lapse set-up

2.10.2 Image acquisition

Images were recorded with a chilled digital camera (Hamamatsu 1394 ORCA-285 S/N) mounted on the microscope and connected to a computer. Image acquisition was under the control of Simple PCI software (DigitalPixel). Both phase contrast illumination and epifluorescence were used. EGFP was excited using a mercury arc lamp with a custom EGF filter set (Q515LP dichroic and a HQ545/50m emission filter). Standard exciter filter sets with accompanying dichroics were used to enable visualisation of Rhodamine, Texas Red, FITC or CY5-conjugated secondary antibodies with narrow band-passes (all filter sets and dichroics from Chroma Technology). The Simple PCI software was used to control all motorised functions of the microscope; time-lapse interval and duration, image properties (exposure, resolution) and logging up to 100 fields of interest by assigning x,y,z coordinates and controlling image capture at each of these positions every 15 minutes until the end of the experiment. After recording, the cells were fixed and prepared for immunocytochemistry. Image capture of antigen expression was performed within the timelapse set up. It was not necessary to use immunocytochemistry for EGFP detection since its fluorescence barely quenches even after fixation.

2.10.3 Analysis of timelapse recordings

For each position in the culture dishes a cdx file was created which contained a series of images taken at 15 minute intervals compiled as a film of that position over the course of the experiment. Analysis of these cdx files was performed using the Simple PCI software which enables the progression through each film in a frame by frame manner. In this way, each clone could be traced through the course of the experiment and a lineage tree determined by observing all of the divisions that occurred and following each daughter cell that was derived. The timing of each cell division observed within a clone could be determined to an accuracy of within 15 minutes. The total number of daughter cells yielded could also be determined and the antigenic identity of surviving cells was accounted for by immunocytochemical analysis. Some clones were too complex for accurate lineage analysis and cells may also migrate out of the recorded field of view. Lineage trees are therefore not described for every cell filmed.

EGFP expression was visualised directly in live cells in transgenic cultures. EGFP-expressing and EGFP-negative cells were traced throughout the recording as described above, and in addition the time at which EGFP appeared was also logged.

Each experiment yielded large numbers of cells that were filmed and traced to the end. High n-numbers within experiments allowed statistics to be applied to determine significant differences in division times of cells grown in different experimental conditions. Statistical significance between experiments was also tested to ensure consistency and repeatability.

Chapter 3

Olig2 Transgenesis

3.1 Introduction

3.1.1 Chapter overview

In order to study the generation of oligodendrocyte precursor cells (OLPs) *in vitro* by time-lapse microscopy, a transgenic mouse was generated that expresses enhanced green fluorescent protein (EGFP), an engineered form of green fluorescent protein (Chalfie et al., 1994;Chalfie, 1995) under the same transcriptional control as the basic-helix-loop-helix (bHLH) transcription factor *olig2* (*oligodendrocyte lineage transcription factor 2*).

3.1.2 Introduction to *olig2*

bHLH transcription factors are characterised by a conserved basic-helix-loop-helix protein motif which is comprised of two α-helices and an intervening loop. bHLH proteins recognise and bind to a consensus hexanucleotide DNA sequence called an E-box (Ferre-D'Amare et al., 1993;Ma et al., 1994). They act as dimers, with amino acid residues within the bHLH region being responsible for both dimerisation and DNA-binding specificity. Residues in both helices are important for dimerisation, whereas helix1 and the loop region are involved in DNA sequence recognition (Nair and Burley, 2000). bHLH factors are involved in the development of diverse organ systems including muscle, the haematopoietic system and the central nervous system (CNS). While most bHLH factors in the CNS are involved in development of neurons, *olig1* and *olig2* are additionally involved in specification of oligodendrocytes. The *olig* genes form a distinct family of bHLH transcription factors, distinct from their proneural counterparts such as *neurogenin-1* or *mash-1*. *Olig1* and *2* are 78% similar at the amino acid sequence level including particular amino acid clusters at their N- and C-termini (Zhou et al., 2000). The majority of the conserved residues lie mainly in the helix portions of the bHLH motif. Since their

loop regions have minimal amino acid sequence similarity, they likely bind to different DNA sequences (Takebayashi et al., 2000) although this has not been formally demonstrated.

Olig2 contains 2 exons in a transcript 3.13 Kb in length (ensemble v.40) and is found on mouse chromosome 16 about 50 Kb upstream of o*lig1*. In the spinal cord it is first expressed strongly in the ventral third of the spinal cord at embryonic day 9.5 (E9.5) and becomes restricted to a tight band defining the motor neuron progenitor (pMN) domain by E10.5. *Olig2*-expressing cells disperse dorsolaterally from E12.5 (Lu et al., 2000;Zhou et al., 2000) and by E18.5, the entire spinal cord is populated with o*lig2*+ cells. *Olig1* has a similar, but more dynamic expression profile than o*lig2* in the spinal cord; it appears 12 hours later and at a much lower and progressively decreasing intensity, such that by E10.5 it has declined to nearly undetectable levels although it reappears at E12.0 in the same, restricted pMN domain as o*lig2* (Zhou et al., 2000). In the brain, o*lig2* is initially restricted at E12.5 to a ventral domain in the ventricular zone (VZ) of the forebrain, midbrain and hindbrain before o*lig2*+ cells disperse from E14.5 onwards. By E19, the entire forebrain is populated with o*lig2*+ cells although not all of these originate from the early ventral sources (Kessaris et al., 2006).

These patterns of *olig* gene expression correspond to the oligodendrogenic zones of the early embryo (Lu et al., 2000) as defined by *platelet-derived growth factor receptor-α* (PDGFRα) expression which labels OLPs (Hall et al., 1996;Pringle and Richardson, 1993). Indeed many *olig2*+ neuroepithelial cells (NEPs) give rise to *olig2*+ OLPs as confirmed by co-localisation with known OLP markers such as *PDGFRα* and *sox10* (sex determining region Y homeobox 10) by *in situ* hybridisation (Zhou et al., 2000). Furthermore, since *olig2*-null mice lack all oligodendrocyte lineage cells (and motor neurons) in the spinal cord, a required role in early stages of oligodendrocyte development is indicated (Lu et al., 2002;Park et al., 2004;Takebayashi et al., 2002;Zhou and Anderson, 2002). Furthermore, a recent paper by Sun et al (Sun et al., 2006) demonstrates that ectopic *olig2* expression (via the electroporation of an *olig2*-containing vector to the dorsal spinal cord) leads to ectopic expression of *sox10* followed by mature oligodendrocyte markers (MBP and

PLP), providing evidence that *olig2* is upstream of *sox10* in the genetic hierarchy leading to myelin gene expression.

In *olig1*-null mice, OLP production is unaffected, but expression of myelin-forming genes in maturing oligodendrocytes is prevented (Xin et al., 2005). Thus *olig1* may have a more significant role in the postnatal rather than the developing animal. This, along with the more dynamic nature of *olig1* expression with respect to that of *olig2* means *olig2* is likely to be a better marker for identifying multipotent NEPs that are involved in early OLP specification. In addition, unlike the expression profiles of most bHLH transcription factors, which are generally downregulated during cell differentiation, *olig2* persists in mature oligodendrocytes (Lu et al., 2000) and so it marks all cells of the oligodendrocyte lineage from the precursors of OLPs to the mature, differentiated cell. To identify neuroepithelial precursor cell (NEP)-derived lineages in which OLPs are specified, I generated a transgenic mouse line that expresses *EGFP* under *olig2* transcriptional control, thus allowing visualisation of all *olig2*+ cells via EGFP fluorescence.

3.2 RESULTS

3.2.1 Screening of the PAC library for *Olig2*-containing clones

Although much is known about its expression profile, the regulatory elements involved in controlling *olig2* expression have not been described. Therefore, in order to create a transgenic mouse line that would faithfully transcribe an expression vector in the same pattern as *olig2*, phage artificial chromosome (PAC) transgenesis was employed to enable insertion into the mouse genome of large regions of DNA that could include all potential regulatory elements required for authentic *olig2* expression (Lee et al., 2001).

The isolation of PAC clones that included an *olig2*-containing fragment was kindly performed by Mat Grist and Nicoletta Kessaris. A gridded PAC library (RPC121) from the UK HGMP Resource Centre was screened for *olig2*-containing clones using a 300 bp probe isolated by EcoRI/SmaI restriction digest. The probe consisted of a fragment spanning the 5' untranslated region (UTR) and 200 bp of the *olig2* open reading frame (ORF). Three clones were isolated and characterised by restriction enzyme mapping and pulse field gel electrophoresis (PFGE) (Figure 3.1). Inverse polymerase chain reaction (PCR) cloning and DNA sequencing of the ends of the insert mapped the extremities of the *olig2* fragment precisely. PAC clone RPC121 512-G7 (named PAC-G7 herein) was chosen for further use – a 178 Kb clone including the *olig2* ORF with 140 Kb upstream and 38 Kb downstream sequence. This clone excluded *olig1* while including large regions upstream and downstream of the *olig2* open reading frame (ORF) likely to include all the regulatory elements involved in endogenous *olig2* expression.

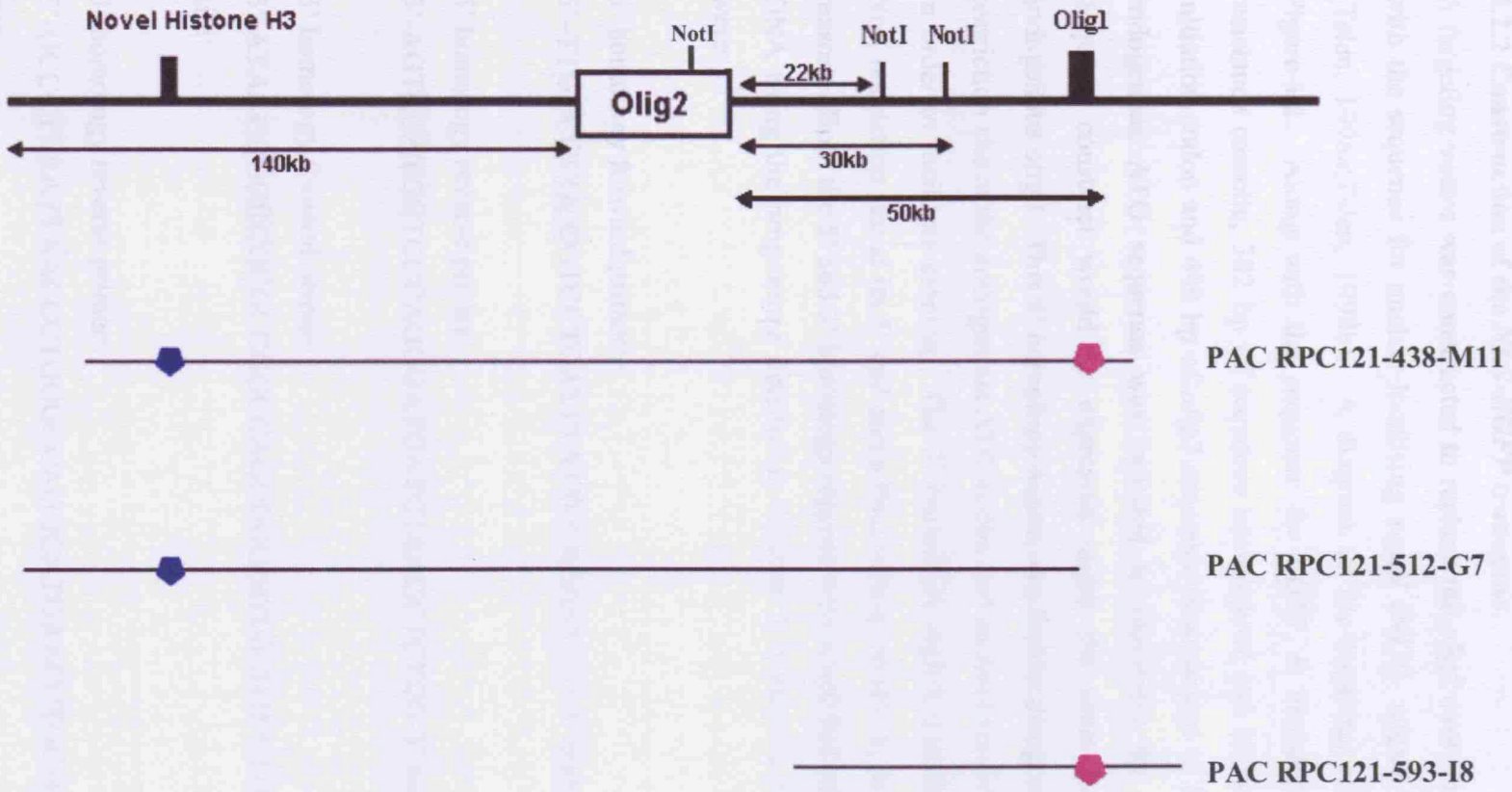

Figure 3.1 Schematic of the genomic region around the *olig2* locus including NotI sites and other known genes within this region (*olig1* 50Kb downstream, and a novel Histone-coding sequence 130 Kb upstream of the *olig2* locus – ensemble v.40). The relative positions of the *olig2*-containing fragments contained within three PAC clones identified by library screening are shown with *olig1* indicated in pink and the novel Histone H3 in blue. The lengths of these fragments were predicted by the genomic mouse sequence (http://www.ensemble.org/) after the extremities were precisely mapped by inverse PCR. PAC RPC121-512-G7 was selected for modification and transgenic mouse production.

3.2.2 Construction of the *NLS-EGFP* transgene

A targeting vector was constructed to replace the *olig2* exon in the PAC-G7 vector with the sequence for nuclear-localising signal (NLS)- tagged EGFP (NLS:EGFP) (Tsien, 1998a;Tsien, 1998b). A diagram of the targeting construct is shown in Figure 3.2. Along with the sequence for EGFP, it included a chloramphenicol resistance cassette, 382 bp of sequence upstream of and including the *olig2* ATG initiation codon and 490 bp of *olig2* sequence downstream of the stop codon. The endogenous ATG sequence was included to maximise the likelihood that the targeting construct would be expressed under the same regulatory control as endogenous *olig2*. This 5' homology region was further designed to include an NcoI restriction site at the endogenous ATG codon and an AscI restriction site at its 5' end in order to facilitate cloning. The 3' homology region was designed to include a NotI restriction site at its 5' end and a PacI restriction site at its 3' end for the same reasons. Both the 5' and 3' homology regions were amplified by PCR from PAC-G7 DNA using the programme detailed in Chapter 2, Section 2.3. The primers used were:

5' homology forward primer:
5'–TTGGCGCGCCGTCCTCATTTATTCCAGGCCGG-3' highlighted AscI site

5' homology reverse primer:
5'-AGTCCATGGTCCCAGGGATGATCTAAGCTCTCG-3' highlighted NcoI site

3' homology forward primer:
5'-ATAAGCGGCCGCGCCGGCCAGCGGGGGTGCGTCCT-3'highlightedNotI site

3' homology reverse primer:
5'-GCCCTTAATTAACCCTGGGCCAGGGATGAACCTGC-3'highlighted PacI site

The PCR products were isolated by agarose gel electrophoresis and purified (Chapter 2, Section 2.3) before being cloned directly into pCRII-TOPO® for DNA

sequencing. Once the sequences were confirmed, the 3' homology fragment was isolated from the TOPO plasmid by NotI/PacI digest and ligated into the pBluePacAsc plasmid to create pBluePacAsc3'h (Figure 3.3).

EGFP coding sequences were amplified from the pBird plasmid (Figure 3.4) using Expand High Fidelity Taq Polymerase (EHFTP) (Roche) with primers that incorporated an NLS and an NcoI restriction site at the 5' end and a SpeI restriction site at the 3'end of the EGFP. The primers used were:

Forward primer:

5'-

CCATGGCACCCAAGAAGAAGAGGAAGGTGGTGAGCAAGGGCGAGGAGC

T-3' highlighted NcoI site

Reverse primer:

5'-ACTAGTTTACTTGTACAGCTCGTCCATGCC-3' highlighted SpeI site

In order to select positively for recombinant clones a chloramphenicol resistance cassette (Cm^R) was included in the construct, inserted between the NLS:EGFP sequence and the 3' homology sequence (Figure 3.2 C). This was obtained by NotI digest from the pI22 plasmid constructed and donated by P. Iannarelli (Figure 3.5). The chloramphenicol resistance cassette includes flanking *frt* sites to allow its removal from the targeting vector prior to pronuclear injection. All the vector components were sequenced to ensure nucleotide sequence fidelity.

The components were individually isolated by appropriate digest and ligated together sequentially. The Cm^R fragment was first ligated into the pBluePacAsc3'h (Figure 3.6) and the NLS:EGFP and the 5' homology fragments were then added as shown in Figure 3.7.

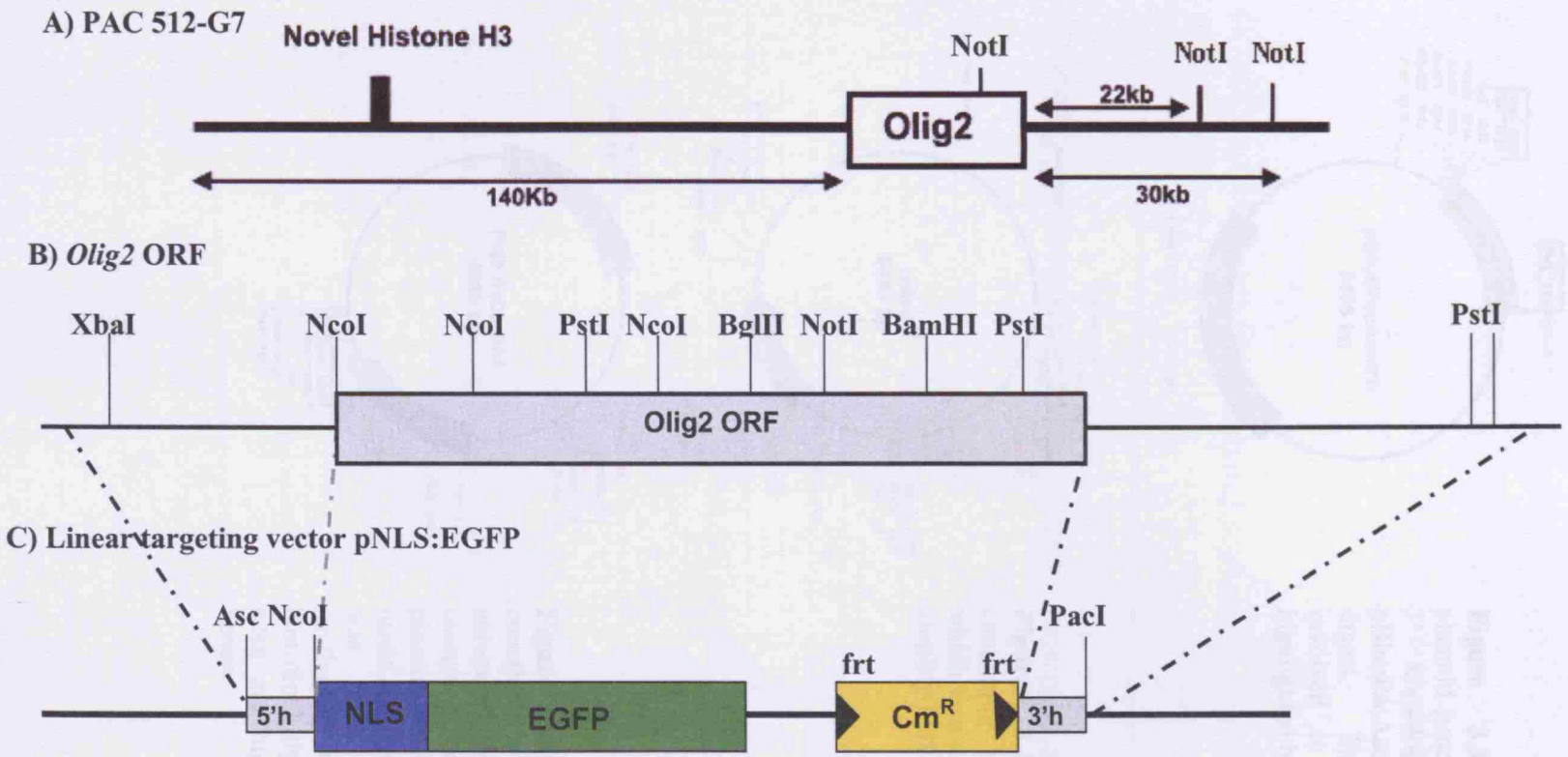

Figure 3.2 A) PAC 512-G7 showing the regions upstream (5') and downstream (3') of the *olig2* locus. The *olig2* ORF is shown along with NotI restriction sites and the novel Histone coding sequence found upstream. B) Schematic of the *olig2* ORF with flanking genomic sequences to include some key restriction sites. C) Schematic of the linearised targeting vector pNLS:EGFP used in homologous recombination via the 5' and 3' regions of homology (homology sequences and sites of recombination with the *olig2* ORF sequence shown as grey boxes and grey dotted lines). The NLS:EGFP sequence and the chloramphenicol resistance cassette (Cm^R) are shown (blue/green and yellow boxes respectively) and the Cm^R is flanked by *frt* sites used for its removal before pro-nuclear injection.

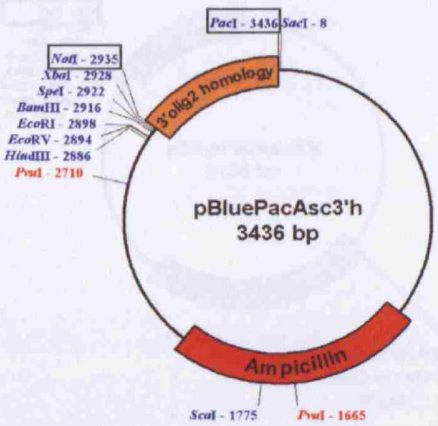

Figure 3.3 pBluePacAsc3'h plasmid generated by ligation of 3' homology fragment into pBluePacAsc via PacI/NotI digest. The restriction sites involved in this ligation are highlighted by black boxes

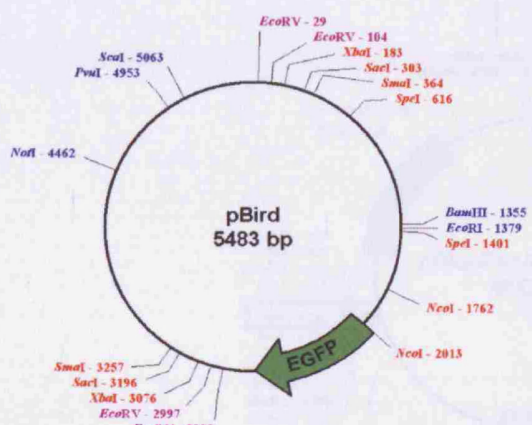

Figure 3.4 pBird plasmid containing an EGFP cassette, which was used as a template to amplify EGFP.

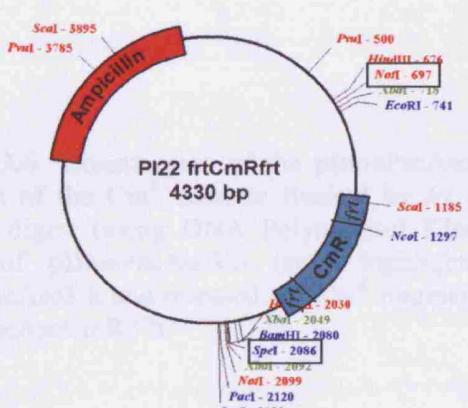

Figure 3.5 pI22 plasmid containing the Cm^R chloramphenicol resistance cassette flanked by *frt* sites. This plasmid was kindly designed and made by Palma Iannarelli and was used to isolate the *frt*-flanked Cm^R fragment via NotI/SpeI digest. The restriction sites are highlighted by black boxes.

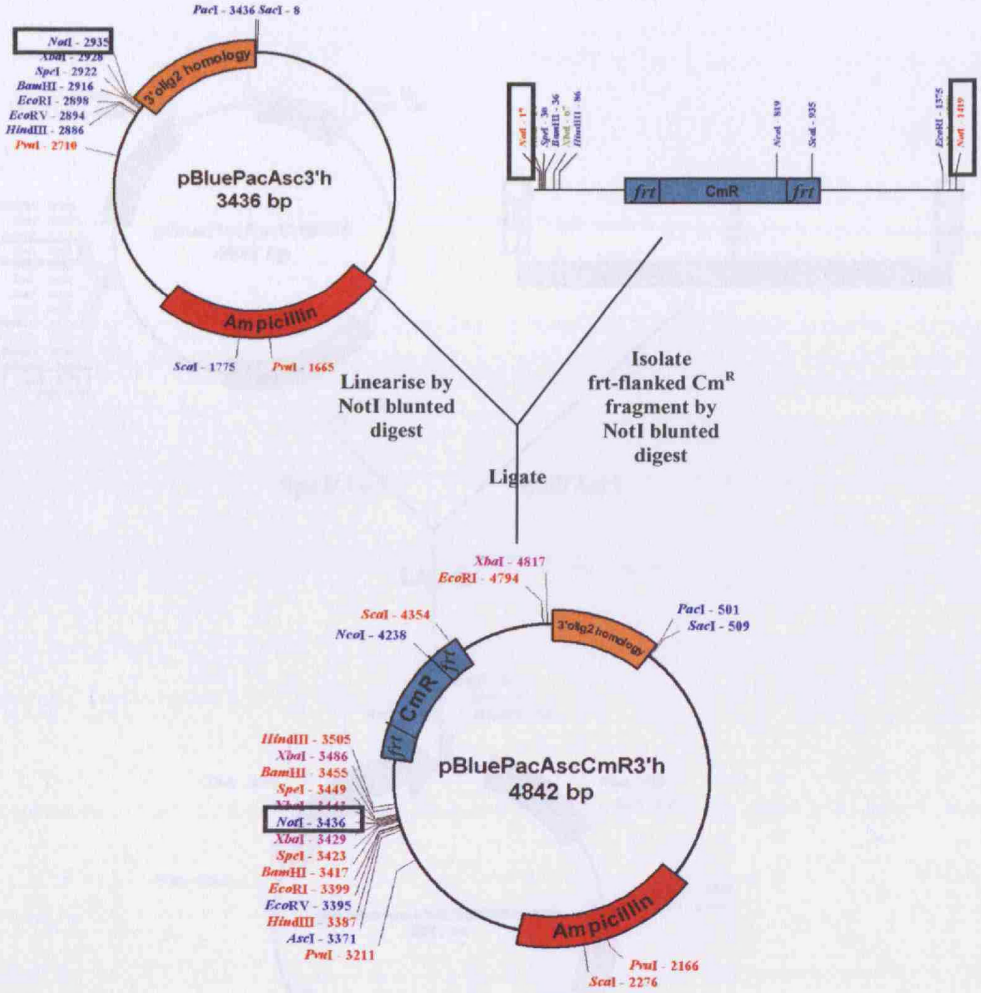

Figure 3.6 Construction of the pBluePacAscCmR3'h vector. The first step was the isolation of the Cm^R cassette flanked by *frt* sites from pI22 (se Figure 3.5) by NotI blunted digest (using DNA PolymeraseI Klenow fragment) along with NotI blunted digest of pBluePacAsc3'h (sites highlighted by black boxes). This linearised pBluePacAsc3'h and released the Cm^R fragment. The two were then ligated to generate pBluePacAscCmR3'h.

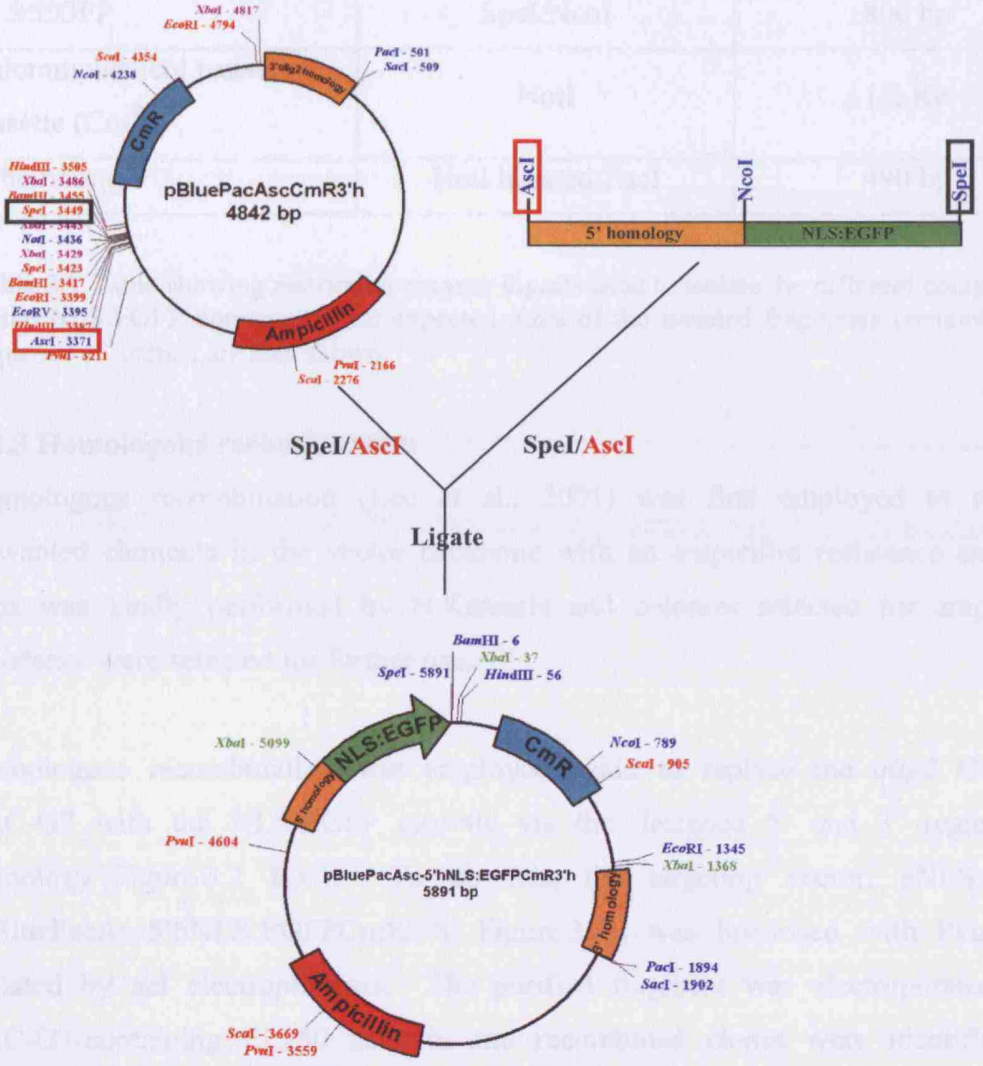

Figure 3.7 Construction of the NLS:EGFP targeting vector by ligation of pBluePacAscCmR3'h with the 5' homology and NLS:EGFP fragments. This was done by restriction enzyme digestion with SpeI and AscI as highlighted by black and red boxes respectively. This generated the complete targeting vector named pBluePacAsc5'hNLS:EGFPcmR3'h - named pNLS:EGFP.

Component	Digest	Fragment size
5' homology	AscI/NcoI	500 bp
NLS:EGFP	SpeI/NcoI	800 bp
Chloramphenicol resistance cassette (Cm^R)	NotI	1.2 Kb
3' homology	NotI blunted/PacI	490 bp

Table 3.1 Table showing restriction enzyme digests used to isolate the different components of the NLS:EGFP construct. The expected sizes of the isolated fragments containing the sequence of interest are also shown.

3.2.3 Homologous recombination

Homologous recombination (Lee et al., 2001) was first employed to replace unwanted elements in the vector backbone with an ampicillin resistance cassette. This was kindly performed by N.Kessaris and colonies selected for ampicillin resistance were selected for further use.

Homologous recombination was employed again to replace the *olig2* ORF in PAC-G7 with the NLS:EGFP cassette via the designed 5' and 3' regions of homology (Figure 3.2 B,C). To do this, the targeting vector, pNLS:EGFP (pBluePacAsc5'hNLS:EGFPCmR3'h; Figure 3.7), was linearised with PvuI and isolated by gel electrophoresis. The purified fragment was electroporated into PAC-G7-containing EL250 bacteria and recombined clones were identified by chloramphenicol selection. Removal of the chloramphenicol resistance cassette from recombined clones was subsequently carried out by arabinose induction of endogenous *flpe* activity. Removal of the resistance cassette was confirmed by Southern blot analysis which detected an 800 bp shift (Figure 3.8) using a probe that spans the 5' homology region of the *olig2* ORF.

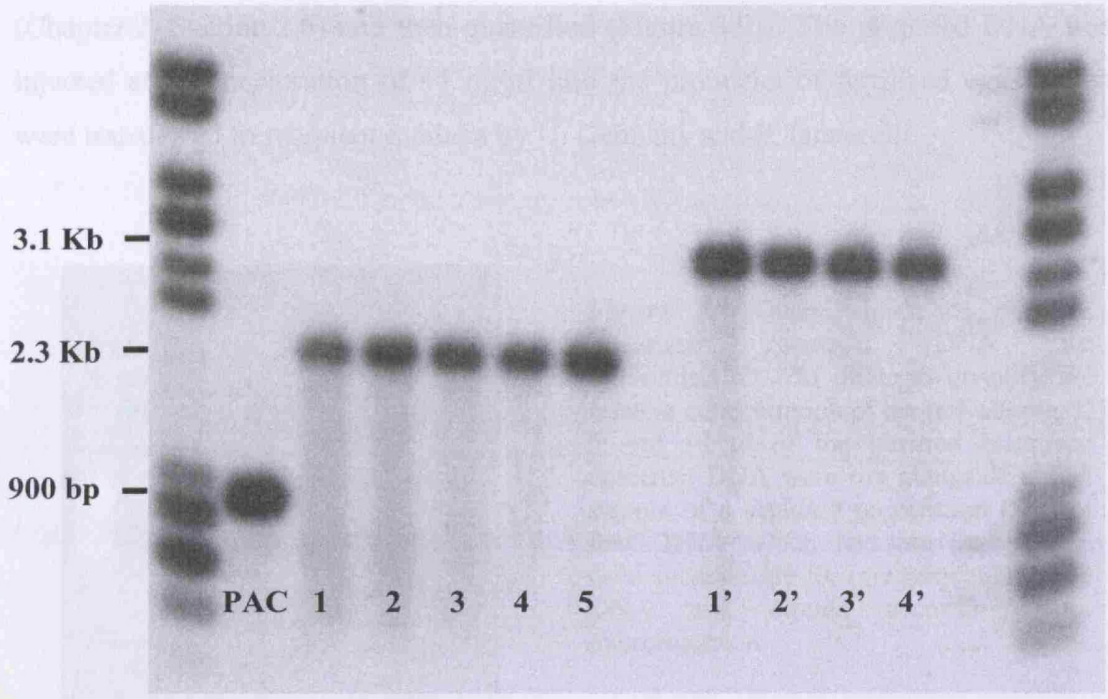

Figure 3.8 Southern analysis following BglII restriction digest of DNA from modified PAC 512-G7 clones before and after Cm^R cassette removal. The digests were probed with a labelled fragment that is complementary to the *olig2* 5' homology from the targeting vector. The first lane is a sample of unmodified PAC 512-G7 vector DNA containing the *olig2* ORF. Samples 1-5 were prepared from modified clones after Cm^R cassette removal by *flpe* activity. Samples 1'- 4' are the corresponding PAC 512-G7 clones before Cm^R removal.

3.2.4 Pronuclear injection of the modified vector construct

The isolated and purified construct was dialysed with microinjection buffer (Chapter 2, Section 2.6) and then quantified (Figure 3.9). The prepared DNA was injected at a concentration of ~1 ng/μl into the pronuclei of fertilised eggs which were transferred to recipient mothers by U. Dennehy and P. Iannarelli.

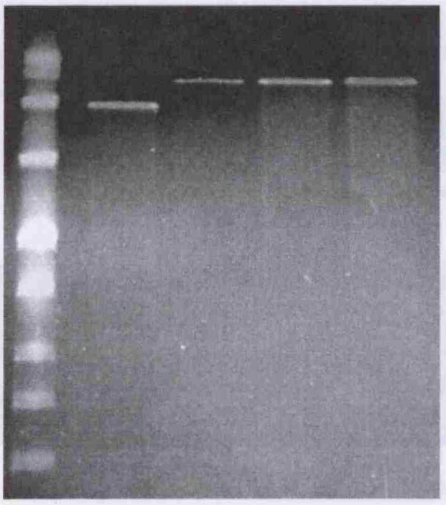

5 μl Std 1 μl 5 μl 10 μl

Figure 3.9 Quantification of purified, linearised construct DNA for microinjection. In order to quantify the relative concentration of the test sample, 1, 5 and 10 μl of the purified linearised construct DNA were run alongside a 5 μl sample of a standard preparation (Std) of PAC DNA which had previously been used successfully for microinjection. The DNA was diluted accordingly for microinjection.

3.2.5 Screening founder litters for the presence of *NLS:EGFP*

Pups born from the recipient mothers were first screened for the presence of the transgene by PCR using genomic DNA as a template. The PCR primers were designed to amplify sequences only if the transgene was present, the forward primer being specific to a sequence in the EGFP fragment of the transgene, and the reverse primer specific to a sequence in the *olig2* 3' homology region.

Forward Primer:

5'- GCCACAACGTCTATATCATGGCC-3'

Reverse primer:

5'-TCCTGGGAGTCTCCTACCCCGCC-3'

PCR analysis identified 13 pups that contained the transgene (Figure 3.11) and this was checked by Southern blot. A probe specific to the 5' homology region was applied to sample genomic DNA digested with BglII. Six of the PCR positives were

confidently confirmed to contain the transgene by Southern blot: 23/3, 24/3, 26/6, 27/1, 27/2, 31/1 (Figure 3.12). However, founders 24/3 and 27/2 appeared to have weak expression and so were not used for initial characterisation of the transgenic lines.

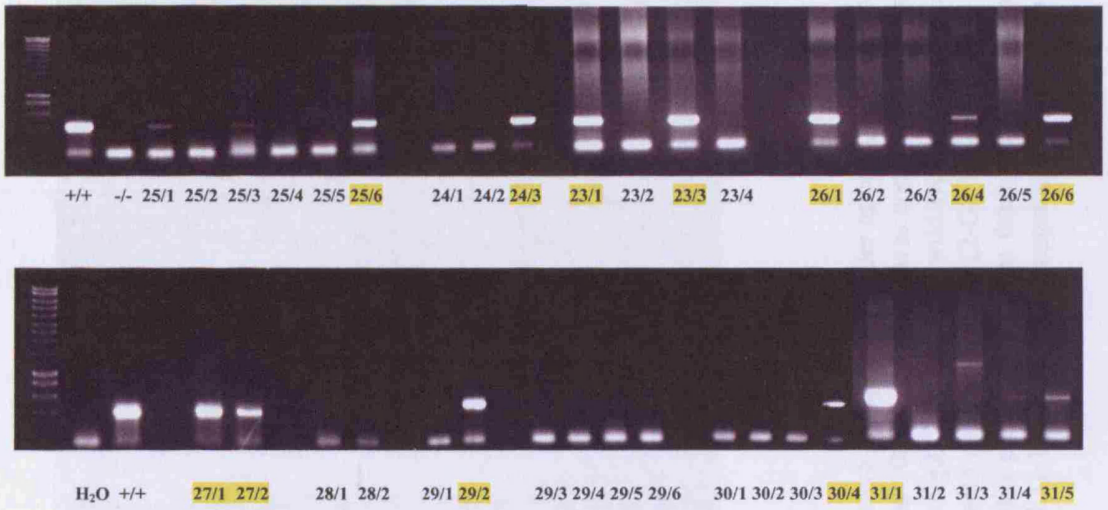

Figure 3.10 Genotyping by PCR of mouse litters born from microinjected eggs. Mice 23/1, 23/3, 24/3, 25/6, 26/1, 26/4, 26/6, 27/1, 27/2, 29/4, 30/4, 31/1 and 31/5 all showed a specific band at 600 bp that was strong enough to be confident that the PCR detected the presence of the transgene. Diluted modified PAC 512-G7 DNA was used as a positive control (+/+) and wild type mouse DNA (-/-) and water (H_2O) were used as negative controls. The forward primer was specific to a sequence in the EGFP fragment of the transgene, and the reverse primer specific to a sequence in the *olig2* 3' homology region

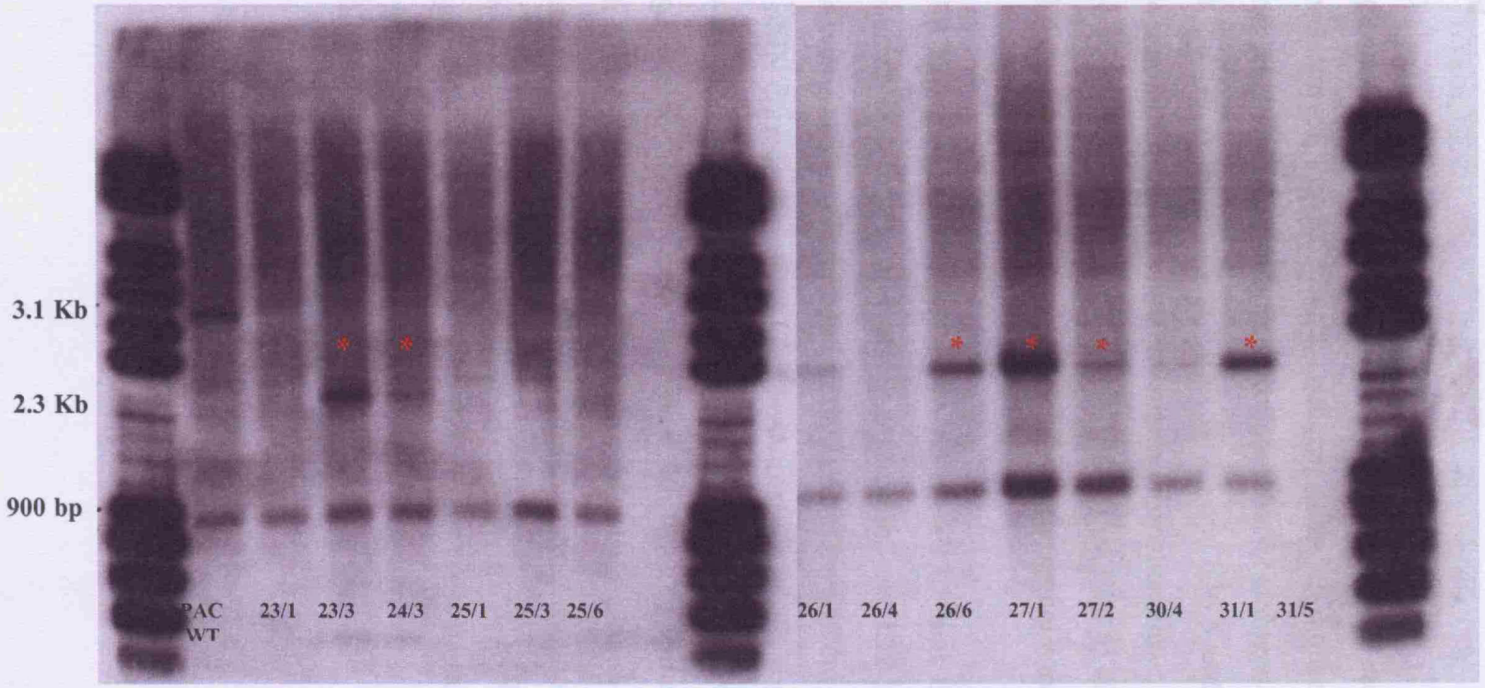

Figure 3.11 Southern analysis of genomic DNA for genotyping of putative transgenic founder mice. Genomic DNA obtained by tail biopsy was digested with BglII. The blot was hybridized with a labeled 500 bp probe that was complementary and hybridised to the 5' homology region found in both the targeting vector and in genomic *olig2*. The expected wild type band can be seen in all samples at 900 bp. As a positive control, a sample of genomic DNA spiked with modified PAC 512-G7 DNA was used and a 3.1 Kb band was, representing a fragment including the transgene with the Cm^R still present. Samples from the putative founders all had the endogenous band at 900 bp and samples 23/3. 24/3, 26/6, 27/1, 27/2 and 31/1 also had the transgenic band at 2.3 Kb (no Cm^R).

3.2.6 Characterising the expression of the *NLS:EGFP* transgene in the spinal cord

Olig2 and EGFP expression in the embryonic spinal cord

Expression of the *EGFP* transgene in founder mouse lines was characterised to assess whether it faithfully recapitulated that of endogenous *olig2*. As a control, wild type mice were harvested at E10.5, E12.5 and E16.5 and analysed for the presence of endogenous Olig2 protein by immunohistochemistry. As expected, Olig2+ cells were seen in a restricted domain (pMN) at E10.5, dispersed dorsolaterally from E12.5 onwards and distributed throughout the spinal cord at E16.5 (Figure 3.13).

EGFP expression was assessed in E10.5, E13.5 and E16.5 *olig2-EGFP* mice and compared with expression of Olig2 protein. At E10.5, like Olig2+ cells, EGFP+ cells were seen in a tight band in the ventral part of the spinal cord corresponding to the pMN domain (Figure 3.14 A). At this age EGFP was present both in the cytosol as well as in the nucleus of expressing cells (Figure 3.14 A inset). Like endogenous Olig2+ cells, EGFP+ cells dispersed through the spinal cord from E13.5 onwards with a high density of EGFP+ cells maintained at the pMN domain (Figure 3.14 B inset 1). They became uniformly distributed throughout the spinal cord by E16.5 (Figure 3.14 C). At these later embryonic ages EGFP was exclusively nuclear (Figure 3.14 B inset 2) demonstrating the effectiveness of the NLS associated with the transgene.

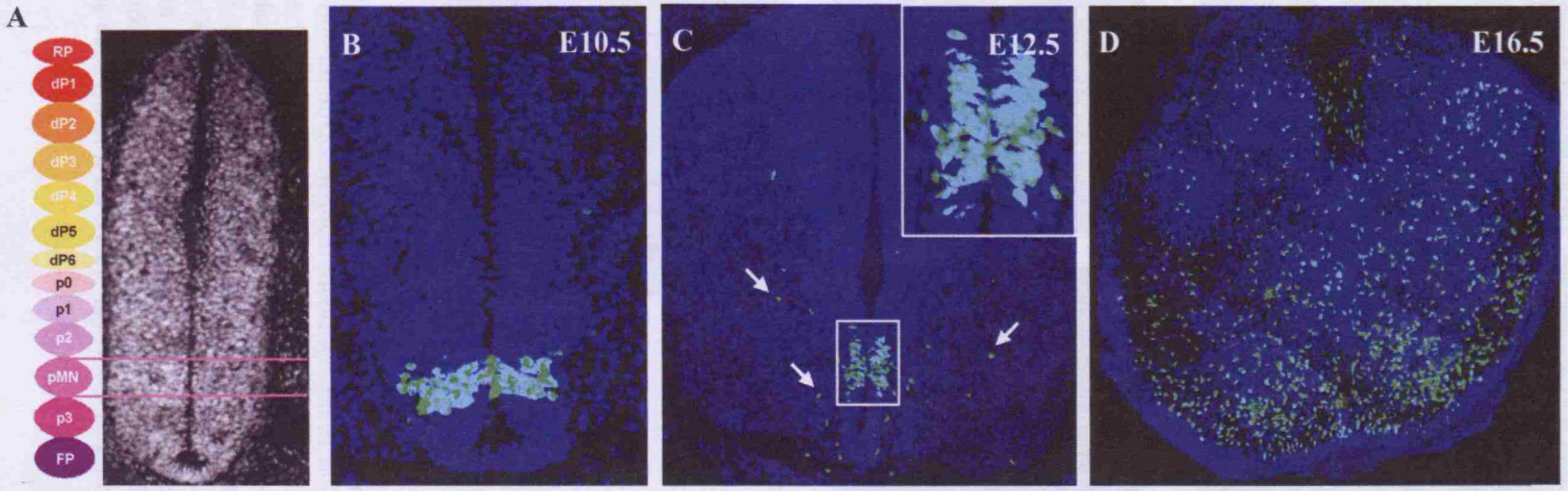

Figure 3.12 *Olig2* expression in the developing embryonic murine spinal cord as detected by immunohistochemistry. At E9.5 the spinal cord is already segregated into tight domains of transcription factor expression (A). *Olig2* is expressed within the pMN domain at this stage and remains restricted until E10.5 (B). From E12.5 (C) onwards some Olig2+ cells disperse dorsolaterally (arrows) from the pMN domain, but a concentrated region of *olig2*-expressing cells within the pMN domain remains (inset). The dispersal continues from E12.5 and the spinal cord contains Olig2+ cells throughout from around E16.5 (D).

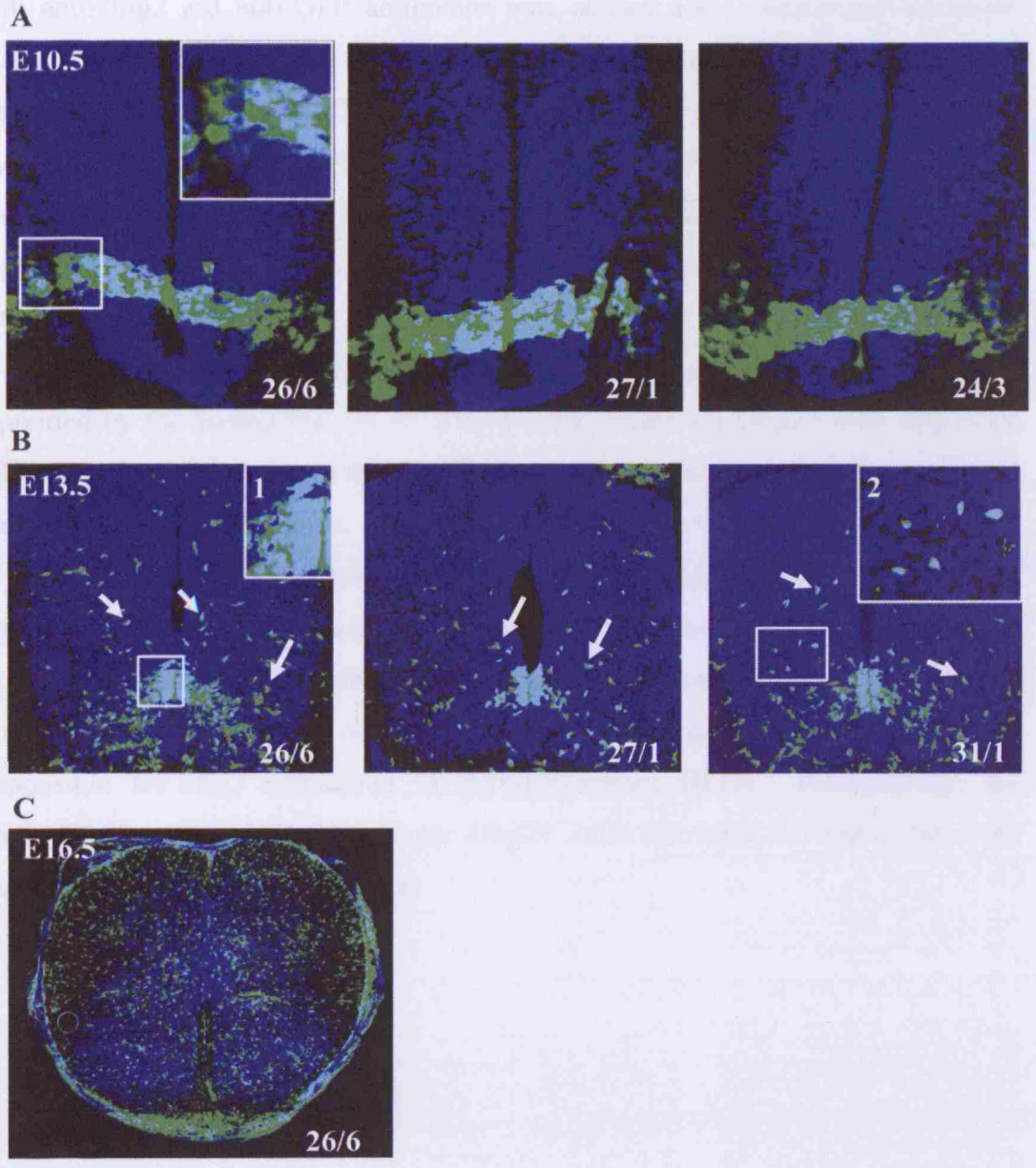

Figure 3.13 EGFP expression in transgenic embryonic spinal cords in different founders as assessed by immunohistochemical identification of EGFP protein. At E10.5 (A), EGFP was seen in a restricted band corresponding to where the pMN domain is located. This was true for all founder lines analysed, three of which are shown here. The EGFP expression at this age was diffuse, being located in the cytosol of expressing cells (inset). At E13.5 (B), like endogenous Olig2 protein, EGFP was found in cells dispersing away from the pMN domain (arrows) with a high density of EGFP+ cells still persisting at the pMN domain (inset 1 for 26/6). Unlike at E10.5, however, by E13.5 the EGFP has been translocated to the nucleus of expressing cells (inset 2 for 31/1). By E16.5 (C) the spinal cord is populated with EGFP+ cells.

In order to confirm that the EGFP co-localised with Olig2 protein, double-labelling with anti-Olig2 and anti-GFP antibodies was carried out. Immunohistochemical analysis was used, since the *in situ* hybridisation probes for EGFP gave a low, unreliable signal. At E10.5, Olig2 and EGFP were found in the same cells although nuclear accumulation of EGFP lagged behind that of Olig2 (Figure 3.14 A). This was true for the three founder lines analysed. At E13.5 however, not all Olig2+ cells expressed EGFP. Olig2+/EGFP- cells were seen predominantly in or near the ventricular zone (VZ) (Figure 3.14 B inset and C) and are likely to be due to a delay in *EGFP* transcription and translation relative to that of *olig2*. This notion is supported by the finding that 96 +/- 2% of older, migrating Olig2+ cells expressed EGFP. At E16.5, there were Olig2+/EGFP+ cells distributed throughout the spinal cord (Figure 3.15). However, there was a difference in the extent of Olig2/EGFP co-localisation in the dorsal and ventral portions of the spinal cords. 93 +/- 6% of Olig2+ cells in the ventral cord co-expressed EGFP, while, in the dorsal cord, only 68 +/- 7% of Olig2+ cells were EGFP+ (Figures 3.15 and 3.16). This might be attributed to the absence of a regulatory element in the transgene that is specifically responsible for *olig2* expression in dorsally-derived OLPs. Alternatively, the Olig2+EGFP- cells might be younger Olig2+ cells that have not upregulated the transgene-derived EGFP at this time.

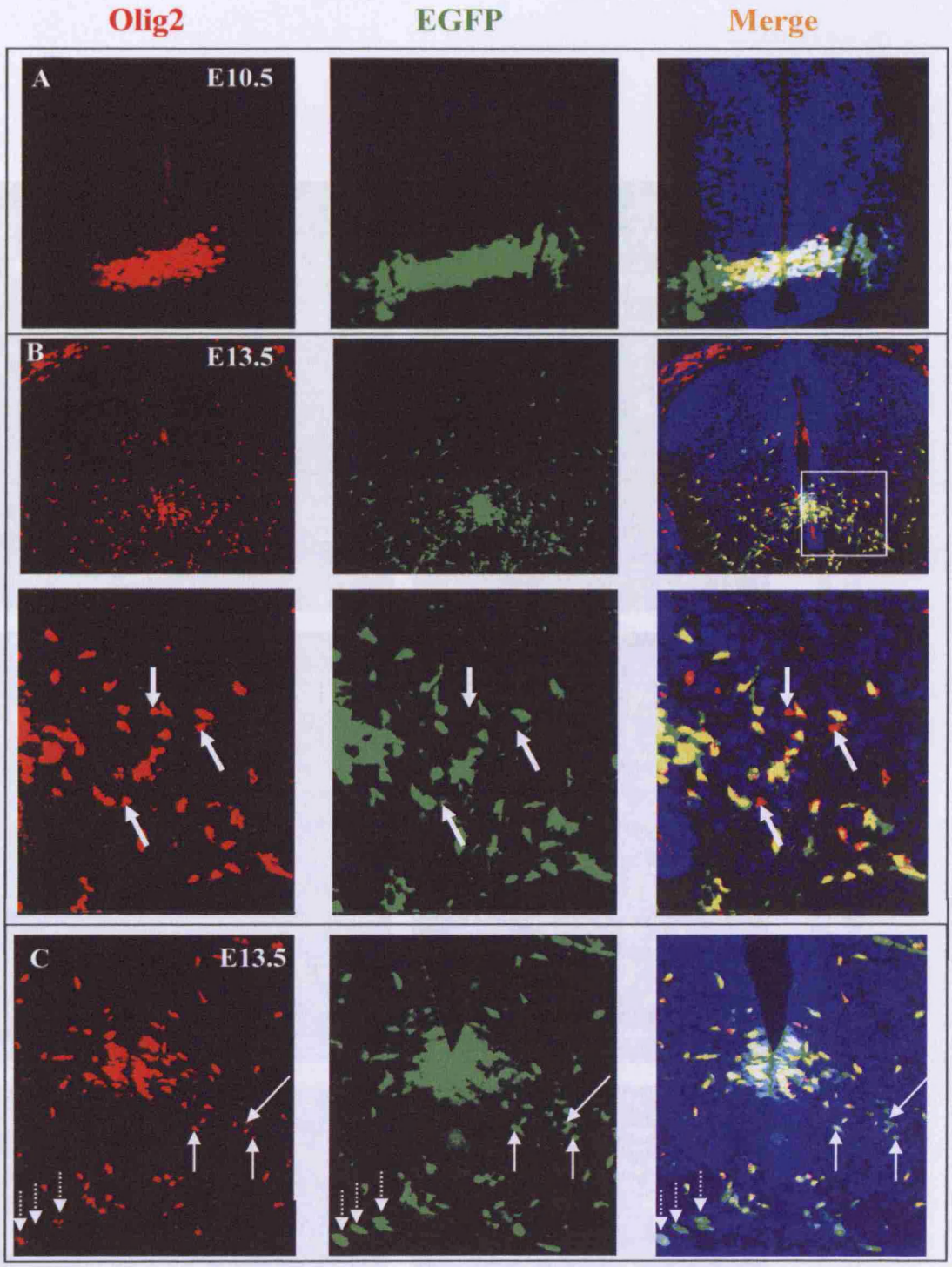

Figure 3.14 Olig2/EGFP co-localisation in transgenic spinal cords at different embryonic ages, as detected by immunohistochemistry. A) At E10.5 Olig2 and EGFP were expressed strictly within the pMN domain with 100% overlap, although EGFP fluorescence was more diffuse than for Olig2 since the protein was present in the cell cytosol as well as in the nucleus. At E13.5 (B,C) 96 +/- 2% of migrating Olig2+ cells were EGFP+. Olig2+/EGFP- cells were mostly found near the pMN domain as shown in panel B (arrows). There were also some EGFP+/Olig2- and EGFP+/weakly Olig2+ cells at E13.5 (C arrows). These were mostly found migrating ventrolaterally (solid arrows) or around the ventral white matter (dotted arrows).

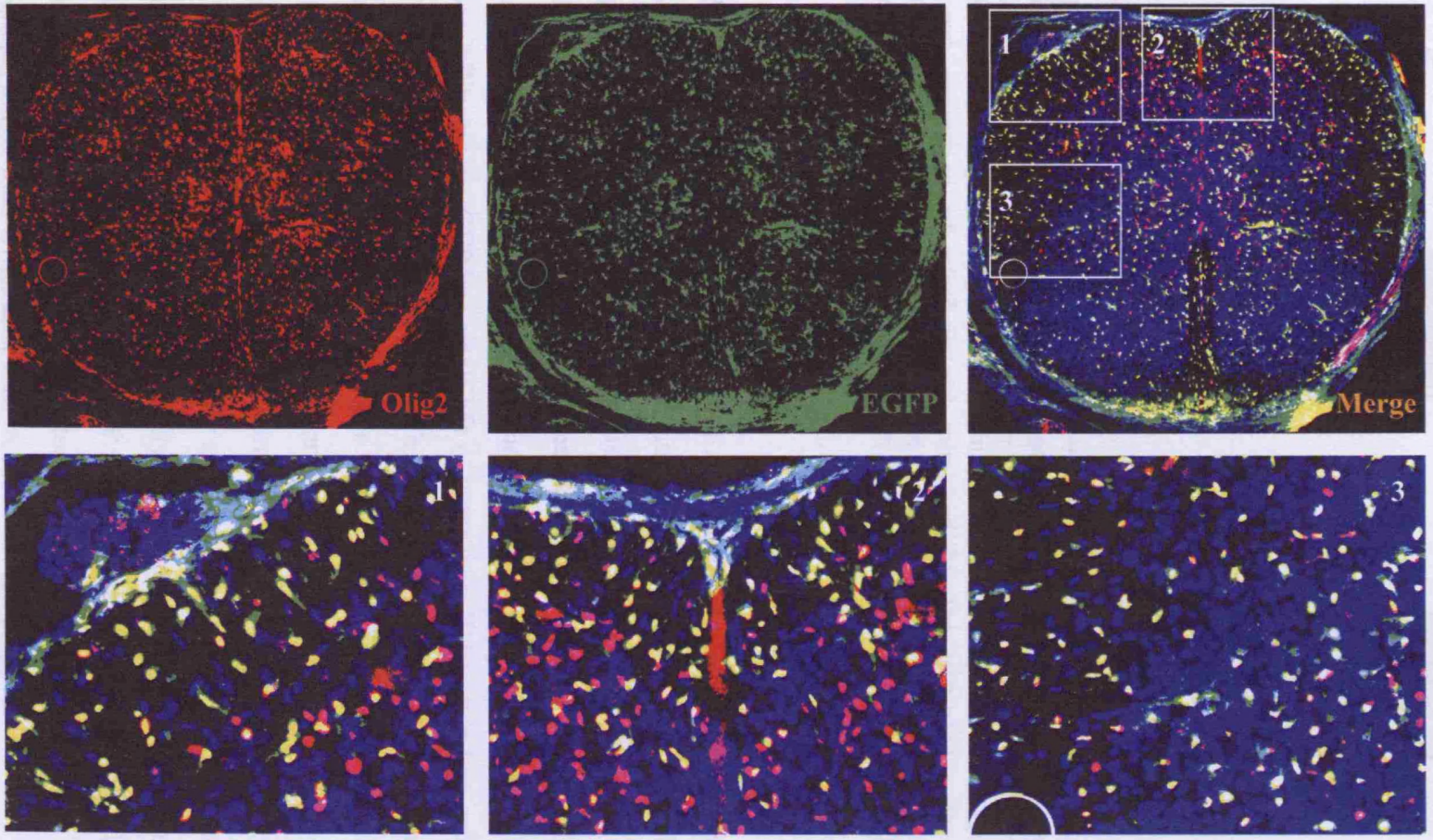

Figure 3.15 Olig2/EGFP co-localisation in transgenic E16.5 spinal cord, detected by immunohistochemistry. 68% of Olig2+ cells were EGFP+ in the dorsal half of the spinal cord (inset 1 and 2) while there was 93% co-localisation in the ventral cord (inset 3).

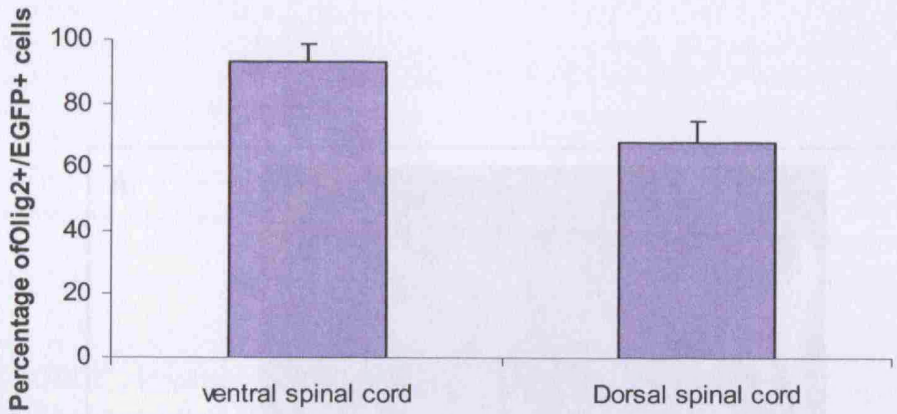

Figure 3.16 Distribution of Olig2+/EGFP+ cells in the dorsal and ventral halves of E16.5 transgenic spinal cords in which there was an apparent discrepancy in co-localisation in these two regions. 93 +/- 7% of Olgi2+ cells were EGFP+ in the ventral spinal cord, 68 +/- 2% pf Olig2+ cells were EGFP+ in the dorsal spinal cord. This suggests that the dorsal expression of *olig2* is not mimicked by the transgene. Percentage of Olig2+/EGFP+ cells is relative to the total number of Olig2+ cells identified. Data is presented as mean +/- standard error mean from 3 animals, 3 sections analysed from each, all from founder line 26/6.

EGFP protein persists in early motor neurons after olig2 down-regulation

Some EGFP+/Olig2- cells were identified in, or close to, the ventral horns of the spinal cord (Figure 3.14 D). Since this is where motor neurons reside, it seemed that these cells might be motor neuron precursors in which *olig2* and *EGFP* transcription had down-regulated, but EGFP protein had not yet been degraded. This is a likely possibility since EGFP has a half life of more than 20 hours in live cells (Corish and Tyler-Smith, 1999), but the half life of Olig2 is likely to be much shorter. To confirm this idea, E13.5 spinal cords were subjected to double-labelling for EGFP and MNR2, an early marker for motor neurons (Tanabe et al., 1998). This revealed co-expression of these two markers in the ventral horns at E13.5 (Figure 3.18 A-D) although there was no co-localisation at E14.5 (Figure 3.18 E-G). *Olig2* is expressed in motor neuron precursors, but rapidly downregulated in post-mitotic motor neurons (Novitch et al., 2001) and since EGFP fluorescence is also absent by E14.5 it appears that *EGFP* is transcribed and translated in parallel with *olig2*, but that EGFP protein persists longer than Olig2 after mRNA synthesis has stopped.

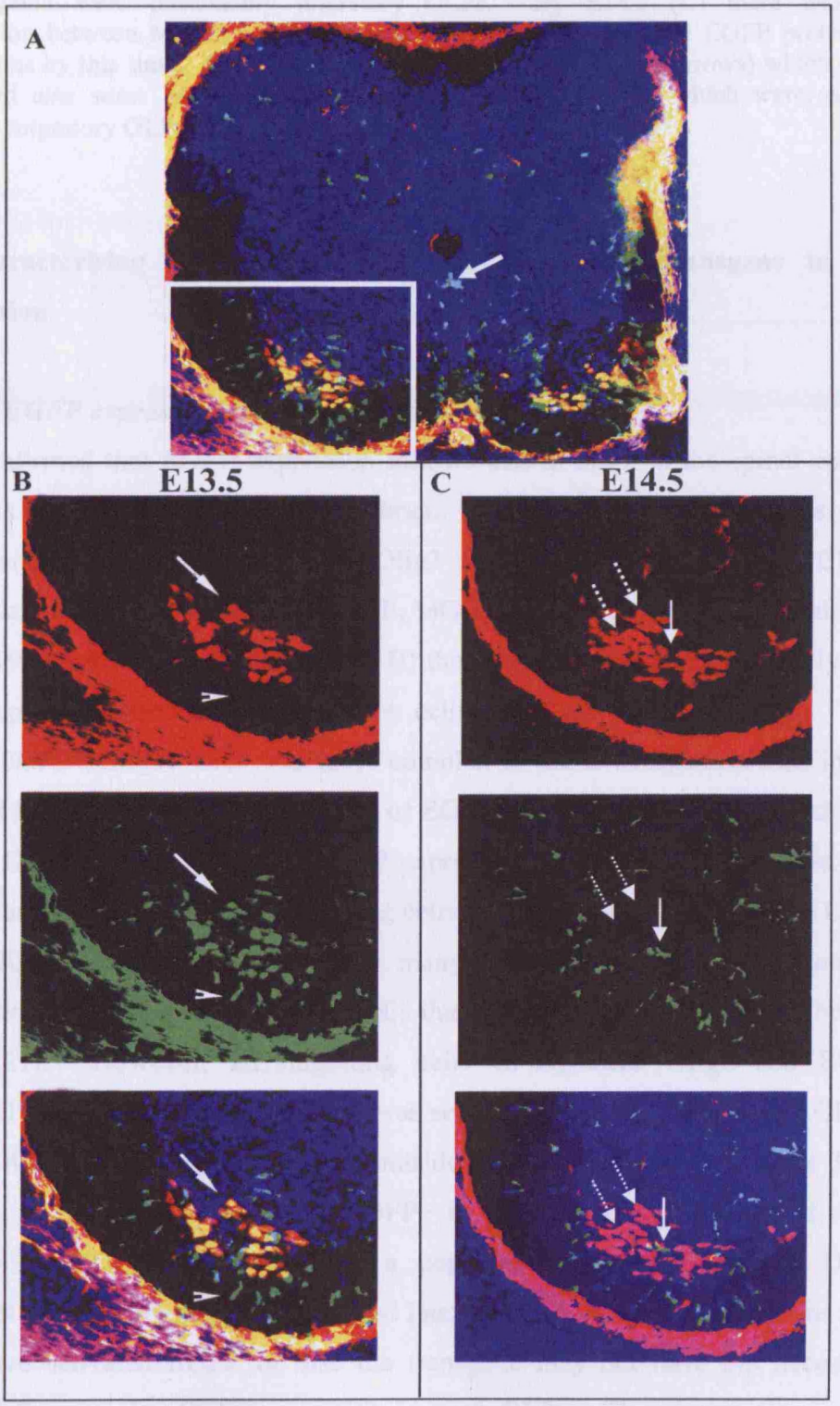
A
B
E13.5
C
E14.5
MNR2
EGFP
Merge

Figure 3.17 (above) MNR2 co-localisation with EGFP in the E13.5 and E14.5 murine transgenic spinal cord. By E13.5 motor neurons have been generated and have migrated to the ventral horns (A). Co-localisation between MNR2 and EGFP is seen in clusters of motor neurons in the ventral horns (arrows, B). There were also EGFP+/MNR2- cells (arrow head, B) which were presumably migratory OLPs. By E14.5 (C) there was no co-localisation between MNR2 and EGFP indicating degradation of the EGFP protein in motor neurons by this time. There were obvious MNR2+ cells (dotted arrows) which were EGFP- and also some EGFP+ cells that are not MNR2+ (arrow) which were, again, presumably migratory OLPs. Founder line 26/6.

3.2.7 Characterising the expression of the *NLS:EGFP* transgene in the telencephalon

Olig2 and EGFP expression in the developing brain

Having confirmed that *EGFP* expression follows that of *olig2* in the spinal cord, I analysed its expression in the developing brain. As a control, wild type brains were sectioned and analysed for endogenous Olig2 protein at E10.5, E13.5 and E16.5. Olig2+ cells were seen at E10.5 in the LGE, MGE, ventral tectum and hypothalamus (Figure 3.19 A). After E13.5 (Figure 3.19 B) they were dispersed dorsolaterally and the telencephalon contained many Olig2+ cells by E16.5 (Figure 3.19 C). The profile of EGFP+/Olig2+ cells was more complex in the telencephalon than in the spinal cord however, with the appearance of EGFP fluorescence being delayed with respect to Olig2 protein. The first EGFP expression in the anterior forebrain was seen at around E13.5, but only in migrating cells, all of which co-labelled with Olig2 (Figure 3.20). In more posterior sections, many more EGFP+ cells were identified although there were only a few Olig2+ cells that co-expressed EGFP within the VZ (Figure 3.21). However, all migrating cells co-expressed Olig2 and EGFP (Figure 3.21). At E16.5 a similar profile was seen since few VZ cells were EGFP+, but 93 +/- 8% of migrating Olig2+ cells outside the VZ were EGFP+ (Figure 3.22) and 88 +/- 5% of Olig2+ cells were EGFP+ in the early cortex. Some of these cortical Olig2+/EGFP- cells could be a population of dorsally-derived OLPs (Kessaris et al., 2006) which are generated later in development and therefore may not yet have activated *EGFP* or else the transgene may not have the necessary regulatory elements for *EGFP* activation in such OLPs. There were also a few EGFP+/Olig2- cells (Figure 3.22) which could be attributed to EGFP protein

persisting after *olig2* down-regulation during differentiation of cortical neurons, as has been described recently by Furusho et al (Furusho et al., 2006). These data indicate a delay in *EGFP* expression with respect to *olig2* in the brain. This was not unexpected since endogenous *olig2* expression is more complex and dynamic in the telencephalon than in the spinal cord. In addition two of the four lines showed ectopic EGFP in the cortex at E13.5 (Figure 3.23) and were thus excluded from further analysis.

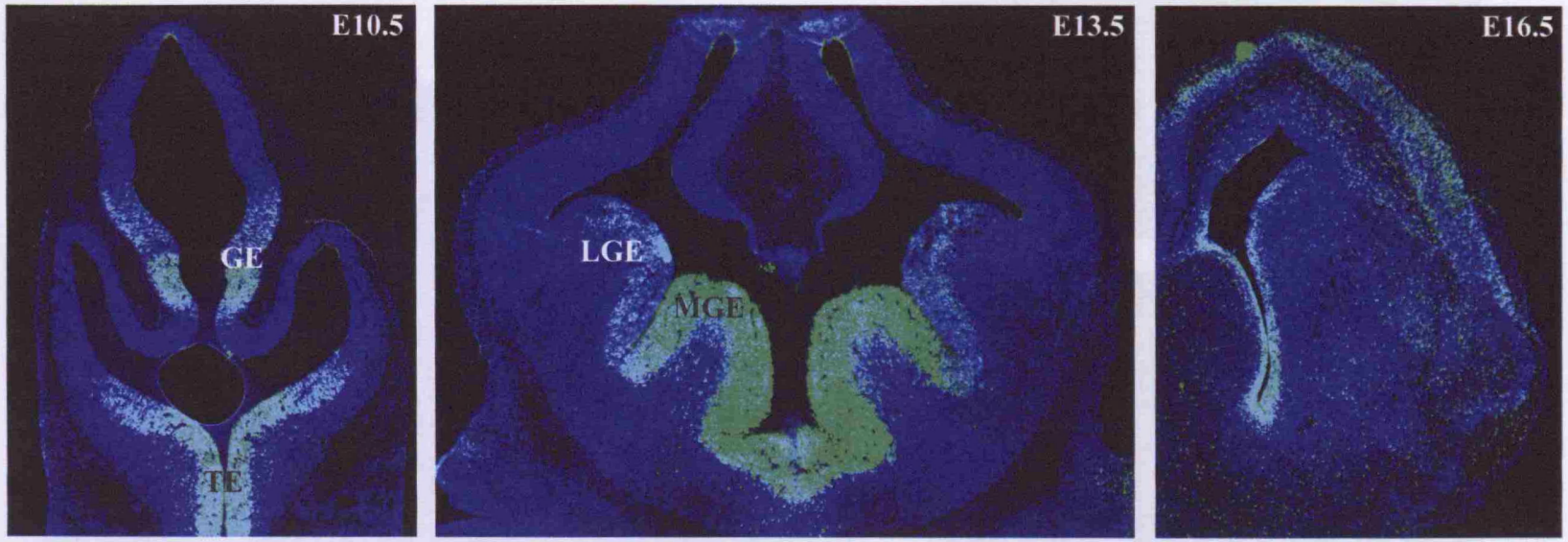

Figure 3.18 Olig2+ cells in the developing embryonic murine brain at the level of the midbrain at E10.5, E13.5, and E16.5 as detected by immunohistochemistry. By E10.5 (A) Olig2+ cells are seen in the ventral tectum (TE) and the ventricular zone of the presumptive lateral and medial Ganglionic eminences (GE). At E13.5 Olig2+ cells are found in the Lateral and Medial Ganglionic eminences (LGE and MGE) and by E16.5 they are found throughout the telencephalon.

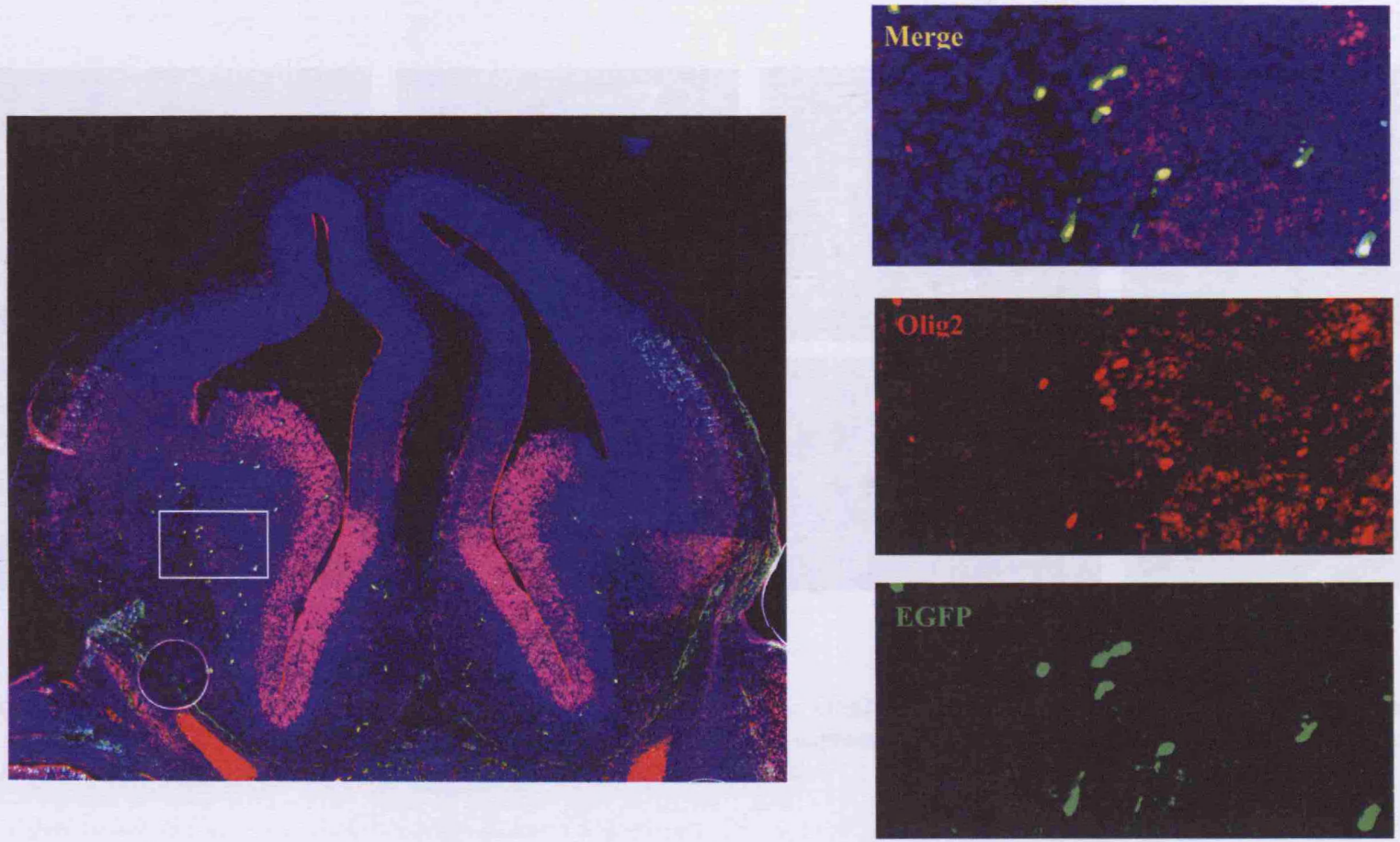

Figure 3.19 Olig2/EGFP co-localisation in the anterior telencephalon at E13.5, as identified by immunphistochemistry. Olig2+ cells at the VZ are EGFP-negative, but all migrating Olig2+ cells co-express EGFP (inset). Founder line 26/6

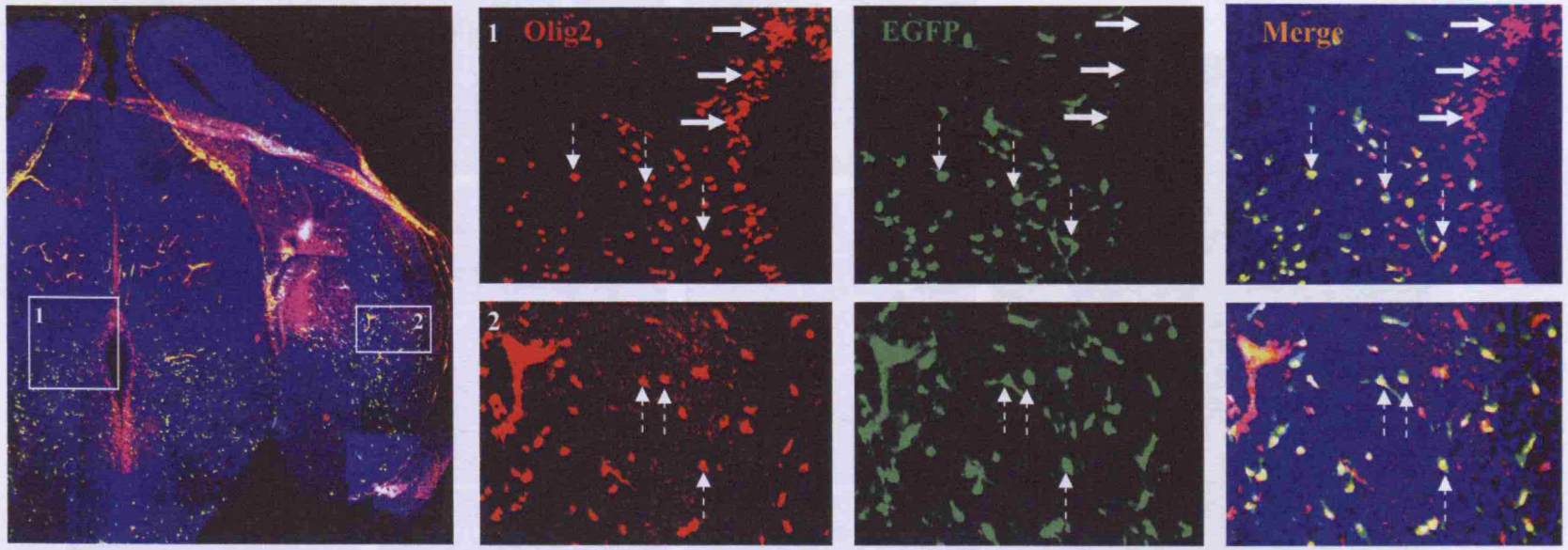

Figure 3.20 Olig2/EGFP co-localisation in the transgenic E13.5 diencephalon. Olig2+ cells around the VZ were EGFP-negative (panel 1 solid arrows), but there were many migrating Olig2+ cells and these all co-expressed EGFP (panel 2 dotted arrows). Migrating cells proximal to the VZ were also EGFP+ (panel 1 dotted arrows). Founder line 26/6.

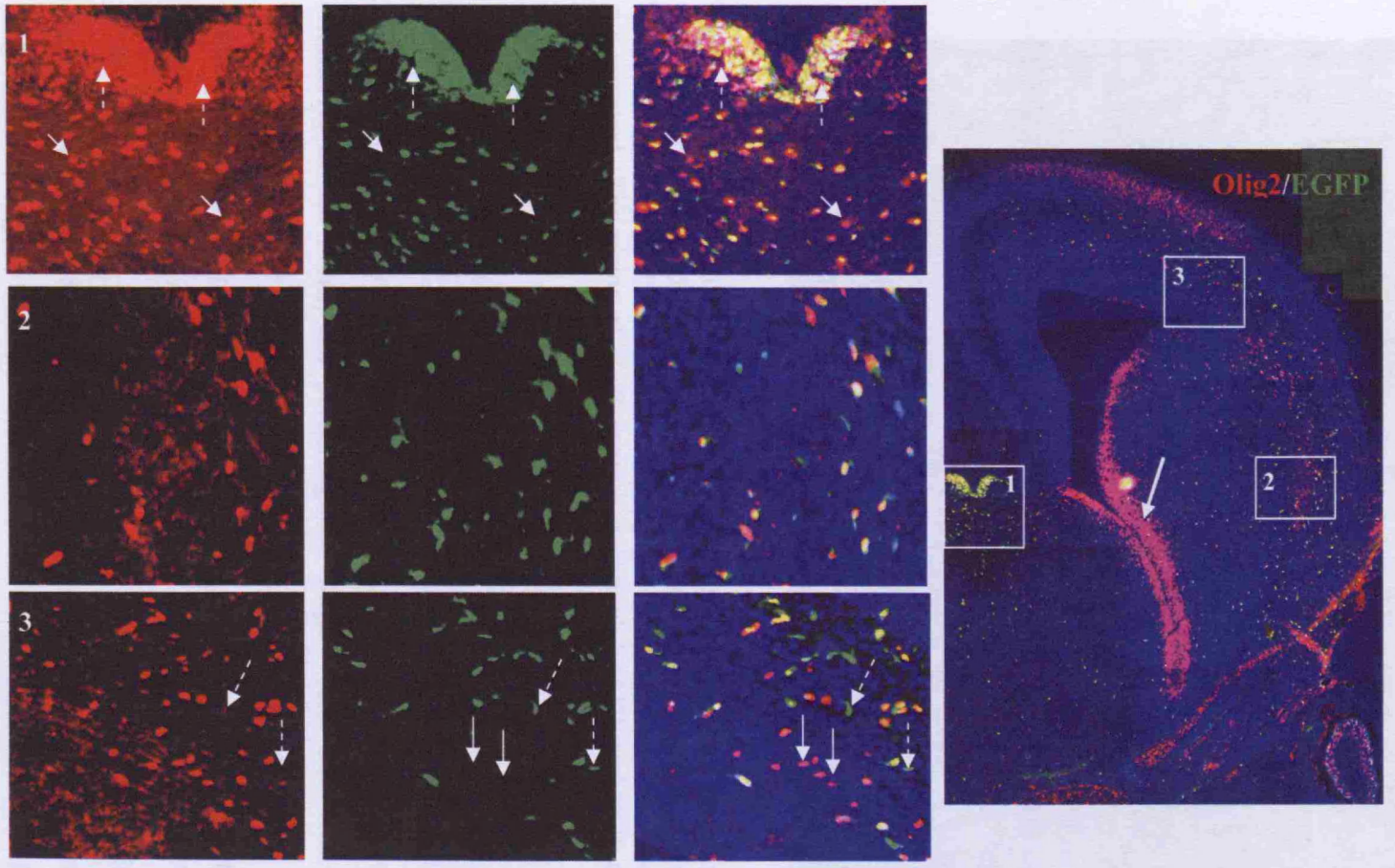

Figure 3.21 Olig2/EGFP co-localisation in E16.5 transgenic brain. Olig2+ cells in the VZ were EGFP-negative (large arrow) indicating delayed *EGFP* activation relative to *olig2*. In the developing corpus callosum (inset 1) where *olig2* has been expressed for longer, most Olig2+ cells co-expressed EGFP (dotted arrows), although there were occasional Olig2+/EGFP- cells (solid arrows). 93 +/- 8% of migrating Olig2+ cells co-expressed EGFP (inset 2). In the cortex (inset 3), 88 +/- 5% of Olig2+ cells co-expressed EGFP with occasional clusters of Olig2+/EGFP- cells being identified (arrows, inset 3). There were also occasional EGFP+/Olig2- cells (dotted arrows, inset 3). Founder line 26/6.

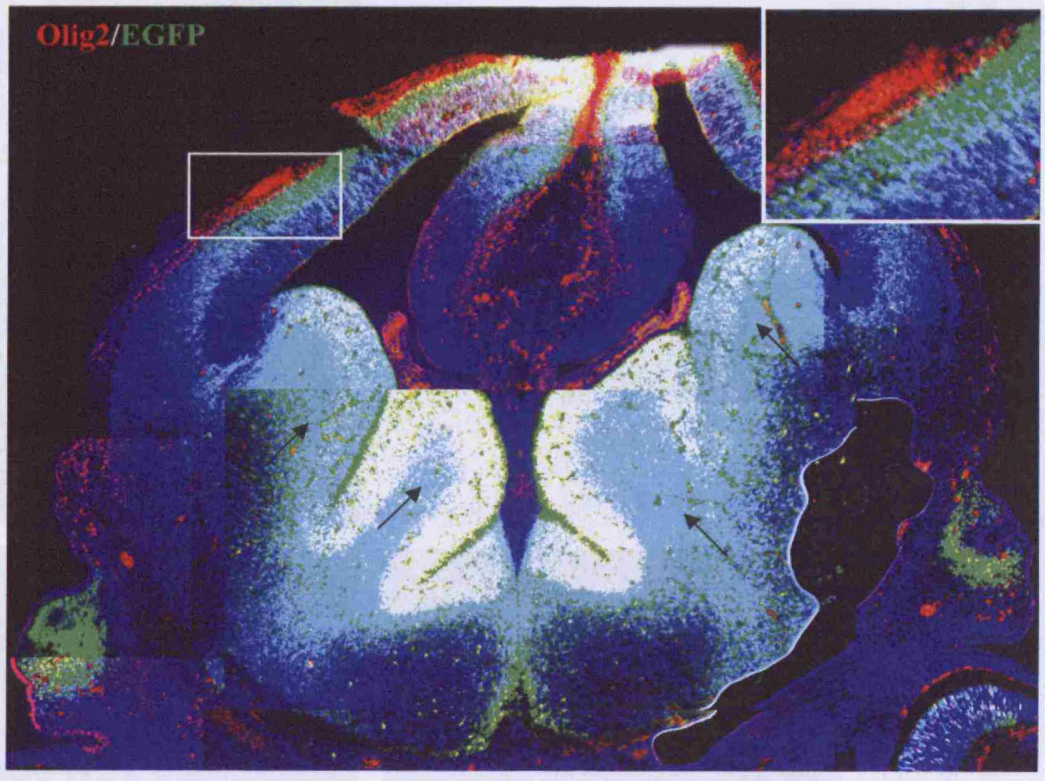

Figure 3.22 Ectopic EGFP expression in E13.5 transgenic brain from founder line 27/1. There was extensive EGFP expression in the developing cortex (inset) where *olig2*+ cells do not exist at this age. The red immunostaining in cortical region is from meninges that were not removed. The region of EGFP expression around the LGE and MGE also far exceeded that of Olig2 (arrows).

3.2.8 EGFP expression in the adult

At P10 in the spinal cord, 70 +/- 3% of Olig2+ cells were EGFP+. However, at P30-45 only 45 +/- 6% of Olig2-expressing cells were also EGFP+ (Figure 3.24). Similarly, in the brain, the percentage of Olig2+ cells that co-expressed EGFP decreased significantly between P10 and P30 - at P10 there was 84 +/- 6% co-localisation in the corpus callosum and 77+/- 11% in the cortex, but this was reduced in P30-45 animals to 47 +/- 1% in the corpus callosum and 68 +/- 6% in the cortex (Figure 3.25). The explanation for this is unclear although it is possible that transcriptional regulation of *olig2* is different in the adult and the embryo and that the *NLS:EGFP* transgene insert lacks adult-specific control elements. Alternatively, the transgene might be selectively inactivated through DNA modification in older animals.

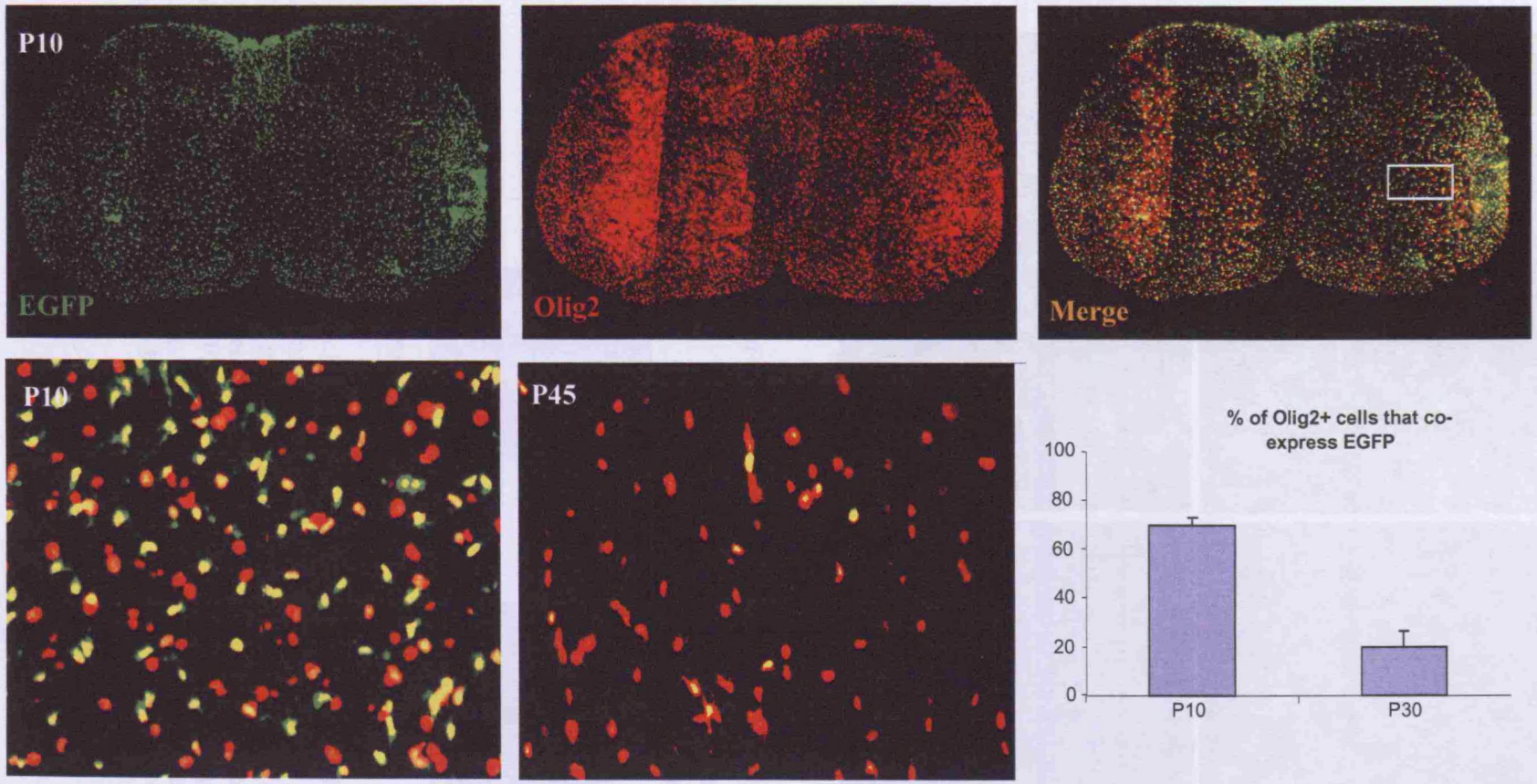

Figure 3.23 Olig2/EGFP co-localisation in the P10 and P30 transgenic spinal cord as determined by immunohistochemistry. At P10, 70 +/- 3% of Olig2+ cells co-expressed EGFP, but this is dramatically reduced by P30 to 20 +/ 7% co-localisation. The total number of Olig2+ cells also decreased at P45. Founder line 26/6.

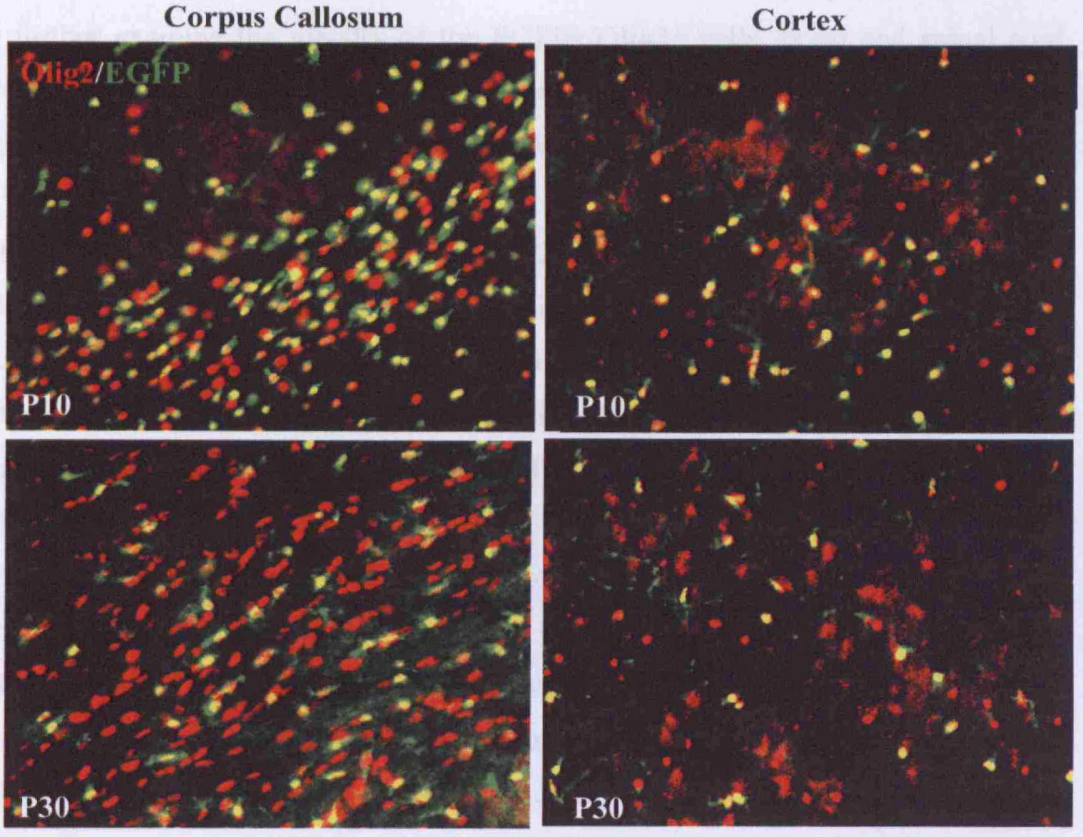

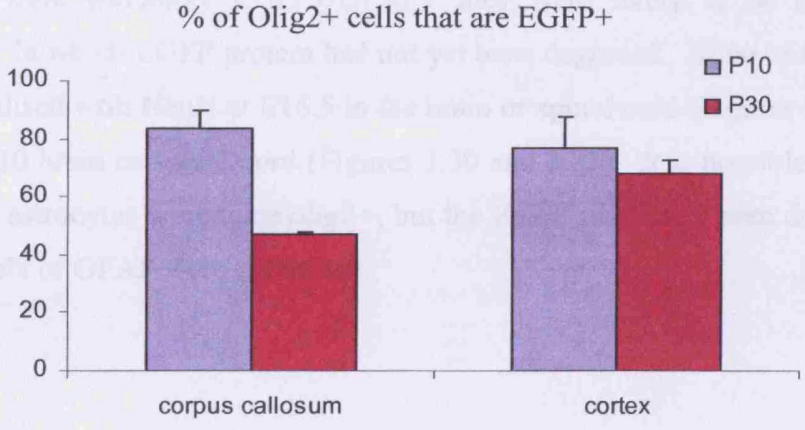

Figure 3.24 Olig2 and EGFP co-localisation in the postnatal transgenic brain as determined by immunohistochemistry. The proportion of Olig2+ cells co-expressing EGFP dramatically decreased between P10 and P30 in the corpus callosum while the proportion of Olig2+/EGFP+ cells (with respect to the total number of Olig2+cells) remained fairly similar in the cortex between P10 and P30. At P10, there was 84% co-localisation in the corpus callosum and 77% in the cortex. At P30-45, there was 47% co-localisation in the corpus callosum and 68% in the cortex. Founder line 26/6.

3.2.9 Confirming the identity of EGFP+ cells in the brain and spinal cord

To further examine the identity of the EGFP+/Olig2+ cells, brain and spinal cord sections were stained with anti-GFP along with either anti-PDGFRα (OLP marker), anti-GFAP (generic astrocyte marker) or anti-NeuN (neuronal marker) antibodies.

In both spinal cord and brain sections, 100% of PDGFRα+ cells co-expressed EGFP at E13.5 (Figure 3.25 and 3.26). However, in the VZ of the brain and spinal cord at E13.5 there were a number of cells that were EGFP+/ PDGFRα -. These could have been early OLPs that had not yet up-regulated PDGFRα or *Olig2*+ progenitors that were not of the oligodendrocyte lineage. GFAP was only looked for in the postnatal animal since expression is weak embryonically. At P10 there was no clear co-localisation of EGFP and GFAP in the brain or spinal cord (Figure 3.27). Some overlap between EGFP+ nuclei and GFAP+ processes was observed in the corpus callosum of the brain and periphery of the spinal cord, but it was difficult to determine whether they belonged to the same cell since cell density was high and assignment of a nucleus to GFAP+ processes was problematic. Since some astrocytes are reported to be derived from *olig2*+ precursors, it is likely that if any of these cells were genuinely EGFP+/GFAP+ they were likely to be such lineal descendants, in which EGFP protein had not yet been degraded. None of the EGFP+ cells co-localised wtih NeuN at E16.5 in the brain or spinal cord (Figures 3.28, 3.29) nor in the P10 brain or spinal cord (Figures 3.30 and 3.31). It is possible that some neurons and astrocytes were once *olig2*+, but the EGFP may have been degraded by the time NeuN or GFAP were expressed.

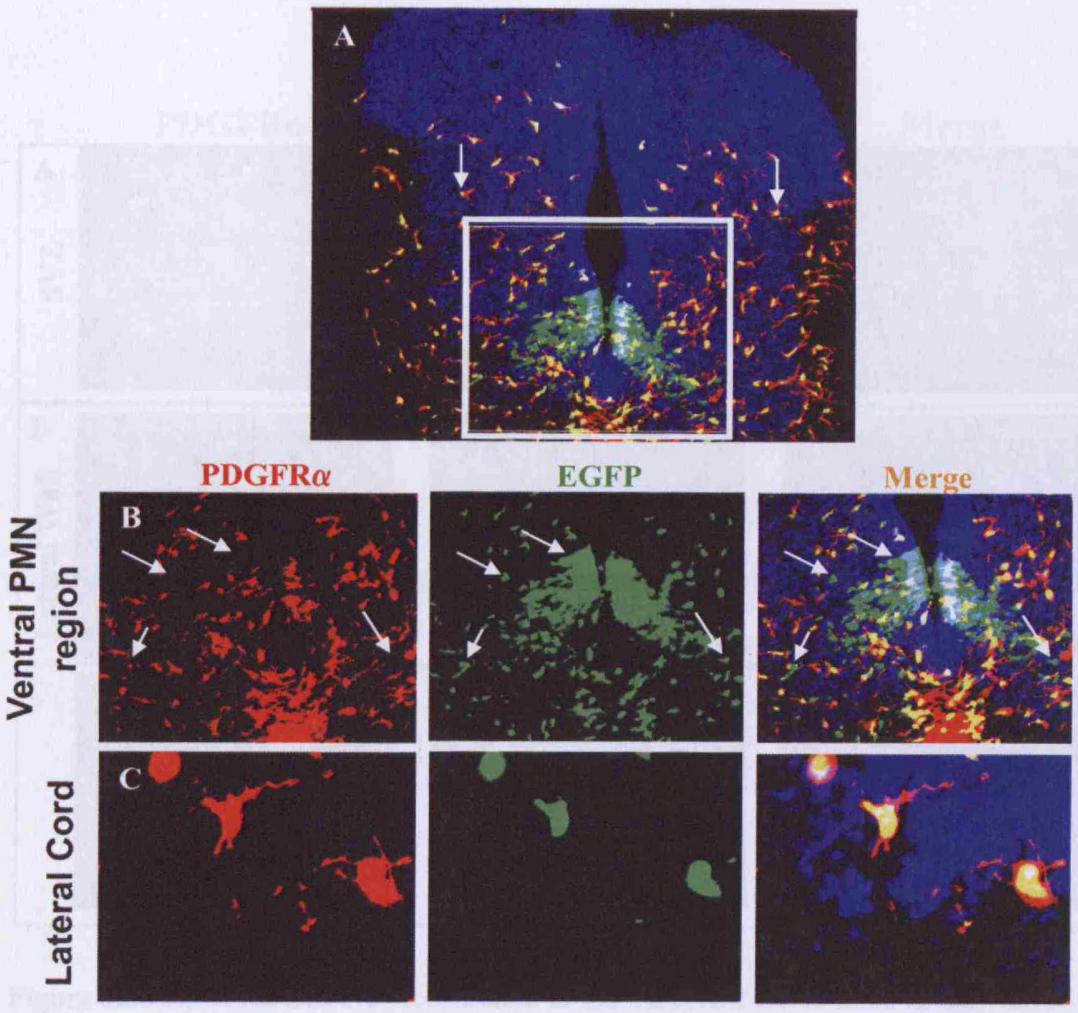

Figure 3.25 PDGFRα/EGFP co-localisation in the transgenic E13.5 spinal cord as determined by immunohistochemistry. 100% of PDGFRα+ cells were EGFP+. These were seen dispersing dorsolaterally from the pMN domain (arrows, panel A). There were, however, many EGFP+/PDGFRα- cells within the pMN domain (arrows, panel B). All EGFP+ cells found more lateral to the pMN co-expressed PDGFRα as shown in panel C. Founder line 26/6.

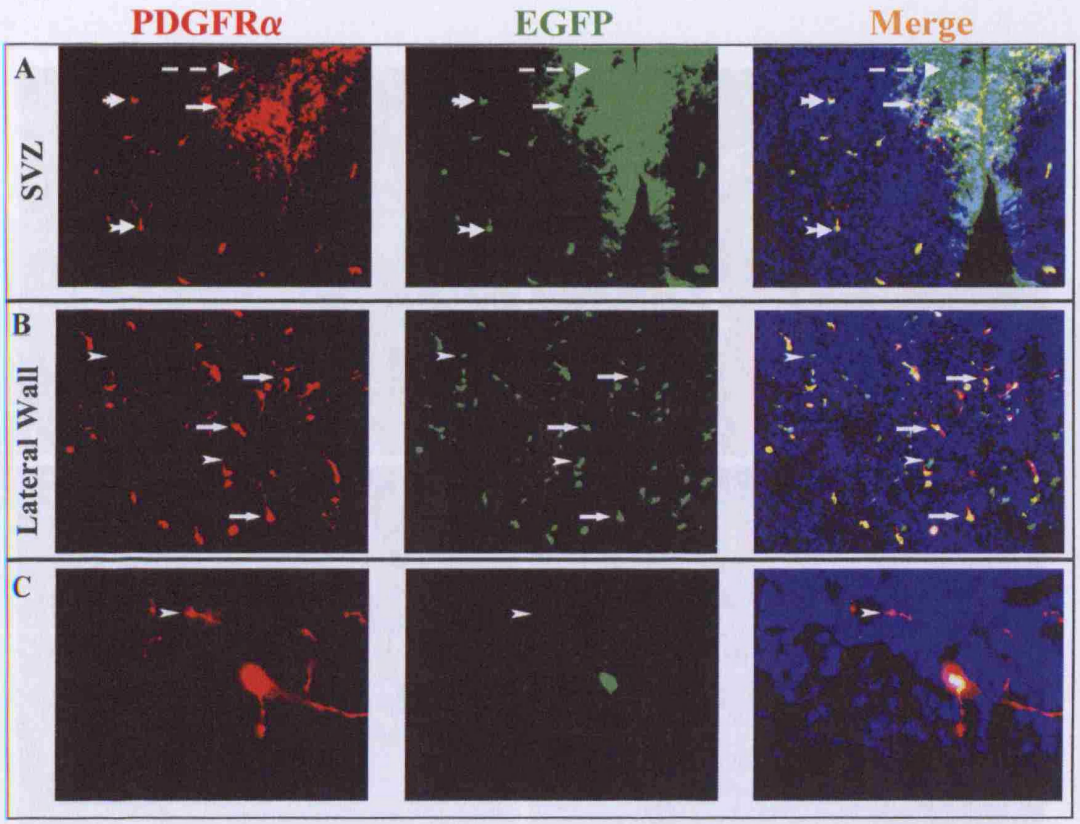

Figure 3.26 PDGFRα/EGFP co-localisation in the transgenic E13.5 brain as determined by immunohistochemistry. All PDGFRα+ cells co-labelled for EGFP (solid arrows A,B). Although some cells appeared PDGFRα+/EGFP- (arrow heads C), upon closer inspection, it was clear that these were cells in which the nucleus has not been included in the section and the PDGFRα+ staining was of cell processes where the presence of EGFP could not be identified. Within the VZ there were many cells that were EGFP+/ PDGFRα- (dotted arrow panel A) and there was the occasional cell that appeared EGFP+/ PDGFRα- in more lateral positions as well (arrow heads, panel B). Founder line 26/6.

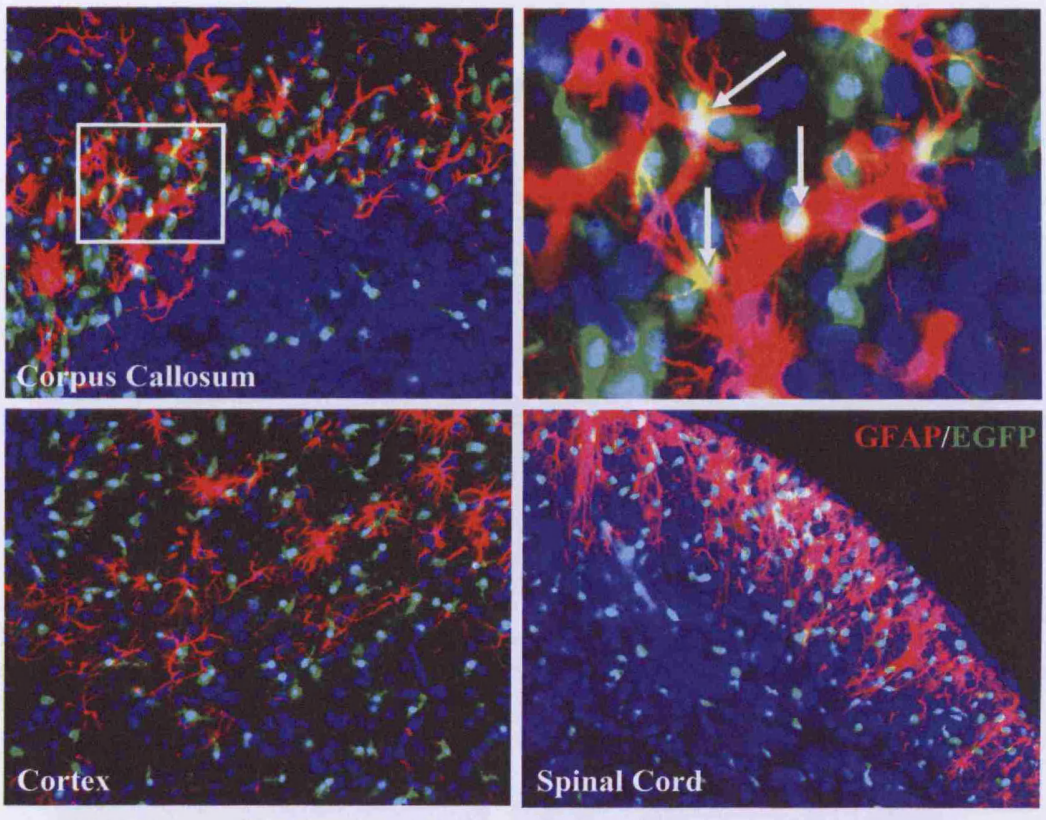

Figure 3.27 EGFP and GFAP expression in the P10 transgenic brain and spinal cord as determined by immunohistochemistry. There was no obvious co-localisation of EGFP and GFAP in the brain or spinal cord at this age. There were instances where GFAP+ processes were proximal and overlapping with EGFP+ nuclei, but these could not be clearly assigned to the same cell (arrows in the magnified image of the inset from the corpus callosum panel). Pictures were taken at low exposure for GFAP fluorescence since it otherwise saturated the image. Therefore, there appeared to be little/no staining in the grey matter of the spinal cord, but at higher levels of exposure, it could clearly be seen and there was no co-localisation with EGFP Founder line 26/6

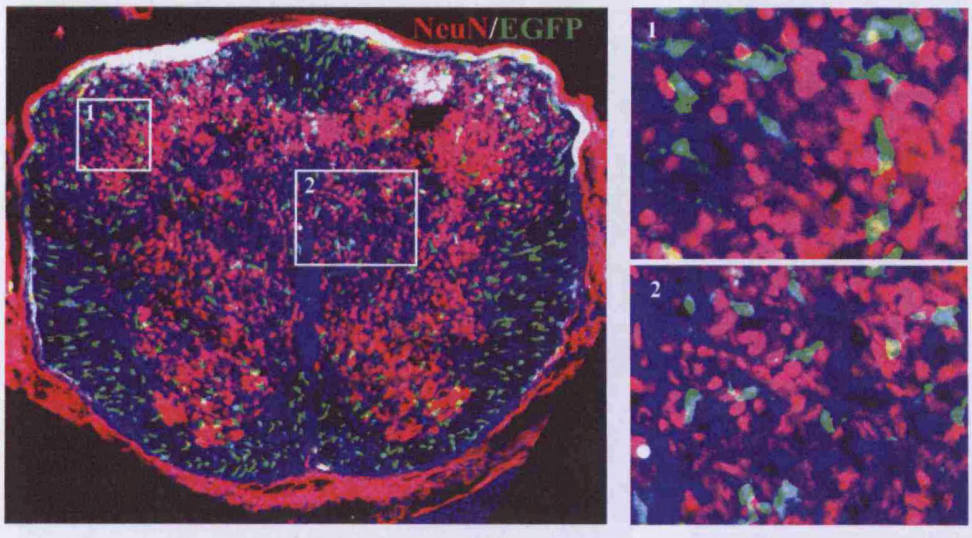

Figure 3.28 NeuN and EGFP expression in transgenic E16.5 spinal cord as detected by immunohistochemistry. There was no co-localisation between NeuN and EGFP in the spinal cord at this age.

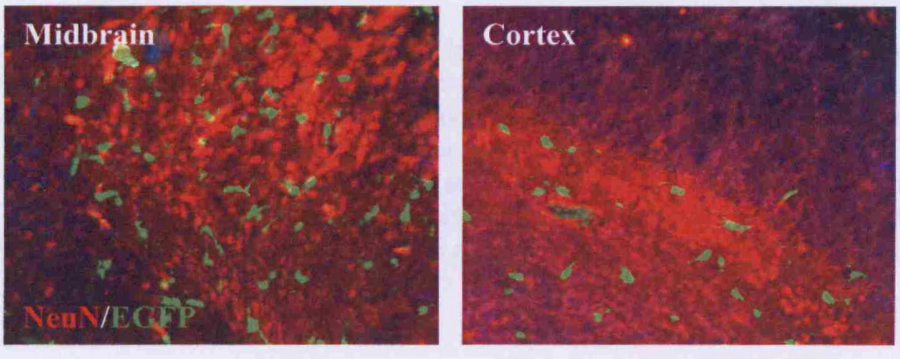

Figure 3.29 NeuN and EGFP expression in the transgenic E16.5 brain as detected by immunohistochemistry. There was no co-localisation between NeuN and EGFP in the brain at this age.

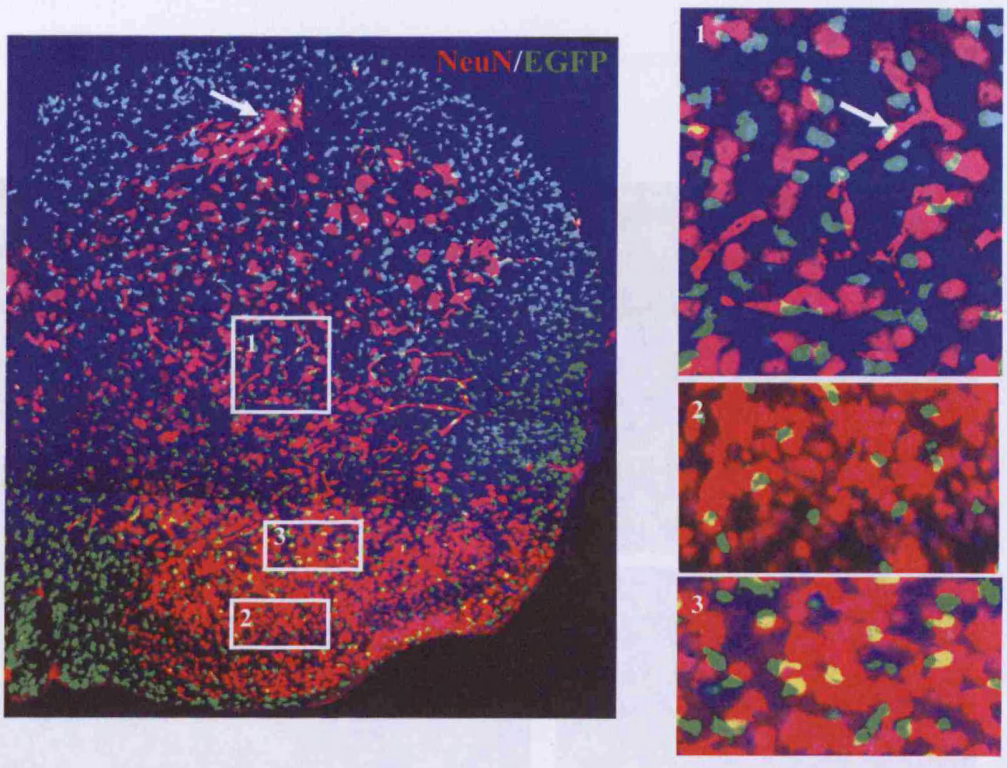

Figure 3.30 NeuN and EGFP expression in the P10 transgenic spinal cord as detected by immunohistochemistry. There was no co-localisation of NeuN and EGFP at this age. Although at first glance there appeared to be some co-localisation, upon closer inspection, it could be seen that this was simply two nuclei close together (inset 2 and 3). The sections were thick (30 μm), meaning that nuclei at different levels throughout the slice could be seen. There were also some blood vessels (arrow in main panel and inset 1) which, when nearby an EGFP+ cell, gave the impression of co-localisation. Founder line 26/6.

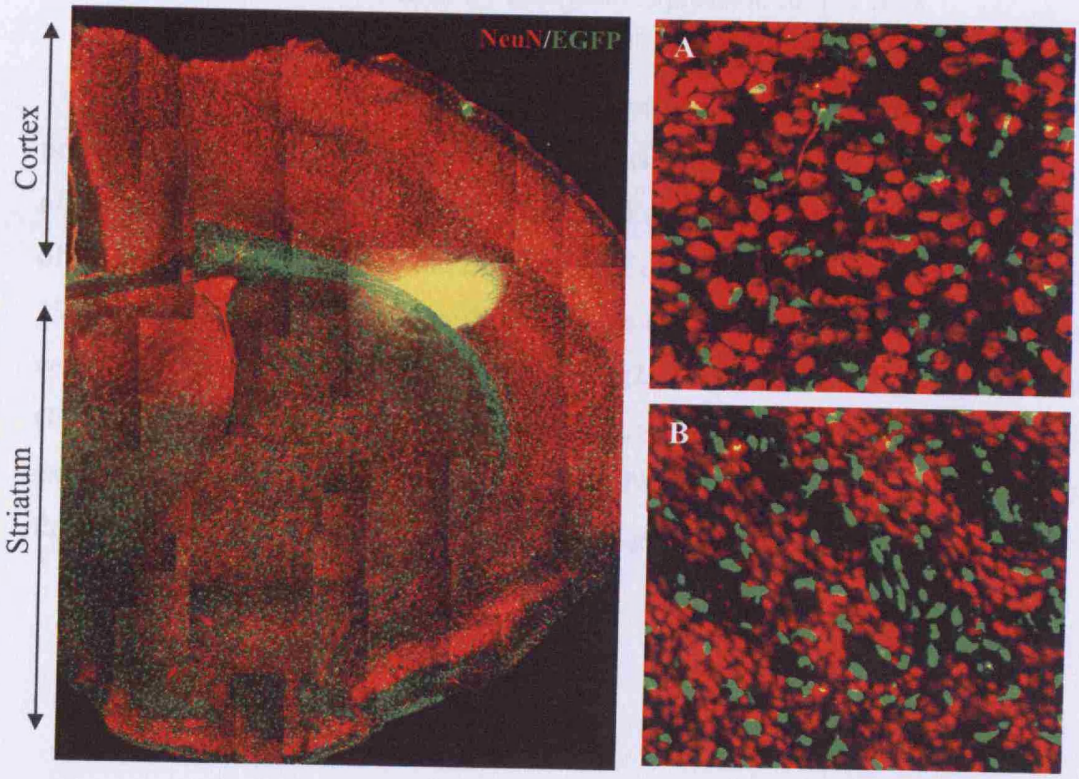

Figure 3.31 NeuN and EGFP expression in the transgenic P10 brain as determined by immunohistochemistry. There was no co-localisation in either the striatum (A) or in the cortex (B).

3.2.10 *In vitro* analysis of EGFP expression

To confirm that EGFP+ cells were bright enough to be useful for live cell imaging, expression was visualised *in vitro*. Smears of spinal cord tissue from freshly killed transgenic mice were examined directly for EGFP fluorescence in live cells. Individual fluorescent cells were visible in the light microscope when spinal cord cells were dissociated. When plated onto Poly-D-Lysine-coated petri dishes the EGFP could also be directly visualised by time-lapse microscopy, confirming that the EGFP could be used to identify transgene expression in live cells.

To determine whether EGFP could be induced in culture in parallel with *olig2*, I prepared cultures from transgenic embryos as follows: E13.5 cerebral cortex from *olig2-EGFP* transgenic mice were dissociated and the NEPs cultured in the presence of 10 ng/ml FGF2 to induce the expression of *olig2* (Kessaris et al., 2004;Qian et al., 1997). EGFP was visualised within 24 hours of plating the cells at which point the cells were fixed and counterstained for Olig2; 100% co-localisation was observed (Figure 3.33). These data confirm that *olig2* induction was mirrored by EGFP expression in this culture paradigm and that NLS:EGFP transgene expression could therefore be used as a reliable surrogate for *olig2* in culture.

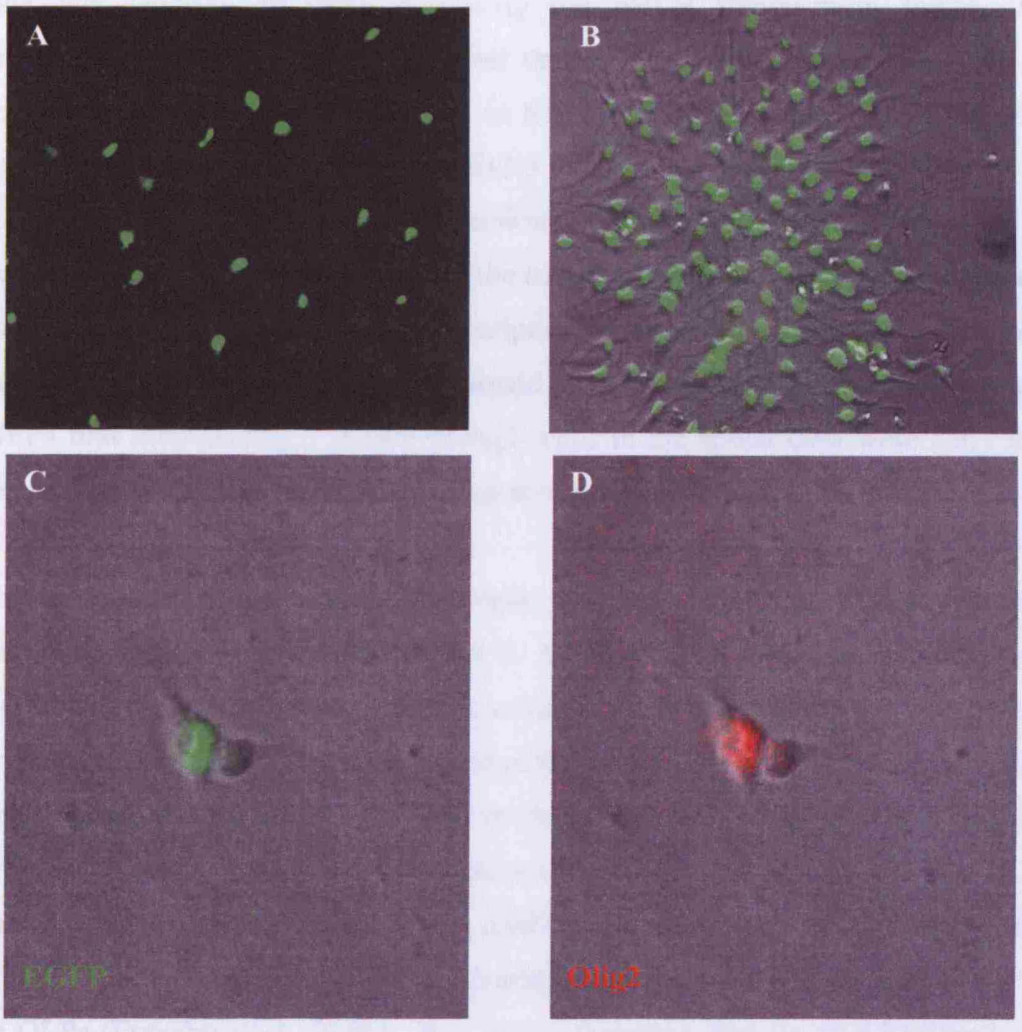

Figure 3.32 Live imaging of EGFP. (A) EGFP+ cells from a smear of spinal cord cells obtained after acute dissection from a transgenic P10 mouse. The EGFP in these cells was imaged directly using a fluorescence microscope. (B) Cells induced to express *olig2,* and therefore the transgene in culture, imaged directly using time-lapse microscopy. To ensure that the first appearance of EGFP corresponded to expression of Olig2 protetin, cortical NEPs cultured in 10 ng/ml FGF-2 were filmed using time-lapse microscopy. Upon the first appearance of EGFP fluorescence (C) the cells were fixed and counter-stained for Olig2 (D). Every EGFP+ cell was Olig2+ and there were no Olig2+/EGFP- negative cells.

3.3 DISCUSSION

3.3.1 EGFP co-localisation with Olig2 in transgenic mice

The aim of the work described in this chapter was to generate a transgenic mouse line that labelled all cells expressing the bHLH transcription factor *Olig2*. Immunohistochemical analysis showed that EGFP expression in the spinal cord mirrored that of endogenous *Olig2*. At E10.5 all Olig2+ cells co-expressed EGFP and vice versa. However, at E13.5 there were also EGFP-/Olig2+ and EGFP+/Olig2- cells in spinal cord sections. The presence of EGFP-/Olig2+ cells could be due to lack of expression of the transgene in some Olig2+ cells, although it is more likely due to a delay in transcription of the transgene with respect to *olig2* since most EGFP-/Olig2+ cells were found close to or within the VZ which is where NEPs first activate *olig2*. EGFP+/Olig2- cells in the spinal cord were early motor neurons as revealed by the fact that they co-expressed MNR2.

Expression in the brain was more complex than in the spinal cord, with appearance of EGFP being delayed with respect to Olig2 protein, although there was more EGFP/Olig2 overlap in more posterior sections and in migrating Olig2+ cells outside the VZ. This is consistent with the idea that activation of transgene expression is simply delayed relative to *olig2*. As in the spinal cord, some EGFP+/Olig2- cells were also found in the brain. It is known that *olig2*+ precursors give rise to both motor neurons and OLPs in the spinal cord (Lu et al., 2002;Takebayashi et al., 2002) and there is also evidence that *olig2*+ precursors in the brain produce neurons as well as OLPs (Furusho et al., 2006). It is likely, therefore, that the EGFP+/Olig2- cells identified here were derivatives of *olig2*+ precursors that had recently down-regulated *olig2* and were not destined to generate OLPs. The question of their identity still remains as there was no co-localisation between EGFP and GFAP or NeuN in the embryo or the adult. However, EGFP might have degraded by the time these markers were expressed. Thus, although most EGFP+ cells are of the oligodendrocyte lineage (as confirmed by PDGFRα labelling), there are populations derived from *Olig2*+ precursors that must belong to other lineages. This should be investigated further. Markers that could be used include Doublecortin to identify neuroblasts, Nestin or Glast to identify early NEPs and S100β for astrocytes.

3.3.2 EGFP expression in the adult

100% of EGFP+ cells co-expressed Olig2 in adult (P30-45) transgenic mice suggesting that, in the adult, all EGFP+ cells are of the oligodendrocyte lineage. This, however, constitutes only 50-70% of the total Olig2+ cells in the adult. Down-regulation of transgene expression in adult cells is not uncommon (Johansen et al., 2002;Pettersson et al., 1989). The insertion site of the transgene can influence the dynamics of expression (Clark et al., 1994). It is also possible that regulatory control of *olig2* differs in the adult and embryo and the transgene might not contain the elements required for accurate expression in the adult.

3.3.3 EGFP expression *in vitro*

Given the discrepancies between transgene vs. endogenous *olig2* expression *in vivo*, it was important to ascertain whether the transgenic mouse was suitable for use as a reporter in an *in vitro* assay. I found that 100% of Olig2+ cells that were specified *in vitro* in response to FGF-2 also expressed EGFP, confirming that the transgene contained the necessary regulatory elements for induction in vitro, and was therefore suitable to use in the time-lapse microscopy experiments described in the next chapter.

Chapter 4

Time-lapse microscopy of neuroepithelial precursor cells in vitro

4.1 Introduction

4.1.1 Chapter overview

The ability of multipotent neuroepithelial precursor cells (NEPs) to give rise to specific neurons and glia at particular times and spatial locations is likely the result of a combination of both cell-intrinsic properties and environmental cues. Many experiments designed to investigate this look at single time-points; analysis of single time points in cultures and fate mapping of labelled populations *in vivo*. The aim of the work described in this chapter was to use time-lapse microscopy to investigate the real-time behaviour of single embryonic cortical NEPs as they divide and differentiate *in vitro* in response to the mitogen FGF-2 (for experimental details see chapter 2 methods and materials, section 2.9).

4.1.2 Introduction to FGF-2 in development

As discussed in chapter 1, members of the FGF family have a catalogue of roles throughout development of the mammalian central nervous system (CNS). FGF-2 is well documented as being involved at multiple stages within the oligodendrocyte lineage (Bansal et al., 1996;Bansal, 2002;Fortin et al., 2005), but of interest here is the potential involvement of FGF-2 in regulating the initial specification of OLPs from NEPs. Developmentally, most OLPs are derived from ventral zones of the CNS (Qi et al., 2002;Richardson et al., 1997;Rowitch et al., 2002;Tekki-Kessaris et al., 2001;Woodruff et al., 2001), their specification critically depending on Sonic Hedgehog (SHH) signalling (Agius et al., 2004;Alberta et al., 2001;Orentas et al., 1999;Tekki-Kessaris et al., 2001;Wijgerde et al., 2002). However, there are also dorsal sources of OLPs which are thought to contribute 10-15% of all

oligodendrocytes in the spinal cord and up to 50% in the forebrain by birth (Fogarty et al., 2005;Kessaris et al., 2006;Richardson et al., 2006) and these are likely to be derived via a SHH-independent mechanism. FGF-2 is a possible candidate for such SHH-independent oligodendrogenesis since it has been shown to induce OLPs *in vitro* from dorsally derived NEPs from the embryonic brain and spinal cord even in the absence of SHH signalling (Chandran et al., 2003;Gabay et al., 2003;Kessaris et al., 2004). Furthermore, Naruse et al (Naruse et al., 2006) recently demonstrated that injection of FGF-2 into cerebral ventricles of E13.5 mouse embryos (time of onset of gliogenesis) induced the precocious emergence of OLPs in the dorsal forebrain of recipient mice, providing *in vivo* evidence for an otherwise culture-based phenomenon.

4.1.3 FGF-2 - mitogenesis vs. cell fate induction

FGF-2 is classically described as a mitogen and is thought to promote cortical precursor proliferation by increasing the rate of transition from G1 to S phase (Li and Cicco-Bloom, 2004). *In vivo*, ectopic exposure of mouse embryonic cortical ventricular zones to FGF-2 at E13 causes a 70-80% increase in the number of glia found in the postnatal brain (Vaccarino et al., 1999), while characterisation of FGF-2-/- knockout mice reveals a much reduced brain size with far fewer neurons and glia than in controls (Murtie et al., 2005;Raballo et al., 2000). Such experimental data leads to the idea that FGF-2 regulates cell number and evidence suggests that this is largely due to effects on cell division since no differences are seen in levels of apoptotic markers, but many more cells are seen to be entering S phase in the presence of FGF-2 (Vaccarino et al., 1999). As well as its role as a mitogen however, FGF-2 signalling is also known to affect cell migration, survival and cell fate determination (Bansal et al., 2003;Besser et al., 1995;Boilly et al., 2000;Ford-Perriss et al., 2001;Fortin et al., 2005;Gabay et al., 2003;Ornitz and Itoh, 2001;Yamaguchi and Rossant, 1995). Of relevance here, it has been shown *in vitro* that FGF-2 induces the expression of *olig2* and the generation of OLPs in cortically derived NEPs within 24 hours of culture (Kessaris et al., 2004;Qian et al., 1997). These *olig2*+ cells are presumed to go on to differentiate into mature oligodendrocytes as identified by markers such as O4 and NG2. Furthermore, increasing numbers of *olig2*+ cells are generated in the presence of higher concentrations of FGF-2 indicating a dose-dependent response. This could be

attributed to increased *olig2* induction, cell division, cell survival or all of the above. One ligand can certainly initiate a range of responses depending on the nature of the receptive cell and its environment. One way of altering a cell's response to a ligand is to alter the potency or duration of ligand binding. An example of this is in neurons and neural networks, in which sustained signalling events result in long term changes in a neuron's transcriptional profile and activity (long term potentiation), whereas transient signals result in short-term intracellular responses (Bliss and Collingridge, 1993). This is also well-described for cell responses to neurotrophin signalling through tropomysin-related kinase (Trk) receptors which promote cell differentiation through sustained signalling events and proliferation through more transient receptor activation (Arevalo et al., 2004;Marshall, 1995). The separation of cell responses to FGF-2 signalling has been documented (Bailly et al., 2000;Boilly et al., 2000;Boilly et al., 2000;Isacchi et al., 1991;Piotrowicz et al., 1999) and there is evidence that different intracellular events are initiated via reception of different bandwidths of FGF-2 concentration (Garcia-Maya et al., 2006).

Another way of achieving differential responses to a given ligand is to alter the receptor compliment of the cell (Lillien and Cepko, 1992;Lillien and Wancio, 1998;Sun et al., 2005). The differential responses of oligodendrocytes to FGF-2 at different stages of differentiation, for example, are meditated via signal transduction through different receptors isoforms as discussed in chapter 1. Recruitment of different signalling pathways downstream of the receptor can also modulate the intracellular responses that are elicited. An example of this is again provided by FGF-2 signalling, since proliferation and migration can be initiated through separable intracellular pathways in a variety of cell types (Besser et al., 1995;Daviet et al., 1990;Piotrowicz et al., 1999;Presta et al., 1989;Sa and Fox, 1994). Pharmacological analysis has indicated that proliferation is commonly induced via activation of protein kinase C (PKC), but a unique pathway for differentiation (of fibroblasts) or migration has not been identified, nor has the mechanism by which different pathways may be recruited independently through activation of a common receptor isoform. The presence/absence of cofactors can also affect the result of the application of a ligand to a cell and heparin sulphate proteoglycans (HSPG) are frequently a critical component of FGF signalling (Barolo and Posakony, 2002;Brickman et al., 1995;Granerus et al., 1993;McKeehan et al., 1999;Nurcombe

et al., 2000). Finally, the extracellular matrix can also affect cellular responses to a ligand. Components of the extracellular matrix can be involved in localising and concentrating ligands in the vicinity of receptive cells and might also take part in signalling events themselves (Barolo and Posakony, 2002;Ingber and Folkman, 1989;Kanda et al., 1999). Thus, a given signalling pathway may be redeployed several times over and yet elicit different cellular effects (Barolo and Posakony, 2002).

4.1.4 Age-dependent changes in response to signalling in development

Edlund and Jessell proposed that, during development, cells undergo a transition from being dependent on exogenous signalling for fate decisions to a cell-intrinsic programme (Edlund and Jessell, 1999). Various developmental systems illustrate this idea with multipotent progenitors at early stages becoming fate-restricted and less responsive to exogenous signals over time (Lo and Anderson, 1995). In CNS development, during which neurons are born before glia, it is possible that there is a time-dependent change in the properties of neural progenitors such that they become inherently more likely to generate glia; alternatively, the environment might change and become more favourable to gliogenesis with time. The environment of cells in the developing embryo is constantly changing with differential availability of extracellular ligands and matrix components which, as discussed above, can elicit various intracellular responses. As a consequence, receptive cells will alter their complement of activated proteins and gene expression and will therefore likely respond differently to a given ligand at different stages of development. Differential responsiveness combined with differential availability of signalling molecules is a fundamental component of CNS patterning and development.

4.1.5 Sonic Hedgehog in CNS development

As a morphogen, Sonic Hedgehog (SHH) is required at a particular concentration for the induction of *olig2* in the pMN domain of the spinal cord (Orentas et al., 1999;Orentas et al., 1999;Poncet et al., 1996;Pringle et al., 1996). Moreover, there is no generation of *olig2*+ cells, OLPs or motor neurons in the spinal cord in the absence of SHH signalling (Alberta et al., 2001;Ericson et al., 1996). In the brain, early elimination of SHH signalling using a conditional mutant, results in both the absence of OLPs and of dopaminergic and serotinergic neurons. Elimination of SHH

at later embryonic ages however, results in these neurons being present, though in reduced numbers compared to wild type mice (Blaess et al., 2006;Dahmane et al., 2001). Thus, between E9 and E11 SHH is evidently important for some neuronal specification in the brain and its continuing presence is required for expansion of neuronal pools along with oligodendrogenesis. This is reminiscent of SHH signalling with respect to MN and OLP specification in the spinal cord pMN domain (Orentas et al., 1999). However, there are also differences between the requirements for SHH in the brain and in the spinal cord. For example, SHH is required for normal development of dorsal structures in the brain (Theil et al., 1999;Tole et al., 2000), whereas its absence in the dorsal spinal cord is a prerequisite for dorsal domain specification and ectopic dorsal SHH signalling leads to ventralisation of these domains. This could relate to the distribution of Gli protein isoforms (Gli1-3) in the brain since these are the main transducers of sonic hedgehog signalling and are thought to transduce SHH signalling differentially (Altaba et al., 2003;Jacob and Briscoe, 2003;Litingtung and Chiang, 2000;Litingtung and Chiang, 2000). The role of SHH signalling in dorsal brain specification is though to be mediated partly via Gli3A activity (Theil et al., 1999;Tole et al., 2000) as well as via repression of ventral cell types by Gli3R activity. The data I describe in this chapter includes analysis of the responses of dorsal cortical NEPs to SHH and FGF-2 with respect to *olig2* induction. SHH is also known to have both proliferative and cell survival effects (Cayuso et al., 2006;Charrier et al., 2001;Placzek et al., 1993;Rowitch et al., 1999) and these properties were therefore also assessed for both FGF-2 and SHH-treated cultures, using time-lapse microscopy.

This chapter also addresses potential of NEPs from cortices of different embryonic ages to respond to different concentrations of FGF-2 over 1-3DIV in order to analyse the responsiveness to FGF-2 with respect to OLP generation. While these experiments only indicate fate potential *in vivo*, they give an indication of the intrinsic ability of these cells to respond to FGF-2 signalling over a short time span.

4.2 RESULTS

4.2.1 Experimental paradigm for investigating the induction of *Olig2* in dorsal NEPs

Preparations of NEPs from the dorsal telencephalic cortex of E13.5 mice were prepared as described in chapter 2, section 2.9. This produced a single cell suspension of NEPs which did not give rise to Olig2+ cells (determined by immunolabelling with anti-Olig2 antibody) when cultured in medium without FGF-2 over 3 days *in vitro* (DIV), but generated many neurons in this time. If left over 7DIV, OLPs were eventually seen to be generated in the absence of FGF-2 However, when FGF-2 was added to the culture medium to a final concentration of 10 ng/ml, Olig2+ cells appeared within 24 hours (as determined by immunolabelling) followed by sequential emergence of late-OLP and oligodendrocyte markers over time (Figure 4.1). All cell preparations were cultured in a 1:1 mixture of Bottenstein and Sato's defined medium (Bottenstein, 1986;Bottenstein and Sato, 1979) with the same medium that had been conditioned over a dense cortical-cell culture prepared from E13.5 embryos. For full experimental details of the preparation of conditioned medium see chapter 2, section 2.9. This mixture of Bottenstein and Sato's defined medium combined with conditioned medium is named 'basic medium' and any supplements that were added are specified.

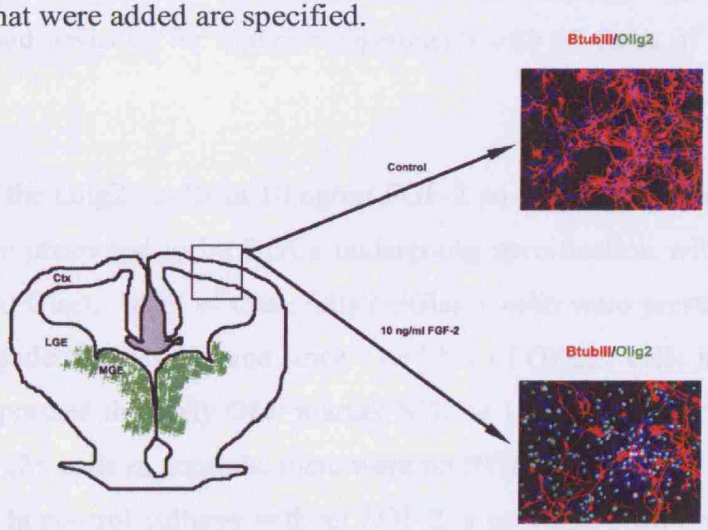

Figure 4.1 Schematic of the experimental culture set-up. The neocortex was excised to exclude the lateral and medial ganglionic eminences (LGE and MGE respectively) such that endogenous zones of oligodendrogenesis (shown in green) at this time were not included in the culture. When cultured in control conditions without FGF-2, no Olig2+ cells emerged over 3 days *in vitro* (DIV) and 100% of counted cells were β-tubulin III positive (red). Conversely, in the presence of 10 ng/ml FGF-2, the number of β-tubulin III+ neurons observed was reduced and many Olig2+ cells (green) were generated.

4.2.2 FGF-2 diverts NEPs from being neurogenic to gliogenic

In a preliminary characterisation of the cells in this culture set-up, immunolabelling was first performed on low density cultures seeded onto PDL-coated glass coverslips at a density of $1x10^4$ cells per coverslip, grown in either basic medium alone or basic medium treated with 10 ng/ml FGF-2. Both control and FGF-2-treated cultures were fixed at 1 or 3 DIV and assessed for the presence of Glast, Olig2, Dcx (Doublecortin) and β-tubulin III to identify radial glial cells (RGC), OLPs, neuroblasts and neurons respectively. At 1 DIV in controls there were no Olig2+ cells, but in the presence of 10 ng/ml FGF-2, 47 +/- 10% of the cells were Olig2+ (Figure 4.2 A, B). However, there were high numbers of Glast+ cells in both controls and FGF-2-treated cultures (Table 4.1; Figure 4.2 A, B).

	% of Olig2+ cells	% of Glast+ cells	% of Dcx+ cells	% of β-tubulin III+ cells
Control	0	69 +/- 12	95 +/- 3	88 +/- 10
10 ng/ml FGF-2	47 +/- 10	55 +/- 10	34 +/- 2	34 +/- 2

Table 4.1 Profile of markers expressed in E13.5 cortical NEP cultures at 1 DIV in control and FGF-2-treated preparations as detected by immunolabelling. Data is presented as mean +/- standard deviation for triplicate experiments with 10 fields of view analysed in each.

81 +/- 12% of the Olig2+ cells in 10 ng/ml FGF-2 co-expressed Glast (Figure 4.2 A) and these were presumed to be RGCs undergoing specification without having yet down-regulated Glast. Most of these Olig2+/Glast+ cells were presumed to go on to follow the oligodendrocyte lineage since 71 +/-5% of Olig2+ cells in FGF-2-treated cultures co-expressed the early OLP marker NG2 at 1 DIV. Corresponding with the absence of Olig2+ cells in controls, there were no NG2+ cells in control conditions at 1 DIV either. In control cultures without FGF-2, a neuronal profile was determined; 95 +/- 3% of cells in control cultures expressed the neuroblast marker Dcx and 88 +/- 10% of cells in controls expressed β-tubulin III (Figure 4.2 C, D) with all β-tubulin III+ cells co-expressing Dcx. Control cultures at 1 DIV were therefore predominantly neuronal. In contrast, in FGF-2-treated cultures only 34 +/- 2% of

cells expressed Dcx (with complete co-localisation with β-tubulin III), which was about 1/3rd of the percentage of Dcx+ cells in controls and none of which co-localised with Olig2. These data suggest that the starting population is inherently neurogenic in the absence of exogenous signalling, but that 10 ng/ml FGF-2 diverts NEPs from generating mostly neurons to generating both neurons and glia even by 1 DIV.

At 3 DIV in 10 ng/ml FGF-2, the number of Olig2+ cells had increased ~5-fold from 68 +/-8 cells per field of view at 1 DIV to 381 +/- 62 cells by 3 DIV which corresponded with a ~5-fold increase in total cell number (Figure 4.3 A, B). The number of β-tubulin III+ neurons doubled over the first two days *in vitro* and remained constant thereafter; 48 +/- 10 neurons at 1 DIV, 108 +/- 10 at 2 DIV, 97 +/- 20 at 3 DIV (Figure 4.3 A; P = 0.7 for number of neurons at 2 vs. 3 DIV). This indicates that neuronal progenitors divided once on average and gave rise to post-mitotic neurons in FGF-2-treated cultures. Conversely, in control conditions without FGF-2, there were no Olig2+ cells generated even by 3 DIV (Figure 4.3 C, D) and the increase in total cell number over 3 DIV was attributable to an increase in the number of β-tubulin III+ neurons; 158 +/- 9 neurons at 1 DIV, 356 +/- 77 at 3 DIV. By 3 DIV in these controls, 100% of the cell population was β-tubulin III+ neurons (Figure 4.3 D). These data indicate an initial induction of *olig2* in NEPs by FGF-2 signalling and a subsequent expansion of this *olig2*+ population.

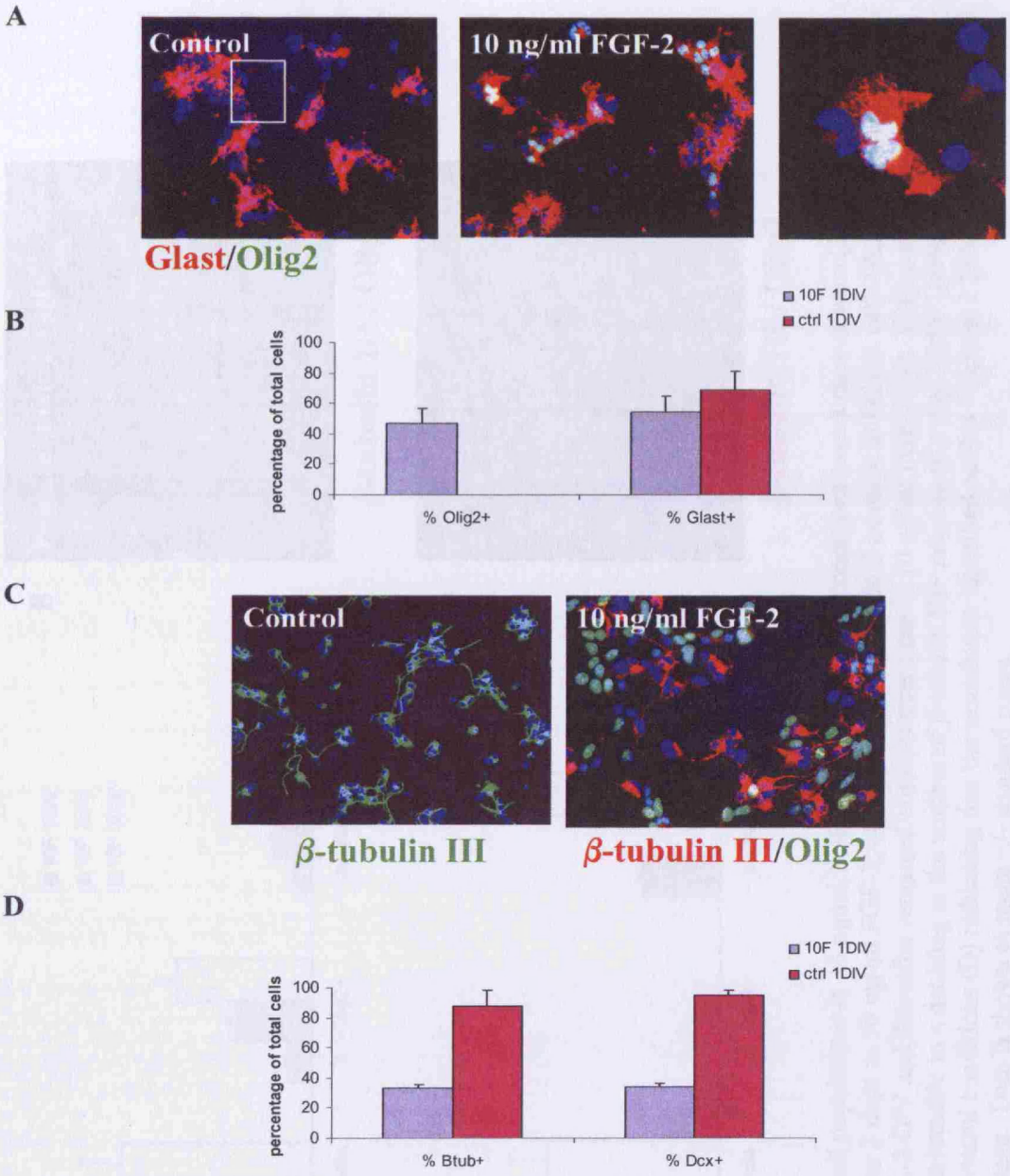

Figure 4.2 Immunolabelling of E13.5 cortical NEPs at 1 day in vitro (DIV) in control and FGF-2-treated conditions. Anti-Olig2, Glast, β-tubulin III and Dcx antibodies were used to identify presumptive glia, radial glial cells, neurons and neuroblasts respectively. 47 +/- 10% of cells expressed Olig2 at 1 DIV in 10 ng/ml FGF-2 (10F) while there were no Olig2+ cells in control conditions (A and B). More than 50% of cells in both conditions express Glast (B) with 81% of Olig2+ cells co-expressing Glast in 10 ng/ml FGF-2 (A middle and right panels). The proportion of β-tubulin III+ neurons was ~three times higher in controls than in FGF-2-treated conditions (C,D) and there was a corresponding distribution of Dcx+ cells (D). All β-tubulin III+ neurons co-expressed Dcx and there was no overlap of Olig2 with β-tubulin III or Dcx in FGF-2-treated cultures (C).

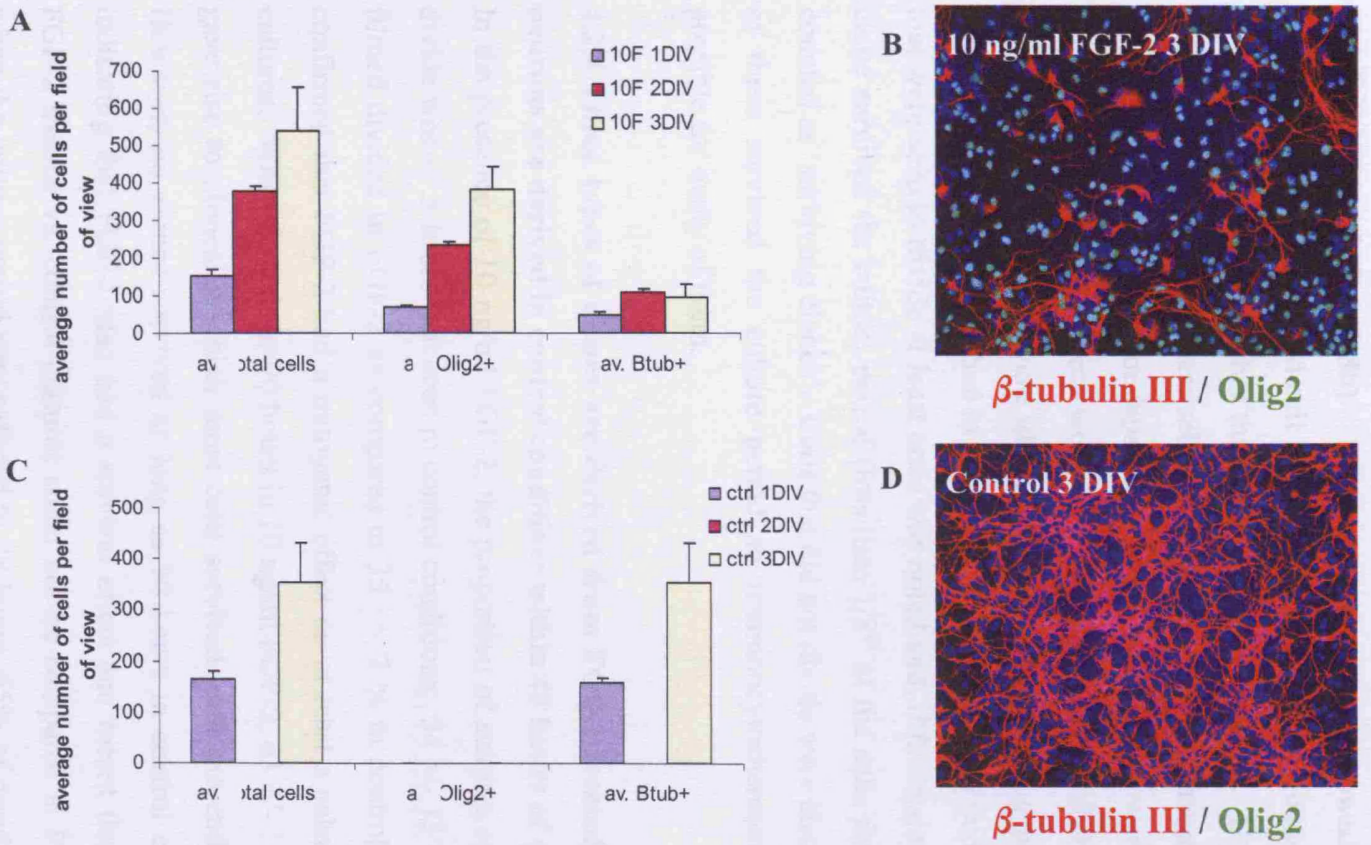

Figure 4.3 Characterisation of cell populations in 10 ng/ml FGF-2 (10F) and control conditions over 3 days *in vitro* (3DIV). Total cell population increased ~5-fold over 3 days in 10 ng/ml FGF-2, corresponding to a ~5-fold increase in Olig2+ cells (A,B). The number of β-tubulin III+ doubled from 1-2 DIV and thereafter remained constant over time in 10 ng/ml FGF-2 (A). Cell number increased in control conditions by ~2-fold, attributable to a doubling in the number of β-tubulin III+ neurons (C). By 3 DIV 100% of cells counted were β-tubulin III+ neurons in control conditions (D) indicating that the neuroblasts identified as Dcx+ cells at 1 DIV have given rise to post-mitotic neurons by this stage. Data is shown as mean +/- standard errors.

4.2.3 Time-lapse microscopy

NEPs were plated at clonal density ($1x10^4$ cells per ml of culture medium) onto 35 mm tissue culture dishes and were allowed to settle overnight before being transferred to the time-lapse set-up. This meant that the start of filming was at 18 hours after plating (18h). Previous experiments showed that there are no divisions over this time and cell survival is improved when cultures are left to settle in a standard incubator rather than in the time-lapse set-up. Up to 120 single cells within the culture dishes were selected to be filmed and an image was captured every 15 minutes to compile time-lapse movies so all divisions were recorded over the culture period. Lineage trees were drawn retrospectively and the cell types derived from each starting NEP were identified by immunolabelling performed within the time-lapse set-up as described in chapter 2, section 2.9. The number of starting cells that were seen to divide at least once was noted and, if the majority of cells within a clone survived the culture period (less than $1/8^{th}$ of the cells dying) then they were counted as 'surviving clones'. Cells that did not divide were also noted although few of these survived the culture period so immunocytochemical analysis was not possible for many of them.

4.2.4 Three types of clones are derived from FGF-2 treated cultures, but only neurons are derived in control conditions within 48 hours of culture

In the presence of 10 ng/ml FGF-2, the proportion of starting cells that was seen to divide was ~1.5-times that seen in control conditions; 54 +/- 13 % of the single cells filmed divided in FGF-2 as compared to 35 +/- 7 % in controls (Table 4.2). This confirmed that FGF-2 had a mitogenic effect on at least a subset of NEPs in these cultures. When filmed for 90 hours in 10 ng/ml FGF-2, 63 +/- 15% of dividing cells gave rise to clones in which most cells survived until the end of the experiment. However, no clones survived as long as 90 hours in control cultures (Table 4.2), indicating that FGF-2 also had a survival effect and meant that clonal analysis of FGF-2 treated vs. control cultures could not be compared at 90 hours. However, when the culture period was reduced to 48 hours, 65% of dividing cells in controls and 75 % in FGF-2 gave rise to surviving clones (Table 4.2). In 48 hour controls, 100% of dividing cells produce only β-tubulin III+ neurons (N-clones; Table 4.3; Figure 4.4 E, F, G).

	% of single cells that divided	% of clones that survived
Control – 48 hours	31 +/- 12	65 +/- 21
Control – 90 hours	40 +/- 18	0
10 ng/ml FGF-2 – 48 hours	47 +/- 8	75 +/- 4
10 ng/ml FGF-2 – 90 hours	62 +/- 24	63 +/- 15

Table 4.2 Comparison of the percentage of single cells in starting cultures that divided during the filming period and percentage of clones that survived for immunocytochemical analysis of control and FGF-2-treated preparations analysed at 48 and 90 hours. Data is presented as mean +/- standard deviation for triplicate experiments (5 experiments for 90 hour data).

	% O+	% O+/O-	%O-	% N
Control – 48 hours	-	-	100	100
10 ng/ml FGF-2 – 48 hours	62 +/- 20	29 +/- 15	9 +/- 5	9 +/- 5
10 ng/ml FGF-2 – 90 hours	46 +/- 15	34 +/- 13	21 +/- 13	0

Table 4.3 Summary of clone types produced in control and 10 ng/ml FGF-2-treated cultures over 48 and 90 hours. Of the surviving clones, the relative proportions of neuron-only (N), Olig2-only (O+), mixed (O+/O-) and Olig2-negative (O-) clones were calculated. Data is presented as mean +/- standard deviation for triplicate experiments (5 experiments for 90 hour data).

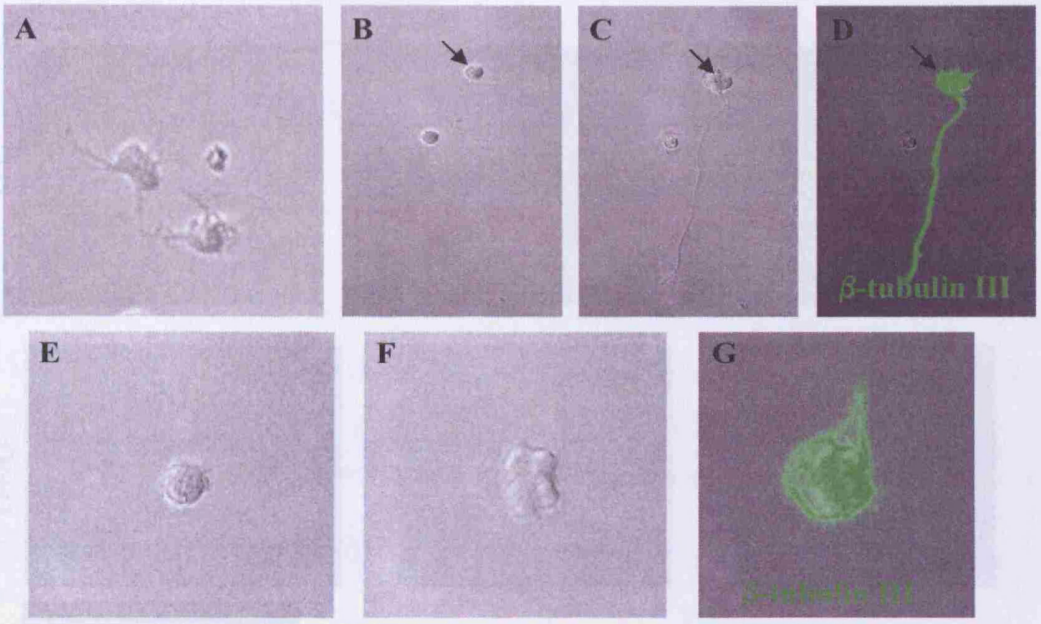

Figure 4.4 Analysis of 48 hour time-lapse cultures in control conditions. A) Brightfield image of a typical neuronal morphology observed for many non-dividing cells and dividing cells that did not survive the culture period. B,C,D are stills from a time-lapse movie of cells in control conditions showing a starting cell (B; arrow) that did not divide, but extended a long neurite by 48 hours (C) and stained for β-tubulin III (D; green). E,F,G are stills from a time-lapse recording of a dividing dedicated neuroblast in control conditions where a starting cell (E) divided twice to give 4 cells at 48 hours (F) which all stained for β-tubulin III (G; green).

In contrast, three main classes of clone types were derived from single cells in 10 ng/ml FGF-2; 62 +/- 10 % produced daughter cells which all expressed Olig2 protein (O+ clones; Figure 4.5 A, B, C), 29 +/-7 % produced a mixed population of daughter cells including Olig2+ and Olig2- cells (O+/O; Figure 4.5 D, E, F) and 9 +/- 3 % contained no Olig2+ cells at all (O- clones; Figure 4.5 G). At 48 hours, all cells in the O- clones in FGF-2-treated cultures were β-tubulin III+ neurons (N-clones) and were derived from 2-3 divisions, therefore yielding 8 neurons as a maximum. However, not all of the Olig2-negative cells in the O+/O- clones were β-tubulin III; some were Glast+ (Figure 4.5 E,F) and some were immunocytochemically unidentified (negative for GFAP, Glast and RC2). Thus, while control conditions yielded only neurons, only 9% of clones were N-clones in FGF-2, indicating that some NEPs were diverted from producing only neurons to being gliogenic in the presence of FGF-2, which is consistent with data from the coverslip cultures (section 4.2.2).

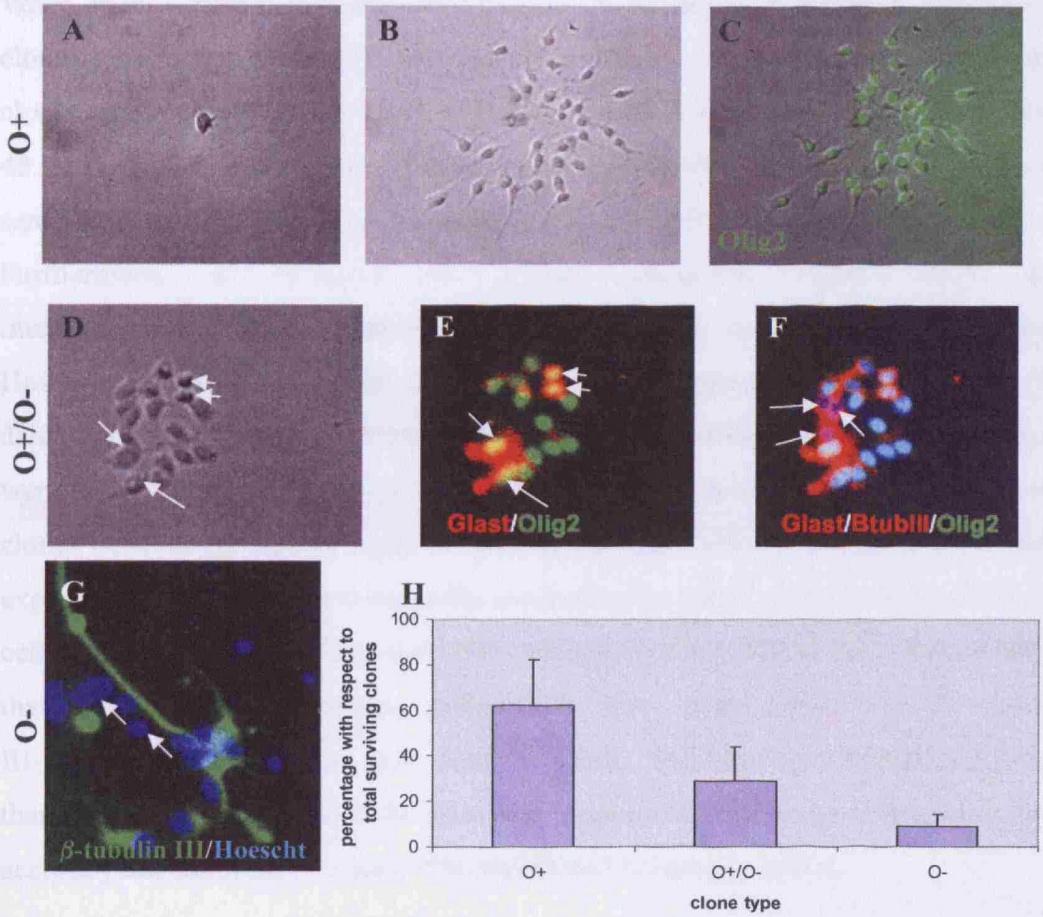

Figure 4.5 Clone types derived over 48 hours in 10 ng/ml FGF-2. An O+ clone derived from a single cell in the starting culture is shown as stills from a time-lapse movie in panels A-C. All the derived daughter cells were Olig2+ at 48 hours (C). Panels D-F, show an O+/O- clone (derived from a single cell) in which some of the Olig2+ cells co-localised with Glast (D,E; white arrows), and the Olig2-negative cells were β-tubulin III+ neurons (F; white arrows). An example of an O- clone in which all cells were β-tubulin III+ neurons is given in panel G. Hoescht-stained nuclei that were apparently β-tubulin III-negative (G; white arrows) were dead cells since they were pyknotic. A graphical representation of the distribution of clone types derived in 10 ng/ml FGF-2 is given in panel H.

Most non-dividing cells did not survive the culture period in either treated or control cultures and could therefore not be identified by immunocytochemistry. However, most of these cells had a morphology indicating that they were neurons since they had extended processes and large cell bodies (Figure 4.4 A). Of the non-dividing cells that did survive, 100% were β-tubulin III+ neurons in both conditions.

4.2.5 Clones change from being O+ to O+/O- in 10 ng/ml FGF-2 over time

When FGF-2-treated cultures were filmed for 90 hours, a different distribution of clone types was seen; 46 +/- 8 % were O+ clones, 33 +/- 6 % were O+/O- mixed clones and 21 +/- 6 % were O- clones (Figure 4.6). Compared to the data collected at 48 hours, the proportion of O+ clones was reduced, O+/O- clones were in about the same proportion, and the proportion of O- clones increased (Figure 4.6). Furthermore, at 90 hours O- clones contained Glast+ cells and/or immunocytochemically unidentified cells as well as β-tubulin III+ neurons. However, in 48 hour cultures, O- clones contained only neurons (N-clones). These data suggest that some β-tubulin III+ cells might de-differentiate over time as there were no neuron-only (N) clones at 90 hours. Since there was also a decline in O+ clones between 48 and 90 hours in culture, the data further indicates that the induced expression of *olig2* is not necessarily maintained in cells. Alternatively, since not all cells within a clone survived even over 48 hours, it is possible that some of the cells that died were multipotent progenitors that could give rise to β-tubulin III-negative/Olig2-negative cells over 90 hours. Cultures were not filmed for more than 90 hours since clone sizes grew too large to be able to trace lineages with any accuracy and cell death could not be monitored accurately either.

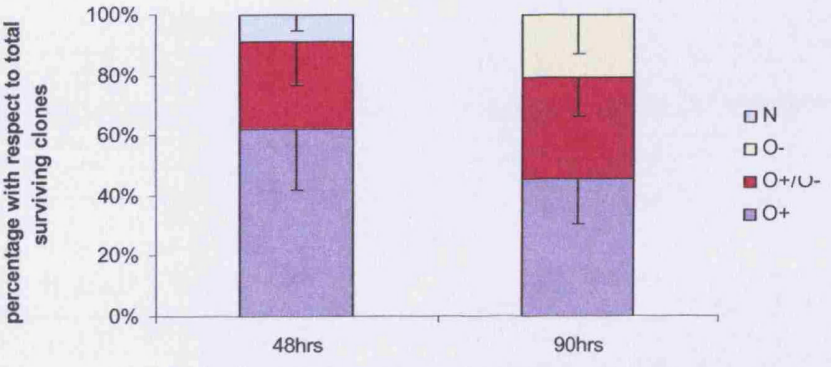

Figure 4.6 Differences in the distribution of clone types derived in FGF-2-treated cultures at 48 hours vs. 90 hours. The percentage of O+ clones was reduced at 90 hours while the percentage of O+/O- clones was roughly the same and the percentage of O- clones had increased. However, at the 90 hour time-point, while the number of O- clones had increased, they all contained both β-tubulin III+ neurons *and* unidentified cells, none of them contained only neurons (N clones). This is in contrast to the 48 hours time-point when all O- clones contained only neurons (N). Data is shown as mean +/- standard deviations.

4.2.6 *Olig2* can be induced at many points within a lineage

To investigate more closely how the different clone types were generated, where possible, lineage trees were drawn from time-lapse recordings.

Many clones demonstrated two distinct branches within a lineage, one O+ and the other O-. Such a lineage is shown in Figure 4.7 in which the two branches contain either only Olig2+ cells or only neurons, respectively. Other lineages gave rise to a mixture of Olig2+ and Olig2-negative cells in a much more irregular distribution as exemplified in Figure 4.8. Such a distribution of Olig2+ cells within a lineage could arise by both up-regulation and/or down-regulation of *olig2* expression at specific branch points and possibly also by induction at the level of the individual daughter cells.

A

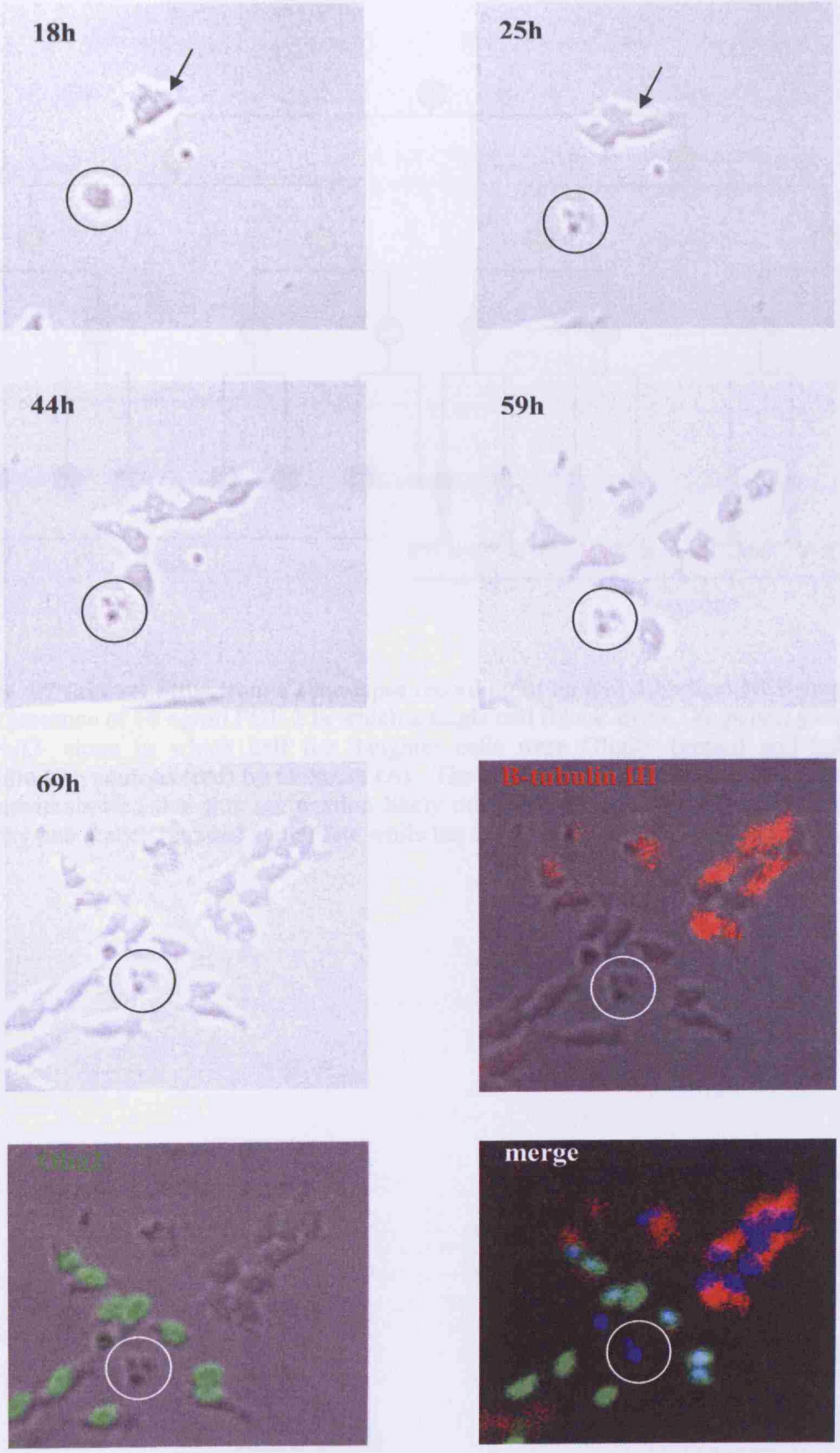

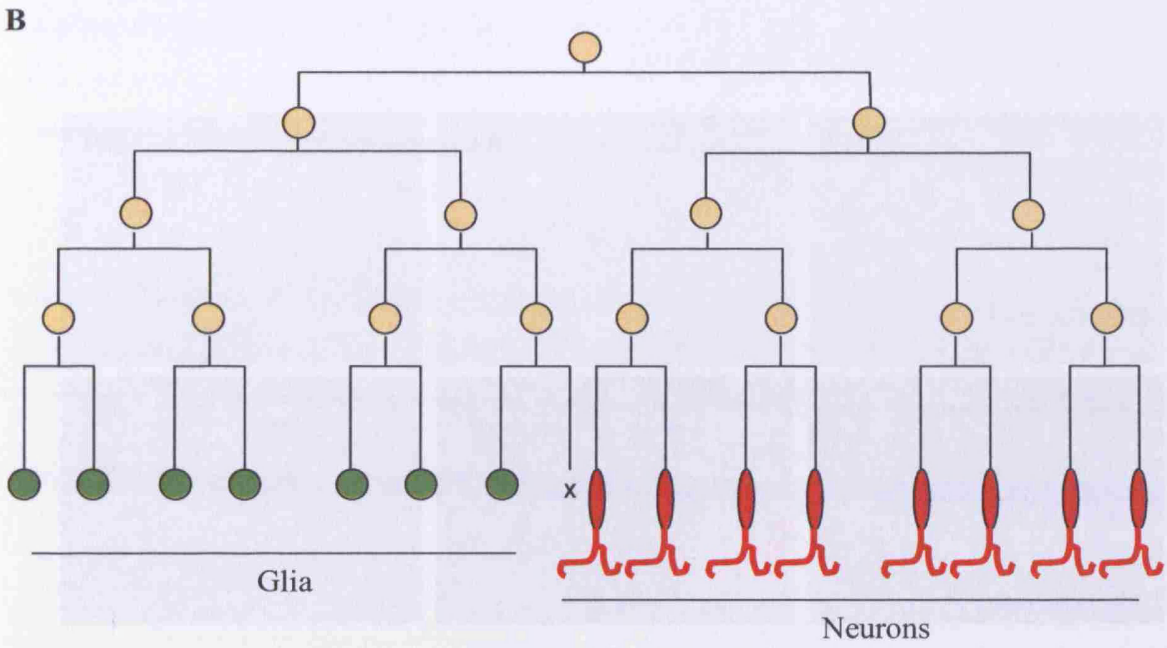

Figure 4.7 (above) Stills from a time-lapse recording of an E13.5 cortical NEP preparation in the presence of 10 ng/ml FGF-2 in which a single cell (black arrow 18h panel) gave rise to an O+/O- clone in which half the daughter cells were Olig2+ (green) and half were β-tubulin III+ neurons (red) by 69 hours (A). The retrospective lineage tree (B) drawn from this movie showed that this segregation likely occurred via an initial asymmetric division whereby one branch pursued a glial fate while the other was neuronal. X = dead cell

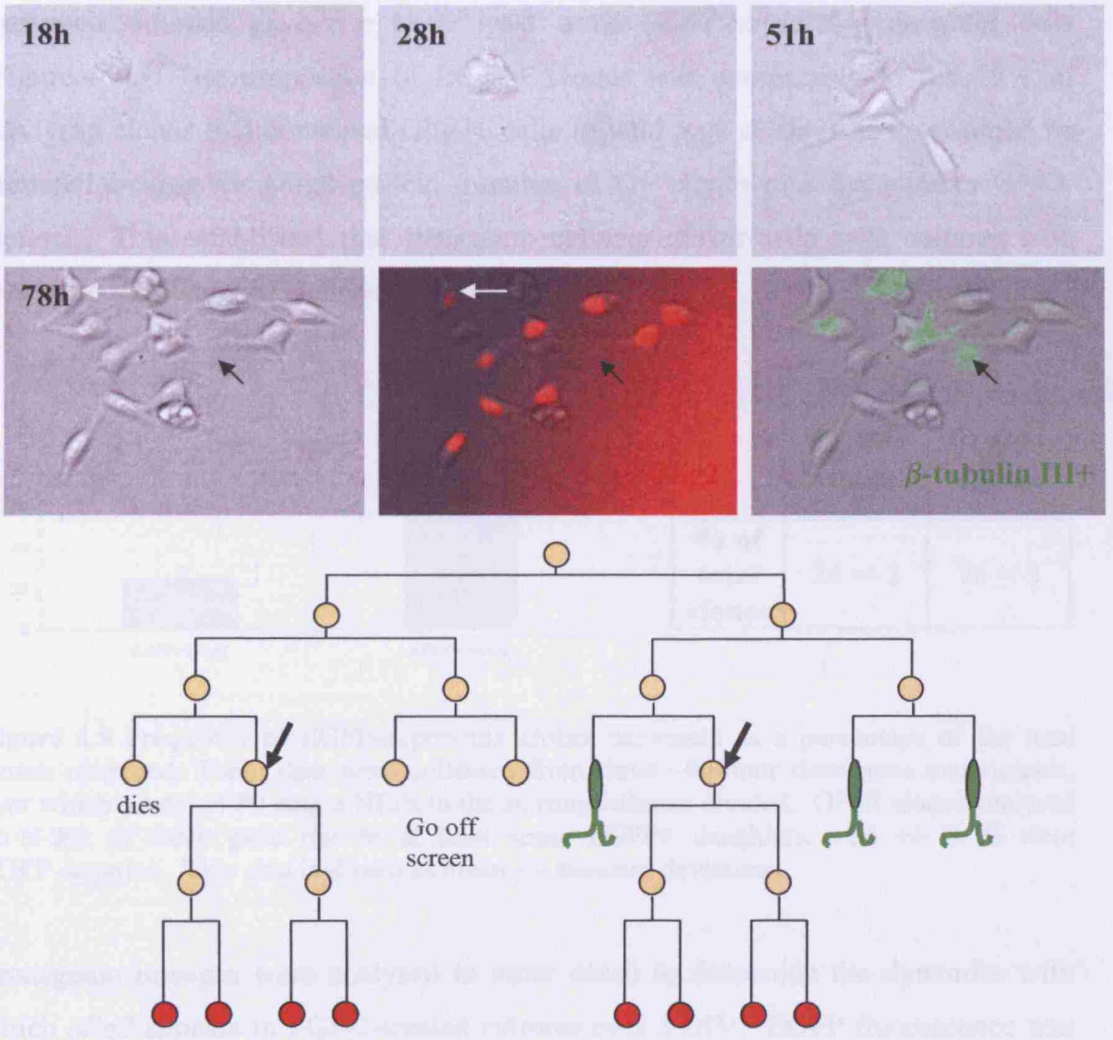

Figure 4.8 Stills and a lineage tree from a time-lapse recording of an E13.5 cortical NEP preparation in the presence of 10 ng/ml FGF-2 in which the distribution of Olig2+ cells in the final clone did not follow a regular pattern. The mixture of Olig2+ and Olig2-negative cells, including β-tubulin III+ neurons, indicated that *olig2* was probably up-regulated late in the lineage, possibly at the two branch points indicated by black arrows on the lineage tree. Note that the Olig2+ cell indicated by a white arrow at 78 hours migrated in from a neighbouring clone and did not belong to this lineage. The green fluorescence in the β-tubulin III-stained panel (black arrows on the stills) was not a cell, but an artefact.

To follow the dynamics of *olig2* expression in real time, *Olig2-EGFP* transgenic mice were used as a source of cells. It was first important however, to confirm that transgenic cultures behaved in a similar manner to wild type. Visualisation of EGFP fluorescence in real time determined that 76 +/- 3 % of dividing NEPs from transgenic animals gave rise to at least some *EGFP*-expressing daughter cells (Figure 4.9). The proportion of EGFP+ clones was comparable to the 79% of surviving clones that contained Olig2+ cells in wild type cultures as determined by immunolabelling for Olig2 protein (number of O+ clones plus the number O+/O- clones). This established that transgenic cultures mirror wild type cultures with respect to frequency of clones that express *olig2*.

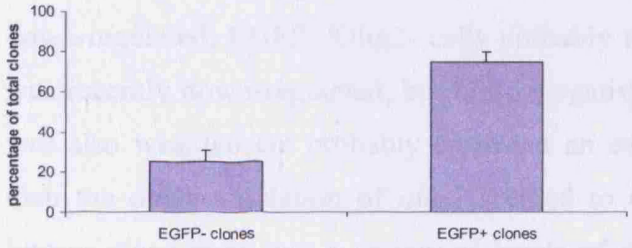

	EGFP- clones	EGFP+ clones
% of total clones	24 +/- 3	76 +/-3

Figure 4.9 Frequency of EGFP-expressing clones expressed as a percentage of the total clones observed. These data were collected from three ~90-hour time-lapse experiments, over which a total of 80 single NEPs in the starting cultures divided. Of all clones analysed 76 +/-3% of these gave rise to at least some EGFP+ daughters. 24 +/- 3 % were EGFP-negative. This data is shown as mean +/- standard deviations.

Transgenic lineages were analysed in more detail to determine the dynamics with which *olig2* appears in FGF-2-treated cultures over 3 DIV. EGFP fluorescence was recorded in real time and the cells were fixed at the end of the recording period to be immunolabelled for Olig2, β-tubulin III and Glast for clone classification (chapter 2, section 2.9).

Figure 4.10 is an example of an O+ clone in which the starting cell upregulated EGFP+ before the first division and maintained in all the daughter cells which were also Olig2+ at 90 hours.

Figure 4.11 is an example of an O+/O- clone which was apparently generated by asymmetric segregation of EGFP (and therefore Olig2) at an early point in the

daughter cells were EGFP+ after a couple of divisions, but the daughter cel
end of the experiment were both Olig2+ and Olig2-negative. Of the Olig2-r
cells, some retained strong EGFP fluorescence, some had weak EGFP fluor
and some had no EGFP fluorescence. Given the lag in EGFP protein degr
with respect to Olig2 protein described in chapter 3, this is an unsurprising
and could actually give an indication of how recently the *olig2* ha
down-regulated; EGFP+/Olig2- cells probably represent populations in whic
was recently down-regulated, but Olig2-negative cells in which EGFP fluor
was also weak/absent probably represent an earlier down-regulation event.
then the down-regulation of *olig2* seemed to occur at multiple points wi
lineage since there was a variety of levels of EGFP fluorescence at the en
experiments, indicating that it is first expressed and then down-regulated i
cells to generate mixed O+/O- clones.

This data provides evidence for the idea that both initial asymmetric segreg
olig2 as well as later *olig2* up- or down-regulation can be responsible fo
O+/O- clones.

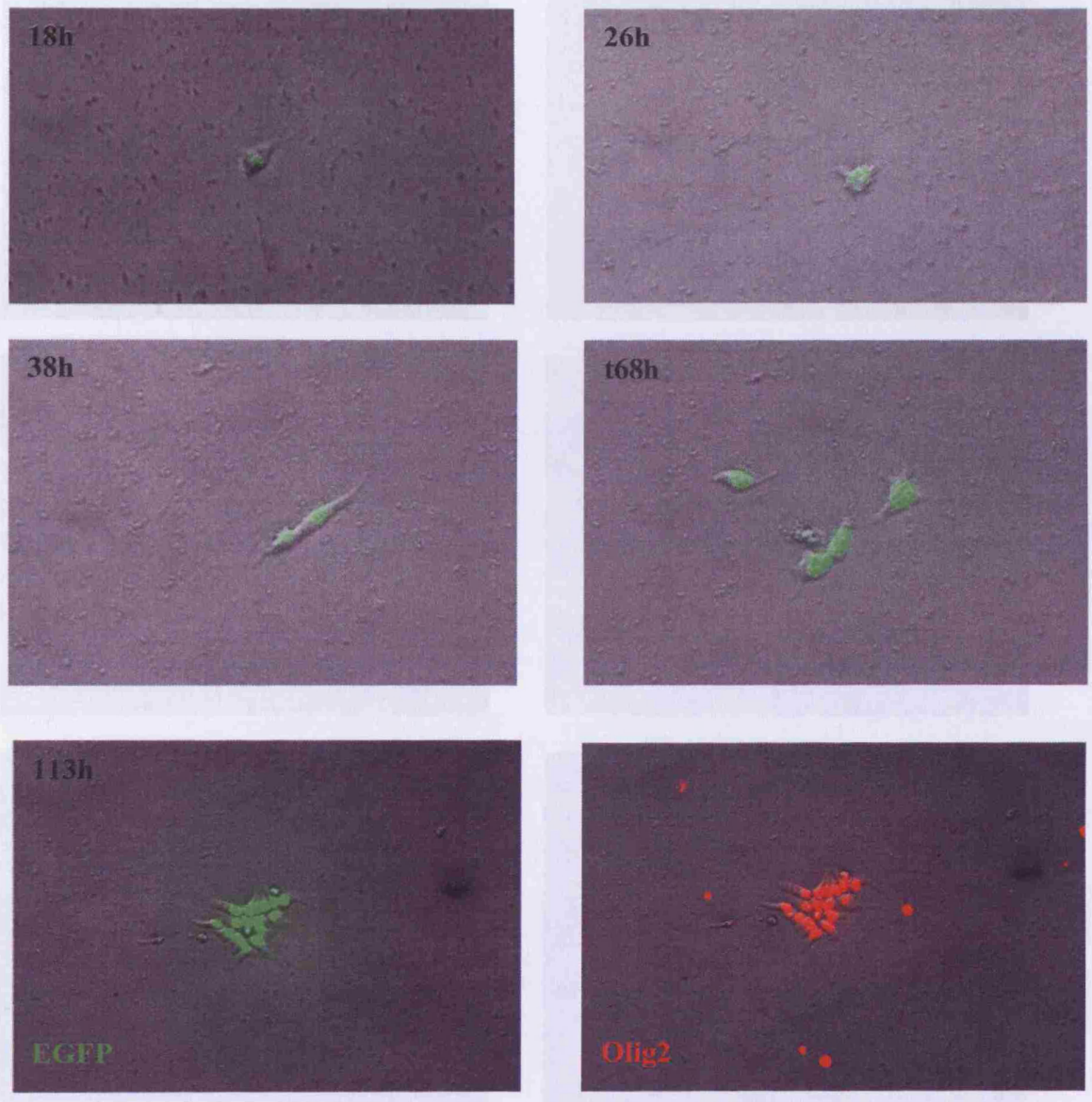

Figure 4.10 Stills from a time-lapse recording of a transgenic E13.5 cortical NEP preparation in the presence of 10 ng/ml FGF-2 in which an O+ clone was generated from a single cell in the starting culture. EGFP was up-regulated in the starting cell before the first division and was maintained in all daughter cells which all labelled for Olig2 at the end. Note that the images of the stills from the experiment (18-68hrs) are cropped to show the cells more clearly and thus appear as though they are at a higher magnification.

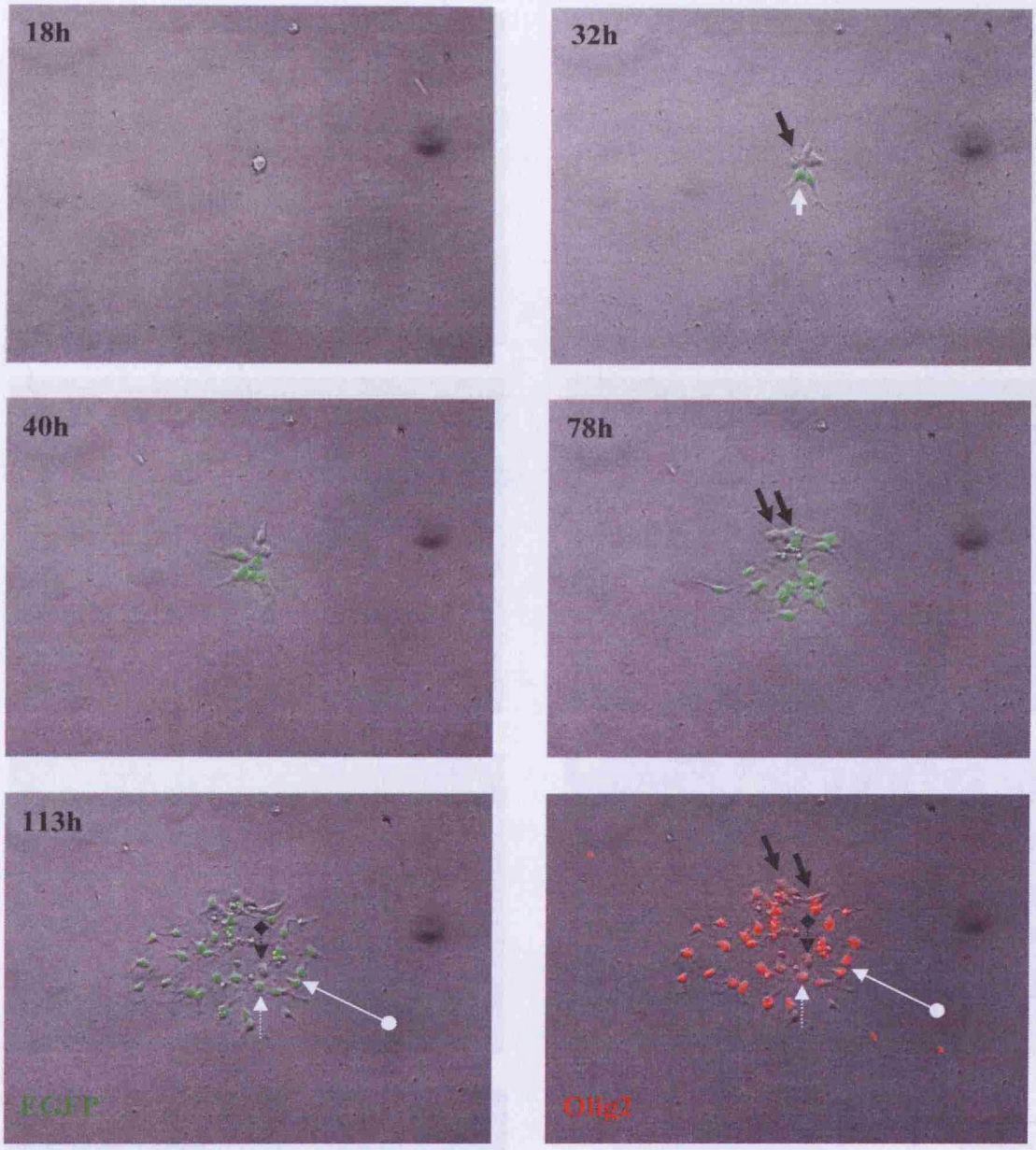

Figure 4.11 Stills from a time-lapse recording of a transgenic E13.5 cortical NEP preparation in the presence of 10 ng/ml FGF-2 in which an O+/O- clone was generated. The starting cell was EGFP-negative, but 2 of 4 daughters were EGFP+ by 32 hours (white arrow). One of the EGFP-negative cells (black arrow 32h) divided once, and all were Olig2-negative at 113 hours (black arrows). At 78 hours all the other daughter cells were EGFP+. Some down-regulated by 113 hours and were Olig2-negative (black, diamond-bottomed arrow). Others were EGFP+, but only weakly Olig2+ (white dotted arrow) while other, strongly-EGFP+ cells were Olig2+ at the end (white round-bottomed arrow).

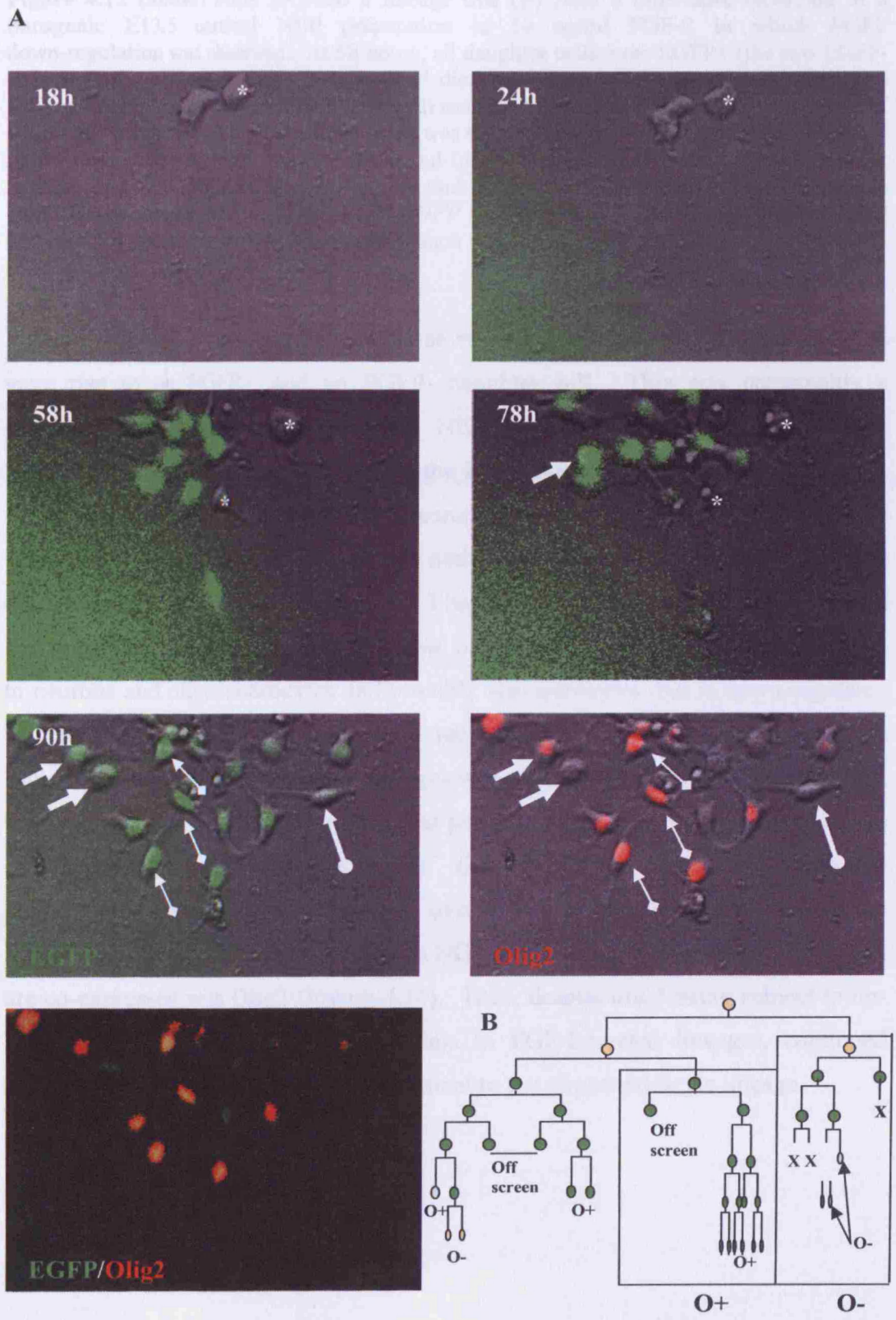
A
18h
24h
58h
78h
90h
EGFP
Olig2
EGFP/Olig2
B
Off screen
O+
O-
Off screen
O+
X
X X
O-
O+
O+
O-

Figure 4.12 (above) Stills (A) and a lineage tree (B) from a time-lapse recording of a transgenic E13.5 cortical NEP preparation in 10 ng/ml FGF-2 in which EGFP down-regulation was observed. At 58 hours, all daughter cells were EGFP+ (the two EGFP- cells at 58h were not part of the clone, and died by 78h). At 78 hours, one EGFP+ cell divided to give rise to two daughter cells with reduced EGFP fluorescence (white arrows), of which one was weakly Olig2+ and the other was Olig2- at 90 hours (white arrows). Brightly EGFP+ cells were strongly Olig2+ at the end (diamond-bottomed arrows) whereas weaker EGFP correlated with weaker Olig2 (round-bottomed arrows) indicating a possible correlation between strength of *olig2* and *EGFP* transcription. The downregulation of *olig2* and *EGFP* appeared to occur at multiple branch points as can be seen from the lineage tree (B).

Figure 4.13 is an example of a genuine asymmetric division since the first division gave rise to an EGFP+ and an EGFP- daughter cell. This was presumably a cell-intrinsic behaviour of the starting NEP since the environment of the two daughter cells was identical. Although the EGFP-negative cells in this clone died, they did not divide again and had a neuronal morphology. They were therefore presumably neurons. The EGFP+ cells maintained EGFP fluorescence throughout the lineage, but not all were Olig2+ at 113 hours meaning that *olig2* down-regulation had occurred in some cells. Since, *in vivo, olig2*+ precursors are known to give rise to neurons and oligodendrocytes and possibly also astrocytes, but is down-regulated as these cells differentiate, it is possible that these time-lapse movies are observing such differentiation events. While lineages were not filmed for more than 90 hours, some cultures were maintained over longer periods of time in order to account for the differentiation of cells beyond 90 hours. *Olig2* is maintained in oligodendroglial progeny and OLPs are seen to emerge over 4-5 days in FGF-2 according to the appearance of early OLP markers such as NG2 and galactocerebrosidase (GC) which are co-expressed with Olig2 (Figure 4.14). Thus, despite *olig2* being subject to up- and down-regulation at early time points in FGF-2-treated lineages, continued expression for 4-5 days indicates commitment to the oligodendrocyte lineage.

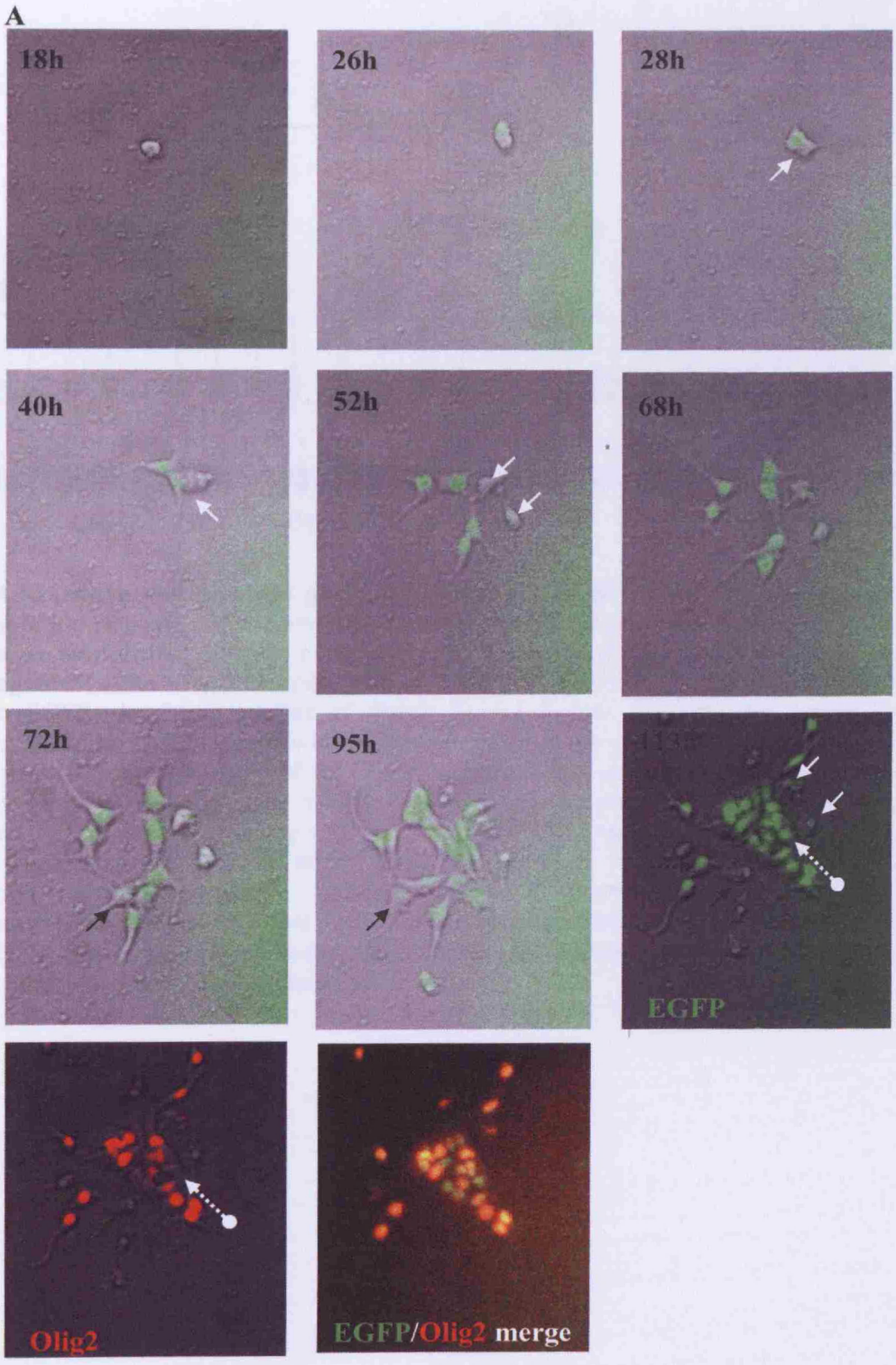
A
18h
26h
28h
40h
52h
68h
72h
95h
EGFP
Olig2
EGFP/Olig2 merge

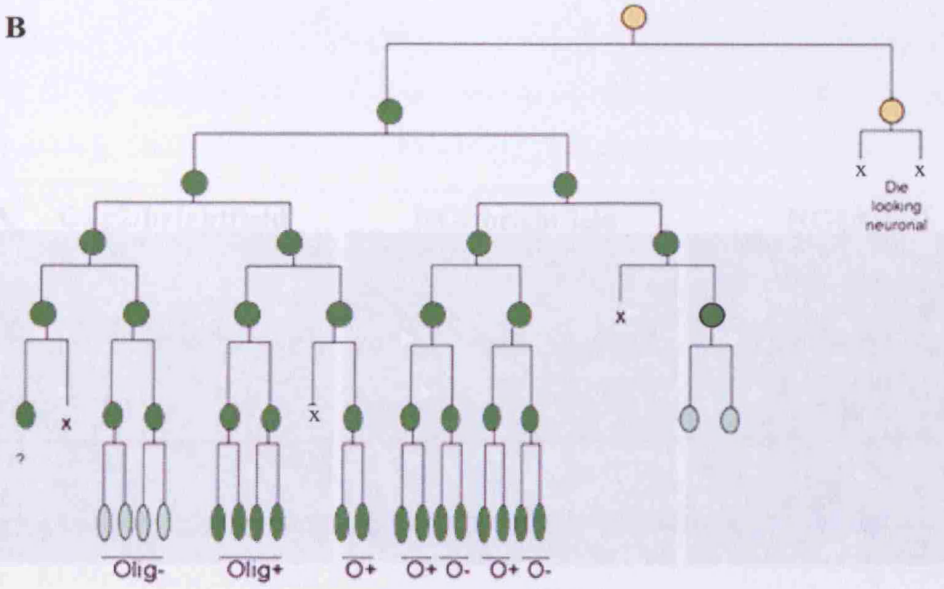

Figure 4.13 (above and previous page) Stills (A) and lineage tree (B) from a time-lapse recording of a transgenic E13.5 cortical NEP preparation in the presence of 10 ng/ml FGF-2 in which an asymmetric division of the starting NEP gave rise to one EGFP+ and one EGFP-negative (white arrow) daughter cell by 28 hours. The EGFP- cell divided once to give two EGFP- daughters, neither of which divided further, but extended neurite-like processes and died by 95 hours (white arrows). These were presumed to be neurons as labelled in the lineage tree (B). Of the EGFP+ daughter cells some began to downregulate EGFP by 72 hours (black arrow) and these were Olig2-negative at 113 hours indicating complete *olig2* downregulation by this time. EGFP+/Olig2-negative cells (white dotted arrows) might indicate a more recent down-regulation of *olig2* when EGFP protein degradation has not yet occurred. Strongly EGFP+ cells were Olig2+ at the end (black dotted arrows) indicating cells that they maintained *olig2* throughout the lineage. The retrospective lineage tree (B) indicated that *olig2* down-regulation could have occurred at multiple branch points within the clone.

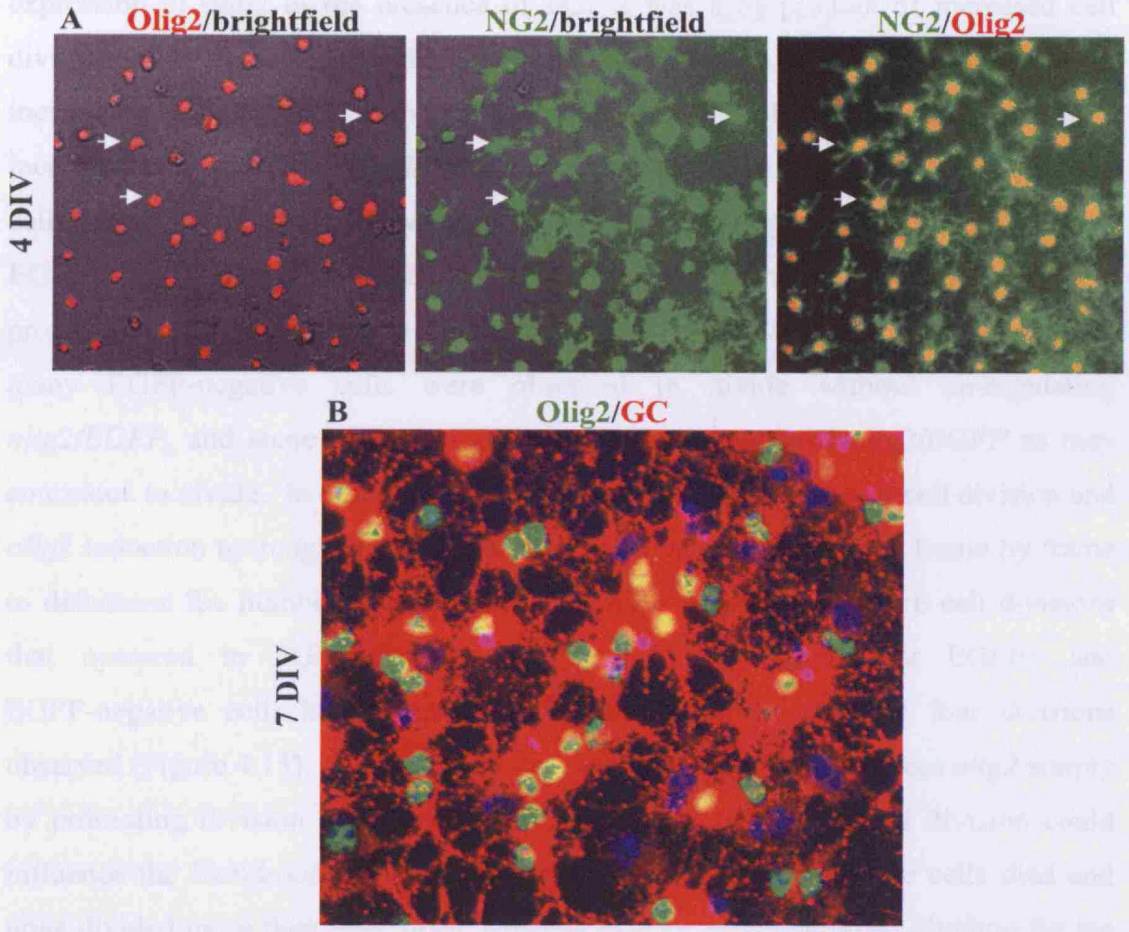

Figure 4.14 Sustained *olig2* expression correlates with the acquisition of oligodendrocyte markers. After 4DIV in the time-lapse set-up, all Olig2+ cells co-expressed NG2 (A,white arrows). At 7DIV, Olig2 co-localised with GC (B). There were some persisting Olig2- cells at this stage, and were probably neurons.

4.2.7 FGF-2 increases cell division in the starting population independently of *EGFP/Olig2* induction

Unpublished data from the Richardson laboratory has shown that *olig2* induction by FGF-2 in the cultures described here requires cell division since blocking the cell cycle with aphidicolin abolishes the effect. It is conceivable, therefore, that the expression of *olig2* in the presence of FGF-2 was a by-product of increased cell division rather than a direct induction by FGF-2 signalling. However, the increase in incidence of Olig2+ lineages in FGF-2 compared to controls far exceeded the relative increase in the number of single cells that were induced to divide; 76.3% of dividing cells in 10 ng/ml FGF-2 gave rise to EGFP-expressing cells compared to zero EGFP+ cells in control conditions, whereas there was only a ~1.5-fold increase in the proportion of cells induced to divide by FGF-2 relative to controls. Furthermore, many EGFP-negative cells were observed to divide without up-regulating *olig2/EGFP*, and some dividing EGFP+ cells down-regulated *olig2/EGFP* as they continued to divide. In order to investigate the relationship between cell division and *olig2* induction more quantitatively, time-lapse lineages were traced frame by frame to determine the number and duration of EGFP+ vs. EGFP-negative cell divisions that occurred in FGF-2-treated cultures. It was found that EGFP+ and EGFP-negative cells had comparable division times for the first four divisions observed (Figure 4.15). It is therefore very unlikely that FGF-2 induces *olig2* simply by promoting division in a permissive environment or that *rate* of division could influence the likelihood of *olig2* expression. Many EGFP-negative cells died and none divided more than four times, whereas EGFP+ cells continued dividing for the entire 90 hours of filming. This demonstrated that EGFP+ cells were differentially responsive to the sustained mitogenic activity of FGF-2.

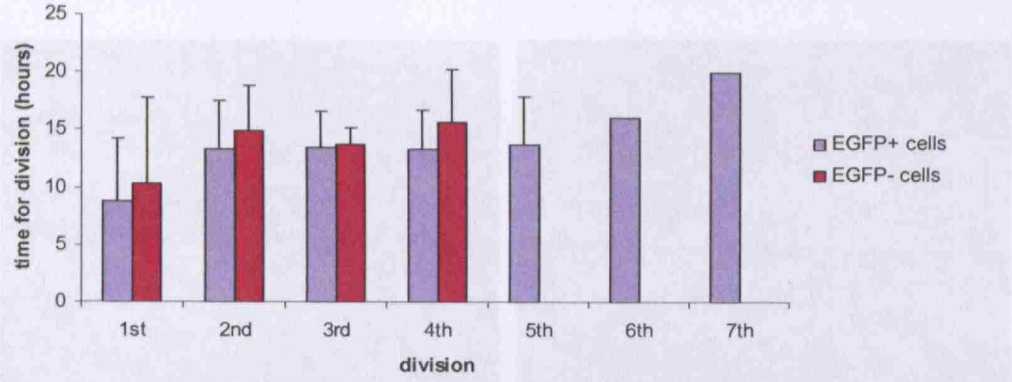

Figure 4.15 Comparison of division times of cells in EGFP+ vs EGFP- clones. There was no significant difference between division times for EGFP+ vs. EGFP-negative cells ($P > 0.1$ for division times for EGFP+ vs. EGFP- cells for divisions 1-4). However, EGFP-negative cells rarely underwent more than 4 divisions and most died before the end of the experiment. Therefore, divisions were not sustained in EGFP-negative clones. Note that the 'first' divisions indicate the time after the start of filming at which the first division was seen to occur. Subsequent divisions are quoted as absolute cell cycle time.

4.2.8 EGF does not induce *olig2* expression

Both FGF-2 and EGF have been implicated in the emergence of oligodendrocytes from neurospheres following mitogen withdrawal (Chandran et al., 2004;Kondo and Raff, 2000;Qian et al., 1998). Furthermore, Chandran et al showed that neurospheres from E14 rat dorsal spinal cord cells cultured in EGF and FGF-2 were capable of generating oligodendrocytes. I therefore decided to compare the effects of EGF and FGF-2 on the cultures described here. When E13.5 cortical NEPs were cultured on coverslips I found that EGF did not induce *olig2* even at concentrations up to 20 ng/ml, unlike the strong inductive effect of 10 ng/ml FGF-2. EGF-treated cultures were indistinguishable from controls with no apparent effect on cell division or expression of any differentiating cell markers (Figure 4.16). Therefore, even though these cells express EGF Receptor (EGFR) at this developmental stage (Tropepe et al., 1999), EGF does not elicit the same effect as FGF-2 with respect to *olig2* induction. As a positive control, the same batch of EGF was used successfully in contemporaneous experiments by other lab members in a different culture paradigm. Thus, the absence of effect here must be attributed to an unresponsiveness of the cortical NEPs. The reason for this is unclear, but is most likely to be due to absence of necessary intracellular components or appropriate levels of EGFR.

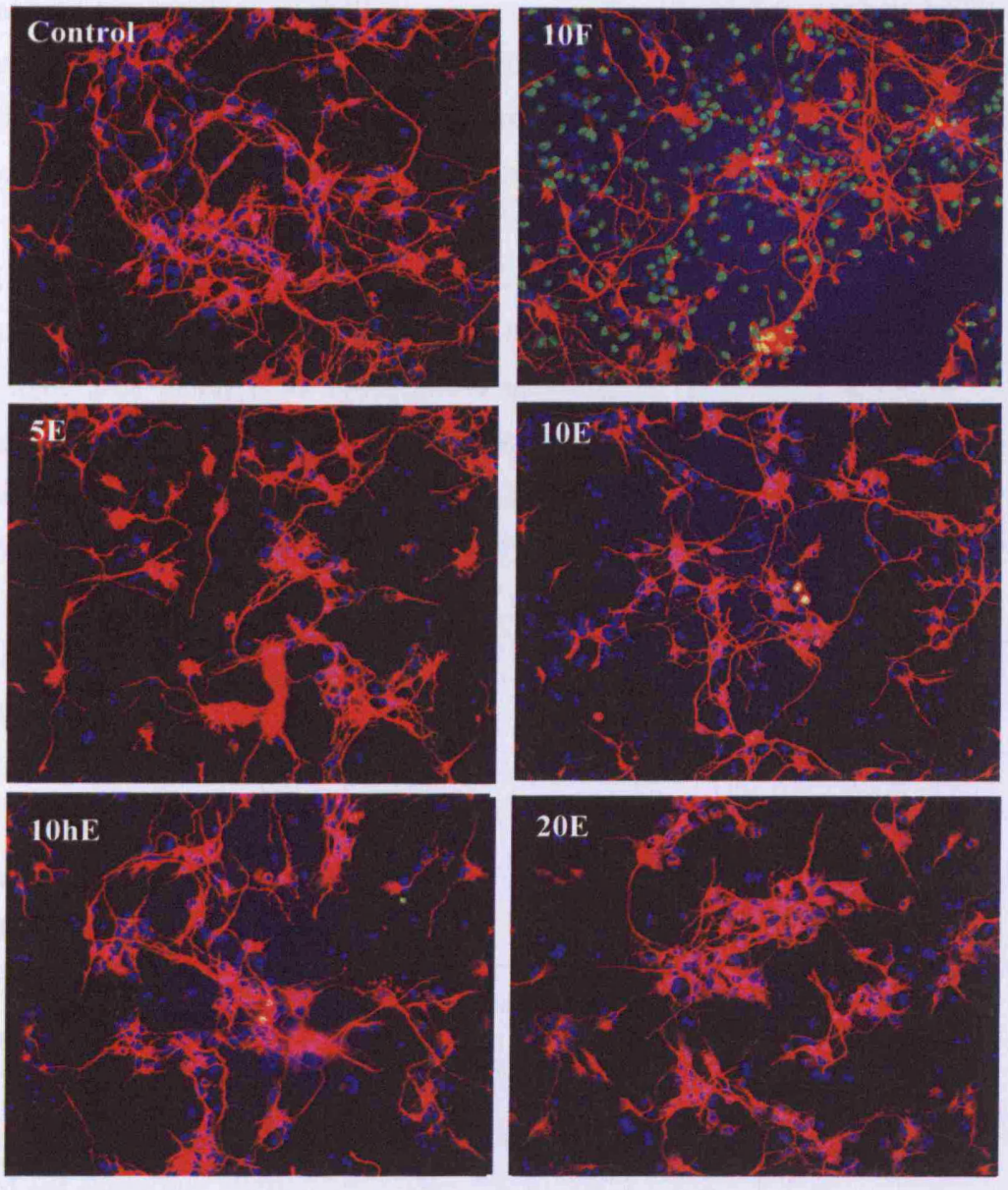

Figure 4.16 E13.5 cortical NEP cultures at 2 DIV in 10 ng/ml *FGF2* (10F), 5, 10 or 20 ng/ml mouse EGF (5, 10, 20E) or 10 ng/ml human recombinant EGF (10hE) versus control conditions. In all concentrations of EGF and in control conditions there was the occasional appearance of Olig2+ cells in doublets (10E, 10hE), but most cells were β-tubulin III+ neurons. In comparison, most cells were Olig2+ (green) in 10 ng/ml FGF2. Furthermore, there was no significant difference in total cell number across any of the EGF-treated cultures or relative to controls.

4.2.9 Dose-dependent response of cortical neuroepithelial precursors to FGF-2

Increasing concentrations of FGF-2 generates significantly higher numbers of OLPs (as determined by NG2 staining) in dense cortical NEP cultures assessed at a single time point (Kessaris et al., 2004). I therefore decided to investigate this effect at the level of individual clones, using time-lapse microscopy.

E13.5 cortical NEPs cultures were prepared and recorded by time-lapse microscopy in the presence of 1-50 ng/ml FGF-2 over ~90 hours. Both transgenic and wild type mice were used in different experiments according to availability and data were collated. The proportion of single cells that divided over the recording period was comparable in all concentrations of FGF-2, but significantly higher than that in controls (Table 4.4):

Concentration of FGF-2 (ng/ml)	**0 (control)**	**1**	**10**	**15**	**25**	**50**
% of single cells that divided	35 +/- 7	39 +/- 9	62 +/- 24	61 +/- 18	62 +/- 10	45 +/- 20
% of clones that survived	0	75 +/- 14	63 +/- 15	66 +/- 16	63 +/- 10	0

Table 4.4 Comparison of percentage of single cells from E13.5 NEP preparations that divided and clones that survived for immuocytochemical analysis in different concentrations of FGF-2. Data is shown as mean +/- standard deviation of triplicate experiments performed (data from 5 experiments were assimilated for 10 ng/ml FGF-2 inputs). There was no significant difference between the figures for concentrations of 10 ng/ml FGF-2 and above, but they ware all significantly different to the data collected for the 0 ng/ml and 1 ng/ml FGF-2 controls.

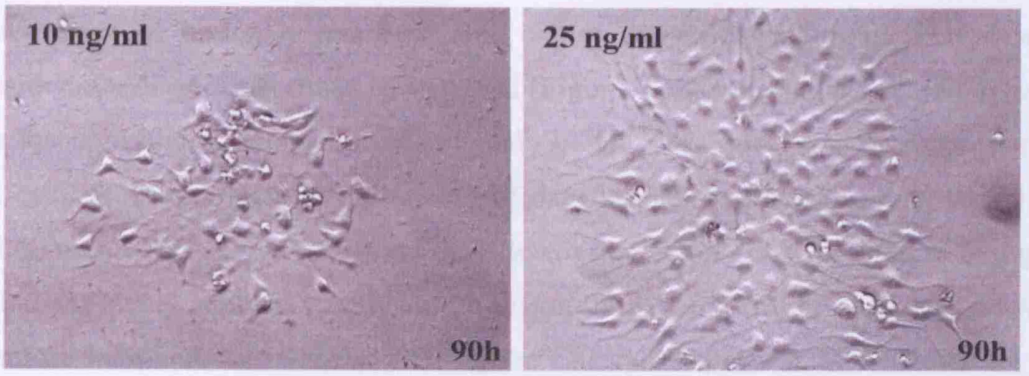

Figure 4.17 Two typical clones from a single experiment in which individual NEPs from the same preparation were cultured in either 10 or 25 ng/ml FGF-2. After 90 hours in culture, clones in 25 ng/ml FGF-2 were considerably larger than those derived in 10 ng/ml FGF-2, reflecting their shorter cell cycle time (Figure 4.18).

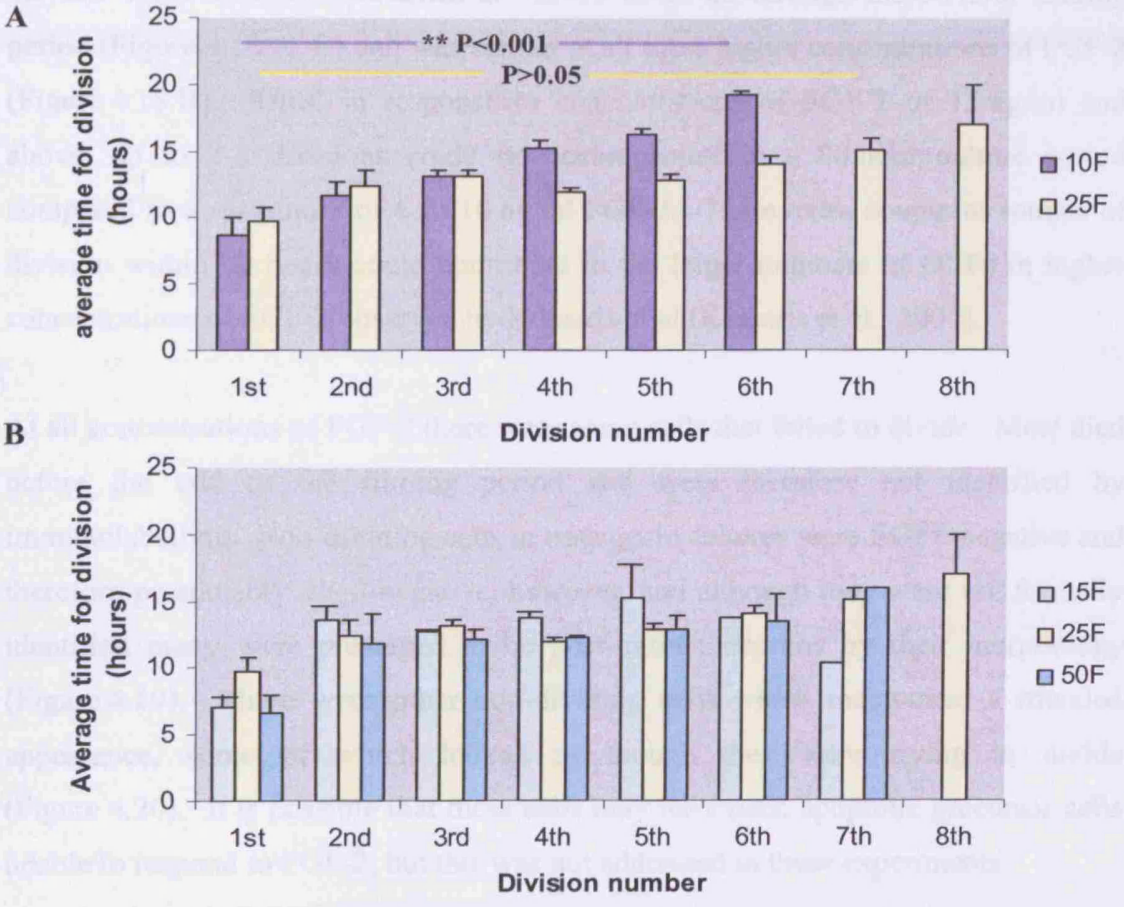

Figure 4.18 Division times of cells in E13.5 cortical NEP cultures over 90 hours in different concentrations of FGF-2. Cell cycle time got progressively and significantly longer in 10 ng/ml FGF-2 with a maximum of 6 divisions occurring in 90 hours (A). Conversely, there was no significant difference in division time over 7 divisions in higher concentrations of FGF-2 and up to 8 divisions occurred in the culture period (A). There was no significant difference in division times in concentrations of 15 ng/ml FGF-2 and above (B). Note that the 'first' divisions indicate the time after the start of filming at which the first division was seen to occur. Subsequent divisions are quoted as absolute cell cycle time.

Despite there being no difference in the number of single cells that were seen to divide after 18 hours, it was clear that clones derived in 25 ng/ml FGF-2 were considerably larger than those in 10 ng/ml (Figure 4.17) suggesting that cell division was faster in higher concentrations of FGF-2. This was quantified by recording the cell cycle time for successive divisions of daughter cells within clones at 10, 15, 25 and 50 ng/ml FGF-2. Although an insufficient number of cells survived in 50 ng/ml FGF-2 for clonal analysis (Table 4.4), division times could still be recorded and were therefore included. In 10 ng/ml FGF-2, the cell cycle time was 12-15 hours for the first couple of divisions, but became progressively longer with each additional division (Figure 4.18 A). Thus, in a 90 hour culture period the cells divided a maximum of 6 times in 10 ng/ml FGF-2. However, in 15 ng/ml FGF-2 and above, the cell cycle time was sustained at ~12-15 hours all through the 90 hour filming period (Figure 4.18 A, B) and was similar at all these higher concentrations of FGF-2 (Figure 4.18 B). Thus, in response to concentrations of FGF-2 of 15 ng/ml and above, up to 7-8 divisions could be accomplished in a 90 hour culture period compared to a maximum of 6 in 10 ng/ml FGF-2. These extra couple of rounds of division within 90 hours could contribute to the larger numbers of OLPs in higher concentrations of FGF-2 observed by Kessaris et al (Kessaris et al., 2004).

At all concentrations of FGF-2 there were some cells that failed to divide. Most died before the end of the filming period and were therefore not identified by immunolabelling. Non-dividing cells in transgenic cultures were EGFP-negative and therefore presumably *olig2*-negative, however, and although they were not formally identified many were presumed to be post-mitotic neurons by their morphology (Figure 4.19). There were other non-dividing cells which maintained a rounded appearance, some of which looked as though they were trying to divide (Figure 4.20). It is possible that these cells may have been apoptotic precursor cells unable to respond to FGF-2, but this was not addressed in these experiments.

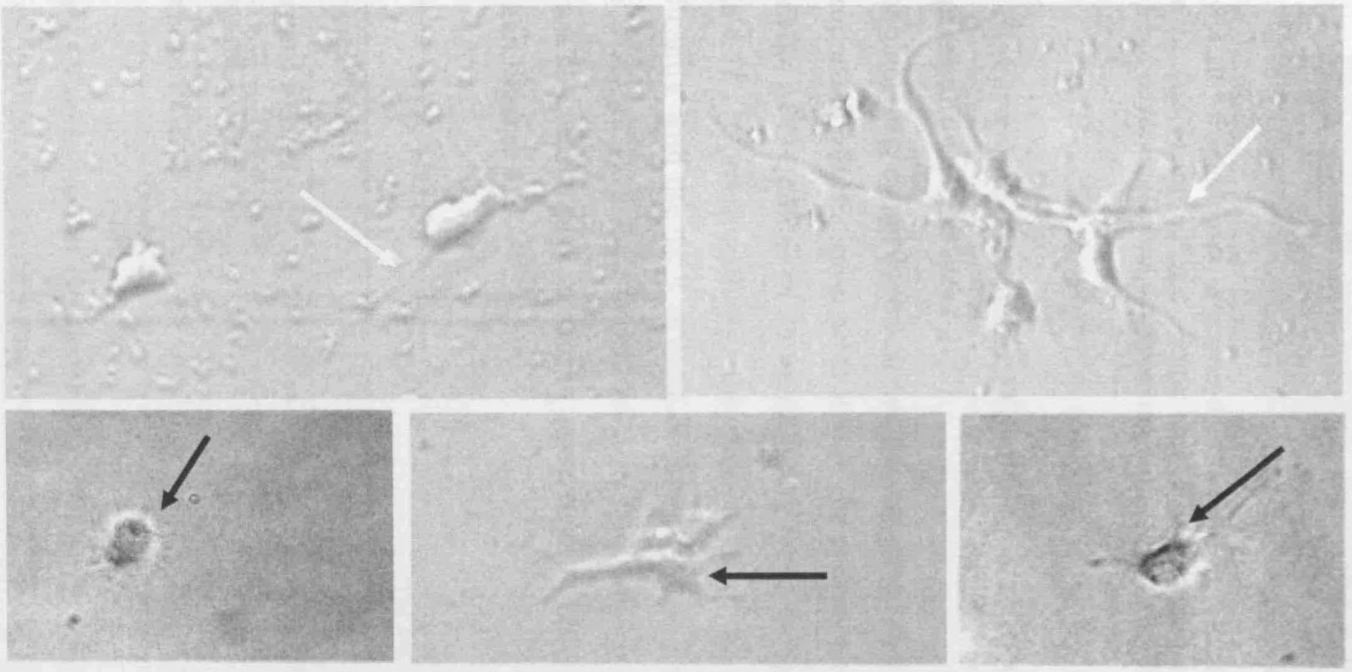

Figure 4.19 Putative neurons. Some had neutrite-like processes (white arrows) and others had large cell bodies with many processes (black arrows) which resembled the morphology of some β-tubulin III+ neurons identified in other clones.

Figure 4.20 Morphologies of rounded cells seen in cultures that did not divide, but died before the end of the culture. Some looked as though they were trying to divide (white arrow), but never underwent cytokinesis. It is possible that these were apoptotic NEPs.

4.2.9 Higher concentrations of FGF-2 induce more NEPs in the starting culture to express and sustain *olig2*

Immunolabelling of surviving clones demonstrated that there was a clear increase in the proportion of O+ clones generated in the presence of higher levels of FGF-2, the percentage of O+ clones in 25 ng/ml being twice that generated in 10 ng/ml FGF-2 (Table 4.5). Correspondingly, the proportion of O- and O+/- clones decreased significantly with the most striking difference being that there were no O- clones at all in 25 ng/ml FGF-2 compared to 21% O- clones in 10 ng/ml FGF-2 (Table 4.5; Figure 4.21). Examples of clones generated in 15 ng/ml and 25 ng/ml FGF-2 are shown in Figures 4.22- 4.27.

	%O+	%O+/O-	%O-
1 ng/ml FGF-2	1 +/- 2.1	17 +/- 8	83 +/- 8
10 ng/ml FGF-2	46 +/- 15	34 +/- 13	21 +/- 13
15 ng/ml FGF-2	64 +/- 6	26 +/- 11	9 +/- 7
25 ng/ml FGF-2	89 +/- 10	11 +/- 10	0 +/- 0

Table 4.5 Comparison of the distribution of clone types generated in E13.5 cortical NEP cultures in different concentrations of FGF-2. Data is presented as mean +/- standard deviation for triplicate experiments (5 experiments for 10 ng/ml FGF-2)

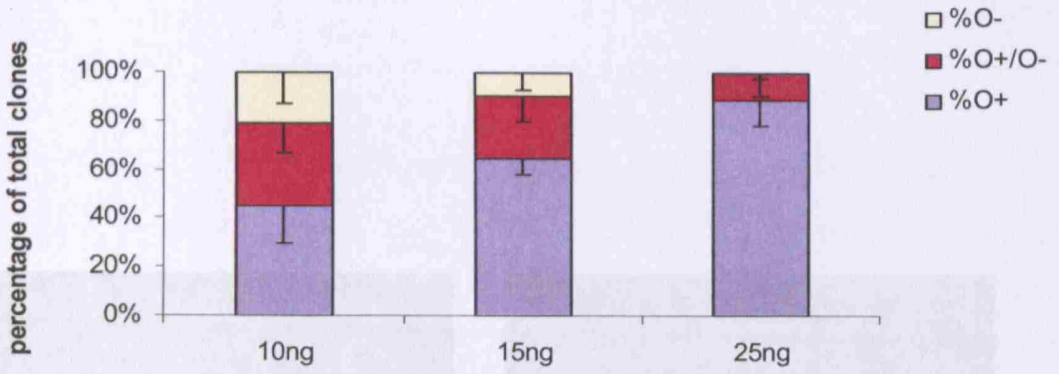

Figure 4.21 Clones derived from E13.5 cortical NEP preparations in the presence of different concentrations of FGF-2. The trend is towards an increase in *olig2*-containing clones as FGF-2 concentration increases. O- clones are absent in 25 ng/ml FGF-2 and mixed clones are reduced in favour of O+ clones.

Figure 4.22 Stills from a time-lapse recording of an E13.5 cortical NEP preparation in 15 ng/ml FGFG-2 in which an O- clone was generated from a single cell in the starting culture. In this example, one daughter cell was a β-tubulin III+ neuron, one looked as though it may have started to express β-tubulin III (arrow) and the other was immunocytochemically unidentified.

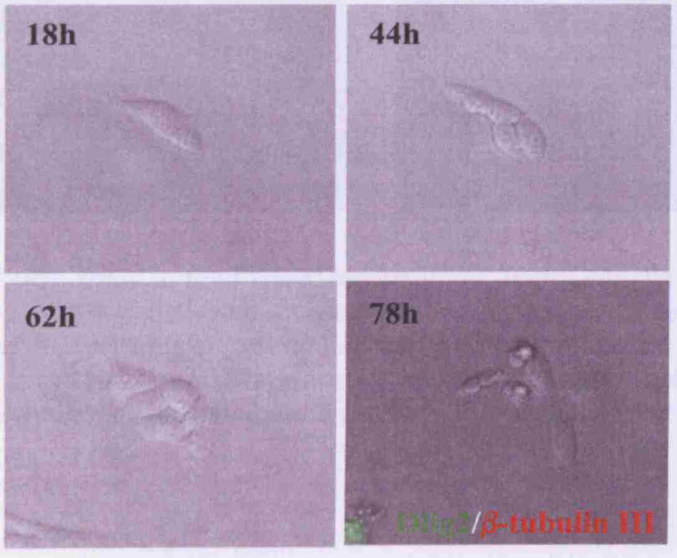

Figure 4.23 Stills from a time-lapse recording of an E13.5 cortical NEP preparation in 15 ng/ml FGF-2 in which an O- clone was generated. None of the cells were identifiable by Olig2 or β-tubulin III labelling.

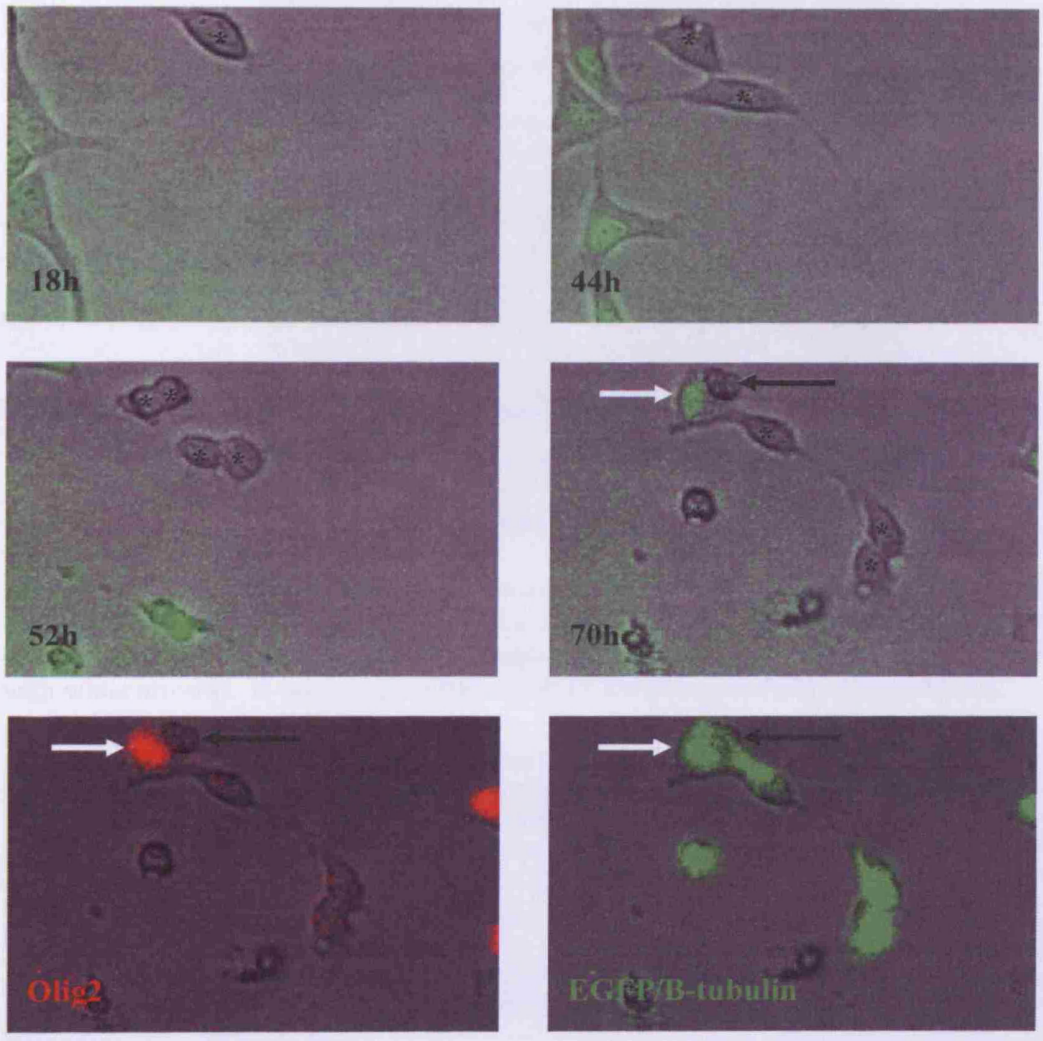

Figure 4.24 Stills from a time-lapse recording of transgenic E13.5 cortical NEPs in 15 ng/ml FGF-2. After two divisions, four β-tubulin III+ cells were generated (starred cells). At 70 hours, an EGFP+/Olig2+ cell and an unidentified cell moved into the field of view from a nearby clone (white and black arrows respectively). These should not be confused with the dividing cell that generated green β-tubulin III+ neurons (starred cells).

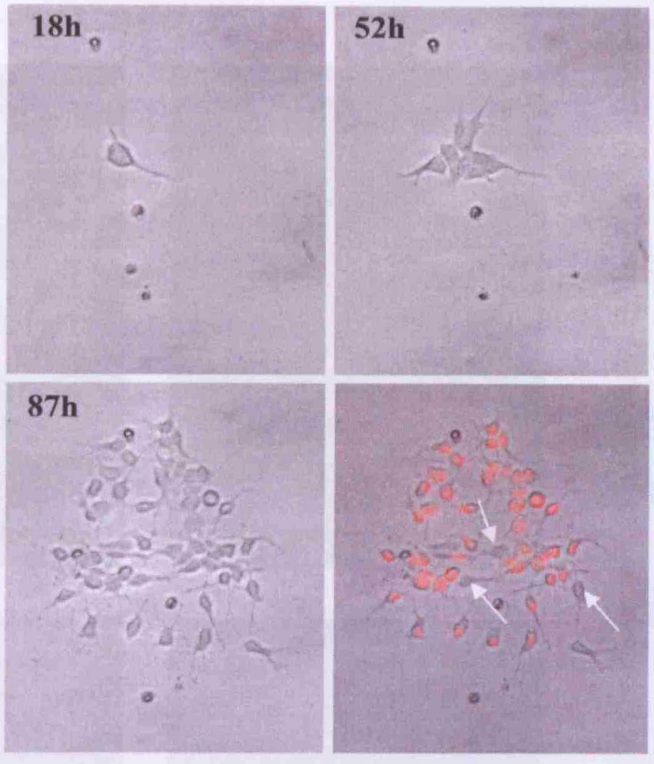

Figure 4.25 Stills from a time-lapse recording of an E13.5 cortical NEP preparation in 15 ng/ml FGF-2 in which an O+/O- clone was generated from a single cell in the starting culture. There were only a few Olig2-negative cells in the final clone (some are indicated with white arrows). It was not possible to follow the lineage of this complex clone.

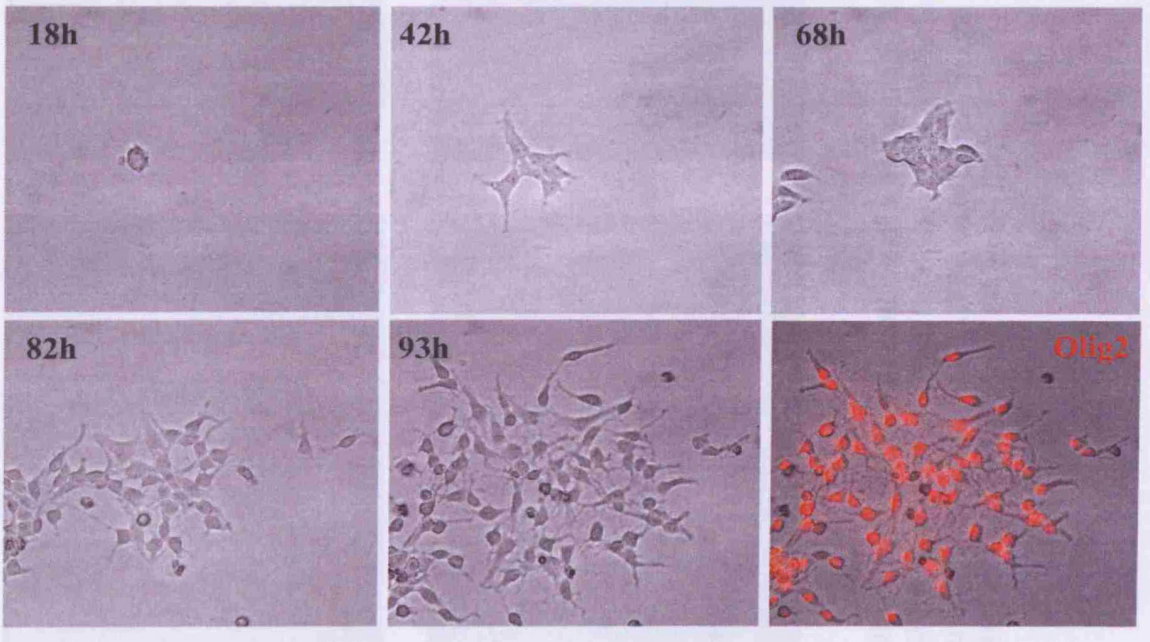

Figure 4.26 Stills from a time-lapse recording of an E13.5 cortical NEP preparation in 15 ng/ml FGF-2 in which an O+ clone was generated. The cells became too numerous and crowded to allow the lineage to be determined.

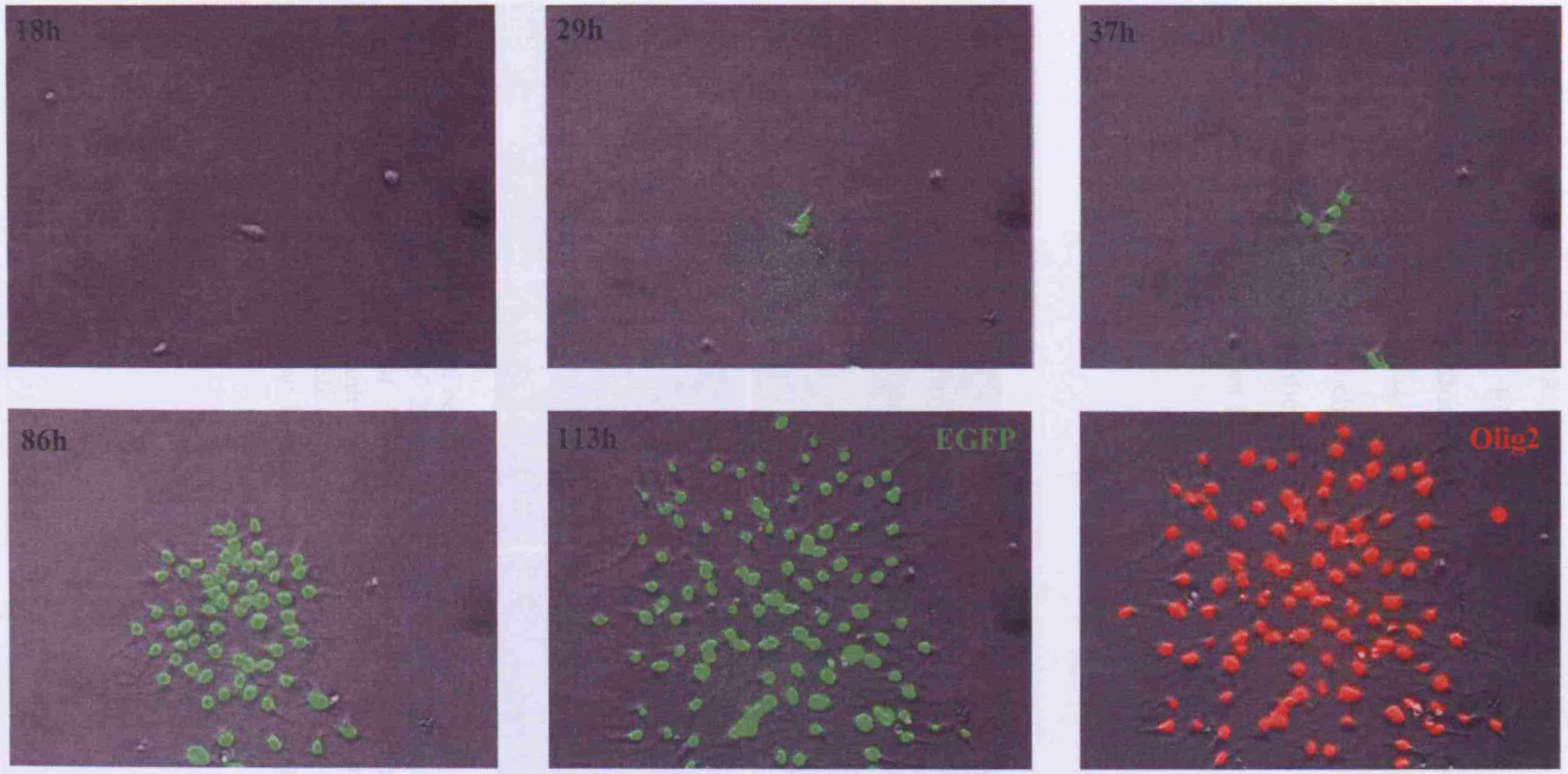

Figure 4.27 Stills from a time-lapse recording of a transgenic E13.5 cortical culture in the presence of 25 ng/ml FGF-2 in which an O+ clone was generated. EGFP was appeared after the first division, just before the second division occurred at 29 hours. Thereafter, all daughter cells were brightly EGFP+, resulting in a large clone of EGFP+ cells by 113 hours. Counter-staining with antiOlig2 (red) determined that all of these cells were additionally Olig2+. This was therefore a O+ clone.

The dose-dependent decrease in proportion of O- clones and increase in proportion of O+ clones suggested that there was not only an increase in the induction of *olig2* expression, but that maintenance of *olig2* expression in cells was also increased at higher concentrations of FGF-2. Indeed, there was little evidence for down-regulation of EGFP fluorescence at all in transgenic cultures in 25 ng/ml FGF-2. However, clone sizes were large in concentrations of 15 ng/ml FGF-2 and above, so individual cell behaviour was very difficult to trace. Examples of transgenic clones including the few clones in which down-regulation of EGFP was observed are shown in Figures 4.27- 4.30.

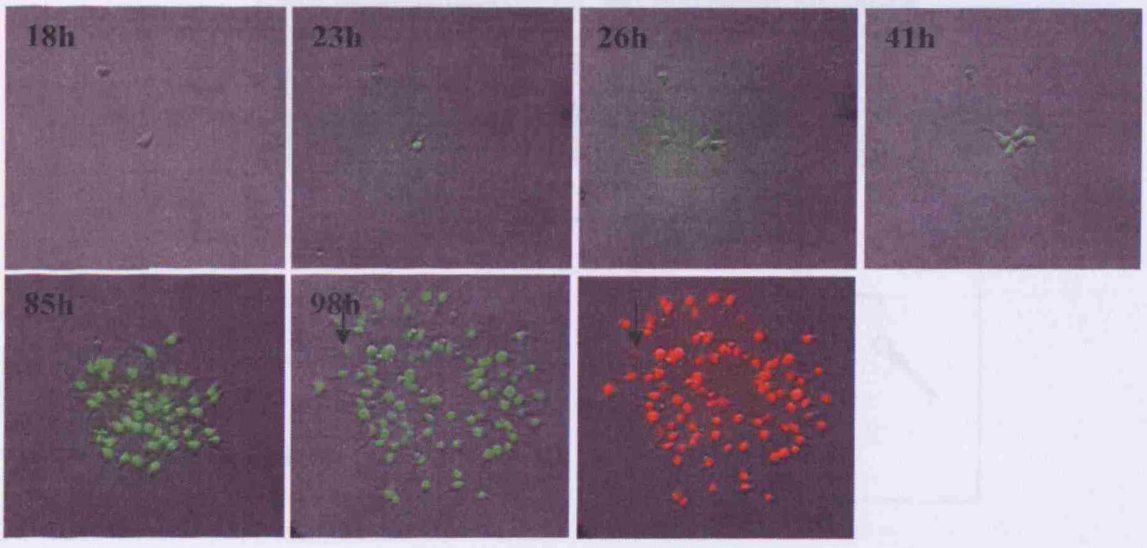

Figure 4.28 Stills from a time-lapse recording of a transgenic E13.5 cortical NEP preparation in the presence of 25 ng/ml FGF-2. In this clone, EGFP fluorescence was detected at the time of the first division at 23 hours and appeared to be maintained in all daughter cells thereafter. Counter-staining for Olig2 at 98 hours determined that all cells were Olig2+, although one cell (arrow) had weak Olig2 and EGFP fluorescence. This appeared to be an O+ clone, but if the single arrowed cell was genuinely Olig2- this could indicate *olig2* down-regulation

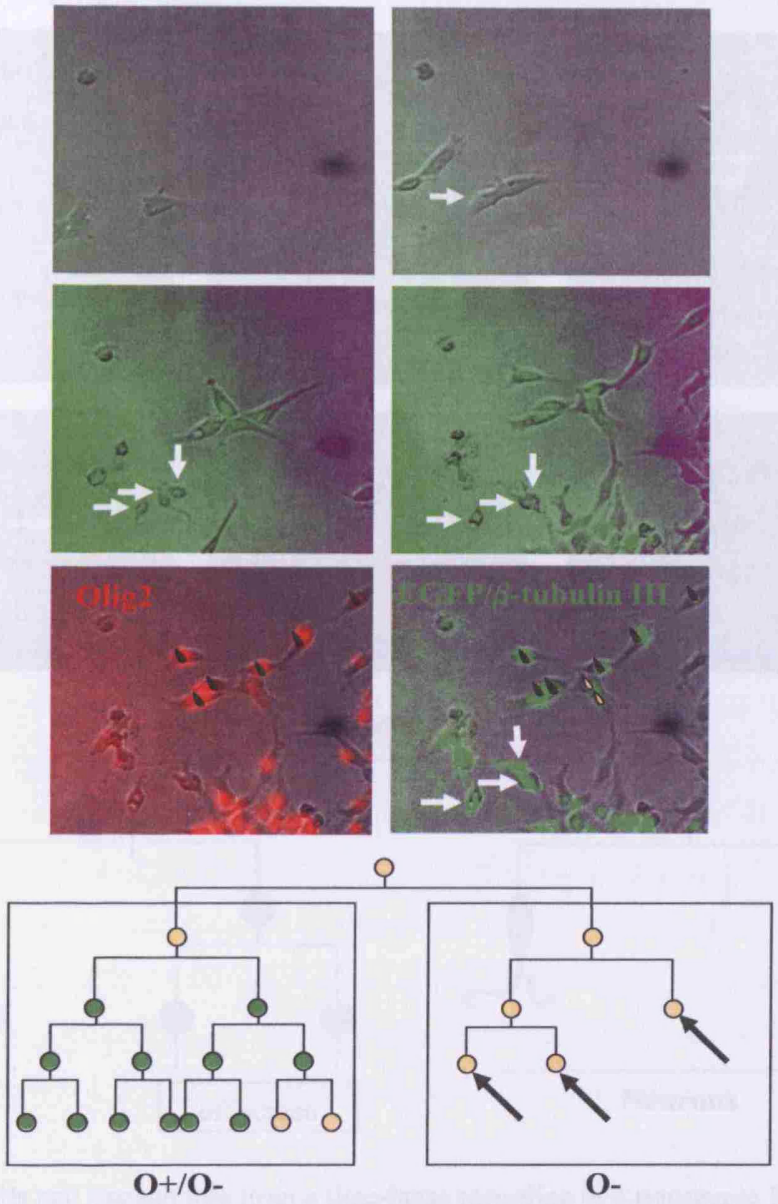

Figure 4.29 Stills and lineage tree from a time-lapse recording of a transgenic E13.5 cortical NEP preparation in 15 ng/ml FGF-2. An asymmetric lineage was derived with an O- and an O+/O- branch. Although the EGFP and β-tubulin III staining were the same fluorescent bandwidth, the two were separable by performing sequential immunolabelling such that the EGFP image was captured before β-tubulin III staining was performed. Thus the three neurons (white arrows on the stills, black arrows on the lineage tree) could be identified. In the O+/O- branch, EGFP was upregulated by the second division and was maintained in all daughter cells. All but two of the daughter cells were strongly Olig2+ (black teardrops). The other two (cream teardrops) were weakly Olig2+ at 90 hours indicating *olig2* down-regulation.

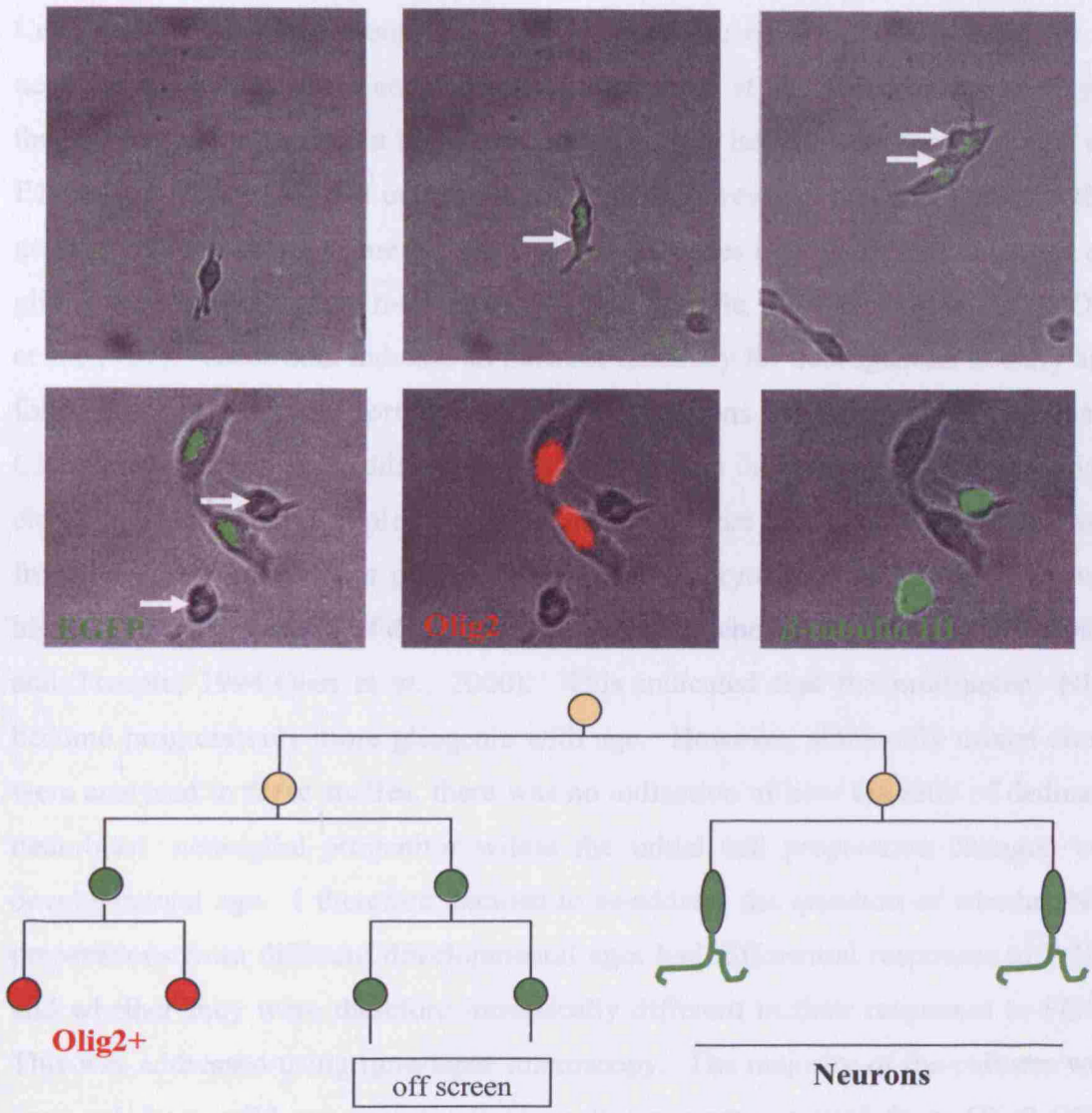

Figure 4.30 Stills and lineage tree from a time-lapse recording of a transgenic E13.5 cortical NEP preparation in 15 ng/ml FGF-2 in which an asymmetric O+/O- clone was generated. EGFP was up-regulated in one daughter cell after the first division and maintained in all daughter cells thereafter (green circles in the lineage tree). Two migrated out of the field of view, but the remaining two EGFP+ daughters were Olig2+ at 90 hours (red). The other, EGFP-negative daughter cells (white arrows) were β-tubulin III+ neurons (green at t90).

No EGFP+/Olig2- cells were identified in any transgenic clones in concentrations of FGF-2 above 10 ng/ml, suggesting that *olig2* down-regulation was infrequent. Anecdotally, in dividing cells, EGFP fluorescence was brighter in the presence of 25 ng/ml FGF-2 than in lower concentrations, indicating higher levels of *olig2* transcription. Thus, the observed effects of FGF-2 were two-fold; a mitogenic effect that saturated at concentrations of FGF-2 above 10 ng/ml and an inductive effect on *olig2* which continued to increase at concentrations of FGF-2 above 10 ng/ml.

4.2.10 Changes in fate potential of cortical NEPs during development

Cells acutely dissected from E10 – E17 embryonic cortices stain principally for neuronal markers (Barolo and Posakony, 2002;Qian et al., 2000) corresponding to the fact that neurogenesis in the cortex occurs mainly between the ages of E12.5 and E17 in the mouse. When cultured over 7 days however, while most E10.5 NEPs generate only neurons, some give rise to mixed clones containing both neurons and glia in unmodified culture medium (Davis and Temple, 1994;Qian et al., 2000;Qian et al., 1997). These data indicate an intrinsic tendency for neurogenesis at early ages followed by gliogenesis, corresponding to the 'neurons first, glia second' dogma of CNS development. The addition of FGF-2 increased the number of glia in a mixed clone and Davis and Temple further demonstrated that the mixed clones generated from NEPs dissected from progressively older embryos contained a progressively higher glia : neuron ratio of daughter cells in the presence of 10 ng/ml FGF-2 (Davis and Temple, 1994;Qian et al., 2000). This indicated that the multipotent NEPs become progressively more gliogenic with age. However, since only mixed clones were analysed in these studies, there was no indication of how the ratio of dedicated neuroblast : neuroglial progenitor within the initial cell preparation changed with developmental age. I therefore decided to re-address the question of whether NEP preparations from different developmental ages had differential responses to FGF-2 and whether they were therefore intrinsically different in their responses to FGf-2. This was addressed using time-lapse microscopy. The majority of the cultures were prepared from wild type mice. Some cultures were prepared from Olig2-EGFP transgenic mice to compare the dynamics of *olig2* expression in younger embryonic ages with the data acquired from E13.5 preparations described above.

4.2.11 E10.5 NEP cultures generate only neurons

Clones derived from E10.5 NEPs were difficult to trace as the cells clumped together if they divided and mostly died when they were plated at clonal density. The rate of cell division was slow in these cultures however, meaning that clones were small; this had the benefit that mixing of neighbouring clones was unlikely. It was therefore possible to plate single cells at a higher density and to include some lumps of less-dissociated tissue without compromising clonal analysis of the single cells that were present. The higher plating-density encouraged better cell survival, likely due to localised self-conditioning of the medium. Divisions remained difficult to

trace within an expanding clone and few clones could be characterised accurately since most single cells died and many cells within expanding clones also died even with the enhanced survival observed upon plating at higher densities. However, it was possible to ascertain that there were no Olig2+ cells, even in large clusters of cells over 3 DIV. Moreover, immunocytochemical analysis identified only β-tubulin III+ neurons throughout the cultures (Figures 4.31 – 4.33). Some of the single cells that produced a traceable lineage proved to be dedicated neuroblasts (N-clones), giving rise only to neuronal progeny (Figure 4.34). This was not quantified however, since there was not sufficient survival to make valid clone classifications in most cases although qualitatively speaking, it could be said that 100% of clones were O-. To ascertain whether the immunocytochemically unidentified cells could be induced to express glial markers with increased FGF-2 signalling, the experiments were repeated in the presence of 25 ng/ml FGF-2. However, this level of FGF-2 seemed to be toxic since none of the cells survived.

In order to investigate the differences in response to FGF-2 for cortical NEPs of different embryonic ages, cultures were also prepared and filmed from E11.5 and E12.5 embryos as described in the next section. None of these cultures were filmed for more than 90 hours in order to make the data comparable to that collected from E13.5 cultures. The limitations of this are that the full potential of these NEPs is not described. Thus, while no Olig2+ cells were observed in time-lapse from E10.5 cultures over 3 DIV, Olig2+ cells are seen to emerge over 7-10 DIV (data not shown) indicating that these NEPs have the potential to generate OLPs, but not over the time frame observed. Nevertheless, the 90 hour data collected indicates a difference in responsiveness to FGF-2 even if it does not reveal the full potential of the NEPs.

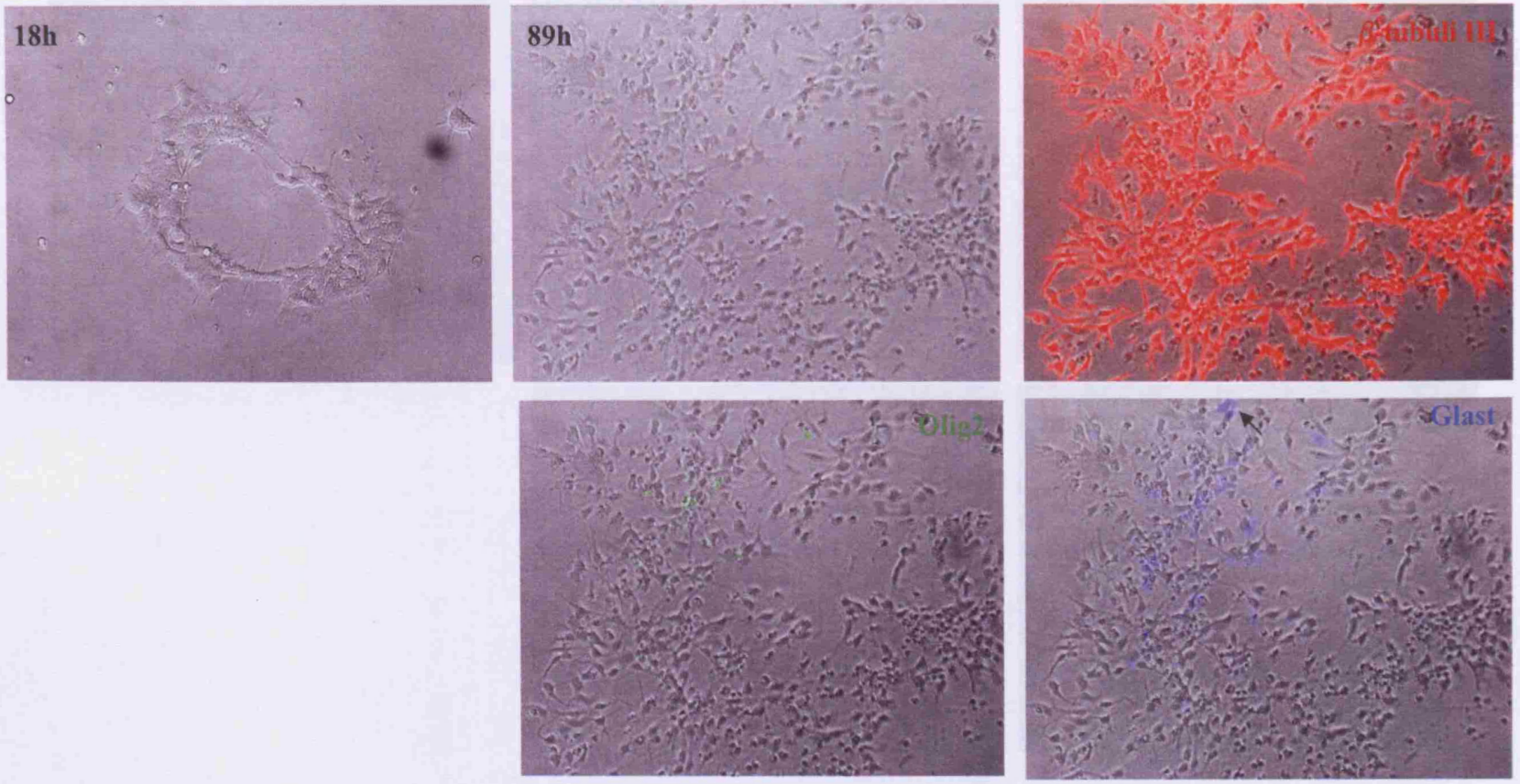

Figure 4.31 Stills from a time-lapse recording of an E10.5 cortical NEP culture. Even in large groups of cells there were no Olig2+ cells and possibly only one Glast+ cell (black arrow) at 89 hours. Most cells were β-tubulin III+ neurons.

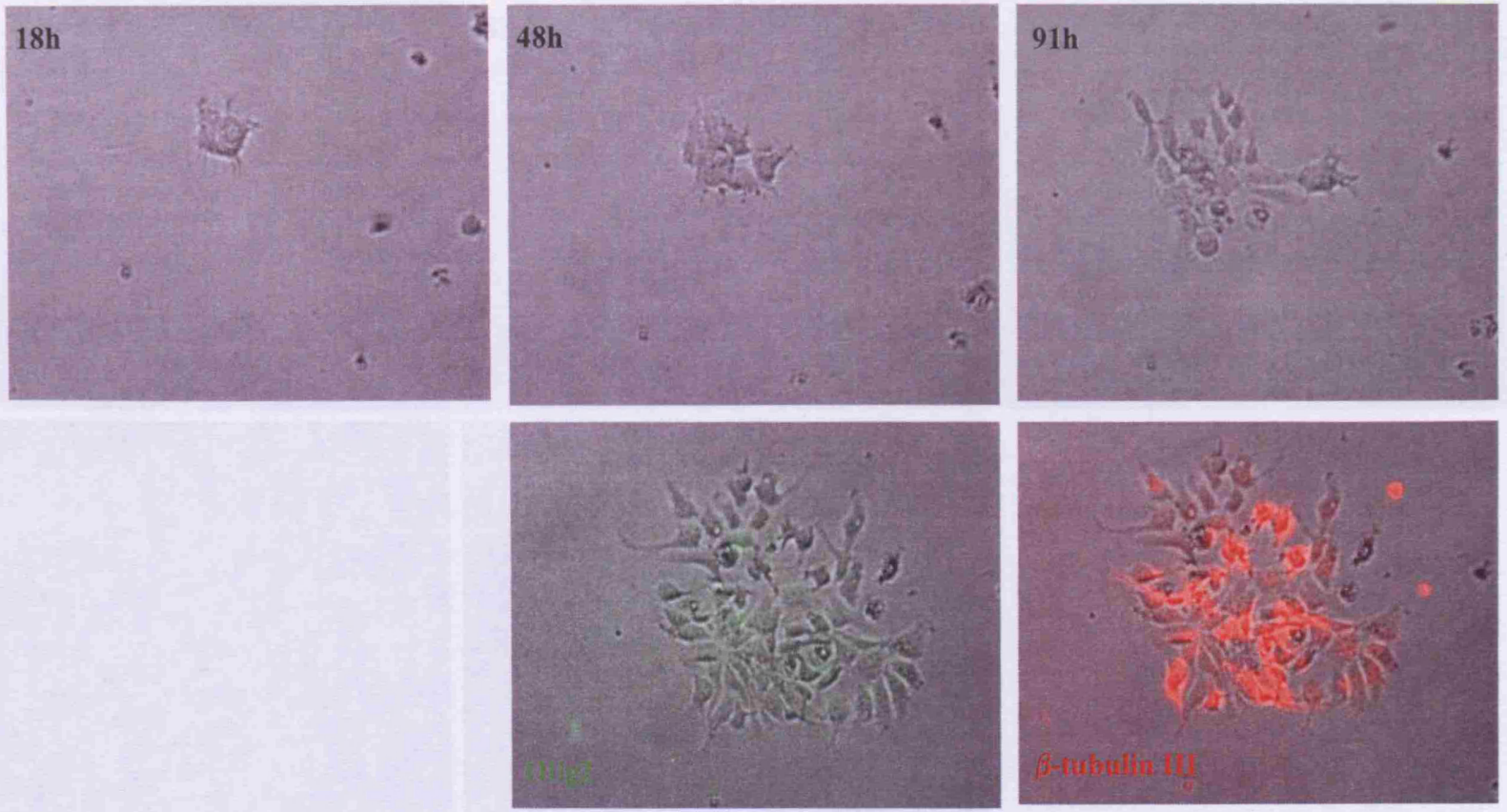

Figure 4.32 Stills from a time-lapse recording of an E10.5 cortical NEP preparation. There were 4 starting cells in this recording, and although their individual lineages could not be distinguished, there were no Olig2+ cells at 91 hours and roughly half of the daughter cells were β-tubulinIII+ neurons. This distribution of cells could arise by N-clones mixing with clones that generate both neurons and unidentified cells or all of the starting cells may have generated a mixed population of daughter cells

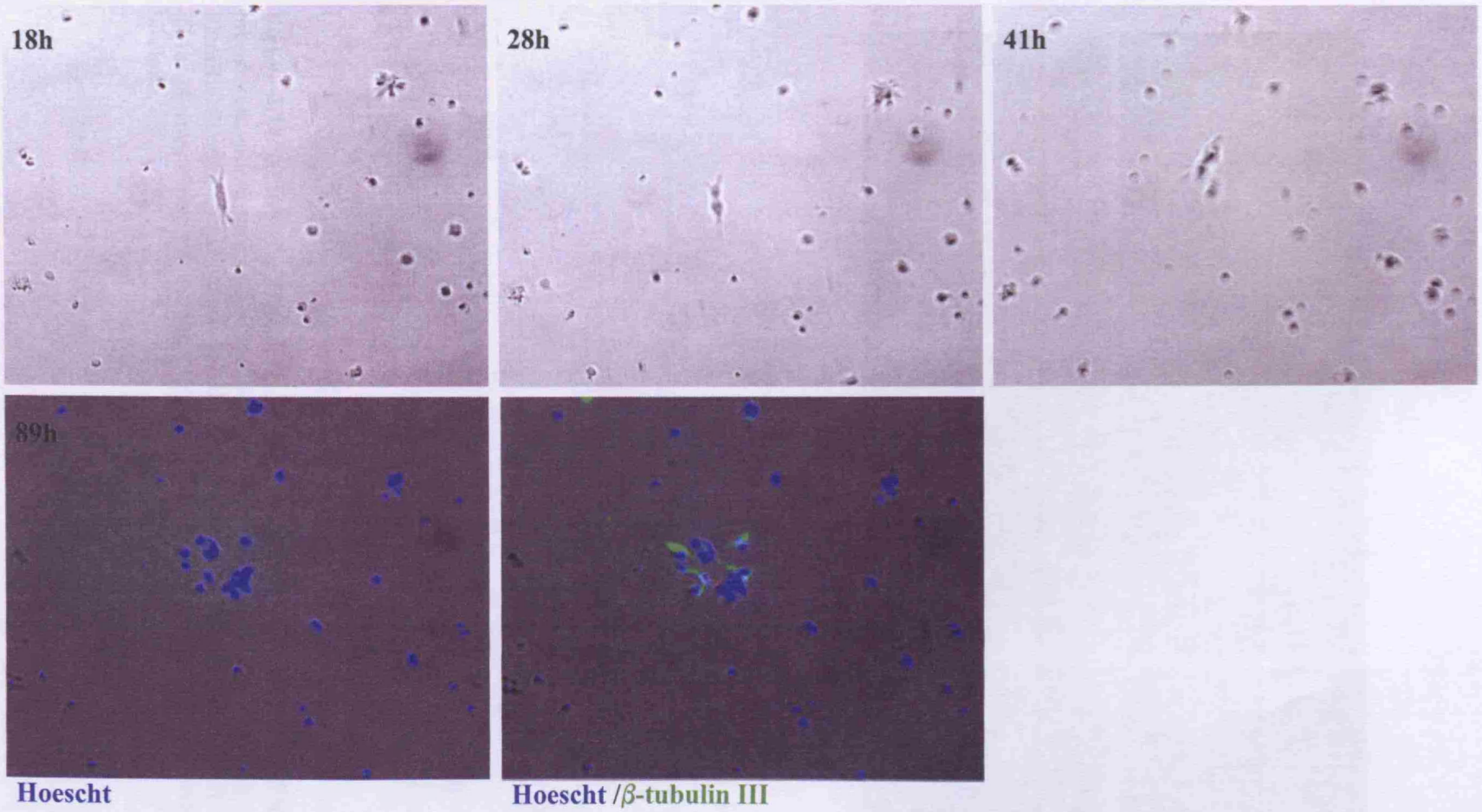

Figure 4.33 Stills from a time-lapse recording of an E10.5 NEP preparation. Over 89 hours in culture, a clone of 12 cells was derived. The focus drifted during the filming so the lineage could not be accurately traced, but a mixture of β-tubulin III+ neurons and immunocytochemically unidentified cells was generated.

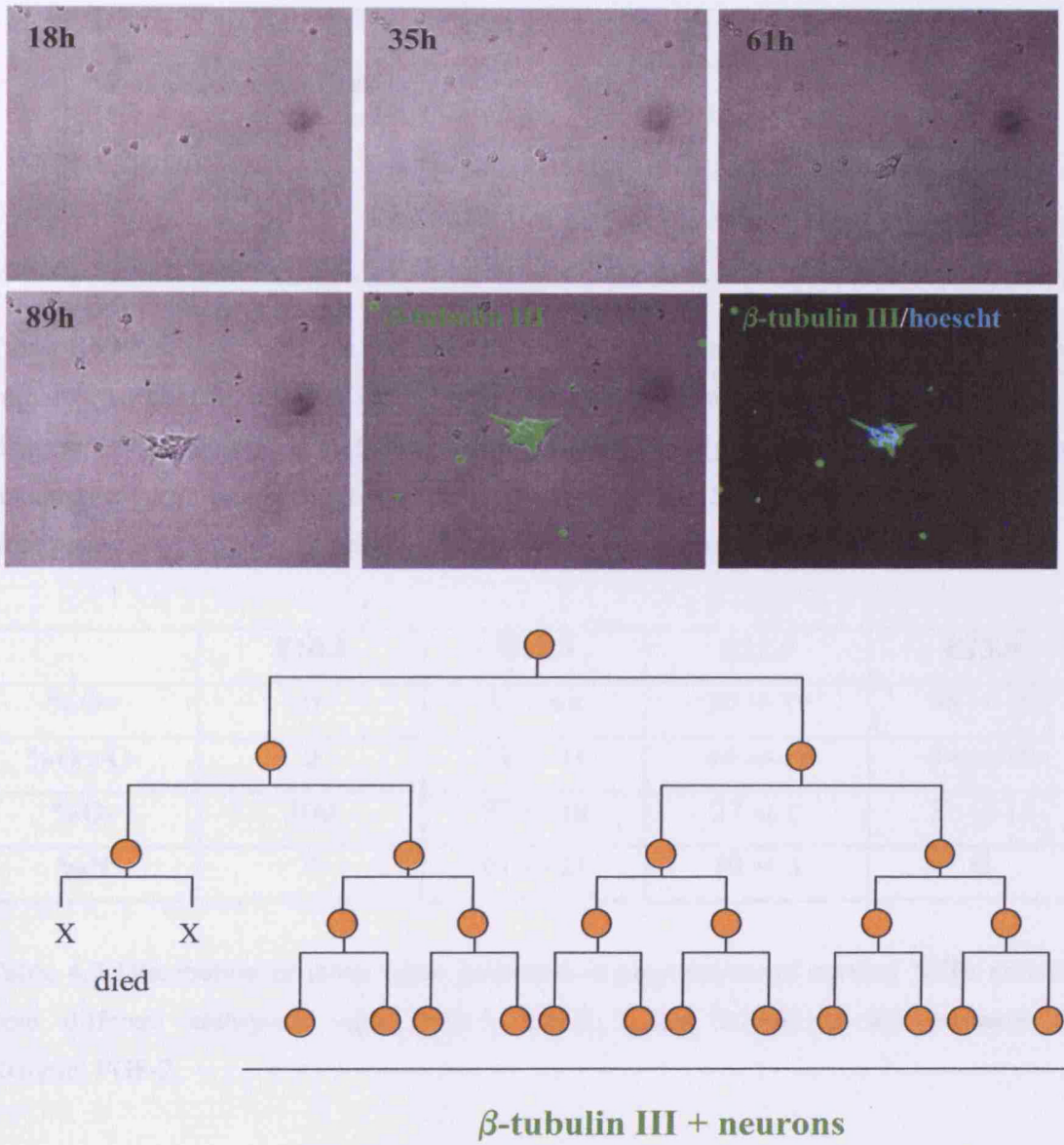

Figure 4.34 Stills and a lineage tree from a time-lapse recording of an E10.5 cortical NEP preparation which gave rise to 12 β-tubulin III+ neurons and two cells that died. Since all identifiable cells were neurons and the two that died had the same morphology as the others, it was presumed that the starting cell was a dedicated neuroblast and this was classified as an N-clone.

4.2.11 NEPs become more gliogenic with age

Preparations from E11.5, E12.5 and E13.5 embryos had good enough survival over ~90 hours (Table 4.6) for quantifiable clonal analysis (Table 4.7).

	E11.5	E12.5	E13.5
% of single cells that divided	38 +/- 9	68 +/- 24	54 +/- 13
% of clones that survived	78 +/- 20	83 +/- 9	69 +/- 8

Table 4.6 Percentage of single cells that divided and percentage of clones that survived for immunocytochemical analysis in 10 ng/ml FGF-2 in preparations derived from cortices of different embryonic ages (E11.5, E12.5, and E13.5). Data is presented as mean +/- standard deviation for triplicate experiments (5 experiments for E13.5). E10.5 data is not included since not enough single cells survived for valid quantitative analysis.

	E10.5	E11.5	E12.5	E13.5
%O+	0	1 +/- 0.8	30 +/- 19	46 +/- 15
%O+/O-	0	22 +/- 15	44 +/- 17	34 +/- 13
%O-	100	77 +/- 16	27 +/- 2	21 +/- 13
%N	?	61 +/- 23	10 +/- 3	0

Table 4.7 Distribution of clone types generated in preparations of cortical NEPs derived from different embryonic ages (E10.5, E11.5, E12.5, E13.5) in the presence of 10 ng/ml FGF-2.

In contrast to E10.5 cultures, the E11.5-derived NEPs gave rise to some, although not many Olig2+ cells; ~1% O+, 22% O+/O- and 77% O-. The total percentage of O- clones was made up of 61% N-clones and 16% contained both β-tubulin III+ and immunocytochemically unidentified cells (Table 4.7). There were many cells that did not divide, and those that survived were found to be β-tubulin III+ neurons. Examples of the different clone types derived from these E11.5 cultures in 10 ng/ml FGF-2 are shown in Figures 4.35 – 4.38.

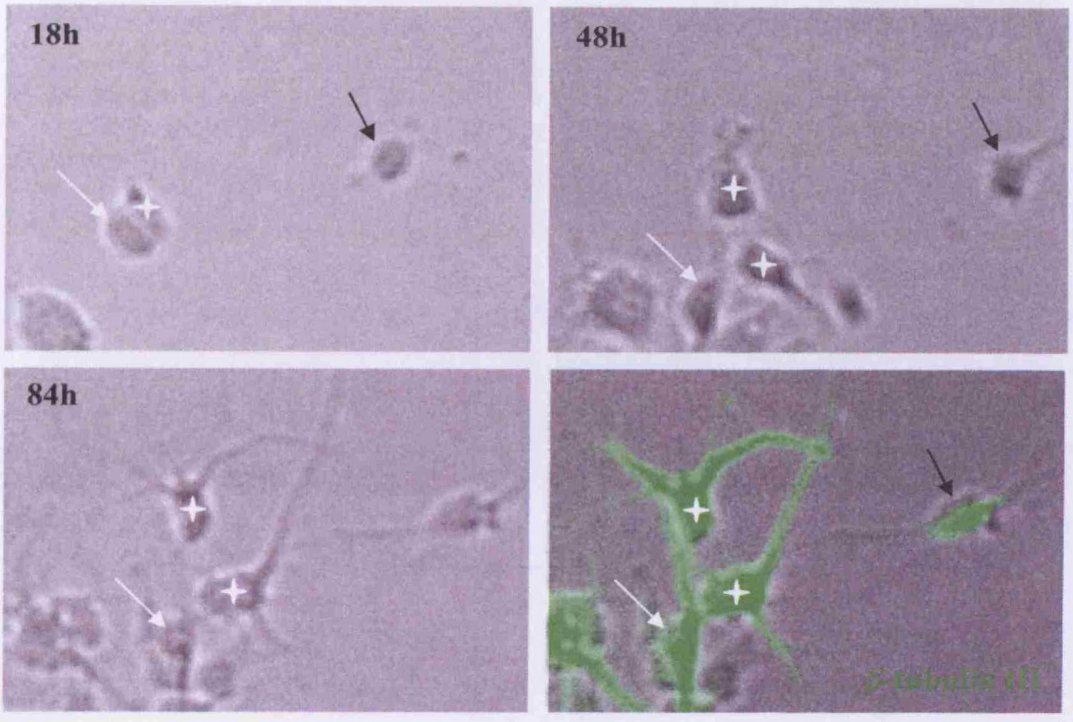

Figure 4.35 Stills from a time-lapse recording of an E11.5 cortical NEP preparation in 10 ng/ml FGF-2 in which both a dedicated neuroblast (white star) and 2 post-mitotic neurons (black and white arrows) were present. Only one cell divided (starred cell at 18h) and it gave rise to 2 β-tubulin III+ neurons and was therefore classified as an N-clone. The starting cell indicated by a white arrow at 18 hours could have been a sister cell to the starred neuroblast since it looked like cytokinesis was just completing at this time. However, because the division itself was not observed, it was not classified as part of the same clone.

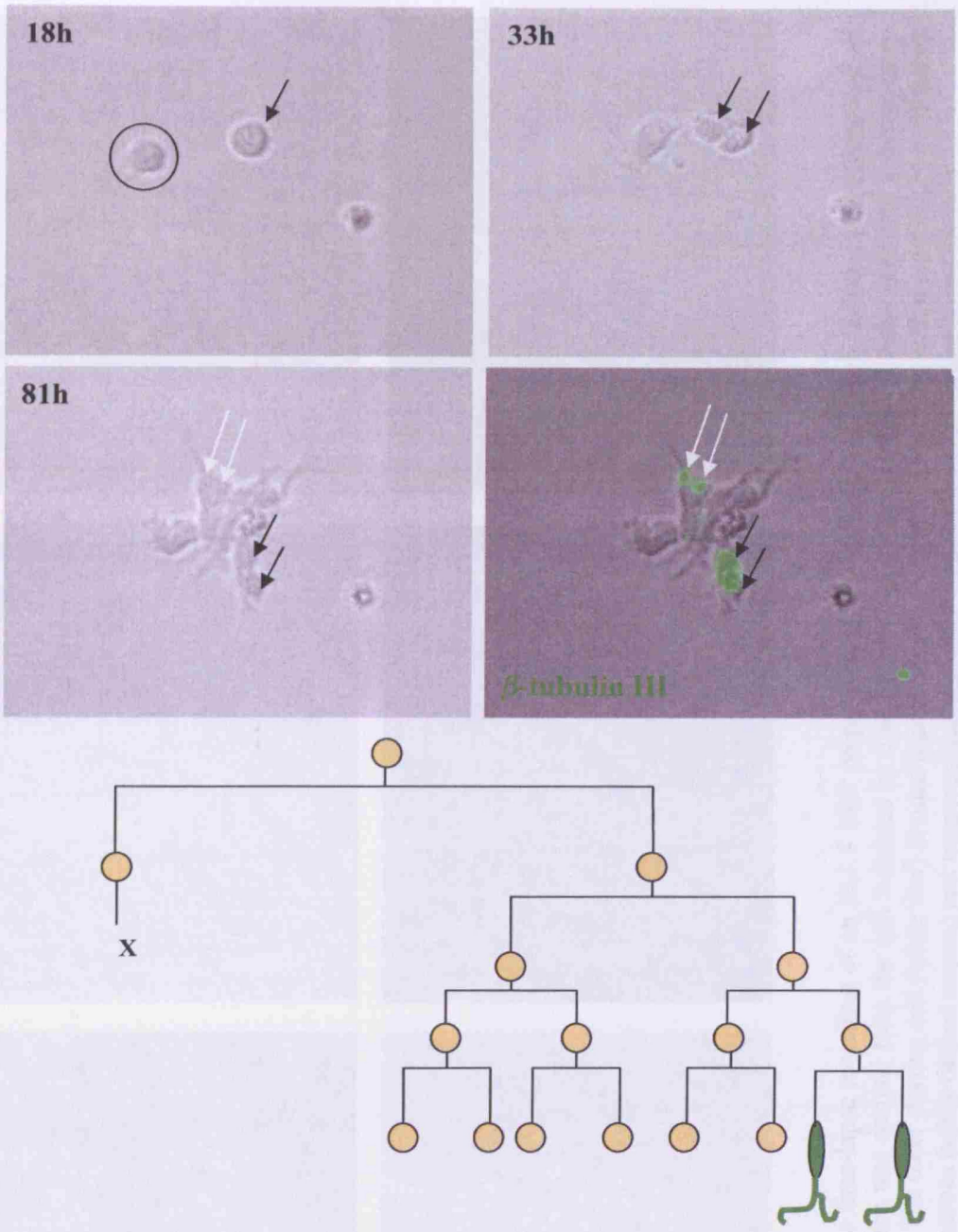

Figure 4.36 Stills and a lineage from a time-lapse recording of an E11.5 preparation in 10 ng/ml FGF-2 which included both a mixed neuronal clone (lineage drawn) and an N-clone. The N-clone derived from what was presumably a dedicated neuroblast (black arrows). The mixed clone (derived from the circled cell) also generated two neurons (white arrows). The remaining cells were unidentified.

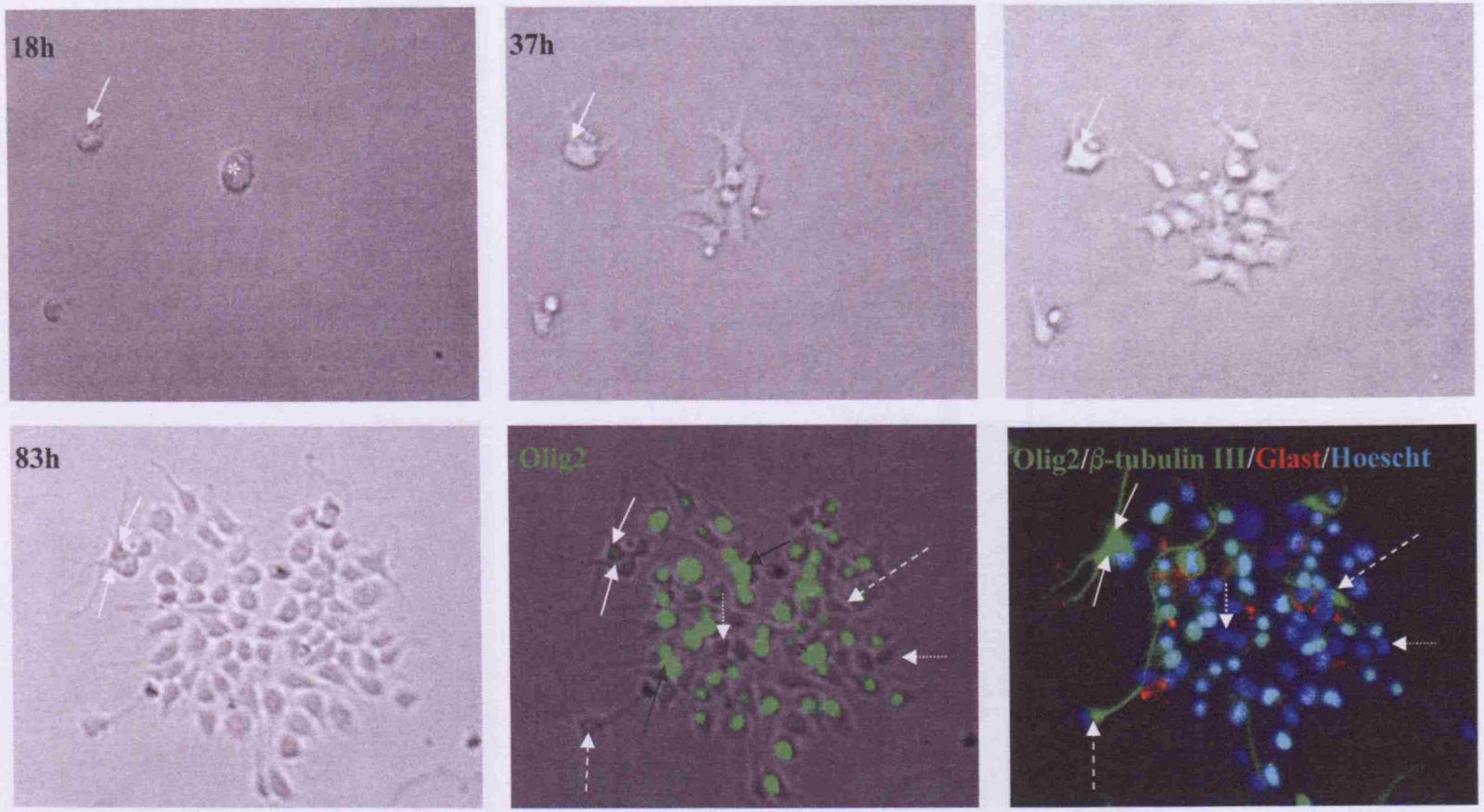

Figure 4.37 Stills from a time-lapse recording of an E11.5 NEP preparation in 10 ng/ml FGF-2 which included an N-clone and an O+/O- clone. The N-clone was derived from the cell indicated by a white arrow at 18 hours which divided once and generated two neurons (white arrows). The other starting cell (white star) divided many times to yield an O+/O- clone with many Olig2+ cells (black arrows), β-tubulin III+ neurons (white dashed arrows) and immunocytochemically unidentified cells (white dotted arrows)

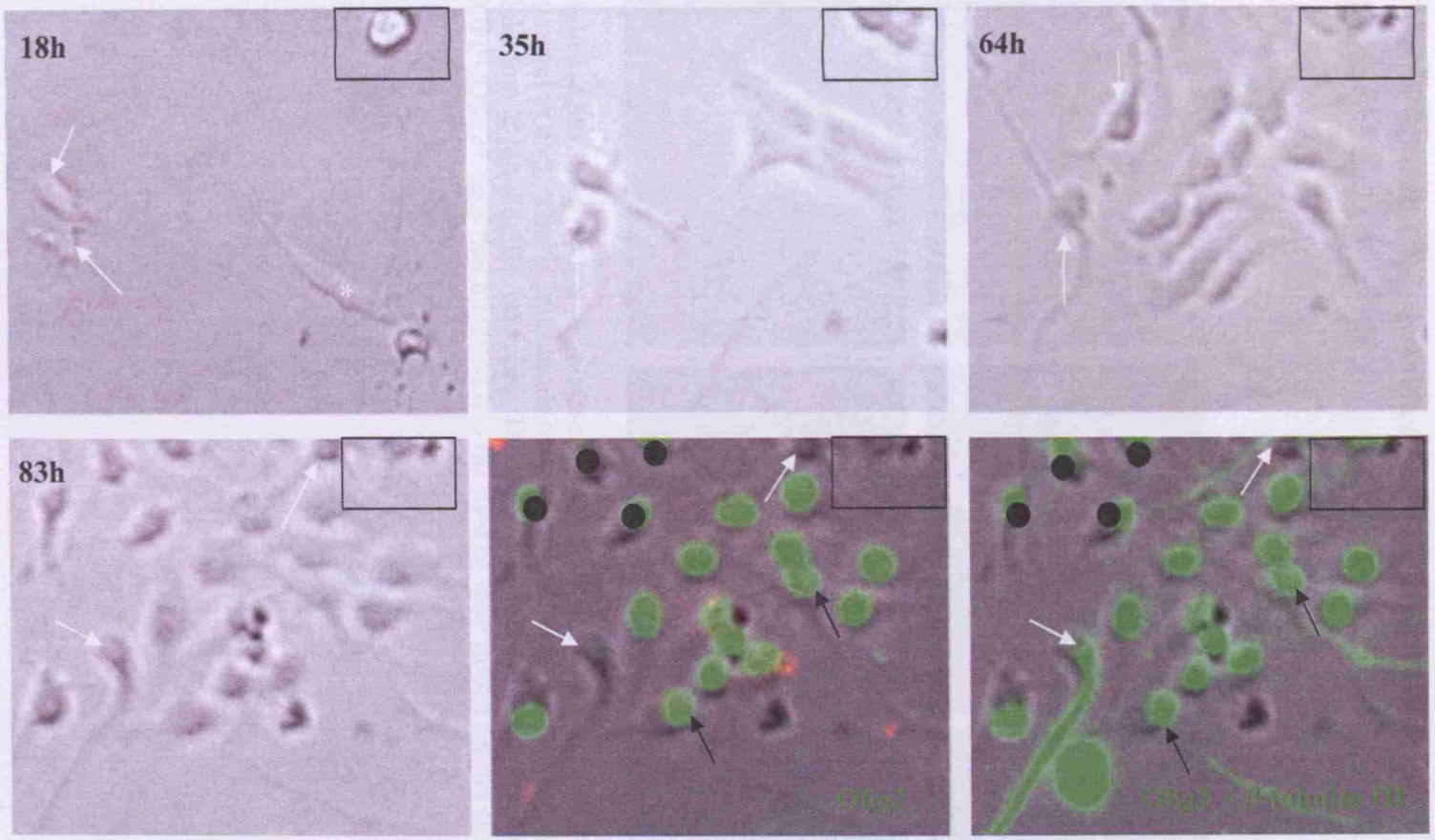

Figure 4.38 Stills from a time-lapse recording of an E11.5 cortical NEP preparation in 10 ng/ml FGF-2. Two cells did not divide and were β-tubulin III+ neurons (white arrows). One cell (starred cell at 18h) divided several times to yield an O+ clone (black arrows). The cells that have been blacked out are cells that entered the field of view from a nearby clone. This is an example of one of the few O+ clones derived from E11.5 cultures. The other starting cell (boxed) at 18 hours underwent several divisions, but mostly outside of this field of view.

In cultures from E12.5 embryos, there was a dramatic increase in the production of Olig2+ cells and a decrease in neurons compared to E11.5 data since 30% of surviving clones were O+ and the total O- clones was 27% with only 10% being N-clones (Table 4.7). Examples of E12.5-derived clones are shown in Figures 4.39 - 4.41.

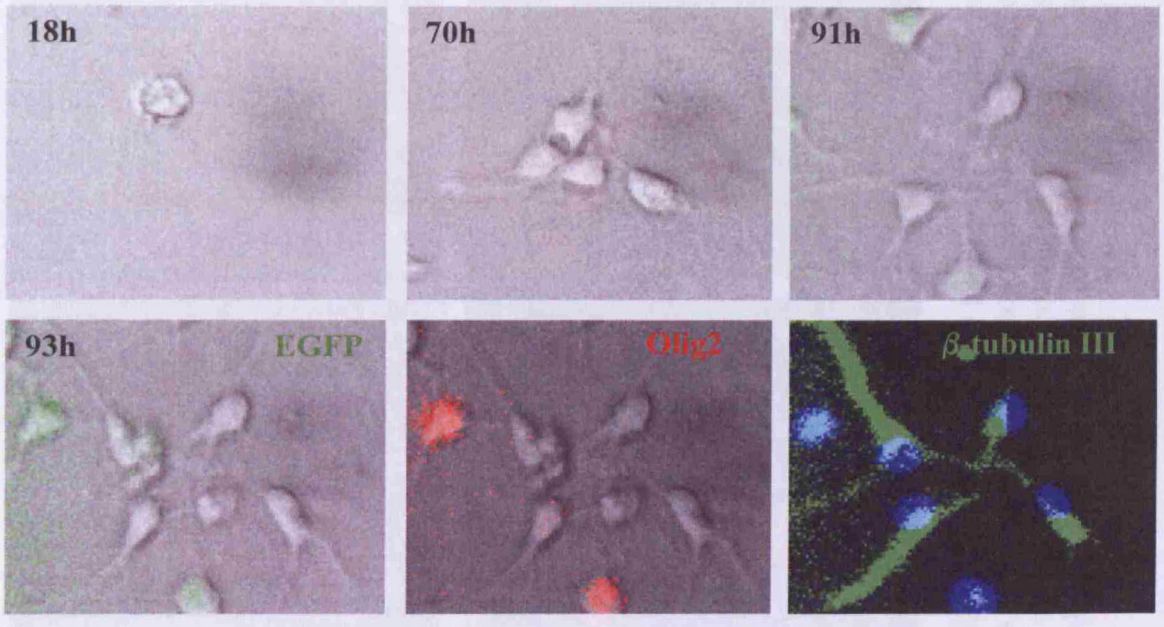

Figure 4.39 Stills from a time-lapse recording of an E12.5 cortical NEP preparation in 10 ng/ml FGF-2. This is an example of an N-clone in which the starting cell divided twice to yield four β-tubulin III+ neurons. The only Olig2 staining here (in red) corresponded to EGFP+/Oilg2+ cells that migrated into the field of view from a nearby clone.

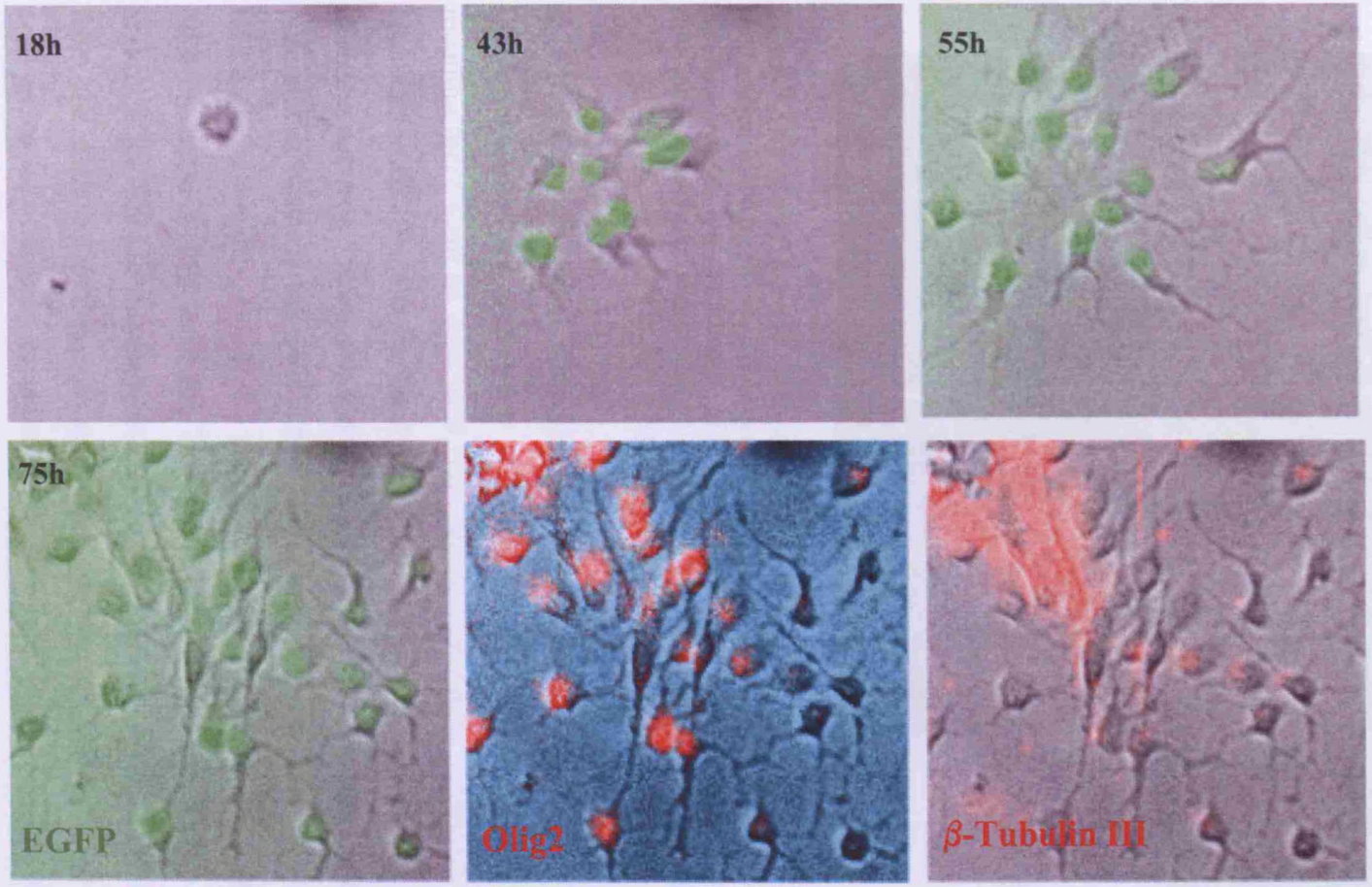

Figure 4.40 Stills from a time-lapse recording of an E12.5 cortical NEP preparation in 10 ng/ml FGF-2 in which one cell gave rise to a mixed clone of Olig2+ and β-tubulin III+ cells as well as some cells which were immunocytochemically unidentified (white arrows). These had elongated processes and might be radial glial cells although they did not stain for the RGC marker Glast. Since all cells were EGFP+ at 55 hours, some down-regulation must have occurred to generate the β-tubulin III+ cells and those which were unidentified. This is another example of the dynamic nature of *olig2* expression in these cultures.

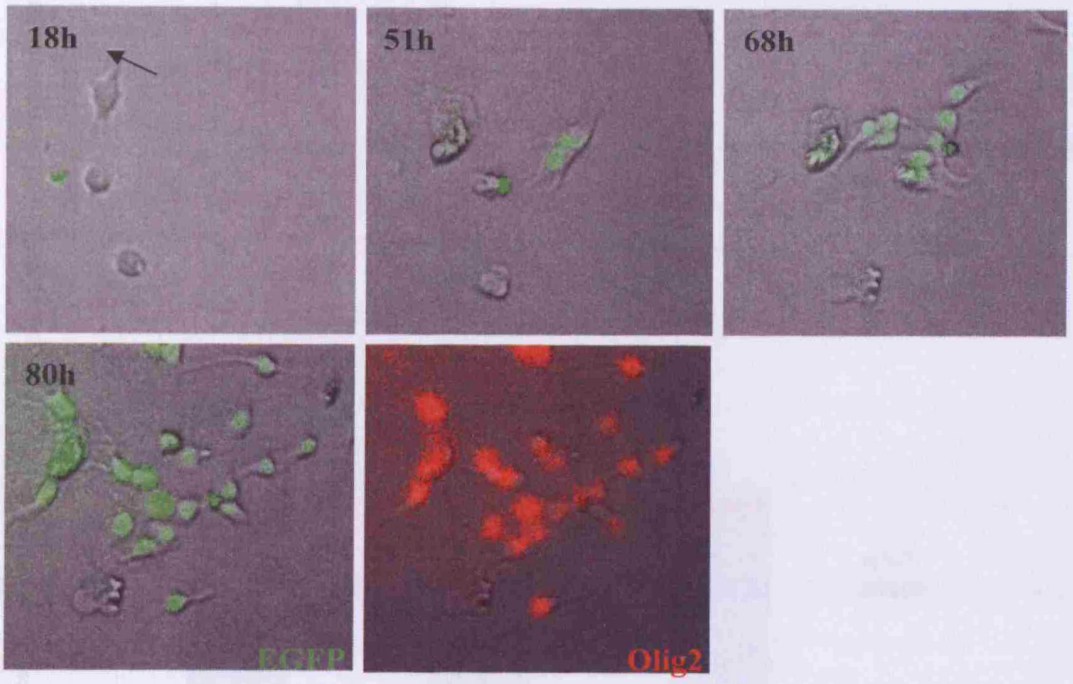

Figure 4.41 Stills from a time-lapse recording of a transgenic E12.5 cortical NEP preparation in 10 ng/ml FGF-2 in which an O+ clone was derived. One starting cell (black arrow) divided and expressed EGFP by 51h. All daughter cells maintained EGFP fluorescence and all counter-stained for Olig2 at 80h. Other cells in the starting field of view died or divided once and died by 68h.

In E13.5 cultures, 46% were O+, 34 % were O+/O- and 21% were O- and all O- clones contained a mixture of β-tubulin III+ neuron and unidentified cells meaning there were no dedicated neuroblasts (Table 4.7). Other than the absence of N-clones in E13.5 cultures, the clone distribution was not dissimilar to that produced in E12.5 cultures. There was therefore clearly a switch from neurogenic to gliogenic potential of NEPs in the presence of 10 ng/ml FGF-2 between the ages of E11.5 and E12.5 (Figure 4.42). Since the percentage of surviving clones was similar in the different cultures (Figure 4.43; Table 4.6; 78% survival for E11.5, 83% for E12.5 and 69% for E13.5), the distributions of clone types derived from cultures prepared from the different embryonic ages were probably a consequence of the genuine emergence of different lineages in response to FGF-2, rather than differential survival of clone types at different ages. Fewer starting cells in E11.5 preparations divided relative to those in E12.5 or E13.5 cultures (Table 4.6), further suggesting that FGF-2 also had a less potent effect with respect to cell division as well as for induction of *olig2* at E11.5.

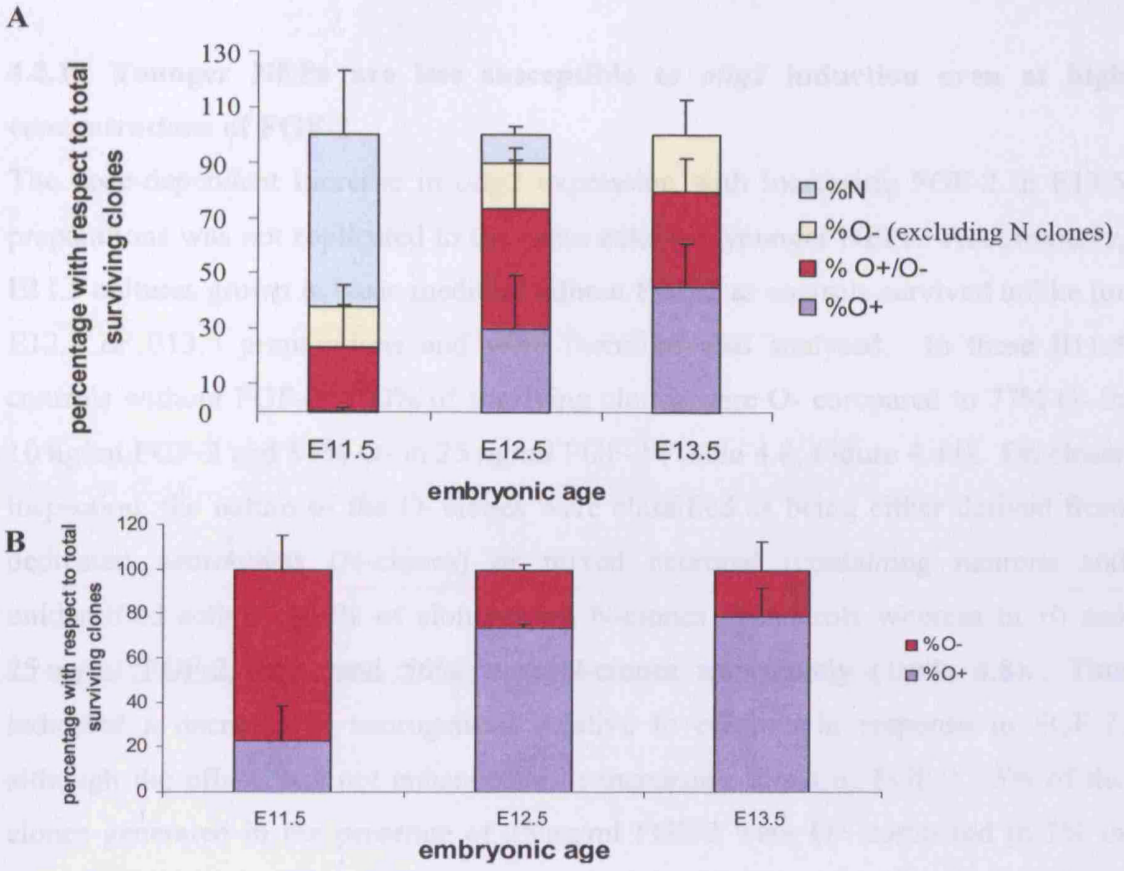

Figure 4.42 A) Distribution of clone types derived from cortical NEP preparations from embryos of different ages. B) Relative appearance of Olig2+ cells in clones derived from cultures from mice of different embryonic ages. O+ clones here indicate the sum of O+ and O+/O- clones. All cell preparations were in 10 ng/ml FGF-2. Data is shown as mean +/- standard deviations. Quantitative analysis could not be done for clones from E10.5 cultures since few survived.

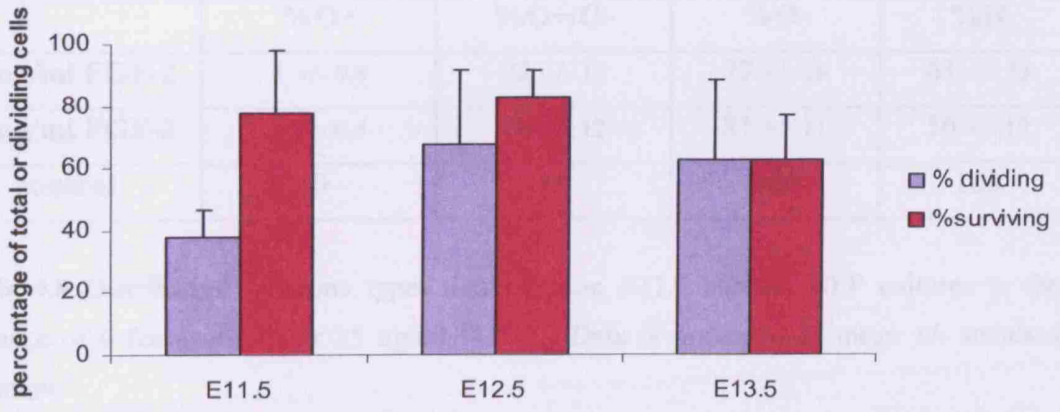

Figure 4.43 Comparison across cortical preparations from mice of different embryonic ages of the percentage of single cells in the starting population that divided at least once (blue) and the percentage of these dividing cells that went on to generate a larger clone which survived the filming period for immunocytochemical analysis (purple). Clones were filmed in 10 ng/ml FGF-2 over 72 hours. Data is presented as mean +/- standard deviation.

4.2.12 Younger NEPs are less susceptible to *olig2* induction even at high concentrations of FGF-2

The dose-dependent increase in *olig2* expression with increasing FGF-2 in E13.5 preparations was not replicated to the same extent in younger NEPs. Anomolously, E11.5 cultures grown in basic medium without FGF-2 as controls survived unlike for E12.5 or E13.5 preparations and were therefore also analysed. In these E11.5 controls without FGF-2, 100% of surviving clones were O- compared to 77% O- in 10 ng/ml FGF-2 and 81% O- in 25 ng/ml FGF-2 (Table 4.8; Figure 4.44). On closer inspection, the nature of the O- clones were classified as being either derived from dedicated neuroblasts (N-clones) or mixed neuronal (containing neurons and unidentified cells). 100% of clones were N-clones in controls whereas in 10 and 25 ng/ml FGF-2, 61% and 56% were N-clones respectively (Table 4.8). This indicated a decrease in neurogenesis relative to controls in response to FGF-2, although the effect was not enhanced with increasing levels of FGF-2. 3% of the clones generated in the presence of 25 ng/ml FGF-2 were O+ compared to 1% in 10 ng/ml FGF-2. Although this was only a small increase, it was significant (Table 4.8; $P = 0.02$) while the percentage of O- and O+/O- clones did not change significantly (Table 4.8; 22% O+/O- in 10 ng/ml FGF-2, 16% O+/O- in 25 ng/ml FGF-2 $P>0.5$; 77% O- in 10 ng/ml FGF-2, 81 % in 25 ng/ml FGF-2 $P>0.5$).

	%O+	%O+/O-	%O-	%N
10 ng/ml FGF-2	1 +/- 0.8	22 +/- 15	77 +/- 16	61 +/- 23
25 ng/ml FGF-2	3 +/- 0.5	16 +/- 12	81 +/- 11	56 +/- 19
control	0	0	100	100

Table 4.8 Distribution of clone types derived from E11.5 cortical NEP cultures in the presence of 0 (control), 10 or 25 ng/ml FGF-2. Data is presented as mean +/- standard deviation.

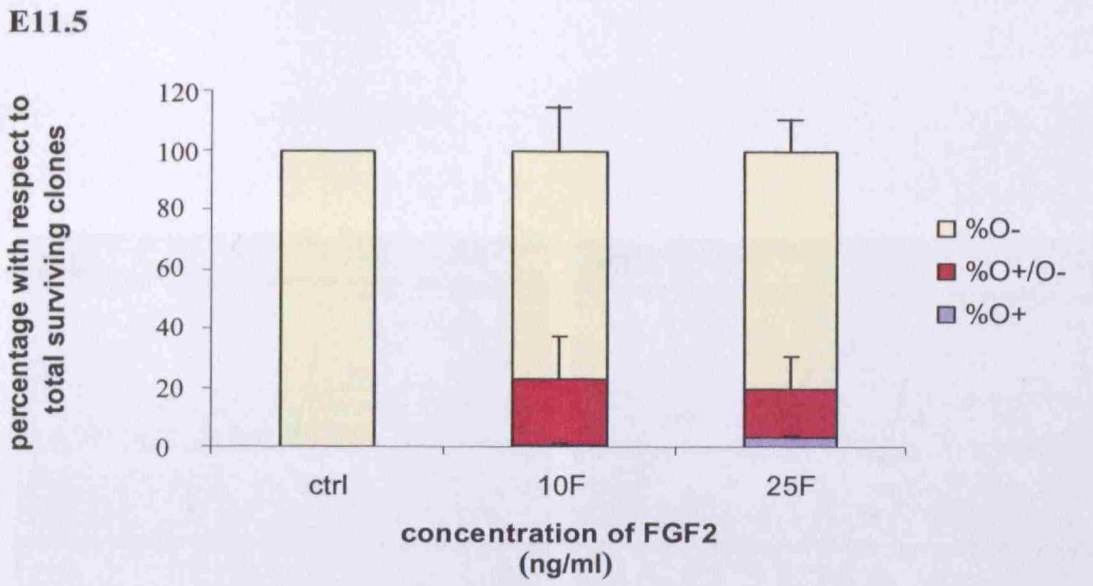

Figure 4.44 Differences in clone types derived from E11.5 cortical NEP cultures in 10 vs. 25 ng/ml FGF-2. The proportion of O- clones did not decrease significantly with increasing FGF-2 ($P>0.5$), but the proportion of O+ clones increased significantly from 1% to 3% ($P = 0.02$). Data is presented as mean +/- standard deviation.

Thus, it appears that increased FGF-2 signalling increased the incidence of *olig2* expression in E11.5 NEP preparations, possibly at the expense of neurogenesis, since the proportion of O+ clones increased while the proportion N-clones decreased (Table 4.8). A selection of clone types derived from E11.5 cultures in 25 ng/ml FGF-2 are shown in Figures 4.45 – 4.48.

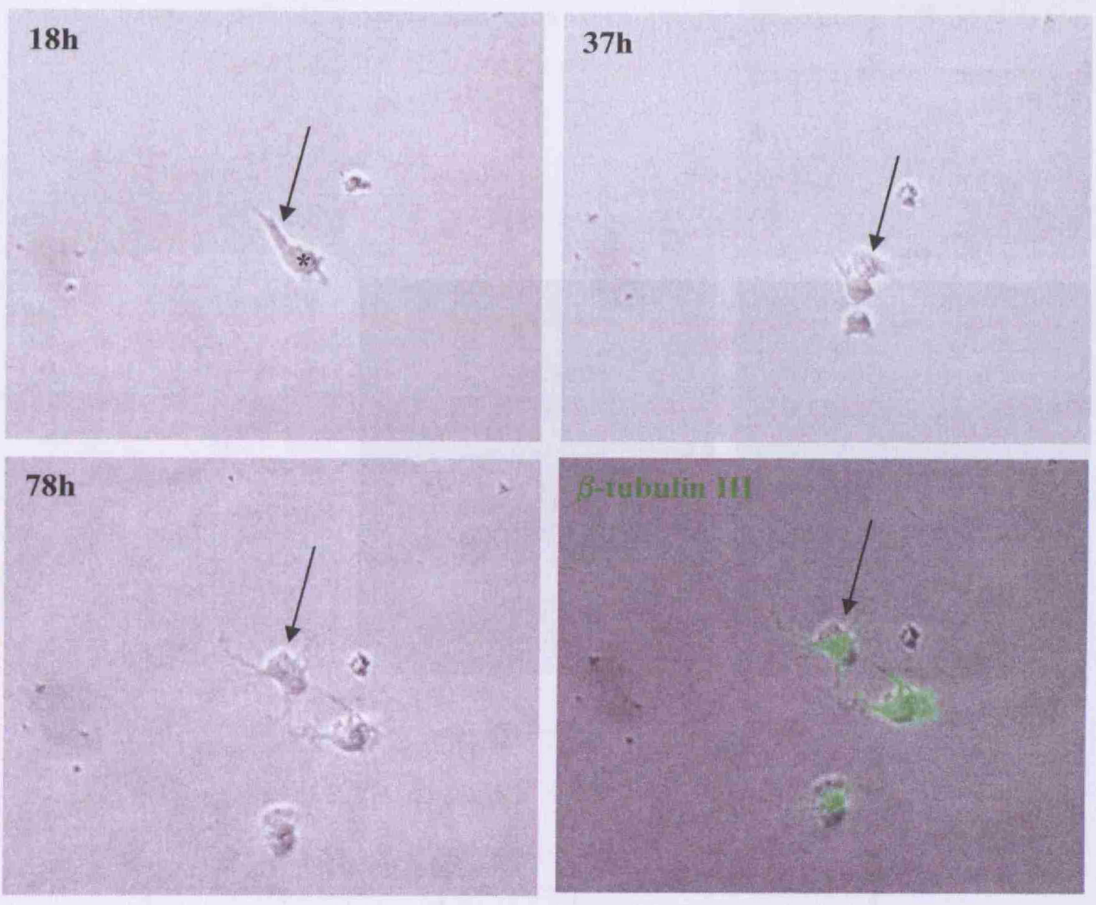

Figure 4.45 Stills from a time-lapse recording of an E11.5 cortical NEP preparation in 25 ng/ml FGF-2. This recording is an example of an N-clone in which two β-tubulin III+ neurons were generated from the division of one starting cell (starred at 18h). The other starting cell (black arrow) did not divide, but was β-tubulin III+ at 78 hours. 56% of clones were neuroblasts in 25 ng/ml FGF-2 as compared to 73% in 10 ng/ml FGF-2 and 100% in controls.

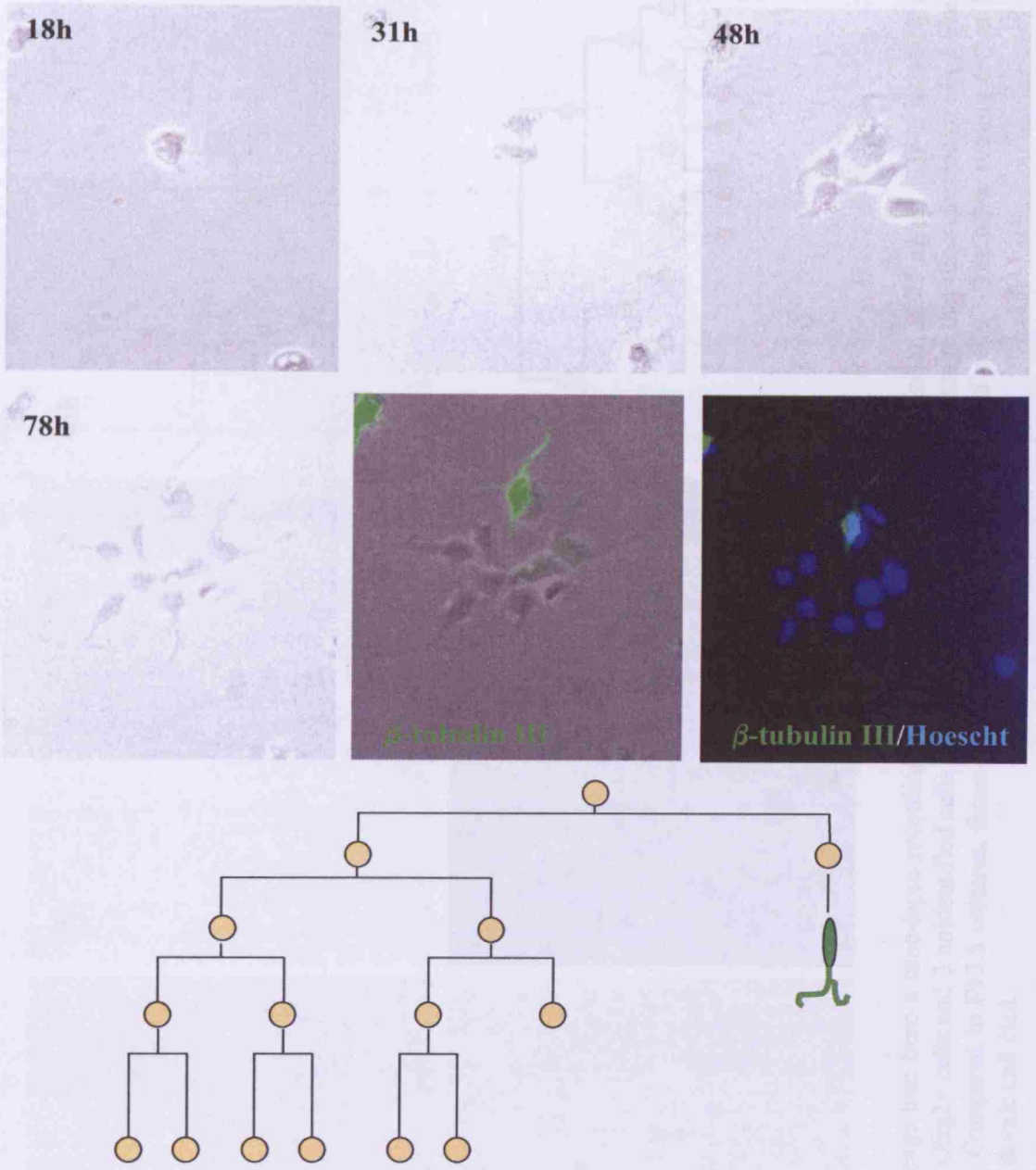

Figure 4.46 Stills and a lineage from an E11.5 cortical NEP preparation in 25 ng/ml FGF-2 in which a mixed neuronal clone was generated. Only one neuron was generated after the first division and all other cells were unidentified. There were no Olig2+ cells, thus classifying this as an O- clone.

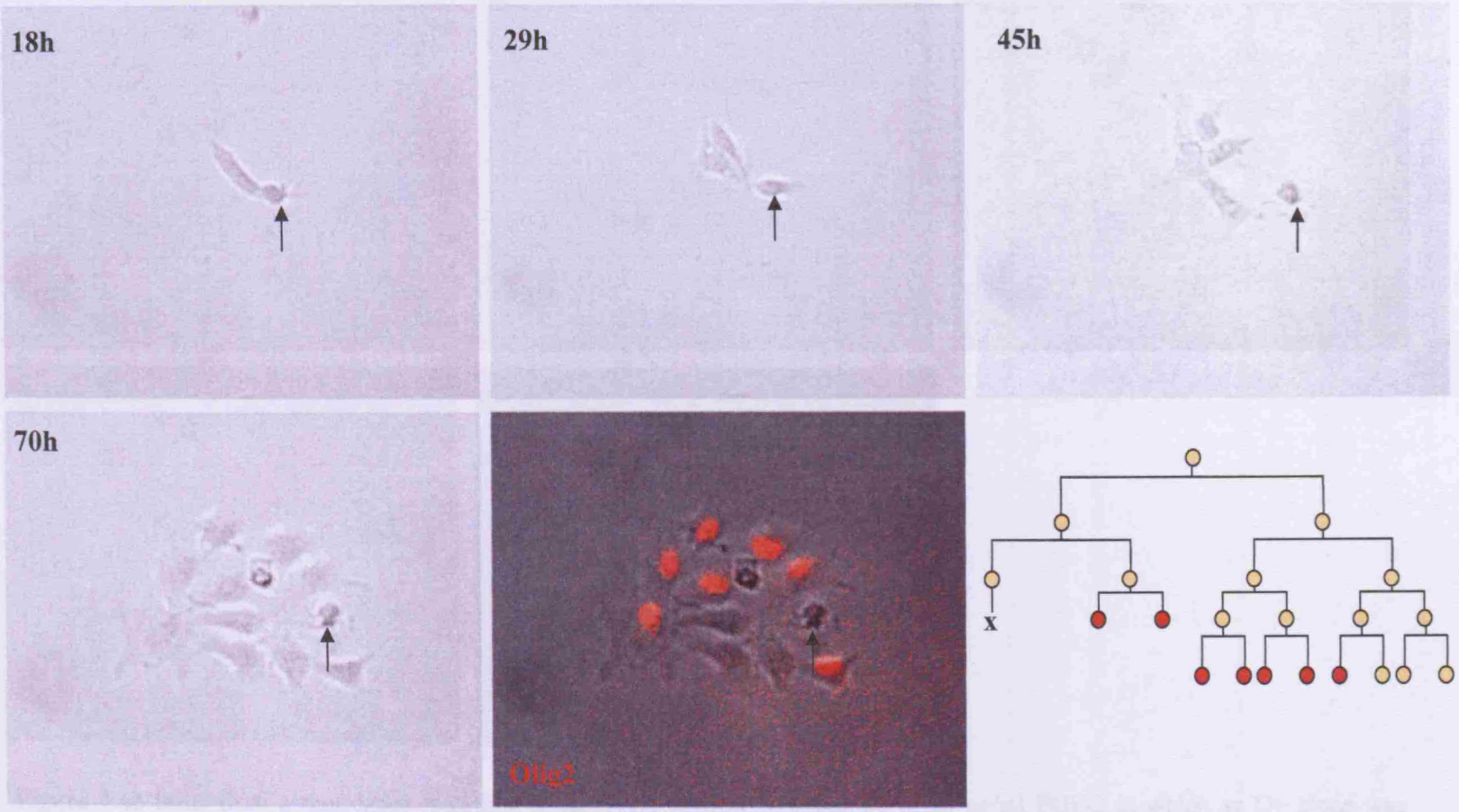

Figure 4.47 Stills and a lineage tree from a time-lapse recording of an E11.5 cortical NEP preparation in 25 ng/ml FGF-2 in which an O+/O- clone consisting of 7 Olig2+ cells and 3 unidentified cells was derived. It seems from the lineage that the induction of *olig2* likely occurred late in the lineage. Compared to E13.5 cultures, these clones generated small numbers of cells. The other starting cell at 18 hours (black arrows) did not divide and died.

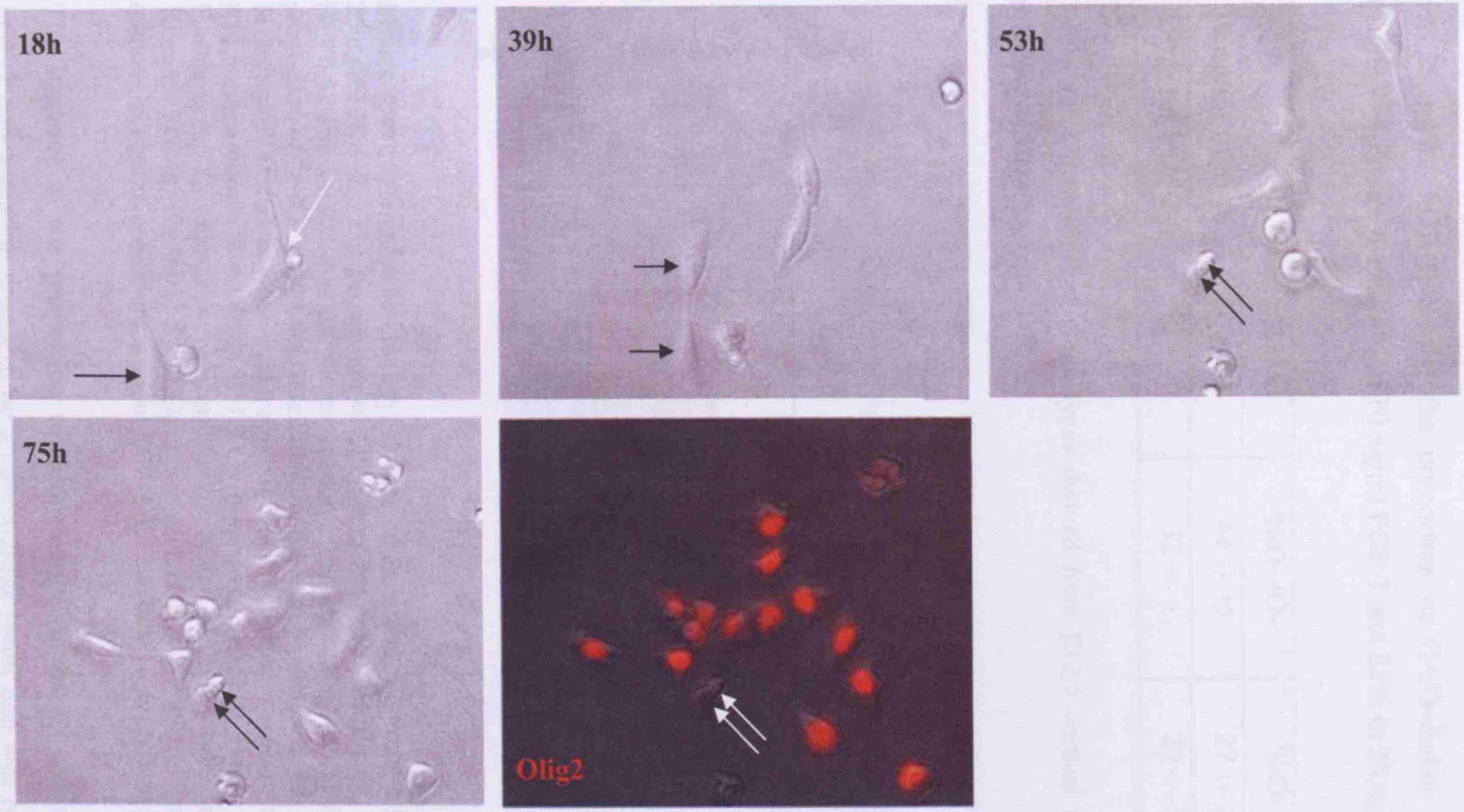

Figure 4.48 Stills from a time-lapse recording of an E11.5 cortical NEP culture in 25 ng/ml FGF-2 in which an O+ clone was generated. The starting cell indicated with a white arrow divided several times to yield 14 Olig2+ daughter cells. The other starting cell (black arrow) divided once and both of these daughter cells (arrows) died.

E12.5-derived cultures also showed only a small increase in O+ only clones with increased FGF-2; from 30% in 10 ng/ml FGF-2 to 40% in 25 ng/ml FGF-2 (Table 4.9). The proportion of N-clones however, doubled (from 10% to 21% in 10 vs. 25 ng/ml FGF-2) whilst the proportion of O+/O-clones decreased slightly (Table 4.9; Figure 4.49; 44% in 10 ng/ml FGF-2 and 32% in 25 ng/ml FGF-2).

	%O+	%O+/O-	%O-	%N
10 ng/ml FGF-2	30 +/- 19	44 +/- 17	27 +/- 2	10 +/- 3
25 ng/ml FGF-2	40 +/- 1	32 +/- 2	29 +/- 3	21 +/- 3

Table 4.9 Distribution of clone types derived from E12.5 cortical NEP cultures in the presence of 10 or 25 ng/ml FGF-2.

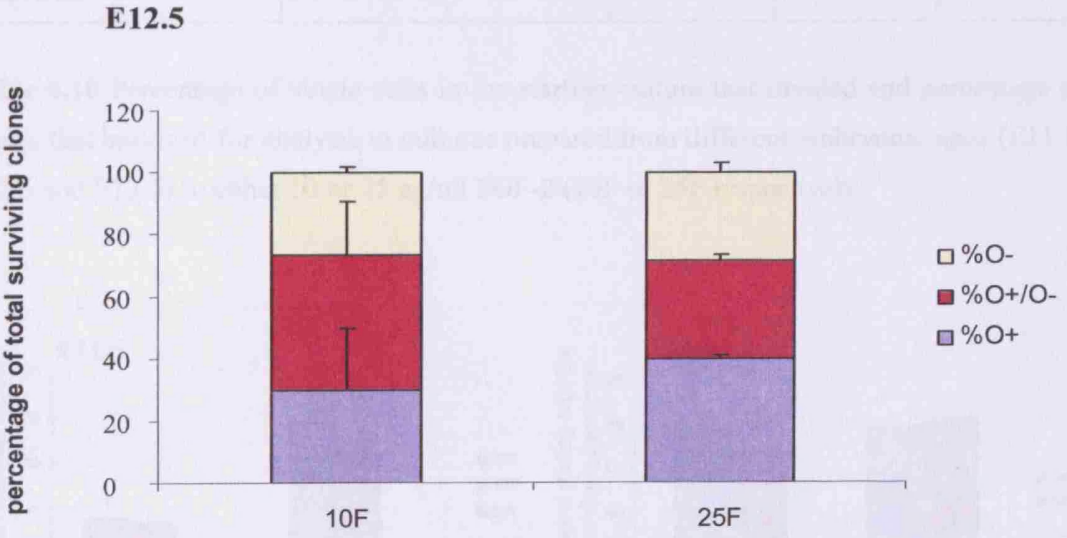

Figure 4.49 Differences in clone types derived from E12.5 cortical NEP cultures in 10 vs. 25 ng/ml FGF-2. The proportion of O+ clones increased marginally, but not significantly (P = 0.62 10F vs. 25F), as did the proportion of neuroblasts (P = 0.55 10F vs. 25F), and the proportion of O+/O- clones decreased marginally, but not significantly (P = 0.52 10 vs. 25F). In 25 ng/ml FGF-2 however, the proportion of O+ clones was significantly larger than in E11.5 preparations (P = 0.0085 E11.5 O+ clones vs. E12.5 O+ clones in 25 ng/ml FGF-2). Furthermore, O- clones were significantly fewer in E12.5 than in E11.5 cultures in 10 ng/ml FGF-2 (P = 0.027 E11.5 O- clones vs. E12.5 O- clones in 10 ng/ml FGF-2). E12.5 cultures in control conditions without FGF-2 did not survive the culture period.

The increase in the proportion of neuron-only clones (N-clones) with increasing FGF-2 concentration seems to be an anomalous result and was only just significant (P = 0.05 for %N clones in 10 vs. 25 ng/ml FGF-2). This anomaly could not be attributed to differences in the percentage of dividing or surviving cells since this

was not significantly different in 10 or 25 ng/ml FGF-2 (Table 4.10; Figure 4.50). It was clear however, that induction of *olig2* was far greater in E12.5 cultures than in preparations from earlier embryonic ages. Examples of the clones generated from E12.5 cultures in 25 ng/ml FGF-2 are shown in Figures 4.51 and 4.52.

	E11.5 10F	**E11.5 25F**	**E12.5 10F**	**E12.5 25F**	**E13.5 10F**	**E13.5 25F**
% of single cells that divided	38 +/- 9	36 +/- 10	68 +/- 24	78 +/- 6	62 +/- 24	62 +/- 10
% of clones that survived	78 +/- 20	78 +/- 1	83 +/- 9	79 +/- 6	63 +/- 15	63 +/- 10

Table 4.10 Percentage of single cells in the starting culture that divided and percentage of clones that survived for analysis in cultures prepared from different embryonic ages (E11.5, E12.5 and E13.5) in either 10 or 25 ng/ml FGF-2 (10F or 25F respectively).

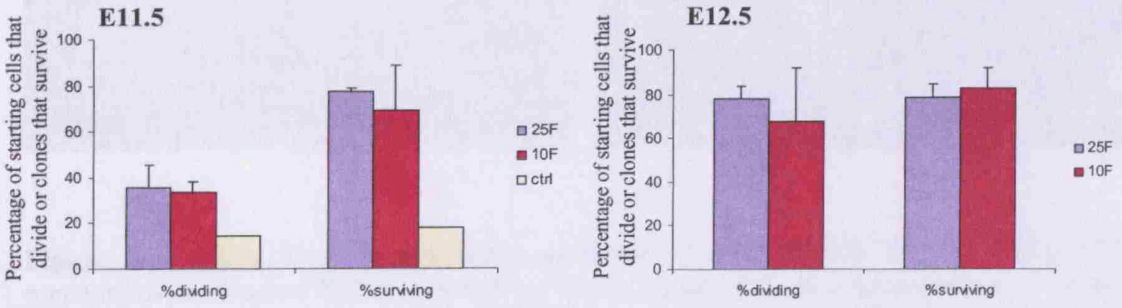

Figure 4.50 Summary of the percentage of starting cells that divided at least once, and the percentage of the dividing cells that gave rise to clones that survived until the end of the experiment in E11.5 and E12.5 cultures in both 10 and 25 ng/ml FGF-2. There was no significant difference in the number of starting cells that divided nor the clone survival at different concentrations of FGF-2.

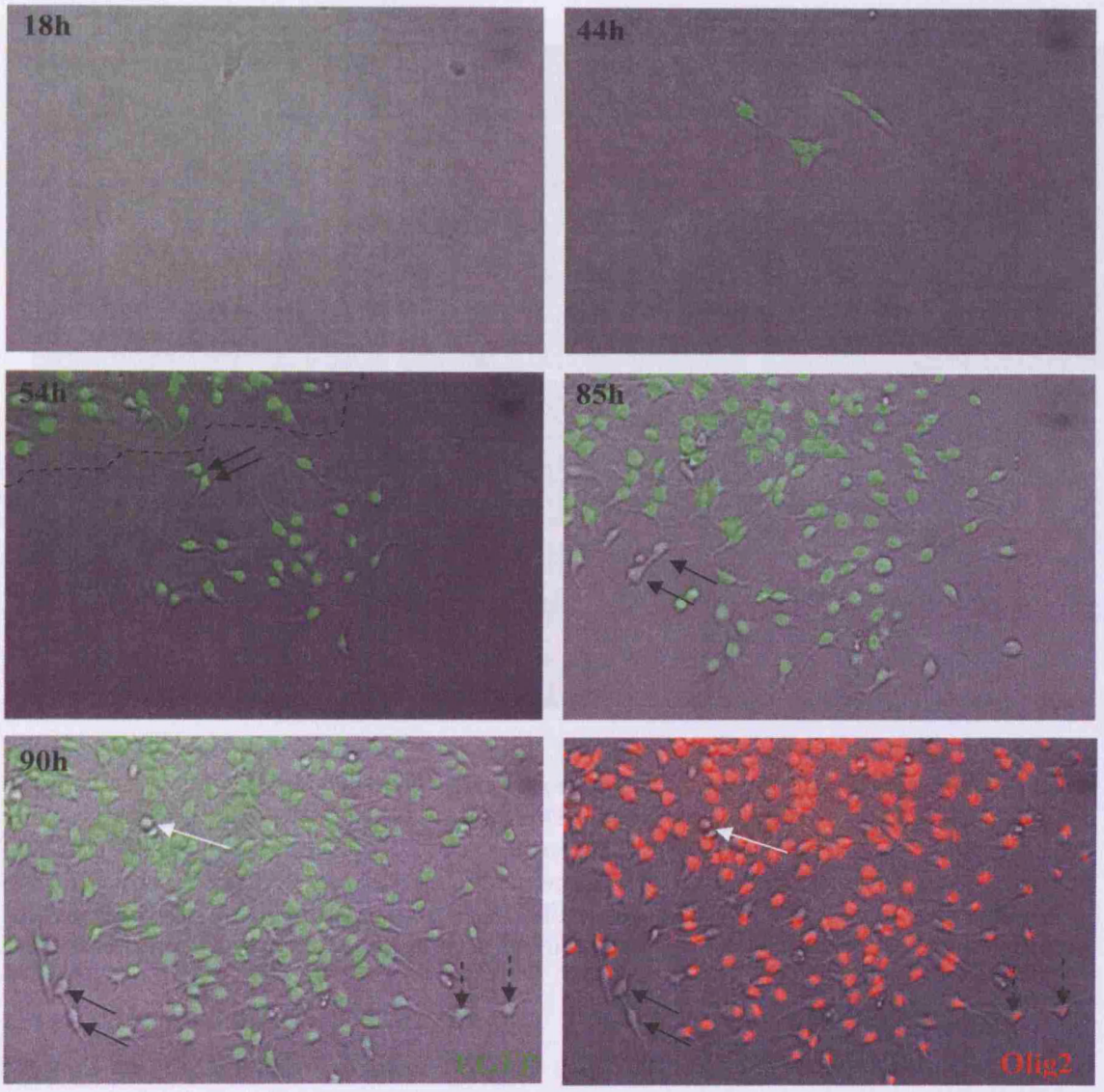

Figure 4.51 Stills from a time-lapse recording of a transgenic E12.5 cortical NEP preparation in 25 ng/ml FGF-2 in which an O+/O- mixed clone was generated. At 54 hours, some cells from a nearby clone entered the field of view (demarcated by dotted line), but the majority of daughter cells from each clone were separable. Note that 2 cells (black arrows) from the original clone were seen to down-regulate EGFP and were Olig2/EGFP-negative at 90h. They were also β-tubulin III-negative and were thus unidentified. A few other cells also seemed to down-regulate EGFP and Olig2 (dotted black arrows). All other cells were Olig2+ meaning the original clone was mixed. A few cells died (white arrows), but the divisions weren't traceable so no lineage tree was drawn.

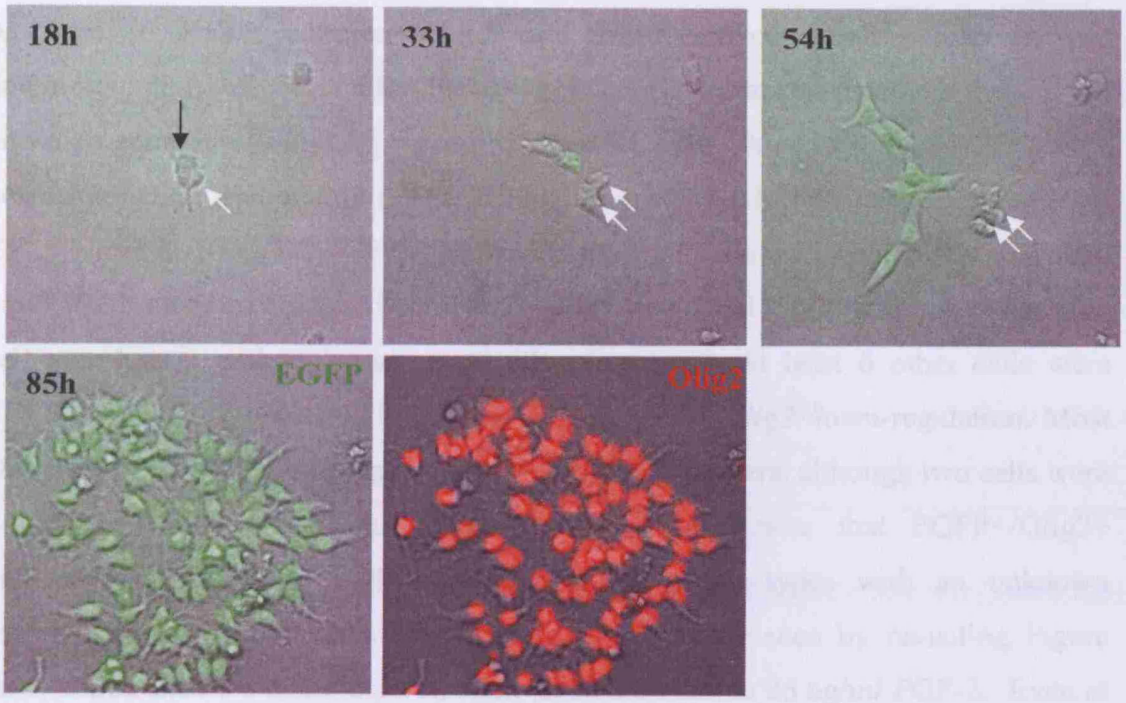

Figure 4.52 Stills from a time-lapse recording of a transgenic E12.5 cortical NEP preparation in 25 ng/ml FGF-2 in which an O+ clone was generated from the starting cell indicated with a black arrow. EGFP was visualized after the first division, but only in one daughter cell. The EGFP-negative daughter was EGFP+ before its second division however, and all daughter cells thereafter were also EGFP+. All daughter cells were EGFP+/Olig2+ at 85h. The other starting cell divided once and both daughter cells died by 54h (white arrows).

Overall responsiveness to FGF-2-induced *olig2* expression increased in cells derived from older embryonic ages. Furthermore, the clone sizes generated in preparations from older embryos were much larger, indicating that cells *within* clones were responding more to the mitotic effects of FGF-2. This was not quantified since divisions were frequently too difficult to trace, but the sizes of the clones and the anecdotal impression that cells were dividing faster in recordings of older cultures indicate that the older NEPs divided faster in response to FGF-2 relative to younger NEPs. Furthermore, NEPs derived from embryos younger than E11.5 were unresponsive to FGF-2 with respect to *olig2* induction even at high concentrations.

4.2.13 *Olig2* up- and down-regulation can account for mixed clones in younger NEP preparations

As seen in E13.5 cultures, E12.5 and E11.5-derived cultures also showed down-regulation of *olig2* after induction in some instances meaning that, at all developmental ages, *olig2* expression is a plastic event. An example of EGFP/Olig2 down-regulation is shown in the earlier Figure 4.40, which is a lineage derived from E12.5 NEPs in 10 ng/ml FGF-2. In this example all cells were EGFP+ by 43 hours, but by 75 hours two cells had completely down-regulated EGFP and had radial glial cell morphology although they were Glast-negative. At least 6 other cells were EGFP+, but Olig2-negative, indicative of more recent *olig2* down-regulation. Most Olig2-negative cells were also negative for all other markers, although two cells were β-tubulin III+ neurons (Figure 4.40). This demonstrates that EGFP+/Olig2+ precursors can become both neurons and other cell types with an unknown immunocytochemical profile. Another example can be seen by revisiting Figure 4.51, which shows a clone derived from an E12.5 NEP in 25 ng/ml FGF-2. Even at this responsive age, in high FGF-2, there was some EGFP and *olig2* down-regulation since two EGFP+ cells were EGFP/Olig2-negative at 90 hours and were also negative for any other markers. EGFP down-regulation was not observed in high concentrations of FGF-2 in E13.5 cultures however, indicating that the tendency to maintain *olig2* expression might also increase with developmental age. Figures 4.52 and 4.53 show lineages in which EGFP (and therefore *olig2*) up-regulation was recorded. In Figure 4.52, one cell was EGFP-negative at 33 hours, but they were all EGFP+ by 54 hours, going on to generate an O+ clone. Figure 4.53 shows a lineage from an E11.5 NEP culture in 10 ng/ml FGF-2 in which EGFP was activated in a selection of daughter cells by 48 hours and by 67 hours almost all cells were EGFP+. There was down-regulation of EGFP thereafter however; yielding an O+/O- clone, including some β-tubulin III+ neurons, by 93 hours. In this example, the brightness of EGFP fluorescence matched that of Olig2 with weakly EGFP+ cells having weak Olig2 immunolabelling and vice versa. Thus, as was seen in the experiments described for E13.5 cultures, *olig2* up- and down-regulation can occur in cultures from younger embryonic cortices as well, but also in high concentrations of FGF-2 which was not seen for E13.5 cultures.

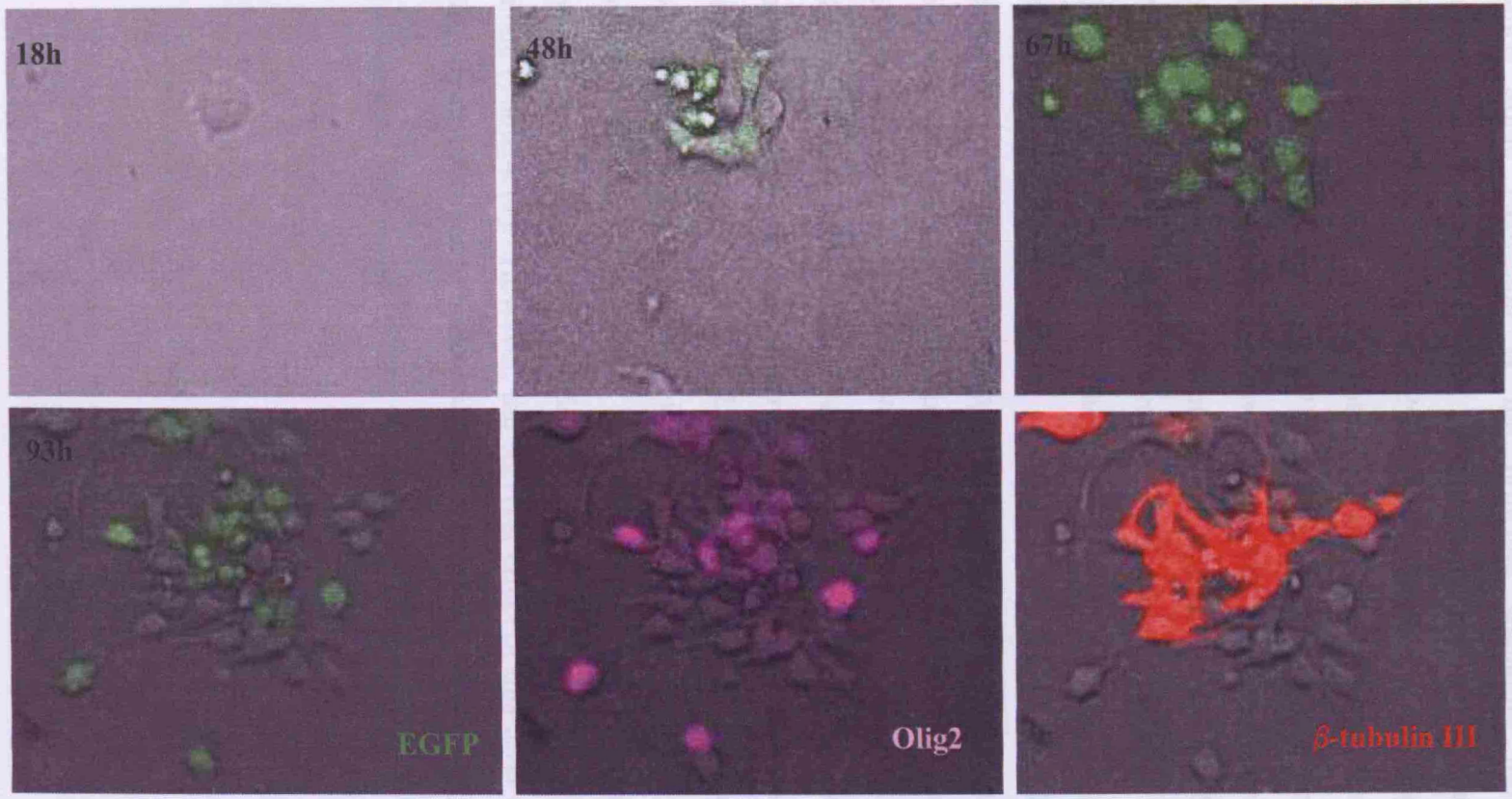

Figure 4.53 Stills from a time-lapse recording of an E11.5 cortical NEP preparation in 10 ng/ml FGF-2 in which a starting cell divided at 18h and yielded a large clone of both EGFP/Olig2+ cells and β-tubulin III+ neurons. The cells were too close together to draw an accurate lineage, but most cells expressed EGFP at some point and many down-regulated it (matched with weak/absent Olig2 staining). Others remained EGFP-negative and of these, some gave rise to neurons.

4.2.14 Effects of Sonic Hedgehog on clonal density cortical neuroepithelial precursor cells

Since Sonic Hedgehog is the principle signalling molecule required for oligodendrogenesis in the CNS, I decided to assess how SHH affected the dynamics of *olig2* expression in cortical NEPs in comparison to the responses to FGF-2. A small-molecule SHH agonist from Curis Inc (Cur-0188168/SHH-Ag1.2, named SAg; (Frank-Kamenetsky et al., 2002)) was used at a working concentration of 100 nM, added to the basic culture medium (Bottenstein and Sato's defined medium, conditioned as described previously). At this concentration, SAg induces *olig2* in dense E13.5 cortical NEP cultures within 20 hours, and NG2+ cells within 72 hours (Kessaris et al., 2004). Furthermore, the numbers of Olig2+ and NG2+ cells generated in 100 nM SAg are comparable to those in 10 ng/ml FGF-2 in dense cultures ($6x10^6$ cells/ml). Thus, 100 nM SAg was deemed an appropriate concentration for the time-lapse experiments described here to enable direct comparison to the effects of FGF-2. Unlike FGF-2-treated cultures, however, I found that cells did not survive well at clonal density in 100 nM SAg and basic medium alone. Survival improved when 1 ng/ml FGF-2 was also added to the medium. This level of FGF-2 did not induce *olig2* in many cells although the occasional O+/O- clone was identified (Table 4.5; Figure 4.54). Furthermore, addition of 1 ng/ml FGF-2 to 100 nM SAg-treated cultures did not affect the percentage of single cells that divided as compared to NEPs grown in 100 nM SAg alone (Table 4.11). However, the survival effect of this level of FGF-2 enabled the SAg-treated cultures to be recorded over 90 hours.

	% of single NEPs that divided	% of clones that survived over 90 hours
Control (0 nM SAg)	40 +/- 18	0
1 ng/ml FGF-2	39 +/- 7	75 +/- 14
100 nM SAg	42 +/- 16	0
100 nM SAg + 1 ng/ml FGF-2	42 +/-9	79 +/- 15
50 nM SAg + 1 ng/ml FGF-2	42 +/- 6	76 +/- 7
200 nM SAg + 1 ng/ml FGF-2	51 +/- 18	75 +/- 10

Table 4.11 Percentage of single cells in the starting culture that divided and the percentage of clones that survived for immunolabelling compared between different concentrations of SAg with and without 1 ng/ml FGF-2, 1 ng/ml FGF-2 alone and controls.

	%O+	%O+/O-	%O-
1 ng/ml FGF-2	1 +/- 2.1	17 +/- 8	83 +/- 8
50 nM SAg +1 ng/ml FGF-2	52 +/- 35	31 +/- 24	18 +/- 14
100nM SAg + 1 ng/ml FGF-2	37 +/- 19	44 +/- 16	20 +/- 10
200 nM SAg + 1 ng/ml FGF-2	49 +/- 32	44 +/- 27	8 +/- 7

Table 4.12 Comparison of distribution of clone types in different concentrations of SAg in the presence of 1 ng/ml FGF-2 and in 1 ng/ml FGF-2 alone.

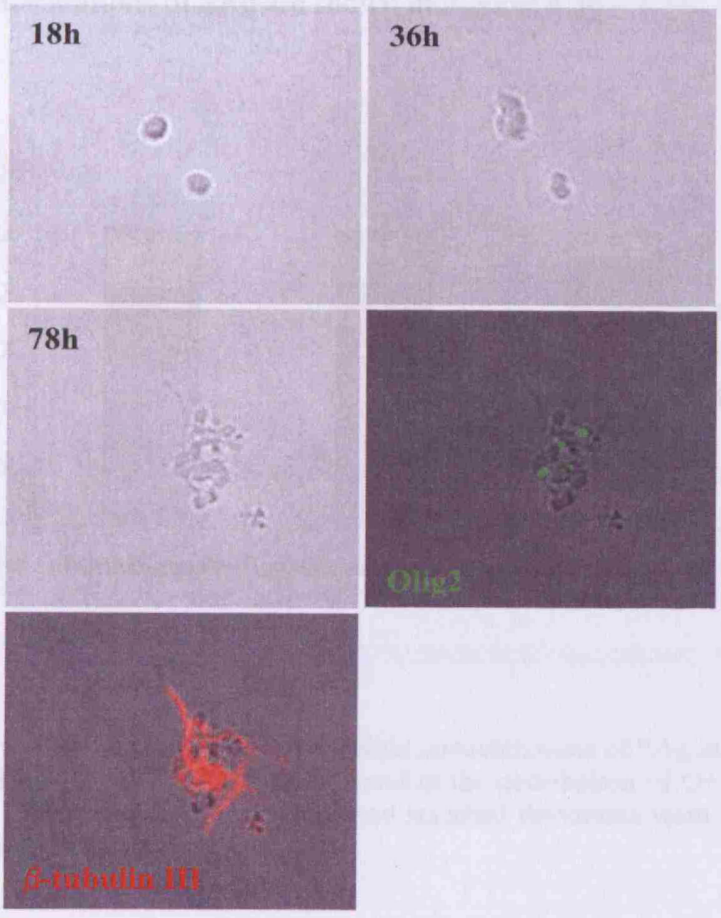

Figure 4.54 Stills from a time-lapse recording of an E13.5 cortical NEP preparation in the presence of 1 ng/ml FGF-2 in which an O+/O- clone was formed. Although *olig2* expression was induced at 1 ng/ml FGF-2, the number of Olig2+ cells was small. The other cells were β-tubulin III+ neurons or remained immunocytochemically unidentified. This sort of lineage with Olig2+ cells was a very rare occurrence as mostly only neurons were generated under these conditions.

4.2.15 Sonic agonist induces *olig2* over a range of concentrations

E13.5 embryonic cortical NEPs were cultured and filmed in the presence of SAg at 50, 100 and 200 nM along with 1 ng/ml FGF-2. The lineages were consistently difficult to trace however, since the cells frequently clumped together making individual divisions difficult to observe. The percentage of single cells that divided within the recording period could be counted however and was similar at all concentrations of SAg (Table 4.11). The proportion of clones that survived for immunocytochemical analysis was also similar across the SAg concentration range analysed (Table 4.11) and were classified as O+, O+/O- or O- clones as previously defined. The ratio of O+ : O+/O- : O- clone types was roughly 2:2:1 in all

concentrations of SAg (Table 4.12, Figure 4.55). Examples of clones generated in the different concentrations of SAg are shown in Figures 4.56 – 4.58.

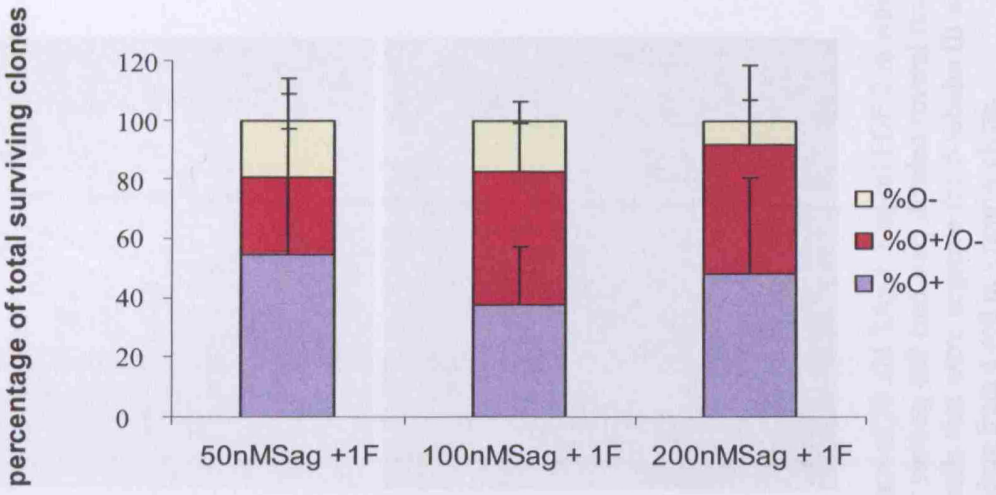

Figure 4.55 Distribution of clone types in different concentrations of SAg in the presence of 1 ng/ml FGF-2 (1F). There was no general trend in the distribution of O+, O+/O- and O- clones across the different culture conditions and standard deviations were large enough to deem any differences as insignificant.

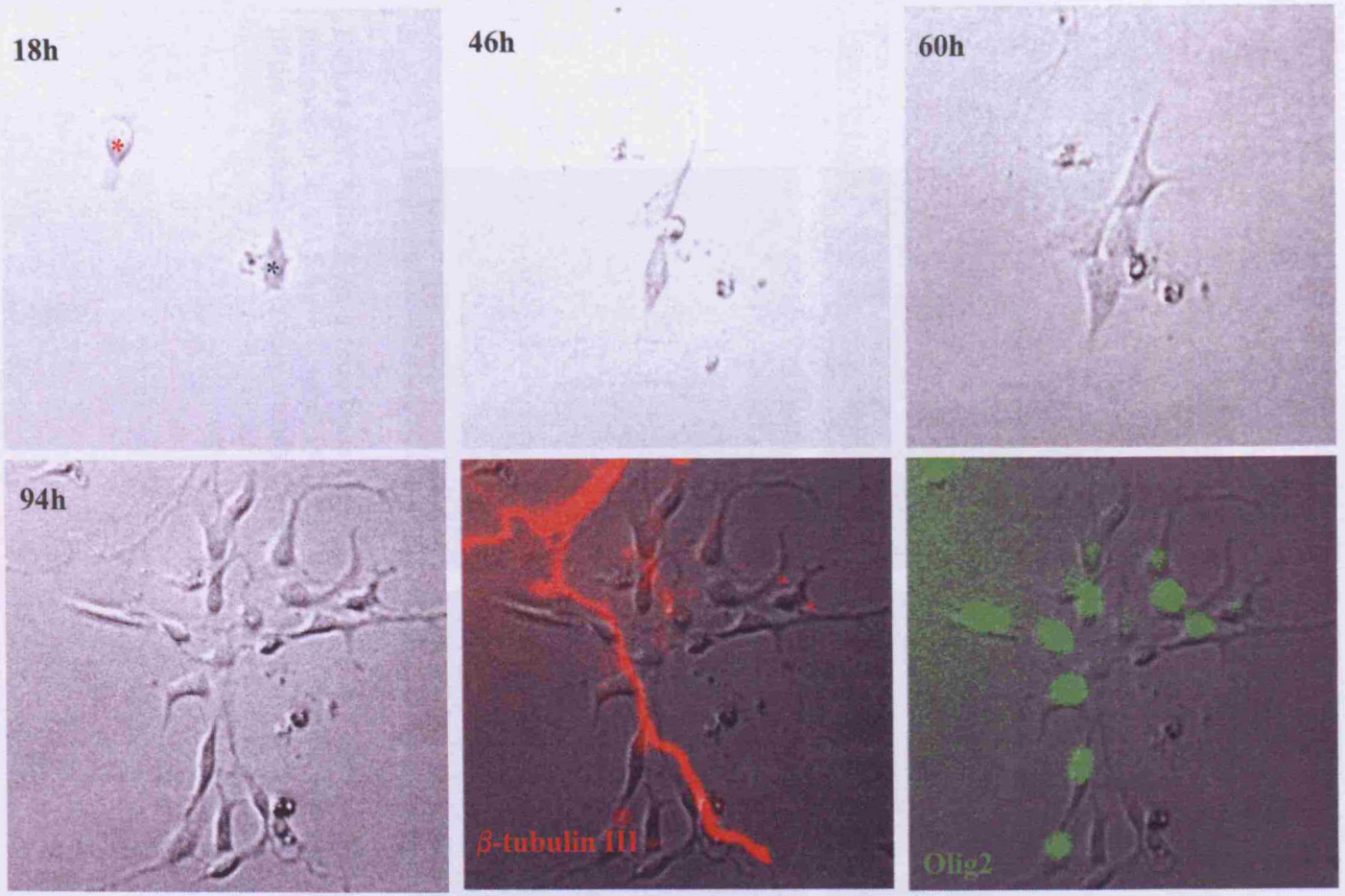

Figure 4.56 Stills from a time-lapse recording of a cortical NEP preparation in the presence of 50 nM SAg + 1 ng/ml FGF-2 in which an O+/O- clone was generated. One cell (black star) divided once and died. The other starting cell (red star) divided several times and gave rise to 8 Olig2+ cells, 3 weakly-expressing Olig2+ cells and 4 unidentified cells that were negative for β-tubulin III and Glast and GFAP. The β-tubulin III staining shown here was for a neuronal process extending from a cell in a nearby clone.

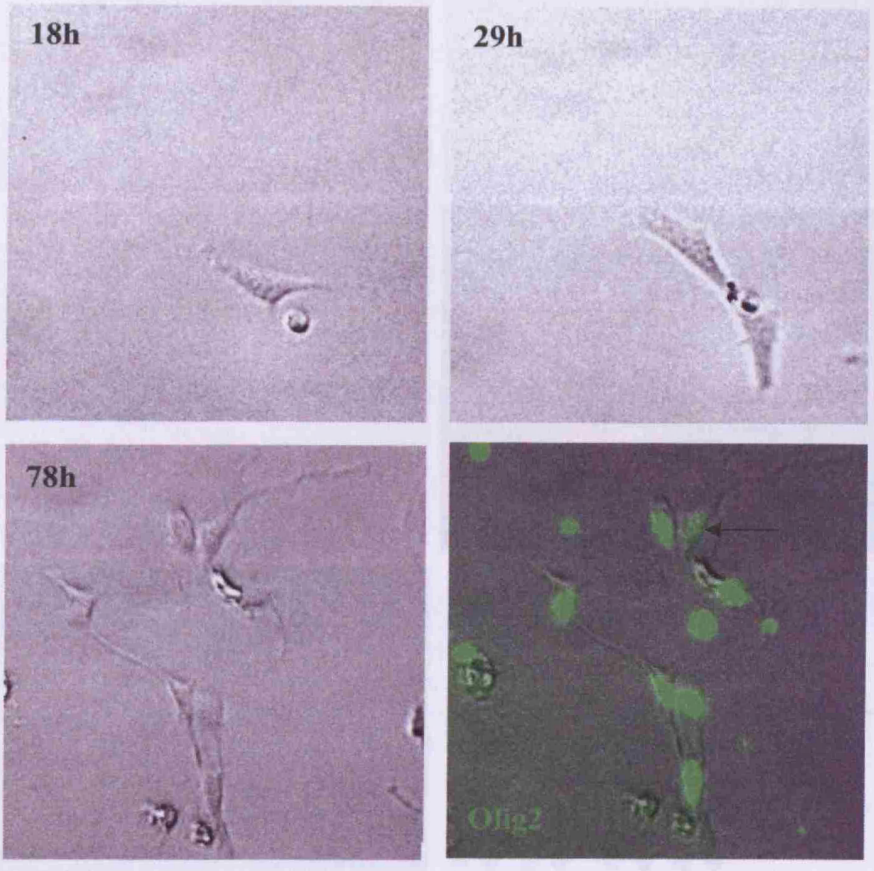

Figure 4.57 Stills from a time-lapse recording of an E13.5 cortical NEP preparation in the presence of 50 nM SAg + 1 ng/ml FGF-2 in which an O+ clone was generated although one of the daughter cells aws only weakly Olig2+ at 78 hours (arrow).

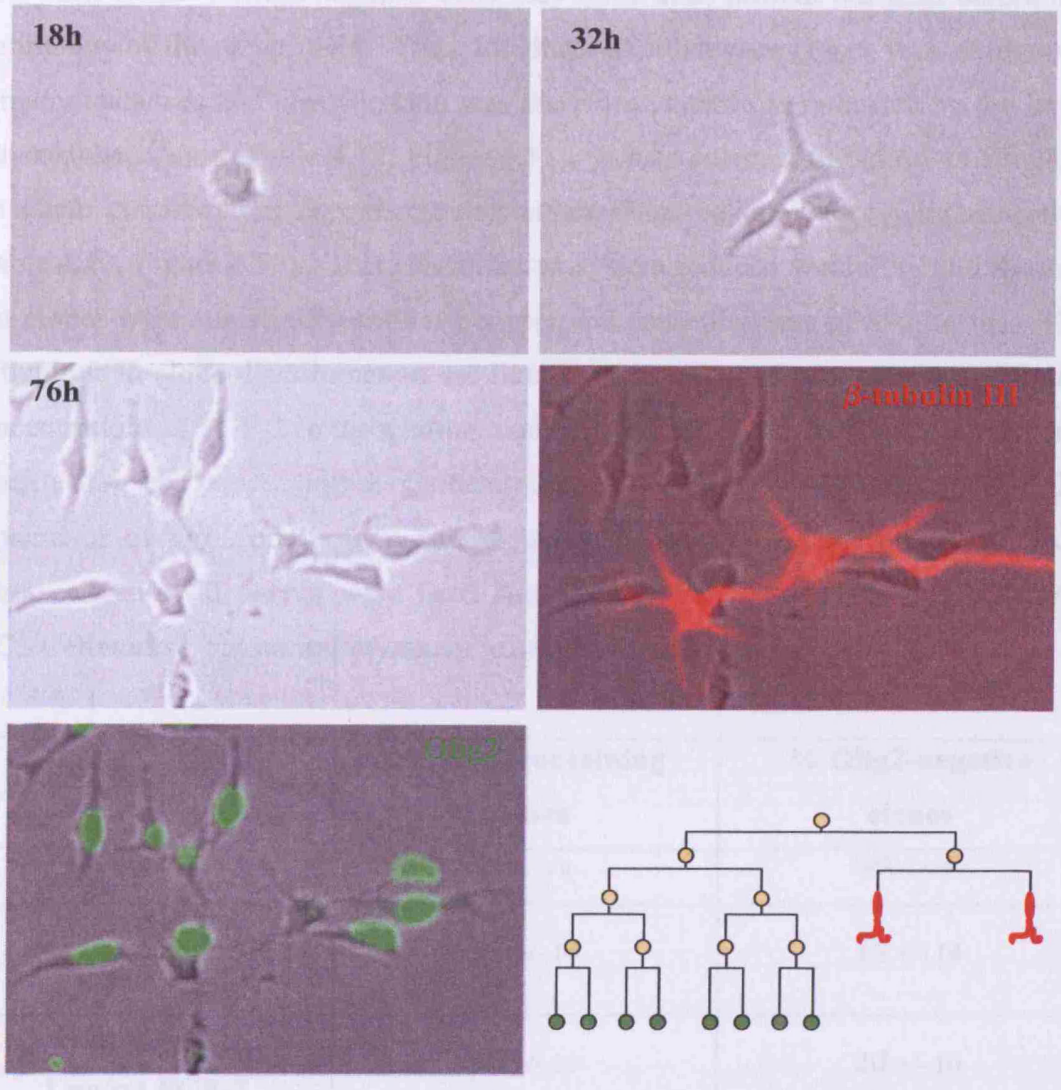

Figure 4.58 Stills from a time-lapse recording of an E13.5 cortical NEP preparation in the presence of 100 nM SAg + 1 ng/ml FGF-2 in which an O+/O- clone was generated with an apparently asymmetric lineage. After two divisions at 32 hours, the four daughter cells had distinct morphologies and two did not divide again and were β-tubulin III+ neurons while the other two continued to divide and generated only Olig2+ cells.

The classification of clones was difficult in many instances however, since many cells died within the lineages. Thus, for example, while the only surviving cells may have been Olig2+, Olig2-negative cells may have been present but died before the termination of the experiment. Thus, the distinction between clones was ambiguous in many instances and classification was therefore variable as indicated by the large standard deviations (Table 4.12, Figure 4.57). It was decided, therefore, to simplify the clone classification as either being either Olig2-containing or Olig2-negative (Table 4.13, Figure 4.59). This classification system reduced variability and showed that clones were statistically similar between the concentrations of SAg tested. The difficulties in clone discrimination are likely a side effect of poor survival. Higher concentrations of FGF-2 in the medium could afford better cell survival, but were not feasible for use since higher concentrations of FGF-2 would also induce the appearance of *olig2* on its own and would thus compromise the effects of SAg. Other cell survival agents were used such as the anti-caspase agent Q-VD-OPH (TCS Cellworks), but no improvement in survival was noted.

	% Olig2-containing clones	**% Olig2-negative clones**
1 ng/ml FGF-2	18 +/- 8	83 +/- 8
50 nM SAg +1 ng/ml FGF-2	82 +/- 14	18 +/- 14
100nM SAg + 1 ng/ml FGF-2	80 +/- 10	20 +/- 10
200 nM SAg + 1 ng/ml FGF-2	92 +/- 7	8 +/- 7

Table 4.13 Comparison of distribution of clone types in different concentrations of SAg in the presence of 1 ng/ml FGF-2 and 1 ng/ml FGF-2 alone for the simplified classification of clones being either Olig2-containing or Olig2-negative.

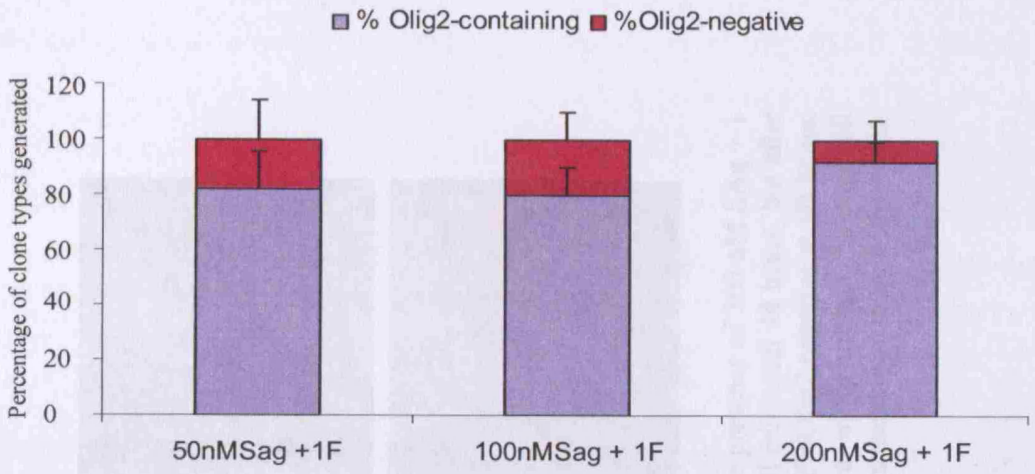

Figure 4.59 Distribution of Olig2-containing vs. Olig2-negative clones generated in different concentrations of SAg in the presence of 1 ng/ml FGF-2 (1F). There was no statistically significant difference in clone type frequencies over the range of SAg concentrations studied (P = 0.28 for Olig2-negative clones and P = 0.29 for Olig2-containing clones).

4.2.16 Olig2 up- and down-regulation was observed in SAg-treated cultures

When transgenic mice were used as a source of cells, both *olig2* up- and down-regulation could be assessed. Figure 4.60 shows a lineage in which the starting cell was EGFP+ at 18 hours and all daughter cells were EGFP+ at 44 hours. There followed complete down-regulation of EGFP in all daughter cells so they were all EGFP/Olig2-negative at 90 hours. Two were β-tubulin III+ neurons, but the other remaining cell was unidentified. It was generally not possible to trace lineages and observe changes in EGFP fluorescence in SAg-treated cultures, so the frequency of *olig2* up- or down-regulation occurring was not ascertainable.

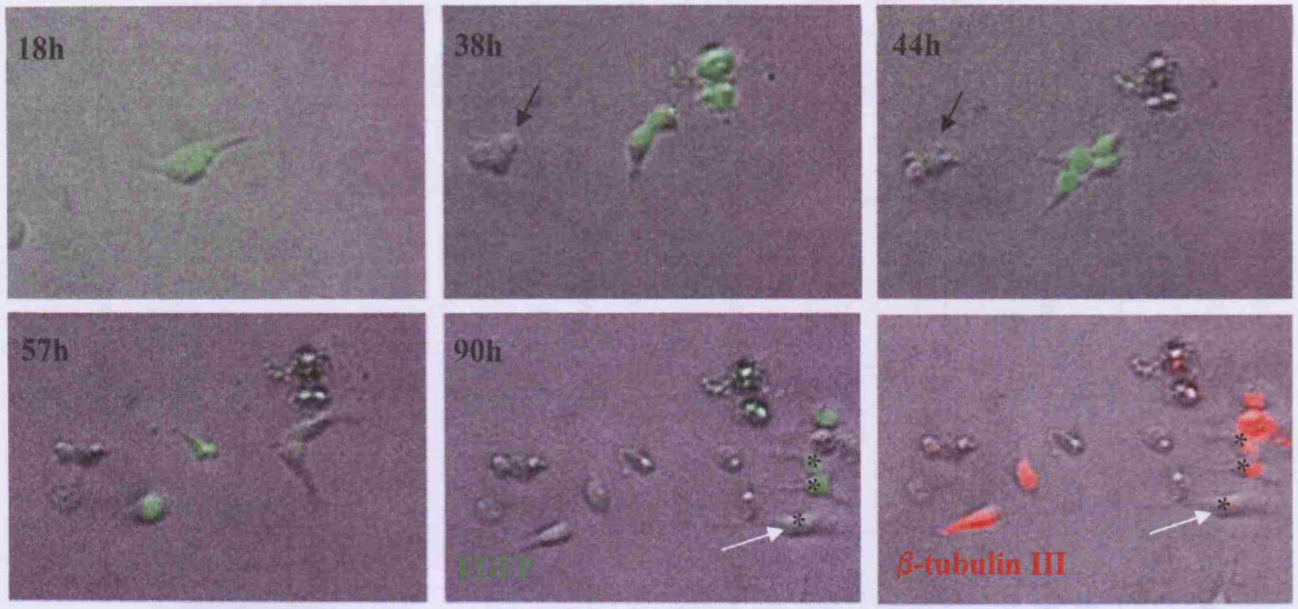

Figure 4.60 Stills from a time-lapse recording of an E13.5 cortical NEP preparation in the presence of 100 nM SAg + 1 ng/ml FGF-2. The starting cell was EGFP+ and EGFP fluorescence was maintained in all cells until 44 hours, but after this time there was complete down-regulation and all remaining daughter cells were EGFP/Olig2-negative at 90 hours. The other daughter cell that survived at 90 hours was unidentified (Olig2, Glast negative, white arrow). Another cell migrated into the field of view at 38 hours (black arrow), but died by 44 hours. At 90 hours there were three EGFP+ cells that migrated into the field of view from a neighbouring clone (black stars).

4.2.17 Cell division times do not vary across the different concentrations of SAg

Over the course of several experiments, sufficient divisions were observed for statistical analysis and it was found that there was no significant difference in division times at different concentrations of SAg (Table 4.14; Figure 4.61). Furthermore, division times did not increase during the course of the filming period, but kept constant over 90 hours. This is in contrast to the effects seen when cells were grown in 10 ng/ml FGF-2 when cell cycle time increased with successive divisions.

	1st division	2nd division	3rd division	4th division	5th division	6th division
50 nM SAg + 1F	8 +/- 1	14 +/- 1	13 +/- 3	14 +/- 3	14 +/- 6	15 +/- 7
100 nM SAg + 1F	7 +/- 1	13 +/- 2	13 +/- 2	15 +/- 2	15 +/- 1	14 +/- 2
200 nM SAg + 1F	7 +/- 2	13 +/- 1	15 +/- 3	16 +/- 4	10 +/- 0	-

Table 4.14 Cell cycle times across a 90 hour filming period for cells in expanding clones in the presence of 50, 100 or 200 nM SAg + 1 ng/ml FGF-2. Division times were not significantly different for cells in different concentrations of SAg, nor did division times change across the 90 hours observed. A maximum of 6 divisions were observed, similar to clones in the presence of 10 ng/ml FGF-2.

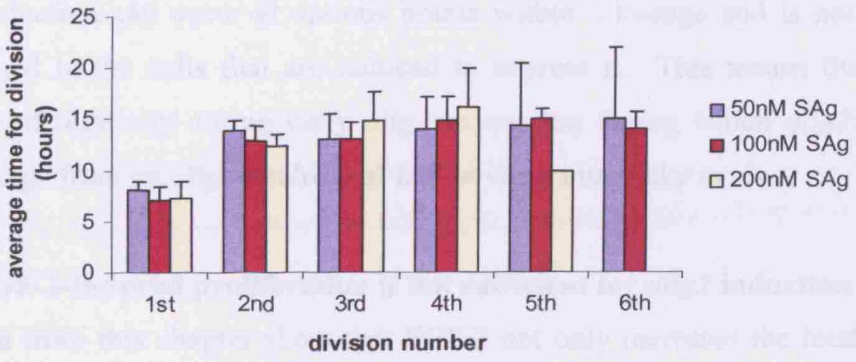

Figure 4.61 Division times for successive divisions of cells within expanding clones in the presence of 50, 100 or 200 nM SAg + 1 ng/ml FGF-2. Division times were similar at all concentrations of SAg analysed and, furthermore, were similar all through the 90 hour filming period. Note that the 'first' divisions indicate the time after the start of filming at which the first division was seen to occur. Subsequent divisions are quoted as absolute cell cycle time.

4.3 DISCUSSION

4.3.1 Summary of Results

With the mounting evidence that FGF-2 is involved in regulating cell fate specification in the developing CNS, I examined how it influenced the generation of Olig2+ cells from NEPs derived from the embryonic dorsal telencephalon. It has previously been shown that FGF-2 can induce the expression of *olig2* and the subsequent generation of OLPs both in culture (Chandran et al., 2003;Kessaris et al., 2004l;Qian et al., 1997) and more recently *in vivo* (Naruse et al., 2006), but whether this was a secondary effect to mitosis or an independent effect had not been clarified. The data I acquired demonstrated that the extent of *olig2* induction by FGF-2 far exceeded the FGF-2-mediated increase in mitosis suggesting that these two activities are independent. Moreover, the proliferative effect was saturating at concentrations of FGF-2 above 10 ng/ml while the induction of *olig2* continued to increase up to 25 ng/ml FGF-2 in E13.5 preparations. The induction of *olig2* was greatly reduced in preparations from younger animals, however, even in the presence of high FGF-2. This indicated a relative insensitivity to FGF-2 at E10.5 and E11.5. In comparison, the response of E13.5 NEPs to SAg was less pronounced relative to the response to FGF-2, although *olig2* induction was observed at a significant level relative to controls. In contrast, no response to EGF was observed at all. I further showed that *olig2* induction can occur at various points within a lineage and is not necessarily maintained in the cells that are induced to express it. This means that there is a window of plasticity during early *olig2* expression during which *olig2*+ cells may still diverge from an oligodendroglial fate *in vitro,* much like *in vivo.*

4.3.2 FGF-2-induced proliferation is not sufficient for *olig2* induction

The data from this chapter show that FGF-2 not only increases the total number of dividing cells in culture, but that the rate of division also increases. This effect was true for both EGFP+ and EGFP-negative cells, since they divided at the same rate, but EGFP-negative cells rarely underwent more than 4 successive divisions. Thus, although the induction of *olig2* might be independent of cell division, its expression correlates with a more proliferative cell type, meaning that Olig2+ clones are expanded more than Olig2-negative ones. Unpublished data from our lab has shown

that induction of *olig2* by FGF-2 is abolished by the application of aphidicolin, which arrests the cell cycle at the G1/S phase interface or within S phase itself. This data together with my observations suggest that, while progression through the cell cycle is necessary, it is not sufficient for *olig2* induction.

The indication that proliferation and *olig2* induction might be independent responses to FGF-2 should be investigated further. The identification of differential components involved in cell division vs. induction of transcription could give valuable insights into the possible role of FGF-2 in CNS patterning and development, which has its roots in the balance between cell division and cell specification. In support of the idea that the two responses are separable, FGF-2 has been shown previously to be capable of eliciting a variety of cellular responses independently (Boilly et al., 2000). In NIH-3T3 cells, a mutant variation of FGF-2 (FGF-2 S117A) continues to be able to stimulate differentiation, but not proliferation (Bailly et al., 2000). Similarly, a 6-amino acid deletion mutant of FGF-2 can induce proliferation as normal while migratory responses are considerably reduced in foetal bovine aortic endothelial cells and in NIH-3T3 cells (Isacchi et al., 1991). The dissociation of responses to FGF-2 has also been achieved pharmacologically; inhibition of protein kinase C (PKC) (a downstream effector of FGF-2 signalling) in NIH-3T3 cells prevents FGF-2-induced migration, but not proliferation (Besser et al., 1995;Isacchi et al., 1991;Presta et al., 1989).

4.3.3 FGF-2 increases the generation of Olig2+ cells over 3DIV by a combination of proliferation and induction of *olig2*

95% of cells acutely dissected from E13.5 embryos expressed Dcx+ (a neuroblast marker) in the absence of FGF-2. Furthermore, all clones that were generated in control cultures without FGF-2 contained only neurons over 3DIV, indicating that most NEPs at E13.5 were neurogenic. Thus, the finding that 79% of clones contained Olig2+ cells in the presence of 10 ng/ml FGF-2 means at least some early NEPs were re-programmed to a more gliogenic fate. Furthermore, the finding that, at 48 hours, O- clones contained only β-tubulin III+ neurons, but at 90 hours they contained a mixture of β-tubulin III+ neurons and unidentified cells implies that neurons themselves may be able to de-differentiate under FGF-2 signalling. This could however, be a misleading result since there were very few O- clones counted at

all at 48 hours and, moreover, the occasional cell within O- clones died leaving it unidentified. Although these consistently had the morphology of a neuronal cell, their identity was unconfirmed and it is therefore possible that, in these neuronal O- clones (N-clones) there may have been multipotent cells that died before immunocytochemical analysis. This will have to be investigated further to be confident of this idea.

The induction of *olig2* in response to FGF-2 increased as concentration of FGF-2 increased in E13.5 cultures, reminiscent of the dose-dependent effect seen by Kessaris et al in dense cultures (Kessaris et al., 2004). Although the proliferative response to FGF-2 was saturated at concentrations of FGF-2 above 15 ng/ml, increased proliferation no doubt also contributed to the increase in NG2+ cells observed in dense cultures. The data I described in fact indicate that it is a combination of responses to FGF-2 that could account for the increase in NG2+ cells in a dense population of cortical NEPs with increasing FGF-2:

* recruitment of more starting cells to generate *olig2*+ clones
* maintenance of *olig2* in expressing cells
* sustained rapid cell division, enabling the exponential growth of *olig2*-expressing clones

It would be of interest to investigate what down-stream signalling components are involved in the induction of *olig2* and proliferation in response to FGF-2 at different concentrations. Maher et al (1999) determined that p38MAPK, but not Erk (extracellular regulated kinase) activity was involved in FGF-2-stimulated proliferation of NIH-3T3 fibroblasts via FGFR1 signalling at 25 ng/ml FGF-2 (Maher, 1999). Garcia-Maya et al, however, demonstrated that both high (>10 ng/ml) and low (0.1 ng/ml) concentrations of FGF-2 were associated with cell survival and differentiation in fibroblast NIH3T3 cell line cultures while *intermediate* concentration ranges (1-10 ng/ml) induced proliferation along with inhibition of cell differentiation (Garcia-Maya et al., 2006). These differential responses related to changes in profiles of the intracellular components FRS-2 (a downstream effector of FGF signalling, chapter 1), Erk and p38MAPK. For example, p38MAPK and FRS-2 were rapidly down-regulated in higher

concentrations of FGF-2 (Garcia-Maya et al., 2006). Despite differences in proliferative response at high concentrations of FGF-2 identified by these two groups, p38MAPK was universally identified as being involved in a proliferative response. Components that are uniquely required for FGF-2-induced differentiation have not been confirmed.

FRS2 is a pivotal component of the docking protein complex that associates with FGFRs upon activation and is itself a central molecule for the recruitment of signalling molecules (Schlessinger, 2004). FGF-2 could feasibly have differential cellular effects according to its concentration via the recruitment and activation of more downstream components such as FRS2. Since different FGFR isoforms bind FGF-2 with differing affinities (Ornitz et al., 1996) it is also a possibility that the differential responses seen at higher concentrations of FGF-2 could be via recruitment of lower affinity receptors.

4.3.4 NEPs from embryonic cortices younger than E12.5 are unresponsive to FGF-2-induced expression of *olig2*

Induction of *olig2* did not occur significantly at embryonic ages younger than E12.5. This is complementary to the *in vivo* period of neurogenesis in the embryonic cortex, which occurs in earnest before the onset of neurogenesis. Not only is there an intrinsic tendency for neurons first, glia second therefore, but there is also a change in responsiveness of these embryonic NEPs to FGF-2 over the course of development. How the increase in responsiveness to FGF-2 occurs is not addressed here. Future experiments could be designed to ascertain whether this change in responsiveness is intrinsic by determining whether daughter cells derived from E11.5 preparations cultured over 2-3 DIV in the absence of FGF-2 have the same responsiveness to FGF-2 as freshly-dissected E13.5 cells. A great deal of work would need to be done to establish a suitable experimental design to enable this *in vitro* analysis. Molecular characterisation of the intracellular components that might be involved at different ages should be assessed in order to ascertain the reason for the differential response to FGF-2 at different embryonic ages. This could be achieved by immunolabelling for the presence of PLCγ, PI3-K and PKC as these are different signalling components that are recruitable by FGF-2 signalling. Western blot could also be used to identify the presence of activated components of the

FGFR-associated docking complex (FRS2, Grb, SHC) to determine whether differential transduction of FGF-2 signalling enables differential responses of NEPs from different embryonic ages. FGF-2 signalling has been implicated in the direct regulation of gene transcription following translocation to the nucleus (Bailly et al., 2000;Besser et al., 1995;Isacchi et al., 1991) and it is therefore possible that epigenetic effects within a cell may influence its responsiveness to FGF-2 signalling and this is also something that should be investigated. Whatever the mechanism, the data presented here indicate that neurogenesis is 'protected' at earlier stages of development and that gliogenesis can possibly only be precociously induced later in development, consistent with the idea that a neural network should be established before supporting cells are generated.

The fact that neurons are born before glia and that they may derive from a common precursor in the CNS is well described, as discussed in Chapter 1. The clonal analysis I have described also categorically demonstrates that both neurons and glia can be derived from single progenitors from ages as early as E11.5 (Figures 4.8, 4.37, 4.38 and 4.41). This has previously been demonstrated by Davis and Temple and Qian et al (Davis and Temple, 1994;Qian et al., 1997) where E10.5 preparations were cultured for up to 7 days, over which time glia and neurons were seen to emerge. With the use of transgenic cultures I have also specifically shown that *olig2*-expressing cortical NEPs can give rise to both neurons and glia. The means by which a common precursor changes from being neurogenic to gliogenic are not yet known, although interplay between transcription factors promoting gliogenesis vs. those that promote neurogenesis will certainly be central to this mechanism. An example of this is the co-expression of the neurogenic bHLH factor Neurogenin-2 (*ngn-2*) and *olig2* required for the generation of motor neuron precursors in the pMN domain in the spinal cord (Mizuguchi et al., 2001;Novitch et al., 2001;Scardigli et al., 2001) and the later exclusion of *ngn-2* from *olig2*+ cells that is necessary for the onset of oligodendrogenesis thereafter (Sun et al., 2001;Zhou and Anderson, 2002). The data I have presented indicate that *olig2*+ NEPs can also be a common precursor to both neurons and glia in the developing cortex.

4.3.5 Olig2 expression is dynamic

A significant finding of the work described here is that *olig2* can be down-regulated subsequent to its induction, indicating induced *olig2* expression by FGF-2 does not irreversibly commit E13.5 cortical NEPs to an oligodendrocyte fate *in vitro*. In combination with the possibility that neuronal cells may de-differentiate as described above, these data suggest that cell specification is a dynamic process and that developmental/differentiation programmes can be reversed or modified. It is known that in the spinal cord, motor neuron precursors express *olig2* which is rapidly down-regulated in post-mitotic, terminally differentiating motor neurons. Furusho et al (Furusho et al., 2006) directly described the generation of neurons from *olig2*-expressing precursors in mouse spinal cords. Using tamoxifen-induced *cre-lox* mediated recombination to permanently activate a reporter gene in *olig2*-expressing cells at E12.5 in mice, they found derivative reporter-gene labelled cells in the E18 spinal cord that expressed neuronal markers including ChAT. This is consistent with the *in vitro* data I described here where Olig2+ precursors gave rise to neurons in which *olig2* had down-regulated. There is evidence that *olig2* might also be involved in early specification of a pan-glial progenitor in preference to a neuronal one (Marshall et al., 2005), raising the possibility that some of the cells that down-regulated *olig2* in my experiments, yet did not express β-tubulin III, might be astrocytes or astrocyte precursors. Although no GFAP expression was observed in the cultures analysed here, GFAP is a late astrocyte marker and would not necessarily mark immature astrocytes. Some of the Olig2-negative cells were seen to express Glast, although labelling was usually very weak. The population of cells that remained unidentified is of great interest and their identification is pressing. Markers such as Nestin and S100-β should be used to ascertain whether they express other stem cell or astrocyte-related proteins respectively given that they were negative for Glast, RC2 and GFAP.

The up- and down-regulation of *olig2* observed indicates that there may be a window of opportunity within which cell fate may be plastic even in the presence of an inductive ligand. However, the co-expression of Olig2 with other OLP markers by 120 hours in culture implies that these Olig2+ cells are likely to be firmly committed to the oligodendrocyte lineage. I observed anecdotally that the more intense the initial EGFP fluorescence, the more likely it was that the descendants of that cell

would maintain *olig2* expression. Thus, the initial strength/level of *olig2* expression might influence commitment to the oligodendrocyte lineage. This hypothesis is supported by recent evidence from Liu et al, demonstrating a delayed expression of mature oligodendrocyte markers in heterozygous *olig2* mutants as compared with wild type controls (Liu et al., 2006). They also noted reduced numbers of MBP+/PLP+ mature oligodendrocytes in older spinal cords which was not accountable for by an increase in cell death. Furthermore, prolonged expression of *olig2* in the dorsal chick spinal cord caused mature oligodendrocytes to emerge from dorsal NEPs within 4 days whereas a more transient expression of *olig2* induced oligodendrocytes later and in reduced numbers. This led to the conclusion that dose as well as duration of *olig2* expression is important in oligodendrocyte specification and supports the observations I have made.

4.3.6 Responses to other signalling molecules:

EGF

Comparison of the effects of EGF with those of FGF-2 signalling was important to analyse given their complementary roles in neurosphere formation from cortical stem cells. Furthermore, an asymmetric distribution of EGFR has been demonstrated in subventricular zone cells in the embryonic murine forebrain both *in vitro* and *in vivo* (Sun et al., 2005). This asymmetrical distribution of EGFR is thought to underlie functional differences in daughter cells; High EGFR denotes an astrocytic fate and low EGFR determines that cells that could go on to pursue the oligodendrocyte lineage (Sun et al., 2005). Thus, it was possible that EGF might have had an effect on the induction of *olig2* and astrocyte markers and/or on cell proliferation. However, I found no observable effect of EGF signalling on E13.5 NEP. Furthermore, the addition of EGF in combination with FGF-2 at 10 ng/ml had no effect on the inductive effects of FGF-2 alone. However, while Tropepe et al determined that there is EGFR expression in NEPs at E13.5, this was not confirmed in my experiments and it is therefore possible that there was no EGFR expression in the cultured NEPs that I observed. Even if there was a baseline of EGFR expression, since FGF-2 signalling is known to induce EGFR upregulation, it is possible that in the absence of FGF-2, EGFR expression was not sufficient for an observable response to EGF. Unfortunately, the lack of both available markers and time meant that this question could not be answered. As a possible alternative explanation, the

fact that the NEPs cultured here were at clonal density may have affected their responsiveness to EGF signalling. Tropepe et al determined that the proliferative response to EGF of NEPs derived from E14.5 mouse embryonic brains depended upon cell density; at low density (10 cells/μl), EGF induced a proliferative effect half the magnitude of that of FGF-2, but at high densities (50 cells/μl) EGF induced a proliferative response ~10 times greater than that to FGF-2 (Tropepe et al., 1999). Since the 'low density' in the experiments described by Tropepe et al was equivalent to the clonal density at which cells were plated in my experiments, it is possible and likely that the absence of EGF-induced proliferation or induction could be related to the need for cell-cell contact for this to occur. The suggested importance of cell-cell contact and paracrine signalling between neighbouring cells is an inherent caveat to the data acquired here although it means that the responses observed in these clonal time-lapse experiments reveal a more cell-intrinsic capacity to respond to exogenous signalling.

Sonic Hedgehog

SHH has a well-defined role as a dorso-ventral patterning morphogen in the spinal cord, but its role in the developing brain is less clear. Like in the spinal cord, SHH is involved in both neurogenesis and oligodendrogenesis in the brain, being important in the induction of dopamine-releasing neurons in the midbrain (Hynes et al., 1995) and serotinergic neurons in the ventral forebrain (Ericson et al., 1995;Fedtsova and Turner, 2001;Hynes et al., 1995;Kohtz et al., 2001;Ye et al., 1998) early in development (E9-E12) and important in oligodendrogenesis thereafter. The experiments described in this chapter investigated the effects of SHH signalling on dorsal cortical NEPs from E13.5 mice from a region in which neurogenesis is still ongoing and endogenous oligodendrogenesis has not begun (Ericson et al., 1995;Kessaris et al., 2006). Given that FGF-2 induced *olig2* expression in a dose-dependent fashion in these cultures (Kessaris et al., 2004) and that SHH is a classified morphogen in the CNS (Echelard et al., 1993), it was expected that a dose-dependent induction of *olig2* within a bandwidth of SAg concentrations should be seen. In dense E13.5 cortical NEP cultures this is indeed the case; SAg induces large numbers of OLPs at concentrations between 250 and 500 nM, but above or below these concentrations the numbers of NG2+ cells generated declines significantly (Kessaris et al., 2004). Contrary to this, the data presented in this

chapter indicate that SHH does not act as a morphogen in the same E13.5 cortical NEPs when they are cultured at clonal density. No significant difference in the expression of *olig2* was observed across a range of SAg concentration of 50-200 nM. Furthermore, SAg alone did not enable sufficient cell survival for any level of *olig2* induction to be observed and there was an obligate requirement for the presence of at least 1 ng/ml FGF-2 for sufficient cell survival for analysis. It is known that FGF-2 signalling is required *in vitro* at least for SHH-induced *olig2* expression via the activation of MAPK since blocking FGF-2 signalling with an FGFR1 inhibitor in dense cultures blocks SAg-induced *olig2* expression (Kessaris et al., 2004). This indicates that there is endogenous FGF-2 signalling in dense cultures since SAg was able to induce *olig2* without the exogenous addition of FGF-2, but this is not the case in the clonal cultures recorded here. It could be assumed that in clonal cultures, the benefits of proximal production of FGF-2 by neighbouring cells are removed and it is therefore feasible and likely that the addition of FGF-2 in these experiments facilitated an obligate requirement for FGF-2 signalling in SAg-induced *olig2* expression in addition to a role as a survival factor. Unfortunately, given the poor survival and difficulty in analysing the clones in these cultures, the data was variable. This meant that quantification of the distribution of clone types did not reveal a clear trend across the different concentrations of SAg. Qualitatively, the clones generated in all concentrations were similar although there seemed to be more cell division in the higher doses of SAg. It was also still possible to determine that *olig2* up-and down-regulation occurred in the presence of SAg as it did in FGF-2 meaning that SAg does not induce the irreversible expression of *olig2* and manipulation of differentiation programmes might still be possible. More work will need to be done in order to analyse this more thoroughly.

The absence of morphogenetic activity of SAg on the clonal cultures of E13.5 cortical NEPs described here could be due to expression of downstream effectors in these cells being different to those in spinal cord domain NEPs. If SHH signalling is strong enough it can induce the generation of a weak Gli3 activator isoform (Bai et al., 2004;Wang et al., 2000), while it normally regulates Gli3 post-translationally to alter Gli3R availability. If SHH additionally encouraged the generation of Gli3A in preference to Gli3R in dorsal cells in the brain, SHH signalling may have a more direct activating effect here than in the dorsal spinal cord. To assess this possibility,

the quantification of Gli3A vs. Gli3R should be performed by both Western blot analysis on dorsal cortical NEP cultures both in the presence and absence of SAg. Furthermore, the expression of other downstream components should be analysed in comparison to ventrally-derived NEPs to determine whether the differential effects of SHH could be attributed to availability of intracellular signalling molecules as well as differential regulation of Gli3 isoform modification. If there is the availability of suitable antibodies, the detection of the different Gli3 isoforms may also be detected in real time by in situ immunolabelling and visualization of NEPs using time-lapse. This could give a better idea of the dynamics of Gli3 regulation upon SHH signalling.

The fact that not a huge proliferative or cell survival effect was observed with the addition of SAg indicates that these cells behave differently in low density than in high density cultures. What causes this difference is yet to be ascertained although evidence suggests that is might be related to FGF-2 signalling or, at least, MAPK activation (Kessaris et al., 2004). *In vivo*, FGF-2 is widely available so the effects of SHH are likely to be supported by FGF-2 activation of intracellular events if they are indeed physiologically required. This could potentially be assessed by regionalized blocking of FGF-2 signalling by topical application of FGFR1 inhibitors in oligodendrogenic domains. Whether the sonic agonist has different effects to endogenous SHH is also a contentious issue. Previous experiments have indicated that they induce equivalent effects in dense cultures (Kessaris et al., 2004), however, this should also be quantified for clonal preparations to confirm the observations described here. Certainly, the differences in responses of NEPs cultured in high vs. clonal density should be studied further to help determine what physiological implications data obtained from experiments like these might have.

Chapter 5

Final Discussion

5.1 Summary of results

The aim of this work was to use time-lapse microscopy to observe, in detail, the behaviour of individual neuroepithelial precursor cells (NEPs) cultured at clonal density. In particular, the responses of embryonic cortical NEPs to FGF-2 and a Sonic Hedgehog agonist (SAg) were analysed since these are two factors that play important roles throughout CNS patterning and development and in glial development in particular. FGF-2 has been shown to induce both the expression of *olig2* and the generation of OLPs in culture (Kessaris et al., 2004) and can also induce the generation of ectopic OLPs *in vivo* (Naruse et al., 2006). My experiments examined the induction of *olig2* in cultured NEPs using time-lapse microscopy. NEPs cultured from the dorsal cortex of E13.5 mouse embryos do not express *olig2* over 3 days *in vitro* when cultured in basic medium without added FGF-2. However, *olig2* expression is observed within 24 hours in the presence of FGF-2. Time-lapse analysis of *olig2* expression within the clones generated from dividing NEPs was facilitated by the use of the transgenic mouse line that I generated, which expressed enhanced green fluorescent protein (EGFP) under the same transcriptional control as *olig2*. The main findings were that FGF-2 induced *olig2* expression in a dose-dependent manner over 90 hours in NEPs from E13.5 embryos, but not in NEPs from E10.5 or E11.5 embryos. Filming over only 90 hours meant that the analysis of cell potential was limited to this time frame. Indeed, over longer culture periods, E10.5 NEPs eventually gave rise to Olig2+ cells. However, it was clear that over 90 hours there was a marked difference in response to FGF-2 in NEPs from different embryonic ages; E13.5 NEPs being highly sensitive to *olig2* induction and increased rates of proliferation and younger NEPs being more refractory to FGF-2 signalling.

Furthermore, in E13.5 cultures, higher concentrations of FGF-2 resulted in the maintenance of *olig2* expression in *olig2*+ cells. Consequently, more cells in the final

clones were Olig2+. Since OLP specification seems to require sustained *olig2* expression, it is likely that increasing FGF-2 signalling would increase the number of OLPs that are generated as more cells would maintain *olig2* expression. FGF-2 also had a pronounced effect on cell division and caused E13.5-derived NEPs to divide at an accelerated rate that was sustained over 90 hours in higher concentrations of FGF-2. These data indicate that FGF-2 acts pleiotropically on these NEPs sine both *olig2* expression and proliferation were affected. The combination of maintained *olig2* expression with increased cell division clearly accounts for the dramatic increase in OLPs seen in increasing concentrations of FGF-2 described by Kessaris et al (Kessaris et al., 2004). Since such effects were not observed over 90 hours for NEPs derived from younger embryos, something must change in NEPs between E11.5 and E13.5 making them responsive to FGF-2 and permissive of gliogenesis. Furthermore, since E10.5 NEPs do have the potential to generate OLPs over time, it is possible that the E13.5 NEPs are lineal descendents of the E10.5 NEPs.

The Sonic Hedgehog agonist (SAg) also induced *olig2* in the NEPs, but not in an obvious dose-dependent manner, at least over the concentration range that I used. This was unexpected since, in the dense cultures described by Kessaris et al, SAg induced *olig2* in a dose-dependent way, peaking between 200 and 500 nM (Kessaris et al., 2004). This response to SAg required a basal level of FGF signalling since it was blocked by FGFR inhibitors. It was also blocked in the absence of MAPK activation and an obligate requirement for MAPK activation for OLP generation could be satisfied through FGF-2 signalling (Kessaris et al., 2004). In clonal density cultures there is perhaps insufficient production of FGF-2 by neighbouring cells to meet the requirement for FGF; this might explain the different responses to SAg in clonal density versus high-density cultures.

There still remain several questions that are unanswered. First, through what signalling pathways does FGF-2 elicit proliferation and induction of *olig2* in NEPs and are they genuinely separable responses? Second, what is the basis of the differential effects to FGF-2 at different embryonic ages and are E13.5 NEPs lineal descendents of E10.5 NEPs? Third, what is the difference, if any, in the response of NEPs to SAg (or SHH)

and FGF? These questions could be approached by microarray analysis of the NEPs of different ages and in different conditions in order to establish what signalling components are involved in different scenarios. The use of specific inhibitors may also be useful in determining the signalling pathways which are involved. Finally, the question of identity of the cells that did not immunolabel for any of the markers used here should also be addressed. In order to do this, a good understanding of mechanisms involved in OLP, neuron and astrocyte precursor specification must be established.

5.2 A question of density

The difference in response to SAg in high- versus clonal-density cultures could be attributed to the availability or absence of FGF-2 given the findings of Kessaris et al (Kessaris et al., 2004). Plating density is important with respect to signalling via cell-cell contact and/or paracrine signalling events. This implies that the responses seen in clonal density cultures may not reflect what happens in a high density population of cells. Tropepe et al determined that differential plating density of E14.5 NEPs dramatically affected their mitogenic and neurosphere-forming response to EGF (relative to FGF-2); in low-density cultures, the mitogenic response to EGF was half that seen in response to FGF-2, however, the two mitogens induced comparable mitogenic responses in higher-density cultures, with EGF actually having a slightly stronger effect than FGF-2 (Tropepe et al., 1999). These findings, that cell density influences the potency of cell responses to EGF, might explain the lack of response to EGF in the cortical cultures described here. Moreover, if cell density influences responsiveness to exogenous signalling, then the responses of daughter cells within expanding clones may be different to the original isolated founder cells. Thus, the sustained divisions and maintained expression of *olig2* in the larger clones that were generated in higher concentrations of FGF-2 could possibly be attributed to paracrine signalling events occurring within the clone. This could be assessed by subcloning cells from expanding clones to assess whether they behave in isolation as they do within a clone in response to FGF-2. This process could itself affect cell behaviour however. There is no simple solution to this potential problem, except to observe cells *in vivo*, although the extracellular environment

cannot be easily manipulated *in vivo*. Thus, further progress will probably require a combination of both high- and clonal-density culture and *in vivo* observation.

5.3 *Olig2* in gliogenesis vs. neurogenesis

Olig2 is expressed in the precursors of both neurons and glia; it is subsequently down-regulated in neurons and astrocytes and maintained in the oligodendrocyte lineage (Marshall et al., 2005;Zhou et al., 2001). My data suggest that early expression of *olig2* is plastic and that both up-and down-regulation of *olig2* can occur within clones and that FGF-2 significantly increases the generation of *olig2*+ cells. This was at the expense of neurons and, while no astrocytes were identified, this does not mean they weren't generated since they may not have expressed differentiated markers within the culture period analysed. The maintenance of *olig2* expression in my experiments was associated with oligodendrocyte lineage development. The observation that both Olig2+ cells and Olig2-negative neurons can derive from a single *olig2*+ precursor is reminiscent of the results of *in vivo* fate mapping of the *olig2* lineage which demonstrates that neurons, oligodendrocytes and astrocytes derive from *olig2*+ precursors in the brain and spinal cord (Furusho et al., 2006;Masahira et al., 2006), indicating that *in vivo* events can be recapitulated in these cultures.

In the spinal cord, the onset of motor neuron production is associated with up-regulation of the bHLH factors *ngn 1* and *2* in the pMN domain, resulting in their co-expression with *olig2*. This is followed by rapid down-regulation of *olig2* in differentiating motor neurons (MNs) as MN-specific genes such as *hb9* are activated (Novitch et al., 2001). Although down-regulation of *olig2* accompanies MN differentiation, its early expression is necessary for MN specification since there are no MNs (or OLPs) in *olig2*-/- mice. The onset of oligodendrogenesis in the pMN domain is coincident with down-regulation of *ngn-2* and up-regulation of *sox9,* after MN production is over (Lee et al., 2005;Stolt et al., 2003;Sugimori et al., 2007). It is clear that the combination of *olig2* with other bHLH and HD transcription factors is central to cell type specification, but the details are unclear. *Sox9* is first expressed weakly at around E10 in the pMN domain (Stolt et al., 2003) with increasing levels to a peak at E12/13, around the time of OLP specification. It

might be speculated therefore, that *sox9* could be involved in the neuron/glia switch. However, *sox9-/-* mutants have no major phenotype with respect to spinal cord patterning and, although oligodendrocyte generation is slightly delayed and reduced at around E14.5, by E17.5 it is almost normal, indicating that *sox9* is not absolutely necessary for their generation (Stolt et al., 2003). *Sox9* also has a proven role in astrocyte specification (Kordes et al., 2005;Stolt et al., 2003;Wegner and Stolt, 2005). It is possible therefore, that *sox9* is important in the initiation of gliogenesis and whether the resultant progeny are OLPs or astrocytes is dependent upon the presence or absence of *olig2*. The unidentified cells present in the mixed cell clones described here could feasibly be astrocyte precursors which have down-regulated *olig2*, but have not yet up-regulated differentiated astrocyte markers such as GFAP; this will need further investigation. In order to determine which transcription factors might be causally involved in the initiation of the neuron/glia switch, forced expression of transcription factors such as *sox9, mash1* or *ngn2* could be activated via viral transfection and the effects on the generation of neurons and glia analysed by time-lapse microscopy.

5.4 Signalling in gliogenesis and neurogenesis

The combination of *olig2* expression with other bHLH and homeodomain transcription factors is a central component of the specification of neurons versus glia. Sonic Hedgehog and Notch are two important signalling factors that are likely to be involved in co-ordinating the expression of different combinations of transcription factors. Motor neuron precursors are sensitive to SHH early on in their specification, but become independent of SHH signalling post-mitotically (Ericson et al., 1996), whereas sustained SHH signalling is required for OLP specification (Bertrand and Dahmane, 2006;Orentas et al., 1999;Park et al., 2004). This mimics the temporal requirements of *olig2* expression in motor neuron versus oligodendrocyte precursor cells and is also mimicked in the experiments I describe here. In my time-lapse experiments, sustained *olig2* expression was induced by increased FGF-2 signalling, indicating that prolonged FGF-2 signalling could, in principle, produce similar results as prolonged SHH signalling i.e. neurons first and then OLPs.

Notch signalling is also thought to be important in the specification of neurons and glia and might possibly have a role in the neuron/glia switch; over-expression of Notch produces excess OLPs at the expense of motor neurons in the pMN domain and vice versa (Park and Appel, 2003;Yoon and Gaiano, 2005). Furthermore, some cells in the neuroepithelium express Notch1 asymmetrically at their basal pole and the Notch-expressing daughter cell becomes a migrating neuron (Chenn and McConnell, 1995;Park et al., 2004). Time-lapse could potentially be utilised in combination with Notch stimulation of NEPs to determine how the lineal relationships of cells within clones are affected. This could also, in principle, be done using explants and might indicate what qualitative influence Notch signalling has on the ability of NEPs to generate neurons versus glia in a more physiologically relevant context. Lateral inhibition by Notch signalling means that once neuronal fate is induced, neighbours are prevented from following the same fate. This suggests that Notch signalling might be important in regulating numbers or the balance of neurons and glia as well as, or rather than, determining the switch from neurogenic to gliogenic activity. The data I have presented suggests that there might possibly be a cell-intrinsic mechanism governing the neuron/glia switch since I identified asymmetric divisions in the absence of obvious asymmetric stimuli. This suggests that the segregation of transcription factors during cell division could be an important component of the neuron/glia switch although this does not negate the idea that exogenous signalling and lateral inhibition play a part.

5.5 SHH and FGFs – working together?

SHH has a predominantly ventralising role in CNS development, its actions being largely interpreted by Gli proteins as outlined in chapter 1. In culture, the induction of *olig2* in response to SHH seems to be dependent on the activation of MAPK which can be initiated by FGF-2 signalling (Kessaris et al., 2004). Whether this has physiological relevance is another question, although the availability of FGFs and SHH are known to overlap at several stages in CNS development. For example, FGFs and SHH are expressed in the node (early signalling centre during mouse and chick gastrulation) and in the ventral neural tube during spinal cord and telencephalic patterning.

FGF-2 is expressed widely throughout the CNS during development (Ford-Perriss et al., 2001) implying that cell responsiveness is likely to govern whether or not FGF signalling will have an effect. My data show that responsiveness to FGF-2 increases with embryonic age above ~E11.5 meaning that dorsal NEPs may be immune to ventralising signals early on in development, but that oligodendrogenesis in the cortex could be facilitated by FGF-2 thereafter if the signal is strong enough. Sensitivity to FGFs might even be partly dependent on Gli3 expression since Gli3 -/- mutants show expansion of FGF-8 expression with a concomitant decrease in the expression of Wnts, resulting in ventralisation of the dorsal forebrain (Aoto et al., 2002;Gunhaga et al., 2003;Gunhaga et al., 2003;Theil et al., 2002;Theil et al., 1999;Tole et al., 2000). FGFs are known to be ventralising (Crossley et al., 2001) and the repression of FGF-8 expression by Gli3 repressor activity in the dorsal brain may enable dorsalisation at least partly by excluding FGF signalling from these regions. Neurons are known to produce FGF-2 and thus a peak in FGF-2 signalling could feasibly arise at the peak neurogenesis which just precedes the onset of gliogenesis *in vivo*. Although my data indicates that timing of FGF-2 availability is unlikely to provoke oligodendrogenesis *in vivo*, if increased cell responsiveness is accompanied by an increase in neuron-derived FGF-2, this could possibly facilitate the onset of oligodendrogenesis. What causes the observed increase in responsiveness at ~E12.5-E13.5 is not known. However, FGFR1 is up-regulated just prior to gliogenesis in the rat dorsal cortex. Although this should relate to an increase in FGF-2 responsiveness at this time, an induced FGFR1-/- knock out (Kessaris et al unpublished) is phenotypically normal other than having no corpus callosum. Thus, FGFR1 is unlikely to be necessary for normal oligodendrocyte development, although there may be redundancy between FGFR1 and other FGFR isoforms which could compensate for its absence. The physiological role of FGF-2 therefore requires a great deal more investigation as its *in vivo* function is not yet clear.

5.6 Proliferation and cell specification

CNS patterning is a combination of cell specification and directed cell division. FGF-2 is classically a mitogen, but has recently also been shown to be important in cell specification and SHH is classically a morphogen, but also plays a role in cell division,

being highly mitogenic in the cerebellum (Kenney and Rowitch, 2000). Notch activity is also important in determining cell number in a directed fashion, since increased Notch signalling results the generation of more glia at the expense of neurons, while reduced notch signalling causes the emergence of more post-mitotic neurons and fewer glia as outlined in the introduction (Park and Appel, 2003). Notch activity probably regulates cell number by determining the timing of cells exiting the cell cycle and thus facilitating differentiation. Increased activation of CDK inhibitors is observed when Notch signalling is reduced (Park et al., 2005;Park and Appel, 2003), indicating that Notch might act by inhibiting CDK inhibitors normally to keep cells cycling, although the relationship is not necessarily causal. This is unlike FGF-2 which accelerates the cell cycle by increasing the rate of progression form G1 to S phase (Li and Cicco-Bloom, 2004). The mechanisms of SHH-induced cell proliferation are unknown, but it is clear that most signalling factors that are involved in determination of cell fate are also involved in cell division. In combination, they can therefore potentially regulate both the number and distribution of different cell types in the CNS.

5.7 Combinatorial codes in development

There is extensive spatiotemporal overlap of ligand availability during CNS development meaning that CNS development involves the activation of combinatorial signalling pathways. It is also likely that there is a significant degree of redundancy among signalling molecules and transcription factors in order to ensure that small alterations in availability of a single component don't lead to massive failings in developmental programmes. Redundancy amongst the Gli proteins is a good example since, despite their apparently polarised roles in CNS patterning, Gli3 and Gli2 can compensate for the absence of one another. For example, *gli3*, expressed from *gli2* promoter, can reduce the *gli2-/-* phenotype (Bai et al., 2004). Since the activator functions of the different Glis are effectively interchangeable, their expression profiles in combination with post-translational processing must largely determine their developmental role as this governs activator versus repressor functions at different times and places. Signalling molecules themselves might also be able to compensate for the loss of one another. Since FGF-2 can generate OLPs independently of SHH signalling, perhaps is could compensate

for reduced SHH signalling *in vivo* provided the cells were appropriately responsive. Given the ventralising role for FGFs in CNS development, it is feasible that they may facilitate SHH-dependent oligodendrogenesis. There are no OLPs in *shh-/-* mutants, however, meaning that it is unlikely that an SHH-independent mechanism (via FGF signalling or otherwise) is sufficient for ventral oligodendrogenesis.

The data I collected indicates that there is plasticity in the cell types that can be derived from embryonic cortical NEPs according to their exposure to ligands (FGF-2 and SAg described here). Precursor cells throughout the neuroepithelium have the capacity to generate specific glial and neuronal subtypes given the right cues. If the appropriate signalling pathways can be harnessed, there is feasibly, therefore, potential for the manipulation of cell specification during CNS development. This has important implications for intervention in developmental CNS pathologies.

5.8 Unidentified cells in FGF-2-generated cortical clones

A level of plasticity with respect to cell specification is maintained in the adult thanks to resident neural stem cells (NSCs) in the SVZ (Weiss et al., 1996). The lineal relationship between different embryonic NEP populations and postnatal NSCs is currently under investigation. Using Cre-lox fate-mapping in transgenic mice, Young et al (Young et al., 2007) have shown that precursors from throughout the telencephalic neuroepithelium contribute to NSCs in the adult SVZ. It is feasible, therefore, that some of the unidentified cells in the clones described in my experiments could potentially be such stem cells, although this will need further analysis. This could be done by subcloning cells from expanding clones after 90 hours and assaying for stem-cell potential i.e. neurosphere-forming potential with properties of self-renewal and multipotentiality. In order to target the unidentified cells for subcloning, fluorescence assisted cell sorting (FACS) analysis could first be performed in order to isolate the EGFP-negative cells, thus eliminating a large proportion of the identified cells. It is now well documented that there are neural stem cells and glial progenitor cells in many regions of the adult brain. Young et al (Young et al., 2007) demonstrated that embryonic NEPs contribute to these adult populations and there is now also a great deal of interest around whether the

pathways that are involved in cell specification in the embryo are recapitulated in these adult NSCs and glial progenitors.

The distinction between stem cells and restricted precursors and the signals involved in tightly regulated cell differentiation is an area of much current interest. Investigation into fate mapping and linking differentiated cells to particular stem cell or precursor cell populations is vast. The importance of understanding these processes is critical for understanding the biology of development, but also enables insight into the processes that, when disrupted, can result in serious pathologies, such as cancer. Pathways involved in normal progenitor cell proliferation are often the same pathways that are involved in tumour cell proliferation and survival (Garraway and Sellers, 2006). Neural stem cell populations in the subventricular zone of the adult brain are thought to be a significant source of gliomas. The idea that gliomas arise from NSCs could account for the heterogeneity that is characteristic of these tumours; if the tumour derives from a multipotent precursor cell then not only might its progeny be capable of self renewal, but also of differentiation into different glial subtypes. Of particular interest here is the link between *olig2* expression and gliomas since all gliomas have at least a proportion of *olig2*+ cells.

Olig2 is known to be involved in the maintenance of replication competence in glial progenitor cells in development (Lee et al., 2005) and is also required for oligodendrocyte specification. In the adult, subpopulations of NSCs also express *olig2* (Bachoo et al., 2002; Menn et al., 2006) including type B and type C cells which are the adult neural stem cells and rapidly dividing transit amplifying cells respectively (type B cells are thought to give rise to type C cells). Stimulation of *olig2*+ type C cell proliferation can result in glioma formation. Furthermore, Ligon et al (Ligon et al., 2007) demonstrated that *olig2* function is actually *required* for glioma formation and for tumour growth. The majority of the rapidly dividing tumour stem cells in gliomas are *olig2*+ and cells derived from *olig2/olig1* null mice do not generate gliomas in animal models of the disease (Ligon et al., 2007). Given that *olig2* is involved in proliferation and glial differentiation in the developing animal, it is hardly surprising that it could also have a

role in glioma pathology, but this example illustrates quite how closely linked the signalling pathways for development can be to those involved in pathology.

In vitro systems can give an idea of the fate *potential* of cells given the activation of different signalling pathways, even if this potential isn't realised *in vivo*. Nevertheless, the identification of pathways and mechanisms that *could* be involved in normal developmental cell specification is an important start in understanding the potential means of intervention in conditions where normal developmental programmes are defective. I am excited to see what the future holds for *in vivo* manipulation of the NEPs that are the precursors of the CNS.

References

E. Agius, C. Soukkarieh, C. Danesin, P. Kan, H. Takebayashi, C. Soula, and P. Cochard. Converse control of oligodendrocyte and astrocyte lineage development by Sonic hedgehog in the chick spinal cord. *Dev.Biol.* 270 (2):308-321, 2004.

J. A. Alberta, S. K. Park, J. Mora, D. Yuk, I. Pawlitzky, P. Iannarelli, T. Vartanian, C. D. Stiles, and D. H. Rowitch. Sonic hedgehog is required during an early phase of oligodendrocyte development in mammalian brain. *Mol.Cell Neurosci.* 18 (4):434-441, 2001.

A. Altaba, V. Nguyen, and V. Palma. The emergent design of the neural tube: prepattern, SHH morphogen and GLI code. *Curr.Opin.Genet.Dev.* 13 (5):513-521, 2003.

C. R. Altmann and A. H. Brivanlou. Neural patterning in the vertebrate embryo. *Int.Rev.Cytol.* 203:447-482, 2001.

K. Aoto, T. Nishimura, K. Eto, and J. Motoyama. Mouse GLI3 regulates Fgf8 expression and apoptosis in the developing neural tube, face, and limb bud. *Dev.Biol.* 251 (2):320-332, 2002.

J. C. Arevalo, H. Yano, K. K. Teng, and M. V. Chao. A unique pathway for sustained neurotrophin signaling through an ankyrin-rich membrane-spanning protein. *EMBO J.* 23 (12):2358-2368, 2004.

R. M. Bachoo, E. A. Maher, K. L. Ligon, N. E. Sharpless, S. S. Chan, M. J. You, Y. Tang, J. DeFrances, E. Stover, R. Weissleder, D. H. Rowitch, D. N. Louis, R. A. Depinho. Epidermal growth factor receptor and Ink4a/Arf: convergent mechanisms governing terminal differentiation and transformation along the neural stem cell to astrocyte axis. *Cancer Cell 3 (1):269-277, 2002.*

C. B. Bai, W. Auerbach, J. S. Lee, D. Stephen, and A. L. Joyner. Gli2, but not Gli1, is required for initial Shh signaling and ectopic activation of the Shh pathway. *Development* 129 (20):4753-4761, 2002.

C. B. Bai, D. Stephen, and A. L. Joyner. All mouse ventral spinal cord patterning by hedgehog is Gli dependent and involves an activator function of Gli3. *Dev.Cell* 6 (1):103-115, 2004.

K. Bailly, F. Soulet, D. Leroy, F. Amalric, and G. Bouche. Uncoupling of cell proliferation and differentiation activities of basic fibroblast growth factor. *FASEB J.* 14 (2):333-344, 2000.

R. Bansal, M. Kumar, K. Murray, R. S. Morrison, and S. E. Pfeiffer. Regulation of FGF receptors in the oligodendrocyte lineage. *Mol.Cell Neurosci.* 7 (4):263-275, 1996.

R. Bansal and S. E. Pfeiffer. Regulation of oligodendrocyte differentiation by fibroblast growth factors. *Adv.Exp.Med.Biol.* 429:69-77, 1997.

R. Bansal. Fibroblast growth factors and their receptors in oligodendrocyte development: implications for demyelination and remyelination. *Dev.Neurosci.* 24 (1):35-46, 2002.

R. Bansal, S. Magge, and S. Winkler. Specific inhibitor of FGF receptor signaling: FGF-2-mediated effects on proliferation, differentiation, and MAPK activation are inhibited by PD173074 in oligodendrocyte-lineage cells. *J.Neurosci.Res.* 74 (4):486-493, 2003.

S. Barolo and J. W. Posakony. Three habits of highly effective signaling pathways: principles of transcriptional control by developmental cell signaling. *Genes Dev.* 16 (10):1167-1181, 2002.

N. Bertrand and N. Dahmane. Sonic hedgehog signaling in forebrain development and its interactions with pathways that modify its effects. *Trends Cell Biol.* 16 (11):597-605, 2006.

D. Besser, M. Presta, and Y. Nagamine. Elucidation of a signaling pathway induced by FGF-2 leading to uPA gene expression in NIH 3T3 fibroblasts. *Cell Growth Differ.* 6 (8):1009-1017, 1995.

S. Blaess, J. D. Corrales, and A. L. Joyner. Sonic hedgehog regulates Gli activator and repressor functions with spatial and temporal precision in the mid/hindbrain region. *Development* 133 (9):1799-1809, 2006.

T. V. Bliss and G. L. Collingridge. A synaptic model of memory: long-term potentiation in the hippocampus. *Nature* 361 (6407):31-39, 1993.

B. Boilly, A. S. Vercoutter-Edouart, H. Hondermarck, V. Nurcombe, and Bourhis Le, X. FGF signals for cell proliferation and migration through different pathways. *Cytokine Growth Factor Rev.* 11 (4):295-302, 2000.

J. E. Bottenstein and G. H. Sato. Growth of a rat neuroblastoma cell line in serum-free supplemented medium. *Proc.Natl.Acad.Sci.U.S.A* 76 (1):514-517, 1979.

J. E. Bottenstein. Growth requirements in vitro of oligodendrocyte cell lines and neonatal rat brain oligodendrocytes. *Proc.Natl.Acad.Sci.U.S.A* 83 (6):1955-1959, 1986.

Y. G. Brickman, M. D. Ford, D. H. Small, P. F. Bartlett, and V. Nurcombe. Heparan sulfates mediate the binding of basic fibroblast growth factor to a specific receptor on neural precursor cells. *J.Biol.Chem.* 270 (42):24941-24948, 1995.

J. Cayuso, F. Ulloa, B. Cox, J. Briscoe, and E. Marti. The Sonic hedgehog pathway independently controls the patterning, proliferation and survival of neuroepithelial cells by regulating Gli activity. *Development* 133 (3):517-528, 2006.

M. Chalfie, Y. Tu, G. Euskirchen, W. W. Ward, and D. C. Prasher. Green fluorescent protein as a marker for gene expression. *Science* 263 (5148):802-805, 1994.

M. Chalfie. Green fluorescent protein. *Photochem.Photobiol.* 62 (4):651-656, 1995.

S. Chandran, H. Kato, D. Gerreli, A. Compston, C. N. Svendsen, and N. D. Allen. FGF-dependent generation of oligodendrocytes by a hedgehog-independent pathway. *Development* 130 (26):6599-6609, 2003.

S. Chandran, A. Compston, E. Jauniaux, J. Gilson, W. Blakemore, and C. Svendsen. Differential generation of oligodendrocytes from human and rodent embryonic spinal cord neural precursors. *Glia* 47 (4):314-324, 2004.

J. B. Charrier, F. Lapointe, N. M. Le Douarin, and M. A. Teillet. Anti-apoptotic role of Sonic hedgehog protein at the early stages of nervous system organogenesis. *Development* 128 (20):4011-4020, 2001.

A. Chenn and S. K. McConnell. Cleavage orientation and the asymmetric inheritance of Notch1 immunoreactivity in mammalian neurogenesis. *Cell* 82 (4):631-641, 1995.

C. Chesnutt, L. W. Burrus, A. M. Brown, and L. Niswander. Coordinate regulation of neural tube patterning and proliferation by TGFbeta and WNT activity. *Dev.Biol.* 274 (2):334-347, 2004.

A. J. Clark, P. Bissinger, D. W. Bullock, S. Damak, R. Wallace, C. B. Whitelaw, and F. Yull. Chromosomal position effects and the modulation of transgene expression. *Reprod.Fertil.Dev.* 6 (5):589-598, 1994.

P. Corish and C. Tyler-Smith. Attenuation of green fluorescent protein half-life in mammalian cells. *Protein Eng* 12 (12):1035-1040, 1999.

P. H. Crossley, S. Martinez, Y. Ohkubo, and J. L. Rubenstein. Coordinate expression of Fgf8, Otx2, Bmp4, and Shh in the rostral prosencephalon during development of the telencephalic and optic vesicles. *Neuroscience* 108 (2):183-206, 2001.

N. Dahmane, P. Sanchez, Y. Gitton, V. Palma, T. Sun, M. Beyna, H. Weiner, and A. Altaba. The Sonic Hedgehog-Gli pathway regulates dorsal brain growth and tumorigenesis. *Development* 128 (24):5201-5212, 2001.

I. Daviet, J. M. Herbert, and J. P. Maffrand. Involvement of protein kinase C in the mitogenic and chemotaxis effects of basic fibroblast growth factor on bovine cerebral cortex capillary endothelial cells. *FEBS Lett.* 259 (2):315-317, 1990.

A. A. Davis and S. Temple. A self-renewing multipotential stem cell in embryonic rat cerebral cortex. *Nature* 372 (6503):263-266, 1994.

R. Dono, G. Texido, R. Dussel, H. Ehmke, and R. Zeller. Impaired cerebral cortex development and blood pressure regulation in FGF-2-deficient mice. *EMBO J.* 17 (15):4213-4225, 1998.

W. J. Dower, J. F. Miller, and C. W. Ragsdale. High efficiency transformation of E. coli by high voltage electroporation. *Nucleic Acids Res.* 16 (13):6127-6145, 1988.

Y. Echelard, D. J. Epstein, B. St-Jacques, L. Shen, J. Mohler, J. A. McMahon, and A. P. McMahon. Sonic hedgehog, a member of a family of putative signaling molecules, is implicated in the regulation of CNS polarity. *Cell* 75 (7):1417-1430, 1993.

T. Edlund and T. M. Jessell. Progression from extrinsic to intrinsic signaling in cell fate specification: a view from the nervous system. *Cell* 96 (2):211-224, 1999.

J. Ericson, J. Muhr, M. Placzek, T. Lints, T. M. Jessell, and T. Edlund. Sonic hedgehog induces the differentiation of ventral forebrain neurons: a common signal for ventral patterning within the neural tube. *Cell* 81 (5):747-756, 1995.

J. Ericson, S. Morton, A. Kawakami, H. Roelink, and T. M. Jessell. Two critical periods of Sonic Hedgehog signaling required for the specification of motor neuron identity. *Cell* 87 (4):661-673, 1996.

N. Fedtsova and E. E. Turner. Signals from the ventral midline and isthmus regulate the development of Brn3.0-expressing neurons in the midbrain. *Mech.Dev.* 105 (1-2):129-144, 2001.

A. R. Ferre-D'Amare, G. C. Prendergast, E. B. Ziff, and S. K. Burley. Recognition by Max of its cognate DNA through a dimeric b/HLH/Z domain. *Nature* 363 (6424):38-45, 1993.

M. Fogarty, W. D. Richardson, and N. Kessaris. A subset of oligodendrocytes generated from radial glia in the dorsal spinal cord. *Development* 132 (8):1951-1959, 2005.

M. Ford-Perriss, H. Abud, and M. Murphy. Fibroblast growth factors in the developing central nervous system. *Clin.Exp.Pharmacol.Physiol* 28 (7):493-503, 2001.

D. Fortin, E. Rom, H. Sun, A. Yayon, and R. Bansal. Distinct fibroblast growth factor (FGF)/FGF receptor signaling pairs initiate diverse cellular responses in the oligodendrocyte lineage. *J.Neurosci.* 25 (32):7470-7479, 2005.

M. Frank-Kamenetsky, X. M. Zhang, S. Bottega, O. Guicherit, H. Wichterle, H. Dudek, D. Bumcrot, F. Y. Wang, S. Jones, J. Shulok, L. L. Rubin, and J. A. Porter. Small-molecule modulators of Hedgehog signaling: identification and characterization of Smoothened agonists and antagonists. *J.Biol.* 1 (2):10, 2002.

H. Fu, Y. Qi, M. Tan, J. Cai, H. Takebayashi, M. Nakafuku, W. Richardson, and M. Qiu. Dual origin of spinal oligodendrocyte progenitors and evidence for the cooperative role

of Olig2 and Nkx2.2 in the control of oligodendrocyte differentiation. *Development* 129 (3):681-693, 2002.

M. Furusho, K. Ono, H. Takebayashi, N. Masahira, T. Kagawa, K. Ikeda, and K. Ikenaka. Involvement of the Olig2 transcription factor in cholinergic neuron development of the basal forebrain. *Dev.Biol.* 293 (2):348-357, 2006.

L. Gabay, S. Lowell, L. L. Rubin, and D. J. Anderson. Deregulation of dorsoventral patterning by FGF confers trilineage differentiation capacity on CNS stem cells in vitro. *Neuron* 40 (3):485-499, 2003.

M. Garcia-Maya, A. A. Anderson, C. E. Kendal, A. V. Kenny, L. C. Edwards-Ingram, A. Holladay, and J. L. Saffell. Ligand concentration is a driver of divergent signaling and pleiotropic cellular responses to FGF. *J.Cell Physiol* 206 (2):386-393, 2006.

L. A. Garraway and W. R. Sellers. Lineage dependency and lineage-survival oncogenes in human cancer. *Nat. Rev. Cancer* 8 (6): 593-602. 2006.

J. Garrell and S. Campuzano. The helix-loop-helix domain: a common motif for bristles, muscles and sex. *Bioessays* 13 (10):493-498, 1991.

S. Giordano, L. Sherman, W. Lyman, and R. Morrison. Multiple molecular weight forms of basic fibroblast growth factor are developmentally regulated in the central nervous system. *Dev.Biol.* 152 (2):293-303, 1992.

M. Goldfarb. Functions of fibroblast growth factors in vertebrate development. *Cytokine Growth Factor Rev.* 7 (4):311-325, 1996.

M. Granerus, A. Welin, B. Lundh, P. N. Schofield, T. J. Ekstrom, and W. Engstrom. Heparin binding growth factors and the control of teratoma cell proliferation. *Eur.Urol.* 23 (1):76-81, 1993.

N. Gregori, C. Proschel, M. Noble, and M. Mayer-Proschel. The tripotential glial-restricted precursor (GRP) cell and glial development in the spinal cord: generation of bipotential oligodendrocyte-type-2 astrocyte progenitor cells and dorsal-ventral differences in GRP cell function. *J.Neurosci.* 22 (1):248-256, 2002.

R. E. Gross, M. F. Mehler, P. C. Mabie, Z. Zang, L. Santschi, and J. A. Kessler. Bone morphogenetic proteins promote astroglial lineage commitment by mammalian subventricular zone progenitor cells. *Neuron* 17 (4):595-606, 1996.

L. Gunhaga, M. Marklund, M. Sjodal, J. C. Hsieh, T. M. Jessell, and T. Edlund. Specification of dorsal telencephalic character by sequential Wnt and FGF signaling. *Nat.Neurosci.* 6 (7):701-707, 2003.

A. Hall, N. A. Giese, and W. D. Richardson. Spinal cord oligodendrocytes develop from ventrally derived progenitor cells that express PDGF alpha-receptors. *Development* 122 (12):4085-4094, 1996.

M. Hammerschmidt, A. Brook, and A. P. McMahon. The world according to hedgehog. *Trends Genet.* 13 (1):14-21, 1997.

A. Hemmati-Brivanlou, O. G. Kelly, and D. A. Melton. Follistatin, an antagonist of activin, is expressed in the Spemann organizer and displays direct neuralizing activity. *Cell* 77 (2):283-295, 1994.

C. C. Hui, D. Slusarski, K. A. Platt, R. Holmgren, and A. L. Joyner. Expression of three mouse homologs of the Drosophila segment polarity gene cubitus interruptus, Gli, Gli-2, and Gli-3, in ectoderm- and mesoderm-derived tissues suggests multiple roles during postimplantation development. *Dev.Biol.* 162 (2):402-413, 1994.

M. Hynes, J. A. Porter, C. Chiang, D. Chang, M. Tessier-Lavigne, P. A. Beachy, and A. Rosenthal. Induction of midbrain dopaminergic neurons by Sonic hedgehog. *Neuron* 15 (1):35-44, 1995.

D. E. Ingber and J. Folkman. Mechanochemical switching between growth and differentiation during fibroblast growth factor-stimulated angiogenesis in vitro: role of extracellular matrix. *J.Cell Biol.* 109 (1):317-330, 1989.

A. Isacchi, M. Statuto, R. Chiesa, L. Bergonzoni, M. Rusnati, P. Sarmientos, G. Ragnotti, and M. Presta. A six-amino acid deletion in basic fibroblast growth factor dissociates its mitogenic activity from its plasminogen activator-inducing capacity. *Proc.Natl.Acad.Sci.U.S.A* 88 (7):2628-2632, 1991.

J. Jacob and J. Briscoe. Gli proteins and the control of spinal-cord patterning. *EMBO Rep.* 4 (8):761-765, 2003.

J. Johansen, C. Rosenblad, K. Andsberg, A. Moller, C. Lundberg, A. Bjorlund, and T. E. Johansen. Evaluation of Tet-on system to avoid transgene down-regulation in ex vivo gene transfer to the CNS. *Gene Ther.* 9 (19):1291-1301, 2002.

S. Kanda, B. Tomasini-Johansson, P. Klint, J. Dixelius, K. Rubin, and L. Claesson-Welsh. Signaling via fibroblast growth factor receptor-1 is dependent on extracellular matrix in capillary endothelial cell differentiation. *Exp.Cell Res.* 248 (1):203-213, 1999.

A. M. Kenney and D. H. Rowitch. Sonic hedgehog promotes G(1) cyclin expression and sustained cell cycle progression in mammalian neuronal precursors. *Mol.Cell Biol.* 20 (23):9055-9067, 2000.

N. Kessaris, F. Jamen, L. L. Rubin, and W. D. Richardson. Cooperation between sonic hedgehog and fibroblast growth factor/MAPK signalling pathways in neocortical precursors. *Development* 131 (6):1289-1298, 2004.

N. Kessaris, M. Fogarty, P. Iannarelli, M. Grist, M. Wegner, and W. D. Richardson. Competing waves of oligodendrocytes in the forebrain and postnatal elimination of an embryonic lineage. *Nat.Neurosci.* 9 (2):173-179, 2006.

Y. kiyama-Oda, T. Hosoya, and Y. Hotta. Asymmetric cell division of thoracic neuroblast 6-4 to bifurcate glial and neuronal lineage in Drosophila. *Development* 126 (9):1967-1974, 1999.

J. D. Kohtz, D. P. Baker, G. Corte, and G. Fishell. Regionalization within the mammalian telencephalon is mediated by changes in responsiveness to Sonic Hedgehog. *Development* 125 (24):5079-5089, 1998.

J. D. Kohtz, H. Y. Lee, N. Gaiano, J. Segal, E. Ng, T. Larson, D. P. Baker, E. A. Garber, K. P. Williams, and G. Fishell. N-terminal fatty-acylation of sonic hedgehog enhances the induction of rodent ventral forebrain neurons. *Development* 128 (12):2351-2363, 2001.

T. Kondo and M. Raff. Oligodendrocyte precursor cells reprogrammed to become multipotential CNS stem cells. *Science* 289 (5485):1754-1757, 2000.

U. Kordes, Y. C. Cheng, and P. J. Scotting. Sox group E gene expression distinguishes different types and maturational stages of glial cells in developing chick and mouse. *Brain Res.Dev.Brain Res.* 157 (2):209-213, 2005.

T. M. Lamb, A. K. Knecht, W. C. Smith, S. E. Stachel, A. N. Economides, N. Stahl, G. D. Yancopolous, and R. M. Harland. Neural induction by the secreted polypeptide noggin. *Science* 262 (5134):713-718, 1993.

E. C. Lee, D. Yu, de Martinez, V, L. Tessarollo, D. A. Swing, Court DL, N. A. Jenkins, and N. G. Copeland. A highly efficient Escherichia coli-based chromosome engineering system adapted for recombinogenic targeting and subcloning of BAC DNA. *Genomics* 73 (1):56-65, 2001.

J. E. Lee, S. M. Hollenberg, L. Snider, D. L. Turner, N. Lipnick, and H. Weintraub. Conversion of Xenopus ectoderm into neurons by NeuroD, a basic helix-loop-helix protein. *Science* 268 (5212):836-844, 1995.

S. K. Lee, B. Lee, E. C. Ruiz, and S. L. Pfaff. Olig2 and Ngn2 function in opposition to modulate gene expression in motor neuron progenitor cells. *Genes Dev.* 19 (2):282-294, 2005.

B. Li and E. Cicco-Bloom. Basic fibroblast growth factor exhibits dual and rapid regulation of cyclin D1 and p27 to stimulate proliferation of rat cerebral cortical precursors. *Dev.Neurosci.* 26 (2-4):197-207, 2004.

K. L. Ligon, E. Huillard, S. Mehta, S. Kesari, H. Liu, J. A. Alberta, R. M. Bachoo, M. Kane, D. N. Louis, R. A. Depinho, D. J. Anderson, C. D. Stiles, D. H. Rowitch. Olig2-regulated lineage-restricted pathway controls replication competence in neural stem cells and malignant glioma. *Neuron* 53 (4): 503-517. 2007.

L. Lillien and C. Cepko. Control of proliferation in the retina: temporal changes in responsiveness to FGF and TGF alpha. *Development* 115 (1):253-266, 1992.

L. Lillien and D. Wancio. Changes in Epidermal Growth Factor Receptor Expression and Competence to Generate Glia Regulate Timing and Choice of Differentiation in the Retina. *Mol.Cell Neurosci.* 10 (5/6):296-308, 1998.

Y. Litingtung and C. Chiang. Specification of ventral neuron types is mediated by an antagonistic interaction between Shh and Gli3. *Nat.Neurosci.* 3 (10):979-985, 2000.

Y. Litingtung and C. Chiang. Control of Shh activity and signaling in the neural tube. *Dev.Dyn.* 219 (2):143-154, 2000.

Z. Liu, X. Hu, J. Cai, B. Liu, X. Peng, M. Wegner, and M. Qiu. Induction of oligodendrocyte differentiation by Olig2 and Sox10: Evidence for reciprocal interactions and dosage-dependent mechanisms. *Dev.Biol.*, 2006.

L. Lo and D. J. Anderson. Postmigratory neural crest cells expressing c-RET display restricted developmental and proliferative capacities. *Neuron* 15 (3):527-539, 1995.

Q. R. Lu, D. Yuk, J. A. Alberta, Z. Zhu, I. Pawlitzky, J. Chan, A. P. McMahon, C. D. Stiles, and D. H. Rowitch. Sonic hedgehog--regulated oligodendrocyte lineage genes encoding bHLH proteins in the mammalian central nervous system. *Neuron* 25 (2):317-329, 2000.

Q. R. Lu, T. Sun, Z. Zhu, N. Ma, M. Garcia, C. D. Stiles, and D. H. Rowitch. Common developmental requirement for Olig function indicates a motor neuron/oligodendrocyte connection. *Cell* 109 (1):75-86, 2002.

P. C. Ma, M. A. Rould, H. Weintraub, and C. O. Pabo. Crystal structure of MyoD bHLH domain-DNA complex: perspectives on DNA recognition and implications for transcriptional activation. *Cell* 77 (3):451-459, 1994.

P. Maher. p38 mitogen-activated protein kinase activation is required for fibroblast growth factor-2-stimulated cell proliferation but not differentiation. *J.Biol.Chem.* 274 (25):17491-17498, 1999.

V. Marigo and C. J. Tabin. Regulation of patched by sonic hedgehog in the developing neural tube. *Proc.Natl.Acad.Sci.U.S.A* 93 (18):9346-9351, 1996.

C. A. Marshall, B. G. Novitch, and J. E. Goldman. Olig2 directs astrocyte and oligodendrocyte formation in postnatal subventricular zone cells. *J.Neurosci.* 25 (32):7289-7298, 2005.

C. J. Marshall. Specificity of receptor tyrosine kinase signaling: transient versus sustained extracellular signal-regulated kinase activation. *Cell* 80 (2):179-185, 1995.

N. Masahira, H. Takebayashi, K. Ono, K. Watanabe, L. Ding, M. Furusho, Y. Ogawa, Y. Nabeshima, A. varez-Buylla, K. Shimizu, and K. Ikenaka. Olig2-positive progenitors in the embryonic spinal cord give rise not only to motoneurons and oligodendrocytes, but also to a subset of astrocytes and ependymal cells. *Dev.Biol.* 293 (2):358-369, 2006.

M. Mayer-Proschel, A. J. Kalyani, T. Mujtaba, and M. S. Rao. Isolation of lineage-restricted neuronal precursors from multipotent neuroepithelial stem cells. *Neuron* 19 (4):773-785, 1997.

W. L. McKeehan, X. Wu, and M. Kan. Requirement for anticoagulant heparan sulfate in the fibroblast growth factor receptor complex. *J.Biol.Chem.* 274 (31):21511-21514, 1999.

S. Mekki-Dauriac, E. Agius, P. Kan, and P. Cochard. Bone morphogenetic proteins negatively control oligodendrocyte precursor specification in the chick spinal cord. *Development* 129 (22):5117-5130, 2002.

B. Menn, J. M. Garcia-Verdugo, C. Yaschine, O. Gonzalez-Perez, D. Rowitch, A. varez-Buylla. Origin of oligodendrocytes in the subventricular zone of the adult brain. *J. Neurosci.* 30 (26): 7907-7918. 2006.

N. Methot and K. Basler. Hedgehog controls limb development by regulating the activities of distinct transcriptional activator and repressor forms of Cubitus interruptus. *Cell* 96 (6):819-831, 1999.

T. Miki, D. P. Bottaro, T. P. Fleming, C. L. Smith, W. H. Burgess, A. M. Chan, and S. A. Aaronson. Determination of ligand-binding specificity by alternative splicing: two distinct growth factor receptors encoded by a single gene. *Proc.Natl.Acad.Sci.U.S.A* 89 (1):246-250, 1992.

R. Mizuguchi, M. Sugimori, H. Takebayashi, H. Kosako, M. Nagao, S. Yoshida, Y. Nabeshima, K. Shimamura, and M. Nakafuku. Combinatorial roles of olig2 and neurogenin2 in the coordinated induction of pan-neuronal and subtype-specific properties of motoneurons. *Neuron* 31 (5):757-771, 2001.

N. Molotkova, A. Molotkov, I. O. Sirbu, and G. Duester. Requirement of mesodermal retinoic acid generated by Raldh2 for posterior neural transformation. *Mech.Dev.* 122 (2):145-155, 2005.

T. A. Moreno and C. Kintner. Regulation of segmental patterning by retinoic acid signaling during Xenopus somitogenesis. *Dev.Cell* 6 (2):205-218, 2004.

M. Murphy, J. Drago, and P. F. Bartlett. Fibroblast growth factor stimulates the proliferation and differentiation of neural precursor cells in vitro. *J.Neurosci.Res.* 25 (4):463-475, 1990.

J. C. Murtie, Y. X. Zhou, T. Q. Le, and R. C. Armstrong. In vivo analysis of oligodendrocyte lineage development in postnatal FGF2 null mice. *Glia* 49 (4):542-554, 2005.

S. K. Nair and S. K. Burley. Recognizing DNA in the library. *Nature* 404 (6779):715, 717-715, 718, 2000.

M. Naruse, E. Nakahira, T. Miyata, S. Hitoshi, K. Ikenaka, and R. Bansal. Induction of oligodendrocyte progenitors in dorsal forebrain by intraventricular microinjection of FGF-2. *Dev.Biol.* 297 (1):262-273, 2006.

S. Nery, H. Wichterle, and G. Fishell. Sonic hedgehog contributes to oligodendrocyte specification in the mammalian forebrain. *Development* 128 (4):527-540, 2001.

V. H. Nguyen, B. Schmid, J. Trout, S. A. Connors, M. Ekker, and M. C. Mullins. Ventral and lateral regions of the zebrafish gastrula, including the neural crest progenitors, are established by a bmp2b/swirl pathway of genes. *Dev.Biol.* 199 (1):93-110, 1998.

K. Niederreither, P. McCaffery, U. C. Drager, P. Chambon, and P. Dolle. Restricted expression and retinoic acid-induced downregulation of the retinaldehyde dehydrogenase type 2 (RALDH-2) gene during mouse development. *Mech.Dev.* 62 (1):67-78, 1997.

M. Noble, C. Proschel, and M. Mayer-Proschel. Getting a GR(i)P on oligodendrocyte development. *Dev.Biol.* 265 (1):33-52, 2004.

B. G. Novitch, A. I. Chen, and T. M. Jessell. Coordinate regulation of motor neuron subtype identity and pan-neuronal properties by the bHLH repressor Olig2. *Neuron* 31 (5):773-789, 2001.

V. Nurcombe, M. D. Ford, J. A. Wildschut, and P. F. Bartlett. Developmental regulation of neural response to FGF-1 and FGF-2 by heparan sulfate proteoglycan. *Science* 260 (5104):103-106, 1993.

V. Nurcombe, C. E. Smart, H. Chipperfield, S. M. Cool, B. Boilly, and H. Hondermarck. The proliferative and migratory activities of breast cancer cells can be differentially regulated by heparan sulfates. *J.Biol.Chem.* 275 (39):30009-30018, 2000.

D. M. Orentas, J. E. Hayes, K. L. Dyer, and R. H. Miller. Sonic hedgehog signaling is required during the appearance of spinal cord oligodendrocyte precursors. *Development* 126 (11):2419-2429, 1999.

D. M. Ornitz, J. Xu, J. S. Colvin, D. G. McEwen, C. A. MacArthur, F. Coulier, G. Gao, and M. Goldfarb. Receptor specificity of the fibroblast growth factor family. *J.Biol.Chem.* 271 (25):15292-15297, 1996.

D. M. Ornitz and N. Itoh. Fibroblast growth factors. *Genome Biol.* 2 (3):REVIEWS3005, 2001.

H. C. Park and B. Appel. Delta-Notch signaling regulates oligodendrocyte specification. *Development* 130 (16):3747-3755, 2003.

H. C. Park, J. Shin, and B. Appel. Spatial and temporal regulation of ventral spinal cord precursor specification by Hedgehog signaling. *Development* 131 (23):5959-5969, 2004.

H. C. Park, J. Boyce, J. Shin, and B. Appel. Oligodendrocyte specification in zebrafish requires notch-regulated cyclin-dependent kinase inhibitor function. *J.Neurosci.* 25 (29):6836-6844, 2005.

H. L. Park, C. Bai, K. A. Platt, M. P. Matise, A. Beeghly, C. C. Hui, M. Nakashima, and A. L. Joyner. Mouse Gli1 mutants are viable but have defects in SHH signaling in combination with a Gli2 mutation. *Development* 127 (8):1593-1605, 2000.

R. V. Pearse, K. J. Vogan, and C. J. Tabin. Ptc1 and Ptc2 transcripts provide distinct readouts of Hedgehog signaling activity during chick embryogenesis. *Dev.Biol.* 239 (1):15-29, 2001.

S. Pettersson, M. J. Sharpe, D. R. Gilmore, M. A. Surani, and M. S. Neuberger. Cellular selection leads to age-dependent and reversible down-regulation of transgenic immunoglobulin light chain genes. *Int.Immunol.* 1 (5):509-516, 1989.

R. S. Piotrowicz, P. A. Maher, and E. G. Levin. Dual activities of 22-24 kDA basic fibroblast growth factor: inhibition of migration and stimulation of proliferation. *J.Cell Physiol* 178 (2):144-153, 1999.

M. Placzek, T. M. Jessell, and J. Dodd. Induction of floor plate differentiation by contact-dependent, homeogenetic signals. *Development* 117 (1):205-218, 1993.

C. Poncet, C. Soula, F. Trousse, P. Kan, E. Hirsinger, O. Pourquie, A. M. Duprat, and P. Cochard. Induction of oligodendrocyte progenitors in the trunk neural tube by ventralizing signals: effects of notochord and floor plate grafts, and of sonic hedgehog. *Mech.Dev.* 60 (1):13-32, 1996.

P. P. Powell, S. P. Finklestein, C. A. Dionne, M. Jaye, and M. Klagsbrun. Temporal, differential and regional expression of mRNA for basic fibroblast growth factor in the developing and adult rat brain. *Brain Res.Mol.Brain Res.* 11 (1):71-77, 1991.

M. Presta, J. A. Maier, and G. Ragnotti. The mitogenic signaling pathway but not the plasminogen activator-inducing pathway of basic fibroblast growth factor is mediated through protein kinase C in fetal bovine aortic endothelial cells. *J.Cell Biol.* 109 (4 Pt 1):1877-1884, 1989.

N. P. Pringle and W. D. Richardson. A singularity of PDGF alpha-receptor expression in the dorsoventral axis of the neural tube may define the origin of the oligodendrocyte lineage. *Development* 117 (2):525-533, 1993.

N. P. Pringle, W. P. Yu, S. Guthrie, H. Roelink, A. Lumsden, A. C. Peterson, and W. D. Richardson. Determination of neuroepithelial cell fate: induction of the oligodendrocyte lineage by ventral midline cells and sonic hedgehog. *Dev.Biol.* 177 (1):30-42, 1996.

Y. Qi, J. Cai, Y. Wu, R. Wu, J. Lee, H. Fu, M. Rao, L. Sussel, J. Rubenstein, and M. Qiu. Control of oligodendrocyte differentiation by the Nkx2.2 homeodomain transcription factor. *Development* 128 (14):2723-2733, 2001.

Y. Qi, D. Stapp, and M. Qiu. Origin and molecular specification of oligodendrocytes in the telencephalon. *Trends Neurosci.* 25 (5):223-225, 2002.

X. Qian, A. A. Davis, S. K. Goderie, and S. Temple. FGF2 concentration regulates the generation of neurons and glia from multipotent cortical stem cells. *Neuron* 18 (1):81-93, 1997.

X. Qian, S. K. Goderie, Q. Shen, J. H. Stern, and S. Temple. Intrinsic programs of patterned cell lineages in isolated vertebrate CNS ventricular zone cells. *Development* 125 (16):3143-3152, 1998.

X. Qian, Q. Shen, S. K. Goderie, W. He, A. Capela, A. A. Davis, and S. Temple. Timing of CNS cell generation: a programmed sequence of neuron and glial cell production from isolated murine cortical stem cells. *Neuron* 28 (1):69-80, 2000.

R. Raballo, J. Rhee, R. Lyn-Cook, J. F. Leckman, M. L. Schwartz, and F. M. Vaccarino. Basic fibroblast growth factor (Fgf2) is necessary for cell proliferation and neurogenesis in the developing cerebral cortex. *J.Neurosci.* 20 (13):5012-5023, 2000.

M. C. Raff, R. H. Miller, and M. Noble. A glial progenitor cell that develops in vitro into an astrocyte or an oligodendrocyte depending on culture medium. *Nature* 303 (5916):390-396, 1983.

M. S. Rao and M. Mayer-Proschel. Glial-restricted precursors are derived from multipotent neuroepithelial stem cells. *Dev.Biol.* 188 (1):48-63, 1997.

M. S. Rao, M. Noble, and M. Mayer-Proschel. A tripotential glial precursor cell is present in the developing spinal cord. *Proc.Natl.Acad.Sci.U.S.A* 95 (7):3996-4001, 1998.

D. Reimers, M. A. Lopez-Toledano, I. Mason, P. Cuevas, C. Redondo, A. S. Herranz, M. V. Lobo, and E. Bazan. Developmental expression of fibroblast growth factor (FGF) receptors in neural stem cell progeny. Modulation of neuronal and glial lineages by basic FGF treatment. *Neurol.Res.* 23 (6):612-621, 2001.

W. D. Richardson, N. P. Pringle, W. P. Yu, and A. C. Hall. Origins of spinal cord oligodendrocytes: possible developmental and evolutionary relationships with motor neurons. *Dev.Neurosci.* 19 (1):58-68, 1997.

W. D. Richardson, H. K. Smith, T. Sun, N. P. Pringle, A. Hall, and R. Woodruff. Oligodendrocyte lineage and the motor neuron connection. *Glia* 29 (2):136-142, 2000.

W. D. Richardson, N. Kessaris, and N. Pringle. Oligodendrocyte wars. *Nat.Rev.Neurosci.* 7 (1):11-18, 2006.

J. Riese, R. Zeller, and R. Dono. Nucleo-cytoplasmic translocation and secretion of fibroblast growth factor-2 during avian gastrulation. *Mech.Dev.* 49 (1-2):13-22, 1995.

H. Roelink, J. A. Porter, C. Chiang, Y. Tanabe, D. T. Chang, P. A. Beachy, and T. M. Jessell. Floor plate and motor neuron induction by different concentrations of the amino-terminal cleavage product of sonic hedgehog autoproteolysis. *Cell* 81 (3):445-455, 1995.

D. H. Rowitch, B. Jacques, S. M. Lee, J. D. Flax, E. Y. Snyder, and A. P. McMahon. Sonic hedgehog regulates proliferation and inhibits differentiation of CNS precursor cells. *J.Neurosci.* 19 (20):8954-8965, 1999.

D. H. Rowitch, Q. R. Lu, N. Kessaris, and W. D. Richardson. An 'oligarchy' rules neural development. *Trends Neurosci.* 25 (8):417-422, 2002.

G. Sa and P. L. Fox. Basic fibroblast growth factor-stimulated endothelial cell movement is mediated by a pertussis toxin-sensitive pathway regulating phospholipase A2 activity. *J.Biol.Chem.* 269 (5):3219-3225, 1994.

N. Sanai, A. verez-Buylla, M. S. Berger. Neural stem cells and the origin of gliomas. *N. Engl. J. Med.* 353 (8): 811-822. 2005.

Y. Sasai and E. M. De Robertis. Ectodermal patterning in vertebrate embryos. *Dev.Biol.* 182 (1):5-20, 1997.

R. Scardigli, C. Schuurmans, G. Gradwohl, and F. Guillemot. Crossregulation between Neurogenin2 and pathways specifying neuronal identity in the spinal cord. *Neuron* 31 (2):203-217, 2001.

J. Schlessinger. Common and distinct elements in cellular signaling via EGF and FGF receptors. *Science* 306 (5701):1506-1507, 2004.

C. C. Stolt, S. Rehberg, M. Ader, P. Lommes, D. Riethmacher, M. Schachner, U. Bartsch, and M. Wegner. Terminal differentiation of myelin-forming oligodendrocytes depends on the transcription factor Sox10. *Genes Dev.* 16 (2):165-170, 2002.

C. C. Stolt, P. Lommes, E. Sock, M. C. Chaboissier, A. Schedl, and M. Wegner. The Sox9 transcription factor determines glial fate choice in the developing spinal cord. *Genes Dev.* 17 (13):1677-1689, 2003.

K. G. Storey, A. Goriely, C. M. Sargent, J. M. Brown, H. D. Burns, H. M. Abud, and J. K. Heath. Early posterior neural tissue is induced by FGF in the chick embryo. *Development* 125 (3):473-484, 1998.

A. Streit, A. J. Berliner, C. Papanayotou, A. Sirulnik, and C. D. Stern. Initiation of neural induction by FGF signalling before gastrulation. *Nature* 406 (6791):74-78, 2000.

M. Sugimori, M. Nagao, N. Bertrand, C. M. Parras, F. Guillemot, and M. Nakafuku. Combinatorial actions of patterning and HLH transcription factors in the spatiotemporal control of neurogenesis and gliogenesis in the developing spinal cord. *Development* 134 (8):1617-1629, 2007.

T. Sun, B. P. Hafler, S. Kaing, M. Kitada, K. L. Ligon, H. R. Widlund, D. I. Yuk, C. D. Stiles, and D. H. Rowitch. Evidence for motoneuron lineage-specific regulation of Olig2 in the vertebrate neural tube. *Dev.Biol.* 292 (1):152-164, 2006.

Y. Sun, M. Nadal-Vicens, S. Misono, M. Z. Lin, A. Zubiaga, X. Hua, G. Fan, and M. E. Greenberg. Neurogenin promotes neurogenesis and inhibits glial differentiation by independent mechanisms. *Cell* 104 (3):365-376, 2001.

Y. Sun, S. K. Goderie, and S. Temple. Asymmetric distribution of EGFR receptor during mitosis generates diverse CNS progenitor cells. *Neuron* 45 (6):873-886, 2005.

H. Takebayashi, S. Yoshida, M. Sugimori, H. Kosako, R. Kominami, M. Nakafuku, and Y. Nabeshima. Dynamic expression of basic helix-loop-helix Olig family members: implication of Olig2 in neuron and oligodendrocyte differentiation and identification of a new member, Olig3. *Mech.Dev.* 99 (1-2):143-148, 2000.

H. Takebayashi, Y. Nabeshima, S. Yoshida, O. Chisaka, K. Ikenaka, and Y. Nabeshima. The basic helix-loop-helix factor olig2 is essential for the development of motoneuron and oligodendrocyte lineages. *Curr.Biol.* 12 (13):1157-1163, 2002.

Y. Tanabe, C. William, and T. M. Jessell. Specification of motor neuron identity by the MNR2 homeodomain protein. *Cell* 95 (1):67-80, 1998.

N. Tekki-Kessaris, R. Woodruff, A. C. Hall, W. Gaffield, S. Kimura, C. D. Stiles, D. H. Rowitch, and W. D. Richardson. Hedgehog-dependent oligodendrocyte lineage specification in the telencephalon. *Development* 128 (13):2545-2554, 2001.

T. Theil, G. varez-Bolado, A. Walter, and U. Ruther. Gli3 is required for Emx gene expression during dorsal telencephalon development. *Development* 126 (16):3561-3571, 1999.

T. Theil, S. Aydin, S. Koch, L. Grotewold, and U. Ruther. Wnt and Bmp signalling cooperatively regulate graded Emx2 expression in the dorsal telencephalon. *Development* 129 (13):3045-3054, 2002.

S. Tole, C. W. Ragsdale, and E. A. Grove. Dorsoventral patterning of the telencephalon is disrupted in the mouse mutant extra-toes(J). *Dev.Biol.* 217 (2):254-265, 2000.

V. Tropepe, M. Sibilia, B. G. Ciruna, J. Rossant, E. F. Wagner, and Kooy D. van der. Distinct neural stem cells proliferate in response to EGF and FGF in the developing mouse telencephalon. *Dev.Biol.* 208 (1):166-188, 1999.

J. Z. Tsien. Behavioral genetics: subregion- and cell type-restricted gene knockout in mouse brain. *Pathol.Biol.(Paris)* 46 (9):699-700, 1998.

R. Y. Tsien. The green fluorescent protein. *Annu.Rev.Biochem.* 67:509-544, 1998.

F. M. Vaccarino, M. L. Schwartz, R. Raballo, J. Nilsen, J. Rhee, M. Zhou, T. Doetschman, J. D. Coffin, J. J. Wyland, and Y. T. Hung. Changes in cerebral cortex size are governed by fibroblast growth factor during embryogenesis. *Nat.Neurosci.* 2 (9):848, 1999.

A. Vallstedt, J. M. Klos, and J. Ericson. Multiple dorsoventral origins of oligodendrocyte generation in the spinal cord and hindbrain. *Neuron* 45 (1):55-67, 2005.

B. Wang, J. F. Fallon, and P. A. Beachy. Hedgehog-regulated processing of Gli3 produces an anterior/posterior repressor gradient in the developing vertebrate limb. *Cell* 100 (4):423-434, 2000.

M. Wegner and C. C. Stolt. From stem cells to neurons and glia: a Soxist's view of neural development. *Trends Neurosci.* 28 (11):583-588, 2005.

B. Weise, T. Janet, and C. Grothe. Localization of bFGF and FGF-receptor in the developing nervous system of the embryonic and newborn rat. *J.Neurosci.Res.* 34 (4):442-453, 1993.

S. Weiss, C. Dunne, J. Hewson, C. Wohl, M. Wheatley, A. C. Peterson, and B. A. Reynolds. Multipotent CNS stem cells are present in the adult mammalian spinal cord and ventricular neuroaxis. *J.Neurosci.* 16 (23):7599-7609, 1996.

M. Wijgerde, J. A. McMahon, M. Rule, and A. P. McMahon. A direct requirement for Hedgehog signaling for normal specification of all ventral progenitor domains in the presumptive mammalian spinal cord. *Genes Dev.* 16 (22):2849-2864, 2002.

R. H. Woodruff, N. Tekki-Kessaris, C. D. Stiles, D. H. Rowitch, and W. D. Richardson. Oligodendrocyte development in the spinal cord and telencephalon: common themes and new perspectives. *Int.J.Dev.Neurosci.* 19 (4):379-385, 2001.

M. Xin, T. Yue, Z. Ma, F. F. Wu, A. Gow, and Q. R. Lu. Myelinogenesis and axonal recognition by oligodendrocytes in brain are uncoupled in Olig1-null mice. *J.Neurosci.* 25 (6):1354-1365, 2005.

T. P. Yamaguchi and J. Rossant. Fibroblast growth factors in mammalian development. *Curr.Opin.Genet.Dev.* 5 (4):485-491, 1995.

W. Ye, K. Shimamura, J. L. Rubenstein, M. A. Hynes, and A. Rosenthal. FGF and Shh signals control dopaminergic and serotonergic cell fate in the anterior neural plate. *Cell* 93 (5):755-766, 1998.

K. Yoon and N. Gaiano. Notch signaling in the mammalian central nervous system: insights from mouse mutants. *Nat.Neurosci.* 8 (6):709-715, 2005.

K. M. Young, M. Fogarty, N. Kessaris, and W. D. Richardson. Subventricular zone stem cells are heterogeneous with respect to their embryonic origins and neurogenic fates in the adult olfactory bulb. *J.Neurosci.* 27 (31):8286-8296, 2007.

D. Yu, H. M. Ellis, E. C. Lee, N. A. Jenkins, N. G. Copeland, and Court DL. An efficient recombination system for chromosome engineering in Escherichia coli. *Proc.Natl.Acad.Sci.U.S.A* 97 (11):5978-5983, 2000.

P. za-Blanc, F. A. Ramirez-Weber, M. P. Laget, C. Schwartz, and T. B. Kornberg. Proteolysis that is inhibited by hedgehog targets Cubitus interruptus protein to the nucleus and converts it to a repressor. *Cell* 89 (7):1043-1053, 1997.

Q. Zhou, S. Wang, and D. J. Anderson. Identification of a novel family of oligodendrocyte lineage-specific basic helix-loop-helix transcription factors. *Neuron* 25 (2):331-343, 2000.

Q. Zhou and D. J. Anderson. The bHLH transcription factors OLIG2 and OLIG1 couple neuronal and glial subtype specification. *Cell* 109 (1):61-73, 2002.